Identification and functional analysis of pronephric development genes in *Xenopus laevis*.

Subreena Lutchmy Simrick, B.Sc. (Hons.).

A thesis submitted to the University of Warwick

for the degree of Doctor of Philosophy.

Molecular Physiology,

Department of Biological Sciences,

University of Warwick,

Coventry,

CV4 7AL.

June 2006.

Contents

List of Figures

List of Tables

Acknowledgements

A huge thank you goes to my supervisor Liz Oliver-Jones, for her tireless enthusiasm, guidance and drive. I really wouldn't be here if it wasn't for you. Also Karine Massé, who has always been the first port of call for advice or a good chat!

Thank you to everyone who has been in the lab during my stretch, specifically Rob and Stéph for their kind friendship. Not forgetting Surinder who is always at hand with a random joke or two.

I would like to thank my family, namely, "Have you done it yet?" Jim, "Just do it" Didi and "Have you got a job yet..." Mum, who have put up with and supported me.

Finally, I dedicate this thesis to Matthew John Paul, who has been there for me during all the happy and the not so happy moments of this PhD. Thank you for sharing this journey with me.

Declaration

The results presented in this thesis are the work of the author unless specified.

Microinjection and dissections were carried out by Professor Elizabeth Oliver-Jones. Wax-embedding and sectioning were performed by Mr Surinder Bhamra. Hormone injections to *Xenopus laevis* females were given by Mr Robert Taylor and Paul Jarrett.

Sources of information have been acknowledged by reference.

None of this work has been previously used to apply for a degree.

A reprint of the publication obtained during the course of this research can be found at the end of the thesis.

Summary

The formation of the kidney in vertebrates proceeds through a succession of up to three structures, the pronephros, metanephros and mesonephros. This project aimed to identify a suitable target gene involved in the development of the pronephros and study its role in development. By analysing the functional role of a target gene, this thesis ultimately aims to further elucidate the developmental regulation of pronephric organogenesis.

The candidate target genes were identified from 3 sources. Firstly, a *Xenopus laevis* stage 13 cDNA library was screened using a probe made from retinoic acid and activin A treated animal caps. Secondly, four UniGene cluster genes were investigated, after initial analysis indicated they were highly pronephros specific (Personal correspondence Pollet, N). Finally, data mining identified *Xenopus* homologues of important kidney development genes identified in higher vertebrates or newly identified genes expressed in the pronephros. On the basis of preliminary data, *Darmin r* and *Pod 1* were taken forward for functional studies.

Pod 1, a basic-helix-loop-helix transcription factor, was found to be expressed from pronephric initiation with enhanced expression in the pronephros. The expression patterns of *Pod 1* strongly matched that of the mouse homologue, implying a conserved evolutionary role. Pronephros targeted over-expression resulted in the reduction of glomus tissue, with no alteration in pronephric tubule or duct morphology. In addition, targeted knock-down resulted in the absence of cells in the glomus region.

Preliminary analysis of *Darmin r*, a cytosolic non-specific dipeptidase, indicated a role later in pronephric tubule development. Targeted over-expression experiments disrupted tubule morphology and reduced the size of the pronephric anlagen.

Initial promising data clearly placed *Pod 1* and *Darmin r* as important pronephric development genes.

Abbreviations

AP	alkaline phosphatase
APS	ammonium persulphate
ATP	adenosine triphosphate
bFGF	basic fibroblast growth factor
bHLH	basic helix-loop-helix
bp	base pairs
BSA	bovine serum albumin
cDNA	complementary deoxyribonucleic acid
Ci	Curie
C-terminal	carboxyl-terminal
dATP	deoxyadenosine triphosphate
dCTP	deoxycytidine triphosphate
dGTP	deoxyguanosine triphosphate
dH_2O	distilled water
DIG	digoxygenin
DNA	deoxyribonucleic acid
DNase	deoxyribonuclease
dNTPs	deoxyribonucleoside triphosphates
dpc	days postcoitum
E. coli	*Escherichia coli*
EDTA	ethylene diamine tetra acid
EST	expressed sequence tag
FGF	fibroblast growth factor
g	gram
GFP	green fluorescent protein
HCl	hydrochloric acid
H_2O	water
H_2O_2	hydrogen peroxide
l	litre
LBroth	Luria Broth
kb	kilobases
kDa	kilo Dalton
M	molar
MBT	mid-blastula transition
mg	milligram
ml	millilitre
mM	millimolar
MMLV	moloney murine leukaemia virus
MOPS	3-[N-morpholino]propane sulphonic acid
MO	morpholino oligonucleotide
mRNA	messenger ribonucleic acid
NaCl	sodium chloride

ng	nanogram
nl	nanolitre
nM	nanomolar
N-terminal	amino-terminal
PAGE	polyacrylamide gel electrophoresis
PBS	phosphate buffered saline
PBT	phosphate buffered tris
PBST	phosphate buffered tris
PCR	polymerase chain reaction
pM	picomolar
pmol	picomoles
PMSF	phenylmethylsulphonyl fluoride
PNI	Pronephric Index
RA	retinoic acid
RNA	ribonucleic acid
RNase	ribonuclease
rpm	revolutions per minute
RT-PCR	reverse transcription PCR
SDS	sodium dodecylsulphate
ssDNA	single stranded DNA
TBE	tris buffered EDTA
TBS	tris buffered saline
TdT	Terminal deoxynucleotidyl transferase
TEMED	N, N, N'-Tetramethylethylenediamine
Tris	tris (hydroxymethyl) aminomethane
Tris-Cl	tris (hydroxymethyl) aminomethane, pH adjusted with HCl
TUNEL	Tdt mediated dUTP Nick-End labelling
UTR	untranslated region
V	volts
v/v	volume/volume
w/v	weight/volume
U	units
µg	microgram
µl	microlitre
µM	micromolar

Chapter 1

Introduction

1.1 The pronephros; the simplest of the 3 kidney forms

Kidney organogenesis in vertebrates follows a succession of kidney structures, which are formed, degraded, and reformed with increasing structural complexity (Saxén, 1987). Induction of each successive kidney structure requires the previous temporal form for its own induction from the intermediate mesoderm (Brandli, 1999; Vize, *et al.*, 1997). The 3 kidney structures are the pronephros, mesonephros and metanephros (Fig. 1.1, reproduced from Vize, *et al.*, 1997). When functional, the kidney structures all have the same principle role of osmoregulation and waste disposal. This role is achieved by their basic functional unit, the nephron. The pronephros, comprising only one nephron, is the simplest and also the earliest in evolutionary terms. The mesonephros is next, consisting of 10-50 nephron-like structures and finally, the metanephros, with approximately 1 million nephrons is the most sophisticated. The final structural complexity of the kidney is correlated to the complexity of organism. In lower vertebrates, amphibia and fish, the progression is from the pronephros to the mesonephros only, where the mesonephros is the functioning kidney of the adult. In higher vertebrates, mammals and birds, all three kidney stages are created, with the metanephros being the functioning kidney of the adult and the pronephros being vestigial. This thesis will focus on the simplest kidney structure, the pronephros, and its development in *Xenopus laevis*.

1.1.1 *Xenopus* Pronephros: Overview of Structure and Function

The *Xenopus* pronephros, comprising one nephron, has 3 distinct structures; a glomus, the blood capillary network responsible for filtration of the blood; pronephric tubules, used for the selective reabsorption of water and nutrients from the filtrate; and the pronephric duct, which channels waste to the exterior.

The Glomus

The *Xenopus* pronephros is described as a non-integrated nephron, where the vascularised filtration unit, the glomus, is not directly integrated with the tubules.

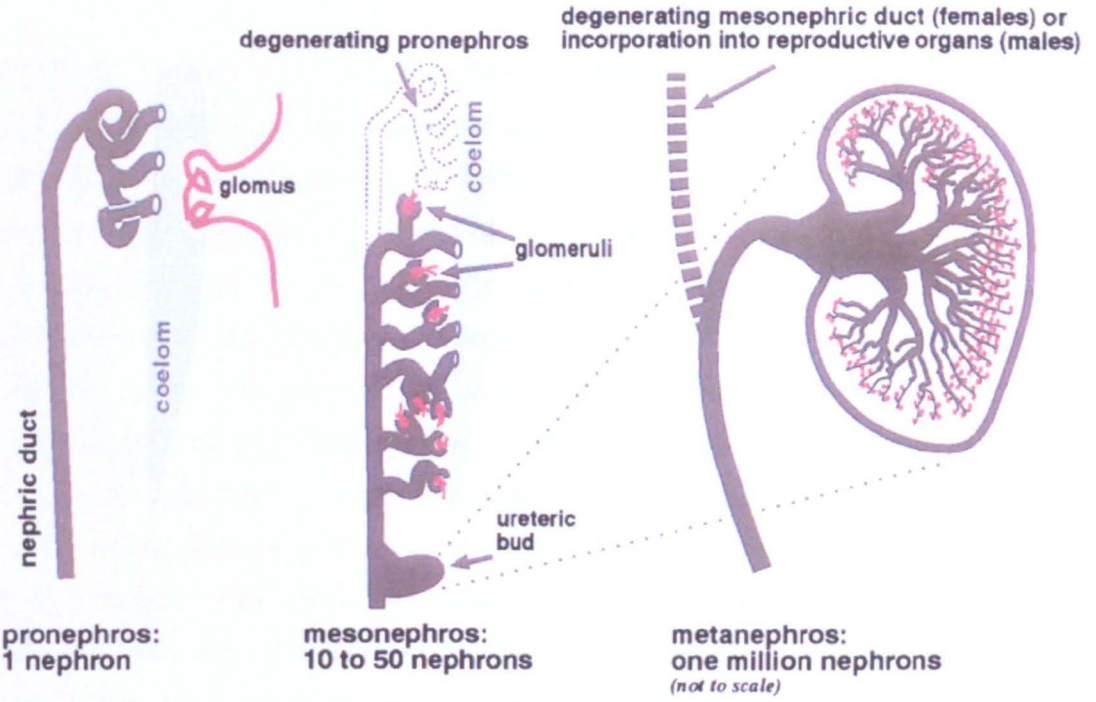

Fig. 1.1 **The pronephros, mesonephros and the metanephros**. Reproduced from Vize, *et al.*, 1997. The pronephros is the first kidney tissue to form in all vertebrates, consisting of one nephron. With a few exceptions, the nephron comprises a glomus/glomerulus, tubule, and duct. The pronephros is the simplest and also the earliest kidney in evolutionary terms. The pronephros is required for the induction of the mesonephros which consists of 10-50 nephron-like structures. Although not forming a fully functioning kidney in mammals, the mesonephros is an important source of hematopoietic stems cells, and in males some mesonephric tubules persist forming sperm carrying tubes. The metanephros is the final and most complex of the kidney structures and is the final kidney structure in higher vertebrates, comprising approximately one million nephrons.

Instead, the glomus and tubules are separated by the coelom and the nephrostomes (Fig. 1.2). Integrated nephrons can be found in the mesonephros and the metanephros.

The glomus is composed of a high pressured capillary network, derived from the dorsal aorta, which projects into the nephrocoel space within the pronephric capsule (Fig. 1.3). Filtration from the high pressured capillary network of the glomus through to the nephrocoel is both passive, through the slit diaphragms, and active, through the podocyte foot processes. The surface of the glomus vasculature 'bulb' is covered by podocytes with foot processed protruding into the basement membrane of the capillaries. The foot processes of metanephric kidneys have been found to have characteristics consistent with high levels of endocytosis (Mundel and Kriz, 1995). Between the podocytes are slit diaphragms which are the dominant size selection element during filtration (Abrahamson, 1986). The matrix of the glomus vasculature 'bulb' is high in podocalyxin and nephrin. Podocalyxin helps maintain foot process structure and function (Schnabel, *et al.*, 1989 and Horvat, *et al.*, 1986) and nephrin is a major component of slit diaphragms (Tryggvason, 1999).

The Pronephric Tubules

The pronephric tubules are joined to the nephrocoel through nephrostomes (Fig. 1.3). Nephrostomes are thin epithelial tubes lined with cilia along their length. The epithelial cells of the nephrostomes are distinct from the pronephric tubule cells by their lack of brush borders and convoluted membranes. The cilia draw fluid from the nephrocoel into the pronephric tubules by ciliary action. The pronephric tubules possess two morphologically distinct segments called the proximal tubules and the distal tubule. The proximal tubules are connected to the nephrostomes and are consistently arranged (Vize, *et al.*, 1997). The epithelial cells forming the proximal tubules have a dense mat of short microvilli on the apical surface (Møbjerg, *et al.*, 2000). This is known as the brush border and serves to increase cell surface area, enhancing water, salt and nutrient uptake. The lateral and basal membranes of the epithelial proximal tubule cells are convoluted and have gap junctions. This morphology may permit the regulation of ion gradients between the epithelial proximal tubules cells and the filtrate. The distal tubule connects the proximal tubules to the pronephric duct. The epithelial cells of the distal tubule do not have a brush border, but have extensive basal membrane convolutions. As with the brush border, these basal membrane convolutions may augment water, salt and

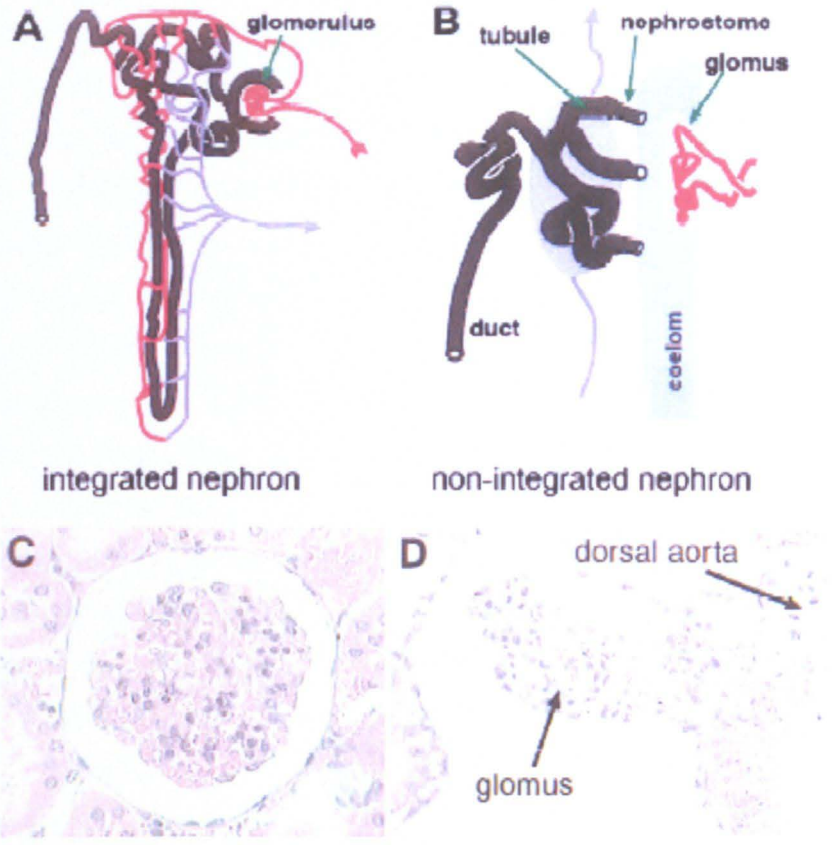

Fig. 1.2 **Integrated and non-integrated nephrons**. (**A**) Integrated nephron organisation. A blood vessel (**red**) enters the Bowman's capsule where wastes are filtered into the Bowman's space. The blood vessel then exits the capsule and surrounds the distal (near the capsule) and proximal tubules. Resorbed nutrients, salts, and water are then returned to the blood stream via the venous system (**purple**). (**B**) Organisation of a non-integrated nephron. Wastes filtered into the **coelom** are collected by tubules. Resorbed materials are returned to the bloodstream via blood sinus (**purple**) derived from the posterio cardinal vein that surrounds the tubules. (**C**) Mammalian glomerulus. (**D**) Amphibian glomus (reproduced from Vize, *et al.*, 1997).

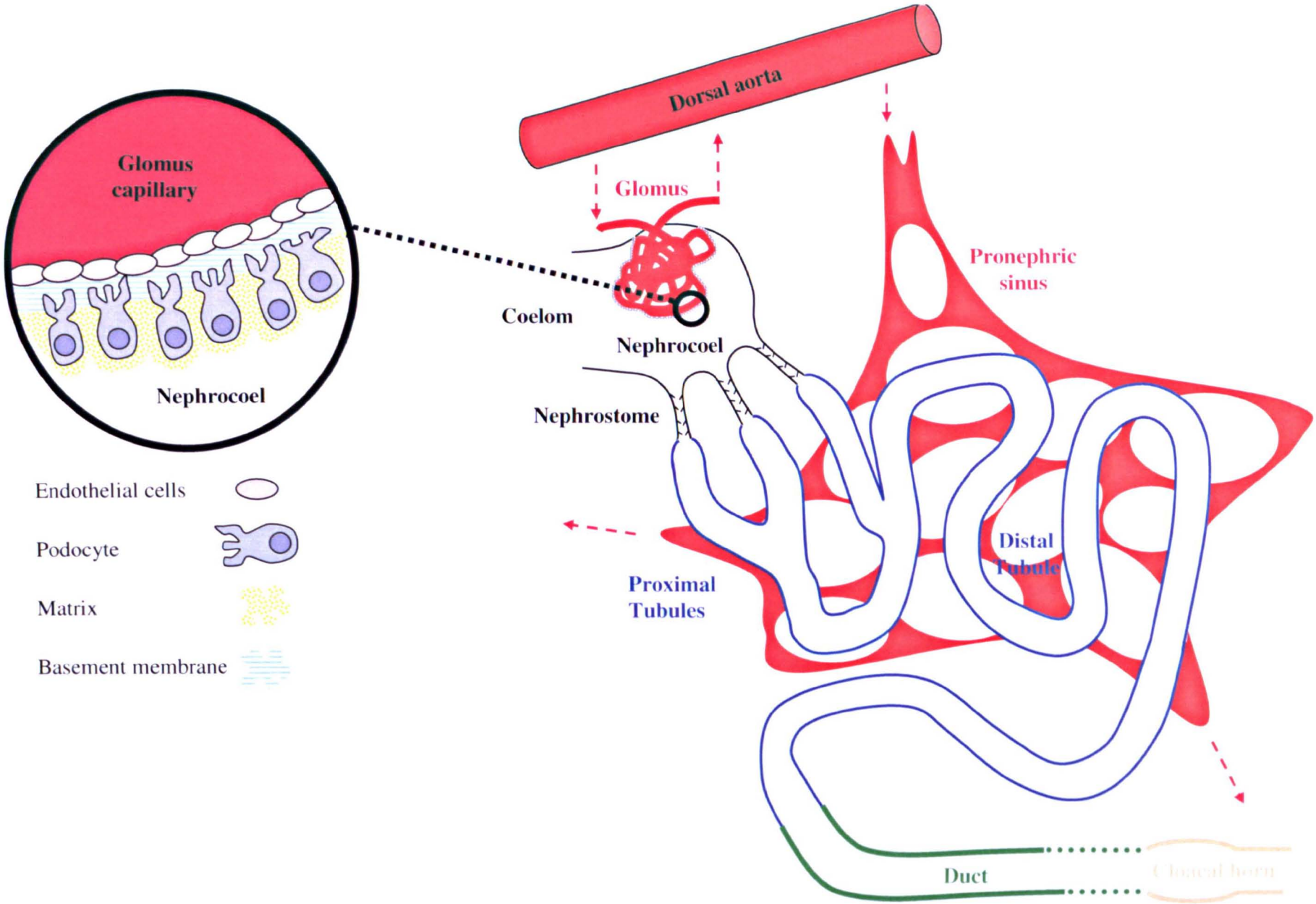
Glomus capillary
Nephrocoel
Endothelial cells
Podocyte
Matrix
Basement membrane
Dorsal aorta
Glomus
Coelom
Nephrocoel
Nephrostome
Pronephric sinus
Distal Tubule
Proximal Tubules
Duct
Cloacal horn

Fig. 1.3 **Structure of the Pronephros.** The glomus is a high pressured capillary network derived from the dorsal aorta. The glomus projects into the nephrocoel space within the pronephric capsule. It is covered by a 'bulb' within the nephrocoel space. This 'bulb' consists of podocytes, an extracellular matrix that contains podocalyxin and nephrin, basement membrane and endothelial cells of the glomus capillary. Filtration from the high pressured capillary network of the glomus through to the nephrocoel is both passive, through the slit diaphragms, and active, through the podocyte foot processes. Once within the nephrocoel, the filtrate is drawn through to the proximal tubules through ciliary action by the nephrostomes. The epithelial cells of the proximal tubules are lined with a brush border which serves to increase cell surface area, enhancing water, salt and nutrient uptake. The proximal tubules are connected to the distal tubules which have extensive basal membrane convolutions, also designed to augment water, salt and nutrient uptake. The pronephric tubules are surrounded by a capillary bed called the blood sinus. The blood sinus returns the reabsorbed water, salt and nutrients, to the blood stream. The resulting filtrate after filtration through the glomus and reabsorbtion through the pronephric tubules is channelled out of the organism though the pronephric duct and cloaca.

nutrient uptake. The pronephric tubules are surrounded by a capillary bed called the blood sinus. The blood sinus returns the reabsorbed water, salt and nutrients, to the blood stream (Brandli, 1999).

The Duct

The epithelial cells of the pronephric duct resemble those of the distal tubule, but have a smooth basal membrane (Møbjerg, *et al.*, 2000). The pronephric duct is fused with a cloacal horn, which extends the structure to the cloaca (Fig. 1.3). The resulting waste after the filtration through the glomus and reabsorbtion through the pronephric tubules is channelled out of the organism though the pronephric duct and cloaca.

1.1.2 *Xenopus* Pronephric Development

The pronephros is derived from the intermediate mesoderm, located between the somites and the lateral plate. The developing pronephros is therefore exposed to signals from the somites, lateral plate and ectoderm. However, the complete picture of the molecular control of pronephros formation is still unclear, although, certain factors have been identified to play a role. The genes actively involved in pronephric development have been reviewed, although this does not include genes expressed by terminally differentiated tissues.

1.1.2.1 The Pronephric anlagen

Morphological development of the pronephric anlagen

Analysis of presumptive pronephric tissues cultured in animal caps revealed the specification of the *Xenopus* pronephros to be between stages 12.5-14 (Brennan, *et al.*, 1998 and Brennan, *et al.*, 1999). However, the first physical sign of pronephric development is not until stage 21, where a slight thickening (condensation) of the somatic lateral mesoderm is observed below somites 3 to 5 (Nieuwkoop and Faber, 1994). This structure will form the body of the pronephros (Fig. 1.4). A second thickening (condensation) of the somatic lateral mesoderm forms below somites 5 to 7 and will give rise to the pronephric duct. The condensation is caused by alterations in cell shape, making the cells elongate along the anterior-posterior axis. The primordia of these two structures fuse at stage 24 and are known as the pronephric anlagen or the

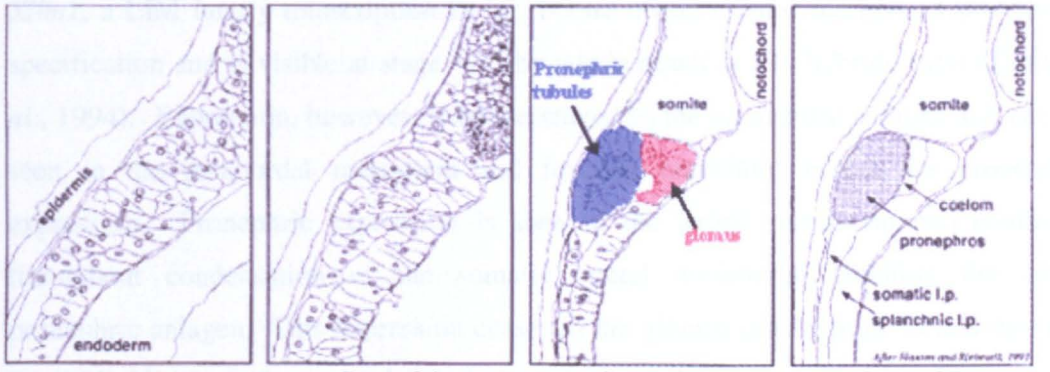

Stage 21 Stage 24 Stage 27 Stage 27

Fig. 1.4 **Segregation of the *Xenopus* pronephric anlagen from the intermediate mesoderm.** At stage 21 slight thickning of the somatic portion o f the lateral mesoderm is caused by pronephric precursor cells becoming more columnar. By stage 24 this forms a compact aggregate, referred to as the pronephric swelling. At stage 27 the pronephric anlage is a distinct mass, lying distal to the lateral plate. The tubule, duct and glomus anlagen can be distinguished at this stage. Cells are arranged radially, which leads to a tiny lumen forming at stage 28. (l.p. lateral plate) (adapted from Vize, *et al.*, 1997).

pronephric swelling. Cells from the pronephric anlagen then become radial and gradually form a lumen at stages 27 through to 32 (Vize, *et al.*, 1997).

Gene expression and regulation in the pronephric anlagen

Xlim1, a LIM family transcription factor, is one of the earliest markers of pronephric specification and is visible at stage 12.5 by wholemount *in situ* hybridisation (Taira, *et al.*, 1994). Expression, however, is not restricted to the pronephric anlagen and can be seen in the prechordal mesoderm and forming notochord before the pronephric expression. Pronephric expression is seen in the lateral mesoderm and continues throughout condensation of the somatic lateral mesoderm, labelling the entire pronephric anlagen. This expression ceases in the glomus primordium around the time that it divides from the pronephric tubule and duct primordium. *Xlim1* expression then continues in the pronephric tubule and duct primordium until late tail bud stages. This loss of expression is concurrent with the initiation of *xWT1*, *Wilms' Tumour 1*, expression in the extreme anterior of the pronephric anlagen, which may indicate an exclusion of *Xlim1* expression by *xWT1* (Carroll, *et al.*, 1999). Indeed, targeted *xWT1* over-expression reduces *Xlim1* expression in the pronephric anlagen (Wallingford, *et al.*, 1998). However, this exclusion is not complete and a small proportion of cells in the extreme anterior of the pronephric tubule and duct primordium do express both transcription factors.

Targeted injection of an inactivated mutant of *Xlim1* does not only result in the loss of the pronephros, but also the anterior somites (Chan, *et al.*, 2000). It is suggested that somites, muscle precursors, appear to have a crucial role in pronephric specification, possibly in supplying inducing factors. Pronephric structures are lost when embryos are extremely UV-ventralised or lithium-dorsalized, removing the anterior somites (Seufert, *et al.*, 1999). To investigate this phenomenon, half of a UV-ventralised blastula and a quarter of a lithium-dorsalized blastula were combined and incubated. The resulting tissue gave pronephric structures in the UV-ventralised tissue, indicating that pronephric inducing signals came from the lithium-dorsalized tissue. Other evidence came from animal cap sandwiches containing lateral mesoderm, somite tissue, notochord tissue and neural tissue alone and in combinations. Only those sandwiches containing lateral mesoderm and somite tissue in combination were able to produce pronephric structures (Tételin and Jones, unpublished).

xPax 8, paired box transcription factor, is another early marker of pronephric specification, and like *Xlim1*, is observed by wholemount *in situ* hybridisation during late gastula (Carroll and Vize, 1999). The expression pattern of *xPax 8* in the developing gastula, differs from that of *Xlim1*. *xPax 8* expression appears more diffuse over the lateral mesoderm and initially, is only expressed in the presumptive glomus and pronephric tubule tissues. Later, between stages 20 to 25, the elongating neurula, *Xlim1* and *xPax 8* expression co-localise to the pronephric anlagen. Over-expression of either *Xlim1* or *xPax 8* in *Xenopus laevis* leads to an enlargement of the pronephros or ectopic pronephroi, indicated by antibody staining for the pronephric tubules. Furthermore, co-injection of the transcription factors has a synergistic effect on this phenotype (Carroll and Vize, 1999). Retinoic acid and activin treatment of dissected animal caps can produce pronephric tissues (Reviewed Chapter in 3). Interestingly, this treatment of dissected animal caps also induces expression of *Xlim1* and *xPax 8* (Heller and Brandli, 1999 and Chan, *et al.*, 2000). In fact, *Xlim1* expression was found to be required for the induction of pronephric tissues in treated animal caps. These data suggests that *Xlim1* and *xPax 8* are involved in pronephric specification and patterning, possibly in collaboration, although, observation of their early expression patterns suggest that they may be regulated by different mechanisms.

Xldb-1, a LIM domain binding protein, has been shown to bind to *Xlim1* and synergize with it to activate the Spemann organizer and neural markers when co-injected (Breen, *et al.*, 1998). Expression is observed in the pronephros and central nervous system in the elongating neurala, stages 23 to 28 (Chan, *et al.*, 2000). However, there is no evidence of their co-activity in the pronephros.

In *Xenopus*, two homologs of the cold-inducible RNA binding protein have been identified, *XCIRP* and *XCIRP-1* (Uochi and Asashima, 1998 and Peng, *et al.*, 2000). *XCIRP* is expressed in the pronephric anlagen at stage 28 through to stage 35 (Uochi and Asashima, 1998). The other homolog, *XCIRP-1*, differs from *XCIRP* by four additional amino acids at the C terminus and has been shown to have a role in kidney morphogenesis (Peng, *et al.*, 2000). Targeting full length *XCIRP-1* antisense mRNA to the C3 blastomere changed the morphogenetic lineage migration of C3 blastomeres and led to defects in the pronephric anlagen at stage 22. *XCIRP-1*, an RNA binding factor, was also found to be required for the induction of pronephric tissues in retinoic acid and

activin treated animal caps. The role of XCIRP-1 is proposed to be required for marking genes or gene transcripts for future activation, where it might change the conformation of the DNA or RNA to establish competence for differentiation programs.

Xwnt-4 and *xPax 2*, another paired box transcription factor, have similar expression patterns to *Xlim1*, although they are observed later in the elongating neurula (Heller and Brandli, 1997 and Carroll, *et al.*, 1999). *Xlim1*, *Xwnt-4* and *xPax 2* expression in the developing pronephric anlagen is entirely co-localised, even as expression is restricted to the pronephric tubule and duct primordium, with a slight over-lap with *xWT1*. The co-expression of *Xlim1*, *Xwnt-4* and *xPax 2* with *xWT1* in the extreme anterior portion of the pronephric tubule and duct primordium is transient and by stage 30, *xWT1* expression is exclusive to the glomus primordium.

NDRG1, *N-myc downstream-regulated gene 1*, expression is initiated between stages 12 and 15 and is observed in the pronephric anlagen at stage 26 by wholemount *in situ* hybridisation (Kyuno, *et al.*, 2003). Over-expression of *NDRG1* resulted in a reduction and disorganisation of pronephric structures and somites. Morpholino oligonucleotide knock-down of *NDRG1* caused a complete oblation of pronephric structures. *NDRG1* is therefore involved in pronephric development, possibly, pronephric anlagen specification events due to the timing of pronephric expression and mis-expression effects on the whole pronephros.

Bone morphogenetic proteins, BMP, are secreted TGF-β superfamily members and have been implicated in a diverse range of biological processes. BMP inhibitors are associated with axis patterning and are believed to be one of the dorsalising factors diffused from the organizer of the blastula (Dale and Wardle, 1999). *BMP4* is expressed in the lateral mesoderm and in the pronephros, although detailed analysis of pronephric expression has not been published (Fainsod, *et al.*, 1994). *BMP4* acts as a morphogen in the specification of ventral tissues, such as blood and epidermis with high concentrations and lateral tissues, such as pronephros and muscle with lower concentrations, in a gradient across the embryo (Dale, *et al.*, 1992 and Dale, 2000). *BMP7* is also expressed widely in the entire marginal zone of early *Xenopus* embryos, including in the mesoderm fated to form the pronephros (Hawley, *et al.*, 1995).

Xwnt-11, expressed in pronephric tubules at stage 28 (Ku and Melton, 1993), has been suggested to provide an important signal during the earliest stages of pronephric development, from preliminary experiments from our laboratory (Tételin and Jones, unpublished).

Notch-1, *Serrate-1*, and *Delta-1* are believed to be involved in a feedback loop within the pronephric anlagen that controls the division of glomus, tubule and duct primordia (McLaughlin, *et al.*, 2000). *Notch-1* and *Delta-1* expression is visible at stage 21/22 in the anterior region of the pronephric anlagen. *Serrate-1* expression is observed in a similar area, a stage later at 23/24. From this similar origin of expression the expression patterns dynamically change, so that at stage 30, *Notch-1* is expressed in the duct, *Serrate-1* is expressed in the pronephric tubules, and *Delta-1* is expressed in the glomus to pronephric tubule border. The role of *Notch-1* in pronephric development was investigated using targeted injection of activated or dominant negative forms of the transcription factor *Su(H)* to mimic or inhibit Notch signaling. Activation of Notch signaling inhibited *Delta-1* and enhanced *Serrate-1* expression and inhibition of Notch signaling inhibited *Serrate-1* and enhanced *Delta-1* expression at stage 30. Surprisingly, activation of Notch leads to an enlargement in tubule and glomus structures and a reduction of duct structures. In addition, inhibition of Notch signaling enhanced duct formation. In fact, activation of Notch promoted *Xlim1* expression in the anterior pronephric anlagen, the area of the presumptive glomus and pronephric tubules, and completely reduced expression in the presumptive duct region at stage 30. *Notch-1* signaling is therefore believed to partition the fates of the pronephric anlagen by a feedback loop with *Delta-1* and *Serrate-1*.

There are three members of the Hepatocyte Nuclear Factor (HNF) transcription factor family that are expressed in the *Xenopus* pronephros, *HNF-1α*, *HNF-1β* and *HNF-4*. *HNF-1β* transcripts are detected in the somatic layer of the intermediate mesoderm at stage 15 and in the pronephric anlage at stage 23, where it is expressed in both the tubules and duct later in development (Demartis, *et al.*, 1994). *HNF1-α* and *HNF-4* are expressed from stage 20 onwards and later in development are detected in the pronephric tubules (Holewa, *et al.*, 1996, Weber, *et al.*, 1996a and Weber, *et al.*, 1996b). It has been proposed that *HNF-4* is at the top of a transcriptional cascade that

leads to the activation of *HNF-1α* via an activin A response element in the promoter to establish tissue-specific gene expression (Weber, *et al.*, 1996a). Expression of a human gain-of-function *HNF-1β* mutant in *Xenopus*, leads to defective development and agenesis of the pronephros. This phenotype is similar to *HNF-1β* mRNA over-expression and demonstrates a conserved role in renal development (Wild, *et al.*, 2000).

1.1.2.2 The Glomus anlagen and development of the nephrocoel

Morphological development of the glomus and nephrocoel

The capillary network of the glomus is derived from the dorsal aorta and is visible at stage 29-30 (Nieuwkoop and Faber, 1994). Although the blood supply to the glomus does not commence until stage 35/36. The nephrocoel and the glomus 'bulb' are formed from the pronephric anlagen containing condensing intermediate mesoderm. During the early tail bud stages, the nephrocoel and the glomus 'bulb' primordium segregate from the pronephric anlagen (Jones, 2005). The area of intermediate mesoderm (within the nephrocoel and the glomus 'bulb' primordium) lying adjacent to the developing glomus capillary network forms a visceral epidermal layer which protrudes into the nephrocoel and forms the glomus 'bulb' (Nieuwkoop and Faber, 1994). The area not lying adjacent to the glomus capillary network is the parietal epidermal layer which forms the lining of the nephrocoel.

Gene expression and regulation in the glomus and nephrocoel

WT1, a zinc-finger transcription factor, is the earliest glomus-specific gene expression in the pronephric anlagen (described in 1.1.2.1 Gene expression and regulation in the pronephric anlagen, Carroll, *et al.*, 1999). Expression is observed in the lining of the nephrocoel and glomus of late tail bud stage embryos and at stage 38 is also detected in the heart (Carroll and Vize, 1996 and Semba, *et al.*, 1996). *xWT1* over-expression disrupts glomus formation and inhibits pronephric tubule development (Wallingford, *et al.*, 1998). It is hypothesised that the function of *xWT1* may be to reserve the fate of pronephric competent cells for the formation of the glomus, possibly by preventing *xPax 2*, *Xlim1* or *xWnt-4* expression, and thus tubule specification, in the glomus primordium. This could account for the difference in timing between initiation of *xWT1* expression and glomus differentiation and the exclusion of the pronephric tubule

development genes from the glomus primordium shortly after the onset of *xWT1* expression.

The other early glomus marker is the LIM domain binding protein xlmx1b, which is expressed from stage 10.5 in neural and presumptive pronephric regions (Haldin, *et al.*, 2003). It is expressed in the glomus primordium at stage 27 and expression continues throughout development. *Xlmx1b* morpholino oligonucleotide knock-down reduces the size of the glomus and disrupts tubule morphology (Haldin and Jones, unpublished). Like *xWT1*, *xlmx1b* has been implicated in early glomus specification, although has yet been shown to inhibit the expression of pronephric tubule development genes.

Nephrin is a trans-membrane protein, expressed in the developing podocytes in the glomus from stage 25 (Gerth, *et al.*, 2005). A component of slit diaphragms, nephrin has been used to study the 3 dimensional structure of the glomus.

VEGF, Vascular Endothelial Growth Factor, and its tyrosine kinase receptor, *flk-1* expression are observed in juxtaposed tissues through-out the *Xenopus* vasculature (Cleaver, *et al.*, 1997). Expression of *VEGF* is seen in the glomus from stage 32. Over-expression analysis reveals an alteration in the vasculature morphogenesis. Ectopic expression in embryos revealed VEGF acts as a chemoattractant for angioblasts, indicating a role in vertebrate vascular development (Cleaver and Krieg, 1998).

1.1.2.3 The Pronephric Tubules

The positioning of the 3 nephrostomes is indicated by the formation of 3 protuberances in the dorsal region of the pronephric anlagen at stage 28 (Fig. 1.5). This is after the segregation of the nephrocoel and the glomus 'bulb' primordium from the pronephric anlagen, leaving the pronephric tubule and duct primordium (Jones, 2005). The nephrostomes are formed before the pronephric tubules and are structurally complete at stage 33 (Nieuwkoop and Faber, 1994). The pronephric tubules begin to form a lumen at stage 30. The first anterior branch of the proximal tubules is formed joined to the two anterior nephrostomes (Fig. 1.5). The final second branch of the proximal tubules is formed joined the more dorsal nephrostome and links the distal tubule. The proximal tubule ultimately joins the pronephric duct. At stage 34, this arrangement is clearly

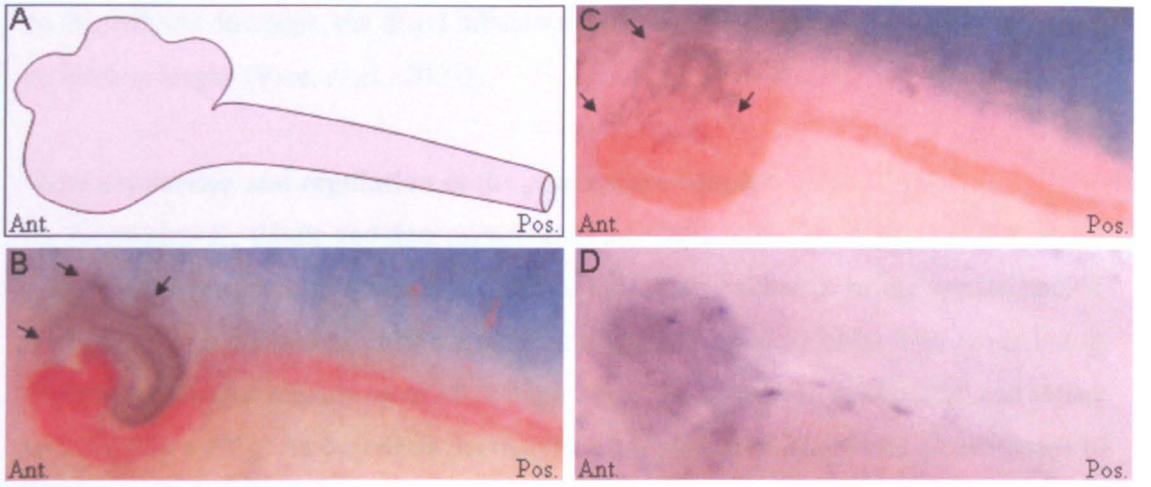

Fig. 1.5 **Formation of the pronephric tubules in *Xenopus* as observed by immunohistochemistry using the tubule specific monoclonal antibody 3G8 and *Darmin r* wholemount *in situ* hybridisation**. (**A**) Cartoon depiction of the pronephric tubule and duct primordium at stage 30 (adapted from Vize, *et al.*, 2003). The 3 protuberances in the dorsal region of the primordium indicate position of developing nephrostomes. (**B**) Wholemount 3G8 and 4A6 antibody staining in a stage 34 embryos. 3G8 staining is observed in the pronephric tubules in purple and 4A6 staining in the pronephric duct in red. At this stage the three nephrostomes can be clearly identified. (**C**) Tubules at stage 36 are more coiled although nephrostomes are still distinguishable. (**D**) Tubules become extended and tightly coiled by stage 42 as indicated by wholemount *in situ* hybridisation using *Darmin r* DIG-labelled antisense RNA probe (Chapter 5).

visible by 3G8 (pronephric tubules) and 4A6 (pronephric duct) immunohistchemistry. As the tadpole develops, the distal tubule extends and coils, forming a convoluted mass by feeding stages (Vize, *et al.*, 2003).

Gene expression and regulation in the pronephric tubules

As the pronephric tubule and duct primordium develops, *Xlim1* pronephric expression is dramatically restricted to the tubules, before becoming exclusive to the nephrostomes, the regions of increased extension and growth (Carroll, *et al.*, 1999). This is similar to the later expression patterning of *xPax 2* but not *xPax 8* (Carroll, *et al.*, 1999 and Heller and Brandli, 1997). As described previously, co-injection of *Xlim1* and *xPax 8* leads to an enlargement of the pronephros or ectopic pronephroi, indicated by antibody staining for the pronephric tubules (Carroll and Vize, 1999). Interestingly, *xPax 2* can also form an enlargement of the pronephros or ectopic pronephroi when co-injected with *Xlim1*. Comparison of *xPax 2* and *xPax 8* with *Xlim1* expression patterns during pronephric tubule morphogenesis shows a much closer relationship of *Xlim1* with *xPax 2*. It has been suggested, therefore, that *xPax 8* is involved with early pronephric patterning events, and *xPax 2* is involved with later pronephric tubule patterning events.

In the developing pronephric tubule and duct primordium, *XWnt-4*, *Xlim1* and *xPax 2* expression coincides with the anterior-dorsal most region of *WT1* expression (Carroll and Vize, 1999). It is not clear whether this environment contributes to the formation of the nephrostomes, or is a result of unspecified cells yet to be determined as glomus or tubule tissue. In zebrafish, nephrostomes are formed transiently, and are derived from the coelom before the tubules develop (Drummond, *et al.*, 1998). In *Xenopus*, however, the nephrostomes are formed from the tubule primordium, but are again formed before tubule morphogenesis (Jones, 2005).

As previously mentioned, *Xwnt-4* is expressed initially in the whole pronephric anlagen and then focuses to the tubules before terminal differentiation. At stage 32, *Xwnt-4* is detected in the nephrostomes (Saulnier, *et al.*, 2002). Embryos injected with Xwnt-4 morpholino oligonucleotide fail to develop tubules, whilst *Xwnt-4* mRNA over-expression appears to perturb morphogenesis of the pronephric tubules with the nephrostomes often fused to form a single structure.

XTRAP-γ is one of four subunits that make up the translocon-associated protein complex which is involved in intracellular protein transport (Li, *et al.*, 2005). Expression was observed in the pronephros from stage 25 in the pronephric tubules. Morpholino oligonucleotide knock-down of *XTRAP-γ* disrupted the pronephric tubule formation and expression of *xPax 2* and *xWnt-4* at stage 30. Conversely for a pronephric tubule promoting gene, *Xlim1* pronephric expression increased in targeted *XTRAP-γ* knock-down embryos. *XTRAP-γ* expression was also found to be required for the induction of pronephric tissues in treated animal caps, which suggests an earlier role in pronephric induction.

Annexin IV is expressed in the pronephric primordium from stage 26 and later on the luminal surface of the pronephric tubules (Seville, *et al.*, 2002). Over-expression experiments resulted in a disruption of *WT1* expression in the glomus, although no effect on *Xlim1* or *xPax 8* expression was observed. Morpholino oligonucleotide knock-down analysis gave a single shortened, enlarged tubule, rather than the branching tubules seen in control embryos.

PKD1 forms part of an ion channel complex with *PKD2* and has been implicated in the activation of intracellular signalling pathways (Burtley, *et al.*, 2005). Expression is observed by dissected pronephric RT-PCR from pronephric initiation, stage 14, and continues until stage 40, the last stage tested. *xPKD1* expression is induced by the treatment of animal caps with retinoic acid and activin to produce pronephric tubules. Inactivation of *xPKD1* ion channel properties by blocking calcium flux where *xPKD1* is expressed, suppresses tubulogenesis.

1.1.2.4 The Duct

The posterior region of the pronephric tubule and duct primordium forms the majority of duct tissue. The pronephric tubule and duct primordium extends posteriorly, forming a lumen at stages 33 to 34. The progressing duct structure fuses with the cloacal horns at stage 37. The cloacal horn originates as a small slit in the cloacal wall at stage 32, which extends anteriorly from the cloaca (Vize, *et al.*, 2003). During metamorphosis, the pronephros degenerates and the mesonephros is formed. The pronephric duct

induces the surrounding mesonephric mesenchyme to form the mesonephros, before gradually regressing to form part of the genital system in males.

Gene expression and regulation in the pronephric duct

A detailed previously, *Xlim1* pronephric expression is initiated at stage 12.5 continues to late tail bud stages (Carroll, *et al.*, 1999). Later expression includes a reducing expression in the anterior duct which is maintained in the portion extending towards the cloacal horns, although not in the cloacal horns themselves. Interestingly, similar to the expression in the pronephric tubules, this is also a region of extension and growth. This expression pattern differs from *xPax 2* in the pronephric duct, which has been comparable in the other pronephric tissues. *xPax 2* expression is ubiquitous over the pronephric duct and includes the cloacal horns.

*X*fz8 is detected in the pronephric anlagen at stage 22 and becomes restricted to the pronephric duct by stage 28. Depletion of Xfz8 results in reduced pronephric tubule branching and a reduction in 4A6 duct staining. *Xfz8* is hypothesised to be involved in epithelium formation in the developing pronephric tubule and duct after specification (Satow, *et al.*, 2004).

At stage 27, *gremlin*, a BMP antagonist, is expressed anteriorly in the early developing duct and proceeds posteriorly as the duct develops (Hsu, *et al.*, 1998). *Xenopus c-ret* has been detected at stage 28 in the caudal tip of the migrating duct primordium and in the tubules (Carroll, *et al.*, 1999).

1.2 Developmental Congenital Kidney Disease

Investigating the development of the pronephros in *Xenopus laevis* can lead to advances in the understanding of vertebrate kidney development and so may impact human developmental congenital kidney disease. The sequential nature of kidney development suggests that there may be a degree of repetition and similarity in the induction of the three kidney structures. Indeed, some critical kidney development genes have been shown to have similar roles in human metanephric and *Xenopus* pronephric development (discussed below). Furthermore, the successive kidney structures develop in a precise spatial and temporal pattern, each requiring the formation of the previous

form for its own induction (Brandli, 1999 and Vize, *et al.*, 1997). Structural defects in the development of the earlier structures may therefore effect the formation of later kidney structures.

Xenopus laevis was the model organism used in this study. The pronephros in *Xenopus* forms just below the epidermal surface, allowing for effortless accessibility. In addition, the morphological development of the pronephros in *Xenopus* has been well documented. *Xenopus*, itself is an ideal organism to use due to its external development, large egg and embryo sizes, ease of embryo culture and adult husbandry. The external development and detailed fate mapping of early division allows for targeted micro-injection of mRNA in over-expression experiments, or morpholino oligonucleotides in knock down experiments. The other common model organism to use in kidney development research is the mouse. However, the metanephric kidneys of the mice are complex and their internal development means embryo manipulation is more difficult. Also the knock-out phenotypes of many kidney development genes are embryo lethal, restricting developmental analysis.

To impress the importance of studying kidney development, four important human and *Xenopus* development genes will be highlighted. *WT1*, *Pax 2*, *Nephrin* and *PKD1* have been previously shown to have critical roles in pronephric development (1.1.2 *Xenopus* Pronephric Development). The roles of these genes in human developmental congenital kidney diseases will now be discussed.

1.2.1 *Wilms' Tumour 1*

Wilms' tumour is a cancer of the kidney that affects 1 in 10,000 children (Discenza and Pelletier, 2004). It is believed to arise when the developing metanephric mesenchyme fails to properly differentiate, forming nephrogenic rests. These rests degenerate, remain dormant, or in the case of Wilms' tumour, proliferate. Human *WT1*, a four zinc-fingered transcription factor, was identified from positional cloning identifying genes on the Wilms' tumor locus human chromosome 11 (p13) (Call, *et al.*, 1990 and Gressler, *et al.*, 1990). However, *WT1* mutations were only found in 10-15% of Wilms' tumours (Gressler, *et al.*, 1994 and Varanasi, *et al.*, 1994), although, *WT1* mutations have been found in nephrogenic rests (Discenza and Pelletier, 2004).

The earliest observation of human *WT1* expression in the kidney is in the developing podocytes of the mesonephros and the metanephros, the condensing metanephric mesenchyme and the tip of the ureteric bud (Discenza and Pelletier, 2004). Expression is also observed in the sex cord region of the urogenital ridge, spleen, epicardium and other epithelial tissues.

Denys-Drash syndrome

WT1 mutations were found at a higher incidence, 90%, with Denys-Drash Syndrome sufferers (Little and Wells, 1997). Denys-Drash syndrome is associated with nephropathy due to diffuse mesangial sclerosis and intersex (Denys, *et al.*, 1967 and Drash, *et al.*, 1970). Denys-Drash syndrome kidneys typically show glomerular lesions, enlarged immature podocytes, thickening of glomerular membranes, reduced capillary lumens and severely damaged tubules. Hypertension is often a symptom, as fibrotic material is produced in the cells lying adjacent to the glomerular, causing the collapse of the arteries (Scharnhorst, *et al.*, 2001). Patients also suffer from a high incidence of Wilms' Tumours (Little and Wells, 1997). 8 out of 10 unrelated Denys-Drash syndrome patients were found to be heterozygous for point mutations in exon 9 of *WT1* (Pelletier, *et al.*, 1991). These point mutations are believed to alter the structure of the third zinc-finger and so hinder the binding of WT1 to the target DNA binding site (Pelletier, *et al.*, 1991, Little, *et al.*, 1993 and Scharnhorst, *et al.*, 2001). Indeed, WT1 DNA binding has been shown to be interrupted *in vitro* by point mutations in exon 9 of the *WT1* gene. Chimeric and heterozygous mice for a mutation that truncates the third zinc finger, coded by exon 9, have been created. Interestingly, the phenotypes observed in the mutant mice were similar to those of Denys-Drash syndrome patients (Patek, *et al.*, 1999). Also co-incident with the human syndrome, >75% of Denys-Drash syndrome mutant mice developed Wilms' Tumours, further implying a link.

WT1 has been shown to repress the *Pax 2* promoter and inhibit its expression (Ryan, *et al.*, 1995). In fact, *Pax 2* down regulation was found to be required for podocyte maturation, (Quaggin, 2002). Unsurprisingly, abnormal *Pax 2* podocyte expression is observed in patients with Denys-Drash syndrome (Yang, *et al.*, 1999). However, it is unclear whether *Pax 2* expression is a cause, or an effect of Denys-Drash syndrome.

Frasier's syndrome

Related to Denys-Drash syndrome, but less severe, Frasier's syndrome was also found to be associated with *WT1* mutations (Barbaux, *et al.*, 1997). Like Denys-Drash syndrome, Frasier's syndrome is characterized by intersex and nephropathy, although, no Wilms' tumours have been detected. The nephropathy, however, is due to focal segmental glomerulosclerosis, where kidneys have fused podocyte foot processes and scar tissue in the glomerulus. The condition is termed focal, as not all nephrons are affected, and segmental due to the localised effect on the filtration barrier of the glomerulus. Frasier's syndrome patients are missing one of the alternatively spliced WT1 isoforms, known as the +KTS isoform (Barbaux, *et al.*, 1997). This loss is caused by mutations in the donor splice site in intron 9 of *WT1*, loosing the addition of three amino acids (KTS) between WT1 zinc-fingers 3 and 4. The 3 additional amino acids are believed to be involved with subnuclear localisation of the WT1 protein (Scharnhorst, *et al.*, 2001).

WAGR syndrome (Wilms' tumour, Aniridia, Genitourinary defects and Mental Retardation)

WAGR syndrome is characterized by development of Wilms' tumours, iris abnormalities (Aniridia), genital defects and mental retardation. WAGR syndrome has been linked with the deletion of part of the short arm of chromosome 11, the region of the *WT1* and *Pax 6* genes (Riccardi, *et al.*, 1978). The reduction of *WT1* expression, due to gene deletion, has been implicated in the unexpected or late-occurring renal failure in some WAGR syndrome patients (Breslow, *et al.*, 2000). The condition of Aniridia has been linked to the deletion of *Pax 6* (Discenza and Pelletier, 2004).

The null *WT1* mouse does not produce any kidney structures, and heterozygous null *WT1* mice have a normal kidney phenotype at birth (Kreidberg, *et al.*, 1993). However, glomerular sclerosis (scar tissue growth in the glomerulus) and albuminuria (thickening of the glomerular basement membrane and fusion of the podocyte foot processes) develops later in heterozygous null *WT1* adult mice (Menke, *et al.*, 2003). This late onset is also associated with loss of *WT1* and *nephrin* expression in the kidneys. Interestingly, the reduced expression of *WT1* appears to have a less severe effect on the kidney than the point mutations described with Denys-Drash syndrome.

WT1 and other vertebrates

Analysis of *WT1* expression in developing quail chick embryos revealed similar expression observed in mouse kidneys, that the mesonephric glomerulus and duct (ureteric bud) and the condensing metanephric mesenchyme (Carmona, *et al.*, 2001). Although no mis-expression experiments have yet been performed, quail expression patterns suggest a link with *Slug*, which is also expressed in podocytes and is involved in their mesenchymal-epithelial transition (Carmona, *et al.*, 2001 and Davidson, *et al.*, 2002).

The null *WT1* mouse lacks kidneys, gonads and adrenal glands (Kreidberg, *et al.*, 1993). Morpholino oligonucleotide knock-down experiments in zebrafish have shown similar phenotypes, with disrupted pronephric and interrenal (adrenal gland) organogenesis. *Ff1b* is a functional homologue of *SF1*, which is a sex determining gene in mammals. *WT1* knock-down in zebrafish was also found to reduce *ff1b* expression, also effecting gonad development (Hsu, *et al.*, 2003).

1.2.2 *Paired box 2*

Pax 2 is part of the paired box transcription factor family. The highly conserved paired box encodes a bipartite helix-loop-helix DNA-binding domain that enables *Pax 2* to bind directly to gene promoters (Sanyanusin, *et al.*, 1996). *Pax 2* is positioned at the boundary band of q24 and q25 of chromosome 10 (Gough, *et al.*, 2003). Comparable with mouse expression, *Pax 2* is believed to be expressed in the pronephric tubule, duct and mesonephric tubules of early human developing kidneys (Eccles, 2002). During induction of the metanephros, expression is observed in the epithelium of the branching ureteric bud and in the condensing mesenchyme. Later expression is observed in the differentiating renal vesicle and the developing nephron, and excluded from the glomerulus. Interestingly, in adulthood, expression has also been observed in regenerating proximal tubule cells following treatment with nephrotoxins. This indicates that *Pax 2* may also be involved in regenerative processes (Eccles, 1998). Other areas of mouse expression include the central nervous system, eye and ear (Favor, *et al.*, 1996).

Papillorenal syndrome / Renal-coloboma syndrome

Papillorenal syndrome is generally associated with a reduced kidney, resulting from reduced ureteric bud branching and a reduced number of nephrons. Other symptoms include vesicoureteral reflux, optic nerve and disc defects, and a high-frequency of hearing loss. Papillorenal syndrome is caused by a single nucleotide deletion in exon 2 or 5 of *Pax 2*, creating a frame-shift of the *Pax 2* coding region creating a premature stop codon which results in a truncated protein (Sanyanusin, *et al.*, 1995 and Sanyanusin, *et al.*, 1999). Symptoms vary in extremity and are increased with homozygous mutations, leading to the hypothesis of haploinsufficiency, where phenotypes are produced from a reduction of healthy protein to inadequate levels (Eccles, 2002).

A spontaneous mutation, typical of the Papillorenal syndrome mutation in humans, has been studied in mice (Favor, *et al.*, 1996). The mutation creates a frame-shift in the helix-loop-helix DNA-binding domain of the Pax 2 protein, resulting in 27 mis-matched amino acids in the DNA-binding domain and a truncated protein. The truncated mutant protein is therefore unable to recognize its normal target genes and so is ineffectual. The *Pax* 2^{1Neu} heterozygous mice were reported to have unaffected, reduced or absent kidneys and eye defects, including severe abnormalities of the optic disc region. The developing homozygous *Pax* 2^{1Neu} mouse had a reduced metanephric anlagen and a deficiency in tubule formation. Other homozygous phenotypes observed in the developing mouse include defects in the mid-hindbrain region, lack of inner ear structures and severely disrupted eye structures. Not only are these phenotypes largely analogous to the symptoms observed in Papillorenal syndrome, but also they display the same variation in intensity. This is again suggestive of haploinsufficiency and collaborates with the inadequacy of the truncated protein.

In mouse metanephric development, the ureteric bud branches into the condensing metanephric mesenchyme, forming a nephron at each ureteric bud tip outgrowth. The number of ureteric bud branches therefore sets the number of nephrons formed for life. *Pax 2* is believed to protect the ureteric bud against apoptosis. Indeed, increased apoptosis was observed in the kidneys of heterozygous *Pax* 2^{1Neu} mice (Porteous, *et al.*, 2000). Analysis using *Pax 2* promoter targeted apoptosis in mice resulted in increased ureteric bud apoptosis and retinal defects similar to Papillorenal syndrome (Dziarmaga,

et al., 2003). In addition, the inhibition of apoptosis in heterozygous *Pax 2*^{1Neu} mice, led to a partial rescue of the decreased ureteric bud branching and nephron number.

***Pax 2* and adult carcinoma**

The role of *Pax 2* in the protection against apoptosis is not restricted to developmental events. Renal cell carcinoma accounts for 3% of all adult aggressive tumours and is the most common malignancy in the adult kidney, 90-95% (Gnarra and Dressler, 1995). Renal cell carcinoma cells lines were found to express *Pax 2*. Inhibition of *Pax 2* by antisense oligonucleotide resulted in the inhibition of cell proliferation. *Pax 2* is therefore a potential anti-apoptotic carcinoma gene. *Pax 2* expression was also observed in Kaposi Sarcoma cells (Buttiglieri, *et al.*, 2004). Kaposi Sarcoma is a cancer of the blood vessels associated with immunodepressive conditions, such as HIV-1 infection and long term post-transplantation therapy. Again, *Pax 2* inhibition, this time by transfection with an antisense *Pax 2* gene, resulted in the reduction of cell proliferation and an enhanced sensitivity to apoptosis.

***Pax 2* and other vertebrates**

Similar to the mouse and human expression, chick *Pax 2* expression is found in the early developing pronephros and mesonephros, the developing ear and brain (James and Schultheiss, 2003 and Hutson, *et al.*, 1999). Also, chick *Pax 2* has been shown to have a role in early kidney induction, where exogenous mesodermal expression was sufficient to produce ectopic kidney structures (Bouchard, *et al.*, 2002). The chick homologue of *Pax 2* has even been shown to have a role in protection against apoptosis, although in the development of the ear, not the kidney (Li, *et al.*, 2004). These common characteristics suggest conserved evolutionary properties of *Pax 2* in development.

Two *Pax 2* zebrafish homologues have been identified, *Pax 2.1* and *Pax 2.2*, however *Pax 2.1* more closely resembles the mammalian *Pax 2* based on its expression pattern (Majumdar, *et al.*, 2000). *Pax 2.1* expression is observed in the central nervous system, ear, optic tracts and pronephros, analogous to the mouse (Majumdar, *et al.*, 2000 and Favor, *et al.*, 1996). The zebrafish *no isthmus* mutant has a truncated form of the *Pax 2.1* gene. Detailed expression analysis of the developing pronephros did not reveal an increase in cell apoptosis, but did show presumptive tubule cells and anterior duct cells ectopically expressing podocyte-specific markers (Majumdar, *et al.*, 2000). This does

not match the increase in apoptosis observed in the kidneys of "Papillorenal syndrome" mice (Porteous, *et al.*, 2000).

1.2.3 *Nephrin*

Nephrin is a major component of the slit-diaphragm of podocytes (Fig. 1.3) (Tryggvason, 1999 and Ruotsalainen, *et al.*, 1999). Without slit-diaphragms, the nephrons are unable to stop large proteins, such as albumin, from entering the tubules and resulting in proteinuria. *Nephrin* was identified using positional cloning to identify the gene responsible for Congenital Nephrotic Syndrome of the Finnish type (See below) (Kestila, *et al.*, 1998). *Nephrin* was found to be located on chromosome 19q13.1.

Congenital Nephrotic Syndrome of the Finnish type

Congenital Nephrotic Syndrome is associated with massive proteinuria at, or shortly after birth (Kestila, *et al.*, 1998). Congenital Nephrotic Syndrome of the Finnish type is autosomal-recessive disorder with an frequency of 1 in 10,000 births in Finland, although significantly less in other European countries. Symptoms of proteinuria and glomerula lesions are observed during embryo development. Structurally, Congenital Nephrotic Syndrome of the Finnish type kidneys have podocytes lacking in foot processes and slit-diaphragms (Fig.1.3), dilated proximal tubules and an increased number of nephrons, resulting in enlarged kidneys. The most frequent cause of Congenital Nephrotic Syndrome of the Finnish type is two nucleotide deletions in exon 2, which result in a frame-shift and a truncated protein. However, many different *Nephrin* mutations have been identified (Koziell, *et al.*, 2002).

Experiments were performed using a human embryonic cell line and 21 mis-sense disease causing *Nephrin* mutations (Liu, *et al.*, 2001). Analysis revealed a localisation of mutant *Nephrin* to the endoplasmic reticulum, not the cell surface of the podocyte. This could explain the lack of slit-diaphragms in Congenital Nephrotic Syndrome of the Finnish type kidneys, and the associated proteinuria.

The homozygous null *Nephrin* mouse dies within the first 24 hours of birth (Putaala, *et al.*, 2001). Consistent with Congenital Nephrotic Syndrome of the Finnish type, the

homozygous and the null *Nephrin* mouse has enlarged kidneys, dilated tubules, massive proteinuria, edema and the absence of slit-diaphragms. Heterozygous null *Nephrin* mice also have similar phenotypes, but these are less severe and proteinuria and edema do not develop until a week after birth.

Nephrin and other vertebrates

In zebrafish, *nephrin* expression is localised to the podocytes (Kramer-Zucker, *et al.*, 2005). Morpholino oligonucleotide mis-translation results in a general edema that spreads throughout the larval body. Embryos die aged 1 week, with pronephric tubule cysts and aberrant glomerulus morphology. The majority of podocytes lack foot processes and no slit-diaphragms are present. The disrupted morphology of the glomerulus reduces the size discrimination of filtration, and large protein deposits are found in the tubules. These phenotypes exactly match the symptoms of Congenital Nephrotic Syndrome of the Finnish type, showing a conserved evolutionary role of *nephrin* in kidney development and a correlation between pronephric and metanephric development.

1.2.4 *PKD1*

PKD1 encodes Polycystin 1, a trans-membrane protein with potential adhesion and protein to protein interactions (Kim, *et al.*, 2000). Polycystin 1 has been found to be expressed in epithelial tissues, endothelial and vascular smooth muscle cells and at cell to cell junctions. In mice kidneys, expression is observed in mature collecting ducts (Gallagher, *et al.*, 2002). *PKD1* has been located chromosome 16 and was identified by its link with Adult polycystic kidney disease.

Autosomal Dominant Polycystic Kidney Disease

Adult polycystic kidney disease is the most common monogenic disease in humans with a frequency of 1 in 400 to 1 in 1000 (Kim, *et al.*, 2000). It is characterised by the formation of cysts in both kidneys, and the progressive destruction of normal renal tissue (Gallagher, *et al.*, 2002). Cyst development in the kidneys normally arises from the tubule or duct tissues. Other symptoms include the formation of cysts in other organs and blood vessel abnormalities (Kim, *et al.*, 2000). In 85-95% of Adult polycystic kidney disease patients, the disease has been linked to a heterozygous

mutation in the *PKD1* gene. In other cases, mutations in related *PKD2* and *PKD3* genes have been implicated (Deltas, 2001 and Paterson, and Pei, 1998).

Mutant $PKD1^{L/L}$ mice were created carrying a mutation similar to that observed in humans (Kim, *et al.*, 2000). The mutation caused a frame-shift in the coding sequence which resulted in a truncated protein. Homozygous $PKD1^{L/L}$ mice died at embryonic day 15.5 from critical vascular defects. Cyst formations were observed in the kidney, although, early metanephric kidney induction did not appear to be affected. Mutant $PKD1^{-/-}$ mice were also created that lacked exon 32, also observed in human Adult polycystic kidney disease (Lu, *et al.*, 1997). Homozygous $PKD1^{-/-}$ mice die during birth from under developed lungs, and have enlarged kidneys with cysts. Renal cyst development was found to originate in the tubules during elongation and maturation.

PKD1 and other vertebrates

Similar to homozygous $PKD1^{-/-}$ mice, polycystic kidney disease medaka fish have enlarged mesonephric kidneys with multiple renal cysts (Mochizuki, *et al.*, 2005). The mesonephric tubule cells have reduced characteristics such as endocytic vesicles, tight junctions and membrane invaginations. Interestingly, cysts were also observed at the microscopic level in the pronephros, suggesting the mutation effects all stages of kidney development.

Studies in zebrafish had indicated that polycystic kidney disease is linked to defects in primary cilia function in the tubules (Low, *et al.*, 2006). It is suggested that a *PKD1/STAT6/P100* pathway is involved in the transduction of a mechanical stimulus into cilia movement. During stimulus, the C-terminal region of polycystin 1 is believed to be cleaved and translocated to the nucleus, where it inhibits the transcriptional activity of *STAT6*. *STAT6* may be under default conditions, reducing cilia activity. The mis-translation of this region due to a frame-shift mutation in autosomal dominant polycystic kidney disease could disrupt this process and inhibit the ability of the cilia to respond to mechanical stimulus.

1.5 Aims of Thesis

This project had two main aims, to identify a suitable target gene involved in the development of the pronephros and then to study its role in development. The identification of a suitable target gene was approached using three different sources of candidate genes. The first source of target genes was the screening of a *Xenopus laevis* stage 13 cDNA library with a subtractive hybridisation probe made from retinoic acid and activin treated animal caps (Chapter 3). This potentially highlighted the genes involved pronephric initiation. The second was the preliminary analysis of a set of UniGene cluster genes that were previously found to be pronephros specific (Personnal correspondence Pollet, N) (Chapter 4). Thirdly, data mining identified *Xenopus* homologues of important kidney development genes identified in higher vertebrates or newly identified genes expressed in the pronephros (Chapter 5).

Subsequent characterisation of the target gene involved mis-expression analysis and regulatory gene network analysis. Over-expression experiments were performed using targeted micro-injection of mRNA into the developing embryo and knock-down analysis was performed using targeted micro-injection of designed morpholino oligonucleotides (Chapters 6 and 8). Investigation into the regulatory gene network was achieved using the animal cap assay system and RT-PCR (Chapter 7).

By analysing the functional role of a target gene, this thesis ultimately aims to further elucidate the developmental regulation of pronephric organogenesis. It is hoped that studies in such a developmental model organism might provide information on human congenital disorders.

Chapter 2

Materials and Methods

2.1 Materials

Materials were sourced accordingly:

Material/Reagent	**Supplier**
^{32}P-GTP	GE healthcare
^{35}S-methionine/cysteine	GE healthcare
Activin A	Invitrogen Life Technologies (Gibco BRL).
Calf intestinal alkaline phosphatase	Roche
Chemicals	Becton, Dickinson and Co., Helena Biosciences, Fisher Scientific, Merck, and Sigma.
DIG RNA labelling kits	Roche
DNA ladder	MBI Fermentas
DNase I	Roche
dNTP	MBI Fermentas
Gel extraction kits	Qiagen
Gentamycin	Sigma
Goat-anti-mouse-AP	Sigma
Hybond nylon membrane	GE healthcare
Miniprep plasmid DNA isolation kits	Qiagen and Sigma.
mMESSAGE mMACHINE™ kits	Ambion®.
Pre-stained protein ladder	New England BioLabs
Proteinase K	Boehringer-Mannheim
Restriction enzymes	Invitrogen
Retinoic acid	Sigma
RNase Inhibitor	GE healthcare
RNase A	Sigma
T4 DNA ligase	MBI Fermentas
Taq/Pfu	Invitrogen
X-ray film	Fuji

2.2 Media and stock solutions

The solutions were made by in house facilities, according to Sambrook, *et al.*, 1989.

2.3 Plasmids

The following plasmids were used in this study and are detailed in the Appendix.

pBLUESCRIPT SK - xl.12848 (IMAGE clone), xl.16795 (IMAGE clone), *Xlim-1* (*In situ* hybridisation probe), RA + A/RA and RA + A/A clones.

pCMV SPORT6	- *Pod 1* (IMAGE clone), *Darmin r* (IMAGE clone), xl. 5110 (IMAGE clone), xl.5983 (IMAGE clone).
pGEM Teasy	- (Promega) initial work on xl.5110, xl.5983, xl.12848, xl.4624, xl.16795, xl.11205, *Pod 1* and *Darmin r* before ordering the selected IMAGE clones.
pGEM T7	- *xWT* (*In situ* hybridisation probe).
PCS2+	- *Pod 1* (mRNA production), *Darmin r* (mRNA production).
pCS3+ MT	- *Pod 1* (c-myc tagged mRNA production).

2.4 Bacterial strains (*E. coli*)

DH5α	F⁻ *supE44 ΔlacU169*(Ø80*lacZΔM15*) *hsdR17 recA1 gyrA96 thi-1 relA1.*
XLI Blue MRF'	Δ(*mcr*A)*183* Δ(*mcrCB-hsdSMR-mrr*)*173 endA1 suppE44 thi-1 recA1 gyrA96 relA1 lac* [F' *proAB lacI*^{q}*ZΔM15* Tn*10* (Tet^{r})].
SOLR	e14⁻(McrA⁻) Δ(mcrCB-*hsdSMR-mrr*)*171 sbcC recB recJ uvrC umuC::*Tn*5*(*Kan*^{r}*) lac gyrA96 relA1 thi-1 endA1* λ^{r} [F' *proAB lacI*^{q} *ZΔM15*] Su⁻ (nonsuppressing).

2.5 DNA Techniques

2.5.1 Agarose gel electrophoresis

Agarose gels of 0.5 – 1.5 % were prepared using TBE (x1) with 0.5μg/ml ethidium bromide. DNA/RNA was separated using electrophoresis in 1 x TBE at 30 – 175 V and then photographed under ultra-violet light (using the GENE DOC). When appropriate, DNA was extracted from the gel using a Qiagen gel extraction kit according to the manufacturer's instructions.

2.5.2 Restriction digests

Restriction digests were carried out following the manufacturer's (Invitrogen) recommendations. Where the digest was for sequence analysis, the reaction mix was 20μl, whereas for other experiments, a larger digest of 50μl was performed. Following digestion of plasmids for ligation, treatment with phosphatase prevented plasmid re-ligation. 1μl of calf intestinal alkaline phosphatase was added per 10μl of reaction, and

the reaction was incubated at 37°C for a further 20 minutes. When necessary, DNA was purified using the Qiagen gel extraction kit according to the manufacturer's instructions.

2.5.3 Ligation of DNA into plasmid vectors

10 – 15ng of vector was mixed with insert digested with appropriate restriction enzymes (molar ratio 1:3) to make a final volume of 20µl with T4 DNA ligase (MBI Fermentas) and ligation buffer. The ligation mix incubated for either 6 hours or over night at room temperature. Where appropriate, PCR products were sub-cloned into pGEM-T Easy® according to the manufacturer's instructions using the t-tailed overhangs.

2.5.4 PCR

PCR reactions were set up as follows:

	µl per sample
PCR buffer (10x)	2.5
$MgCl_2$ (50mM)	1.5
dNTP (10mM)	0.5
Primer mix (25µM) (Table 2.1)	1
Taq polymerase (Invitrogen)	0.1
Water (autoclaved MQ)	18.4
Sample	1

PCR cycle programme:

		First cycle	Next (x) cycles	Last cycle
Denature	(94°C)	3	3	3
Anneal	(55°C)	1	1	1
Elongate	(72°C)	1	1	5
Hold	(4°C)	-	-	∞

Details of all primers used can be seen in table 2.1. After the PCR program had run, 15µl of the products were then run on a 1% agarose gel (0.05µl/ml Ethidium Bromide), at 150V for roughly 45 minutes. A digital image of the gel was then taken under UV light, using the GENE DOC. For Southern blotting and hybridisation (2.9.3 Southern Blotting, 2.9.4 Southern hybridisation), a ruler was placed next to the gel to show the distance travelled of the bands and the gel was kept for further analysis.

Name	5'Sequence3'	Annealing temperature (°C)	Source
EF1α U	CAG ATT GGT GCT GGA TAT GC	55	(Mohun *et al.*, 1989)
EF1α D	CAC TGC CTT GAT GAC TCC TA	55	(Mohun *et al.*, 1989)
ODC U	GGA GCT GCA AGT TGG AGA	55	(Bassez *et al.*, 1990)
ODC D	TCA GTT GCC AGT GTG TGG TC	55	(Bassez *et al.*, 1990)
T3	AAT TAA CCC TCA CTA AAG GG	55	Standard
T7	GTA ATA CGA CTC ACT ATA GGG C	55	Standard
SP6	ATT TAG GTG ACA TAT AG	55	Standard
*Pod*_A	TCT CAG TGA TGT GGA GGA CTT	57	CF270487
*Pod*_B	TGA CGC AGG TGA GCT ATG TAA	57	CF270487
Darmin r A	TTA TGG TCT CCG TGG CAT CTG CTA	57	BC056069
Darmin r B	ATC AGG CAC CAG CCT TAT GGA GAA	57	BC056069
A4229	GAC ACT TGG ATC GTC TGC AAC TTC	55	CA974150
B4229	TTA CAT ACA GGT TCG GCG ACA AGG	55	CA974150
4229C	AAC CGC TGG CAA GTC TAT TC	55	CA974150
A4624	GGA TAC AGG AAG TGA CTC TGG CTA TG	55	AF358133
B4624	CAC ACC AAT GCA GTG ACA AGG ATA GG	55	AF358133
4624C	CTG GAG TCA TAG CTC AGA GT	55	AF358133
A5110	AAA GCT GGG TAC GCG TAA GCT	55	BE508547
B5110	TAG CAC CCA TCT GAT TCT CC	55	BE508547
5110_E	GCT GGT AAG GTA CAG ACA GAG A	53	BE508547
5110_F	GTA AGT GGT GTG CAG CAG TGA A	53	BE508547
A5983	CTC GCA CTT ATG ATC CTA CCA C	55	BC043955
B5983	GTA ATG GAG AGG CGC TTC ATT G	55	BC043955
5983C	TGA AGC GCC TCT CCA TTA CT	55	BC043955
A11205	CCA TCC AGC ACC ACA GAA T	55	AW782622
B11205	CGG CCA GTG CCT AGC TTA T	55	AW782622
11205E	CAA CTG GTC AGG CAG GTA TG	55	AW782622
12848_A	GAC AGG TTG ACA CGC TGC AGA A	55	CA974150
A16795	ATA TCT GCG CTA CTG C	55	CA981992
B16795	TAC CTG CTT CAC TGG TGA C	55	CA981992
16795_C	GCC TAT GAG CTC CAA CTG TTG T	55	CA981992
A22053	CCA GGT GGT GGC AAT AGT T	55	BC043955
B22053	TCA TGA TGG CAT CTC CTC	55	BC043955
6C5_A	CAC CAG CTC CAG TGT AGG CTA A	55	In house sequencing
6C5_B	TCC TAA CAT TCC ACG CAG TGA C	55	In house sequencing
18B1_A	GAA TCT GAA CCG CTG CAT TGC T	55	In house sequencing
18B1_B	GCT GAT CTC TGC AAC TCC TGT A	55	In house sequencing
Rho A F1	TGC GAC CTC TGT CCT ATC CA	55	In house sequencing
Rho 1 R1	TTC TTC TTG CCA CGC CTA CG	55	In house sequencing
5f6(A)	GCT GGT TGC TGT TGG TGA AG	55	In house sequencing
5f6(B)	TGT ACA CCA CTG CGA TGA CT	55	In house sequencing
6a4(A)	GAA TTC GGC ACC AGA	55	In house sequencing
6a4(B)	CGA AGA GTT GCC TAG A	55	In house sequencing
12a1(A)	TGC TGC TCA CTC GGA ATC TG	55	In house sequencing
12a1(B)	TGC CAA GTC ATC TCC ACT GC	55	In house sequencing
15b2(A)	TGG TCG CTC TGC TAA CAG T	55	In house sequencing
15b2(B)	GCT AGC AGT GCA AGA TCT C	55	In house sequencing
15c7(A)	TCT TCT GGT TCC ACG CTG CTT A	55	In house sequencing
15c7(B)	GCC TGG ACT TGA AGA TGG TAT G	55	In house sequencing
xE12/xE47 F2	GGC TTT CCT GCT GCT GTG CTC T	55	X66959/ BC044064
xE12	CTC CTT CTC ACG CTC TGC TTT TG	55	X66959
xE47	TCT CGT ACT CGC ACT CTT TCT CGT	55	BC044064
Xlim 1 U	GAA GGA TGA GAC CAC TGG TGG	55	(Witta and Sato, 1997)
Xlim 1 D	CAC TGC CGT TTC GTT CAT TTC	55	(Witta and Sato, 1997)
xPax 2 U	TCG GAA GAA GAG TGG TCT AC	55	Haldin, C.E. (thesis)
xPax 2 D	GGT ATT CAT ATT CCG CAT TC	55	Haldin, C.E. (thesis)
xPax 8 U	CCA ACA GCA GCA TCA GAT C	53	Haldin, C.E. (thesis)
xPax 8 D	CAA TGA CAC CTG GCC GGA TA	53	Haldin, C.E. (thesis)
xWT1 U	CAC ACG CAC GGG GTC T	60	(Carroll and Vize, 1996)
xWT1 D	TGC ATG TTG TGA TGA CG	60	(Carroll and Vize, 1996)
xITF2b F3	AGC CAG CCG CCA GCA CTT TTC	55	DN059210
xITF2b R3	GGC GCG AGG GAG ACA AAC AGT	55	DN059210
Xlmx1b U	GGA GAG TGG CAT GGA TAT TG	60	(Haldin, *et al.*, 2003)
Xlmx1b D	AGT AGC AGC TGG TGG TGA GG	60	(Haldin, *et al.*, 2003)
xPodocalyxin 1 U	CCA GAG ATG CAG GAG AAA AA	55	BG233342
xPodocalyxin 1 D	GTT TGG TCT GCA TAG TTT TCT T	55	BG233342

Table 2.1 **Primers used in this study**. Primers were either standard primers used in the laboratory, or were designed using Primer designer (Scientific and Educational Software version 3.0) using in house sequencing of clones or EST sequences obtained from NCBI (www.ncbi.nlm.nih.gov) website as indicated.

2.5.5 Primer Design

All novel primers were designed using Primer Designer (Scientific and Educational Software version 3.0). Standard laboratory primers and novel primers can be found in table 2.1.

2.5.6 DNA probe labelling

The screening probe (Chapter 3) was made by Dr Karine Massé according to the protocols of the CLONTECH PCR-Select cDNA Subtraction kit. To label the probe, 4µl probe was added to 31µl of autoclaved MQ water and denatured by heating at 95°C for 3 minutes, then rapidly cooling on ice. Once cool, the denatured probe was centrifuged at 13,000 rpm and cooled again. Under radioactive procedure control, 10µl OLB (200mM Tris.HCl pH 8, 200mM HEPES buffer, dATP, dTTP, dCTP, random hexamer), 2µl BSA 10mg/ml, 5µl ^{32}P dGTP (50µCi), and 2µl Klenow (Invitrogen) was added and the mixture incubated for over 30 minutes at room temperature. After incubation (approximately 3 hours), 23µl T.E. (Tris pH8 and EDTA), 1µl salmon sperm DNA (Invitrogen), 1µl EDTA (50mM), 5µl NaCl 5M and 210µl ethanol was added and the probe mixture immediately centrifuged for 10 minutes at 13,000 rpm. The supernatant was then removed and 500µl T.E. and 50µl NaOH 4M was added. The labelled probe was incubated for 5 minutes at room temperature before adding to the hybridisation buffer (0.5M NaPi, 7% SDS, 5mM EDTA).

2.6 RNA Techniques

2.6.1 RNA extraction from embryos and animal caps

The volumes given below are for 10 animal caps or 2 whole embryos. Where different numbers of animal caps or whole embryos were used, the volumes were adjusted accordingly.

Two whole embryos were homogenized in 300µl extraction buffer (300mM NaCl, 20mM Tris pH 7.5, 1mM EDTA pH8, 1% SDS) with 6µl of proteinase K (15mg/ml) and incubated for 15 minutes at 37°C. Samples were then extracted with an equal volume of phenol and 10µg of glycogen was added to the upper phase. RNA was precipitated with two volumes of ethanol at –20°C for at least 30 minutes and

centrifuged for 20 minutes at 13 000 rpm. The pellet was resuspended in 60µl of DNase I buffer (20mM Tris pH8.3, 30mM NaCl, 2.5mM $MgCl_2$) containing 80u of DNase I and 80u of RNase inhibitor, and incubated for 20 minutes at 37°C. The samples were then extracted with an equal volume of phenol followed by phenol / chloroform, with the aqueous layer being precipitated by adding 2 volumes of ethanol at room temperature for no longer than 30 minutes. This was centrifuged at 13 000 rpm for 20 minutes, the pellet washed with 70% ethanol before being dried and resuspended in 20µl H_2O. 1µl of RNA was analysed on a 1% agarose gel to check the integrity and yield.

Adult tissue RNA was extracted using TRIzol® reagent according to the manufacturer's instructions by Dr Karine Massé. RNA was analysed as above before being stored at – 70°C.

2.6.2 Reverse Transcription PCR

RT-PCR was performed according to Barnett, *et al.*, (1998). 0.5µg of RNA extracted from animal caps, embryo dissections or whole embryos was made up to a total volume of 21.1µl with H_2O, heated at 75°C for 5 minutes before placing on ice. 7.9µl of reaction mix (3.3µM random hexamers, 1 x PCR buffer, 3mM $MgCl_2$, 500µM dNTPs, 1U/µl RNase inhibitor) was added to each tube and incubated at 37°C for 5 minutes before addition of 2µl MMLV reverse transcriptase (200u/µl) and further incubation at 37°C for 1 hour. Reactions were denatured at 95°C for 5 minutes and stored at – 20°C. Samples lacking RNA and RT were added as negative controls. The prepared cDNA was subjected to PCR analysis (2.5.4 PCR). A sample lacking cDNA was checked for contamination in any of the components used and a linearity series (0.2µl, 0.4µl, 0.8µl, 1.6µl) of control cDNA was added to verify that the PCR was in the linear range and semi-quantitative. *EF1α* and *ODC* were used as loading controls, with the amount of cDNA being added equalized with respect to these markers.

2.6.3 Preparation of *in vitro* transcription of mRNA

Plasmid template DNA was linearised with the appropriate restriction enzyme (Appendix) and purified using a gel extraction kit. Capped mRNA was prepared using

the mMESSAGE mMACHINE® kits, T3, T7 or Sp6 (Appendix), according to the manufacturer's instructions (Ambion®).

2.6.4 Wholemount *in situ* hybridisation

Plasmid templates were linearised with the appropriate restriction enzyme (Appendix) and purified using a gel extraction kit. Sense/antisense RNA probes were prepared using digoxygenin (DIG) labelling kit (Boehringer-Mannheim), and single labelled wholemount *in situ* hybridisation was carried out using a standard protocol adapted from Hemmati-Brivanlou, *et al.*, 1990 and Harland, 1991. Where pigmented embryos were used, they were bleached (1% H_2O_2, 5% formamide, 0.5 x SSC in H_2O) on a fluorescent light source following hybridisation for approximately 1 – 4 hours. Internal staining was visualised by clearing the embryos using Murray's solution (benzyl benzoate / benzyl alcohol, 2:1).

2.7 Protein Techniques

2.7.1 *In vivo* translation

Oocytes were injected with 50nl of mRNA at a concentration of 0.5mg/ml and incubated at 18°C for 2 hours. Radio-labelling of proteins was carried out by selecting the best 7 oocytes and incubating them overnight at 18°C in 100µl Barth X containing 10µCi ^{35}S-methionine and cysteine.

Oocytes were washed twice in Barth X before being homogenised in cell lysis buffer (150mM NaCl, 1% NP40, 50 mM Tris-Cl pH8) and 1mM PMSF. Samples were recovered by centrifugation at 13 000 rpm for 5 minutes to remove cell debris and recover the middle layer. 5µl of this layer was mixed with 5µl of protein loading buffer and heated for 3 minutes at 95°C before being loaded onto an SDS-PAGE gel. Samples were stacked on a 4% acrylamide stacking gel at 100V, followed by separation through a 10% acrylamide resolving gel in a tris-glycine running buffer using the BioRad Mini Protean II system. For autoradiography, the gel was dried on for 20 minutes at 80°C.

2.7.2 *In vitro* translation

In vitro translation of 1µg of *in vitro* transcribed mRNA was carried out using the nuclease treated rabbit reticulocyte lysate according to the manufacturer's instructions

(Promega). Reaction products were radiolabelled using ^{35}S-methionine/cysteine. 5µl of product was mixed with 5µl protein loading buffer and heated to 95°C for 3 minutes before being separated on a 10% acrylamide gel as performed for oocyte protein extraction (2.7.1 *In vivo* translation).

2.7.3 Immunostaining

The embryos previously dehydrated in methanol were re-hydrated gradually in PBS. The embryos were then bleached by incubating for 1 hour in bleach solution (1% Hydrogen peroxide, 5% formaldehyde, 2x SSC) in PBS on a light box. Once the embryos had been bleached, the bleaching solution was removed and the embryos washed three times in PBT (2mg/ml BSA, 0.1% Triton X-100 in PBS) for 5 minutes. The embryos were blocked in fresh PBT for 2 hours at 4°C on a nutator before adding 350µl of 3G8 antibody (1/40 dilution in PBT) and incubating overnight at 4°C on a nutator. The excess antibody was washed off by five 1 hour PBT washes at 4°C whilst rotating. The embryos were then incubated overnight in anti-mouse IgG alkaline phosphatase conjugate (1/500 dilution in PBT) overnight at 4°C on a nutator. The excess antibody was washed off by four 1 hour PBT washes at 4°C whilst rotating. The embryos were incubated in colour buffer (0.1M Tris HCl pH 9, 25mM $MgCl_2$, 100mM NaCl, 0.1% Tween-20) for 1 hour before transferring to 350µl of 1/100 dilution of BCIP/NBT in colour buffer. The colour reaction was performed in the dark (plate wrapped in foil) and after 15-20 minutes the colour reaction was stopped by washing with PBS. The embryos were then fixed in MEMFA (2.10.4 Fixing) for 1 hour at 4°C before repeating the process post bleaching with the 4A6 antibody (no dilution) and using FAST RED as the colour reaction substrate.

2.7.4 Western blotting

The 10% SDS PAGE gel (2.7.1 *In vivo* translation) was blotted using a Semi dry blotter according to manufacturers instructions, for 1 hour 30 minutes at 150V. The PVDF (Amersham Biosciences) membrane was blocked in 5% Marvel (Premier International Foods) in PTw (0.1% Tween 20, PBS) for 1 hour whilst rocking. The membrane was then incubated in primary antibody (1/1000 dilution in 5% Marvel in PTw) for 1 hour 30 minutes on a rocker. The membrane was washed five times in PTw, 3 immediate washes, one 5 minutes wash and one 10 minutes wash. The secondary antibody

(1/10000 dilution in 5% Marvel in PTw) was then added and incubated for 1 hour on a rocker. The five washes were then repeated. The membrane was then placed face down on a plastic sheet drizzled with nRNP substrate for 10 minutes before analysing using a PhosphoImager.

2.8 Microbiological Techniques

2.8.1 DNA minipreps and glycerol stock formation

DNA was extracted from overnight cultures set up in 5ml liquid broth, containing antibiotic where desired, in accordance to the QIAprep Spin Miniprep Kit Protocol (QIAGEN). A glycerol stock was made using 0.5ml of the overnight culture containing the plasmid of interest mixed with 0.5ml glycerol solution and stored at –70°C.

2.8.2 Transformation

Where the transformation was to be performed following ligation, 100µl of competent cells (2.8.3 Competent cells) was added to the ligation mix (2.5.3 Ligation). This mixture was left on ice for 15-30 minutes before heat shock at 42°C for 2 minutes, then 2 minutes back on ice. To allow the cells to recover, 900µl of LB (2.2 Stock Solutions) was added and the mix incubated for 1 hour at 37°C. After incubation, the cells were centrifuged for 5 minutes at 3000rpm and 900µl of supernatant removed. The cells were resuspended and plated out onto agar plates containing the relevant antibiotic. For a straight transformation 50µl of competent cells and 1µl of the plasmid miniprep (2.8.1 DNA Minipreps) was used. The bacteria were plated out in 10% and 90% bacterial dilutions. The plates were incubated overnight at 37°C.

2.8.3 Competent cells

An over-night culture of DHL5α (2.3 Bacterial strains) was grown up in LB broth (2.1 Solutions) at 37°C whilst shaking. 500µl of this culture was then grown up in 50ml of Medium A (10mM $MgSO_4$ and 0.2% glucose in LB broth) to OD_{600} 0.5-0.7. This culture was put on ice for 10 minutes before centrifuging at 3000rpm for 10 minutes at 4°C. The pellet was resuspended in 500µl of pre chilled Medium A and 2.5ml of pre chilled Medium B (36% glycerol, 12% PEG, 12mM $MgSO_4$ in LB broth), aliquoted and stored at -80°C.

2.9 Phage Library Screening

2.9.1 Infection of XLI-Blue MRF' with phage

The infection of the XLI-Blue MRF' (2.4 Bacterial strains) bacteria with phage and the plaque lifts were done in accordance to the ZAP-cDNA Gigapack III Gold Cloning Kit instruction manual (STRATAGENE). The N-Hybond (Amersham Biosciences) membranes were then analysed using Southern hybridisation (2.9.4 Southern Hybridisation).

2.9.2 *In vivo* excision

The *in vivo* excisions were done in accordance to the ZAP-cDNA Gigapack III Gold Cloning kit instruction manual (STRATAGENE). The resulting colonies (SOLR, 2.4 Bacterial strains) were checked by PCR using the T3 and T7 primers (Table 2.1).

2.9.3 Southern blotting

The dsDNA PCR products in the 1% agarose gel were denatured by incubating the gel in 0.45M NaCl, 0.5M NaOH at room temperature, for 30 minutes, whilst gently shaking. After denaturation, the gel was washed using MQ water and then neutralised in 0.45M NaCl, 0.5M Tris HCl pH8 at room temperature, for 30 minutes, whilst gently shaking.

The DNA was transferred to N-Hybond (Amersham Biosciences) membrane. This was done by arranging the following materials as in fig. 2.1. The N-Hybond membrane, 2 sheets of Whatmann paper and the tissues were cut to the size of the gel. Care was taken when framing the 1% agarose gel with film strips. The purpose of this was to stop displacement of the ssDNA by the 10x SSC not moving directly vertically. When the materials had been arranged, 10x SSC was poured into the tray, and the edges of the third piece of Whatmann paper was dipped into the liquid. This was then left overnight to allow the ssDNA to transfer onto the N-Hybond membrane.

After the overnight incubation, position of the wells were marked on the N-Hybond membrane, using a pencil. The membrane was then baked for two hours at 80°C, fixing the ssDNA onto the membrane.

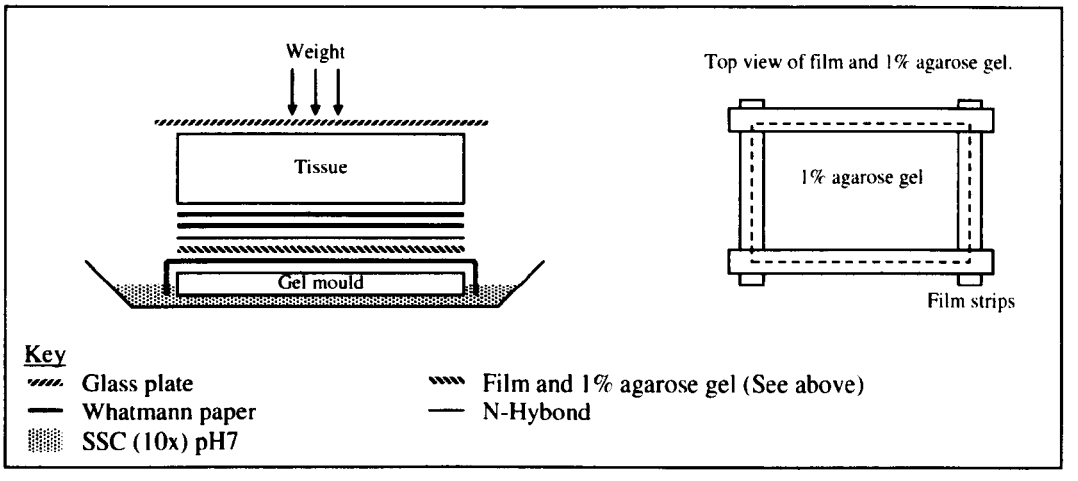

Fig. 2.1 **Arrangement of Southern blotting apparatus.** DNA from a PCR reaction was transferred from an agarose gel to N-Hybond (Amersham Biosciences) membrane using the setup shown. The N-Hybond membrane, 2 sheets of Whatmann paper and the tissues were cut to the size of the gel. Care was taken to frame the 1% agarose gel with film strips to stop displacement of the ssDNA by the 10x SSC not moving directly vertically. When the materials had been arranged, 10x SSC was poured into the tray, and the edges of the third piece of Whatmann paper was dipped into the liquid. This was then left overnight to allow the ssDNA to transfer onto the N-Hybond membrane.

2.9.4 Southern hybridisation

After Southern blotting and baking (2.9.3 Southern blotting), the N-Hybond membranes (Amersham Biosciences) were placed between nylon meshes and inserted into a glass hybridisation tube. To the tube, 100ml of preheated hybridisation buffer (0.5M NaPi, 7% SDS, 5mM EDTA) was added and the hybridisation tube incubated in a rotisserie oven for at least one hour at 42°C. The probe (2.5.6 DNA probe labelling), was then added to the hybridisation tube, taking care that the probe touches the hybridisation buffer before touching the meshes. The hybridisation tube was incubated overnight at 42°C in the rotisserie oven.

The probe and hybridisation buffer mixture was removed and stored safely for further experiments. A wash of 20ml of 2x SSC, 0.1% SDS was added to the hybridisation tube and removed. This was followed by a second wash of 50ml of 2x SSC, 0.1% SDS, and the hybridisation tube incubated in a rotisserie for 10 minutes at 42°C and then the wash was removed. The third wash consisted of 70ml of 2x SSC, 0.1% SDS, with the rotisserie incubation lasting 15 minutes at 42°C. The final wash involved washing in 100ml of 1X SSC, 0.1% SDS, and incubating in a rotisserie for 15 minutes at 65°C.

The N-Hybond membranes were then developed in a cassette for approximately 72 hours at -80°C. The film was then developed using a Fuji developper.

2.10 Embryo culture

2.10.1 *In vitro* fertilisation

Frog husbandry was performed by Mr Robert Taylor and Mr Paul Jarrett. The female *Xenopus laevis* was induced to lay eggs using 2 hormone injections. The first injection, 100 units of follicle stimulating hormone, was given between 8 hours and 4 days before the second injection, 600 units of human chorionic gonadotrophin. The female will start laying approximately 8 hours after the injections at room temperature. To increase this time period, the female is placed in cooled water to lower her body temperature. Whilst the female is laying, she is kept in Barth X, to stop jelly swelling around the eggs. The testis are removed surgically from the male after fatal injection and stored in Barth X on the day of use. To fertilise the eggs, the most of the Barth X was removed from the Petri dish of eggs and the testes teased using a pair of tweezers before brushing over the

eggs. After 5 minutes, 1-2ml of water was added and the eggs left to fertilize for at least 20 minutes.

The embryos were dejellied by treatment with 2% cysteine (pH 8) for 5 minutes. Once the embryos had been dejellied, the cysteine was removed by washing several times with 1/10 Barth X. The embryos were incubated at 12-18°C in 1/10 Barth X and 30µl gentamycin (Sigma) until they reached the required stages.

2.10.2 Staging

The embryos were staged according to Nieuwkoop and Faber (1994).

2.10.3 Micro-injection

Micro-injection was performed by Prof. Elizabeth Jones. For targeted micro-injection, a total of 18nl mRNA/morpholino oligonucleotide was injected into one V2 blastomere to target the left/right pronephros, or both V1 cells to target the heart. As a control, *GFP* mRNA was also injected to confirm targeting (Fig. 2.2). Only those embryos that showed correct targeting by GFP fluorescence were used for analysis and for pronephric targeting, these were sorted for left/right targeting. Oocytes were injected with 50nl of mRNA and cultured as required.

2.10.4 Fixing

The embryos were fixed by incubating overnight (unless otherwise stated) at 4°C in either MEMFA (100mM MOPS pH 7.4, 4% Formaldehyde, 1mM $MgSO_4$, 20mM EGTA pH 8) or Bouin's fix (25% Formaldhyde, 5% acetic acid) (Before bleaching after *in situ* bybridisation only).

2.10.5 Animal cap dissections

All animal cap injections were performed by Prof. Elizabeth Jones. Dissections were carried out using forceps and an eyebrow hair knife. Animal caps were dissected from stage 8/9 embryos and incubated to the required stage according to whole embryo controls.

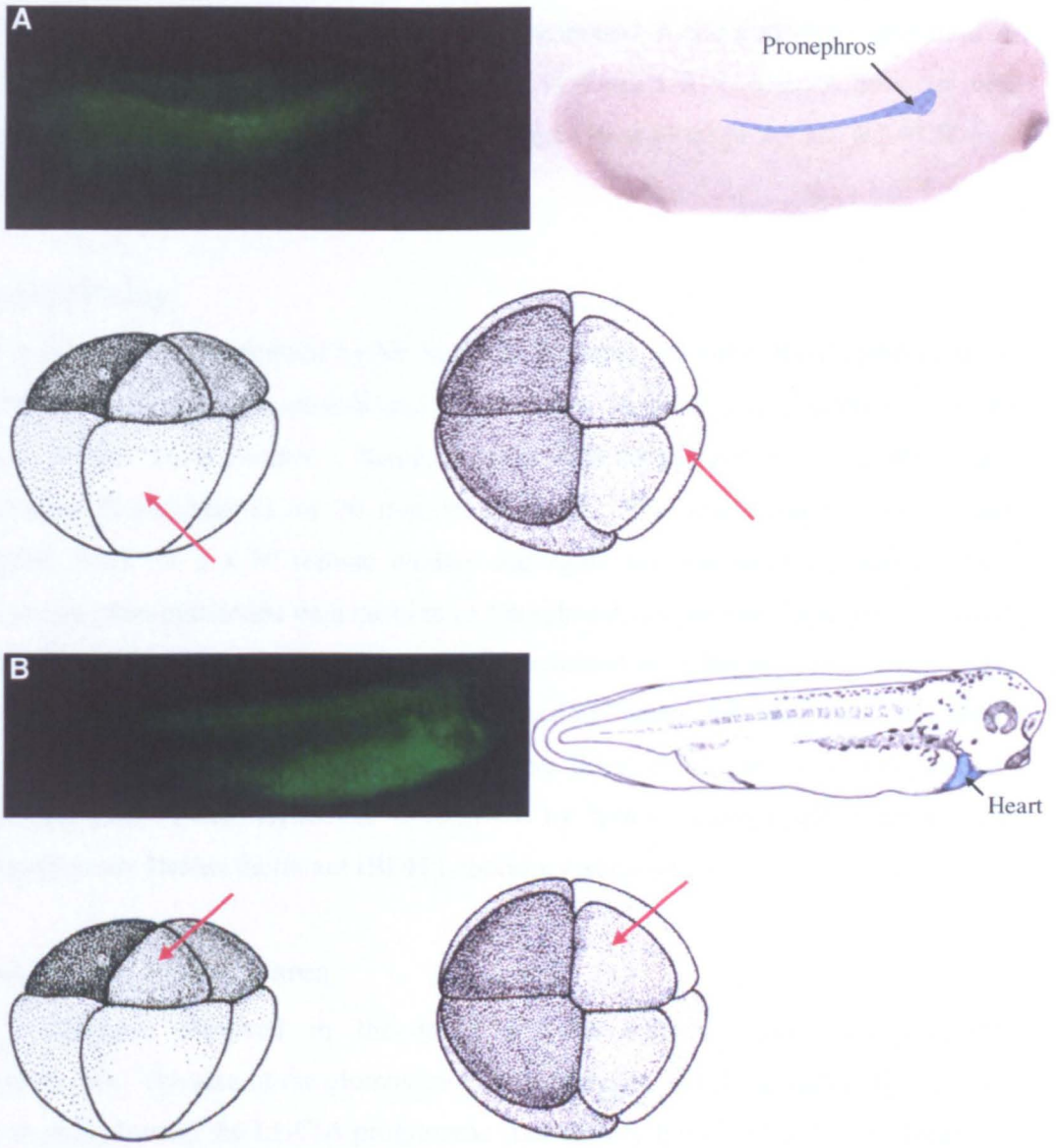

Fig. 2.2 **Targeted mRNA or morpholino micro-injections**. *Pod 1* or *Darmin r* mRNA or morpholino were co-injected with GFP mRNA. The injections were into either V2 cells, to target one pronephros (**A**, as indicated by the **red** arrow), or both V1 cells, to target the heart (**B**, as indicated by the **red** arrow), within an 8 cell embryo. GFP was used as a lineage tracer and would therefore authenticate the pronephric or heart targeting (**A**, **B**). GFP was also used to indicate the left or right pronephric target. Embryos that did not have GFP fluorescence in the required region were discarded from the experiment.

For treated animal caps, the animal caps were incubated in concentrations of activin A and retinoic acid, made up in 1ml volumes of ½ Barth's X with 0.1% BSA 24-well tissue culture plates. They were harvested at equivalent to stage 22 and RT-PCR was performed.

2.10.6 Wax-sectioning

Wax-sectioning was performed by Mr Surinder Bhamra. MEMFA fixed embryos were dehydrated gradually into ethanol and cleared with Histoclear II (Lamb) by 2 x 10 minute washes on a nutator. Samples were then transferred into 1:1 Histoclear II:Paraplast X-tra (Sigma) for 30 minutes at 60°C. This was replaced with molten Paraplast X-tra for 2 x 30 minute washes and again for overnight incubation. One embryo was then embedded on a cushion of Paraplast X-tra per watchglass and allowed to set at room temperature. The blocks were sectioned on a Bright microtome to give 10µm ribboned sections that were collected onto 45°C water and lifted onto Superfrost slides (BDH Laboratory Supplies). Slides were dried overnight on a slide warmer (Phototax), cleared with Histoclear II followed by Xylene washes and mounted with coverslips using DePex mountant (BDH Laboratory Supplies).

2.10.7 Measurement of tissue area

The phenotypes observed in the mis-expression embryos were quantified by measurements. The size of the glomus/pronephric anlagen and the length of the embryo were measured using the LUCIA programme (Laboratory Imaging Ltd.). The length of the embryo was measured to eliminate the factor of the size of the embryo on the size of the glomus/pronephric anlagen (Fig. 2.3).

2.10.8 Pronephric Index

The mis-expression phenotypes of the pronephric tubules were determined using the Pronephric Index (PNI) (Wallingford, *et al.*, 1998) and subsequent statistical analysis. The PNI index is the number of tubule components (Fig. 2.4). A left/right difference in PNI greater than 2 on the same embryo is extremely rare by chance. The embryos were analysed by comparison of the injected side to not injected side only, as slight differences between embryo sets could not be discounted.

B

Length of embryo ±5 mm

Test area ±0.02 mm ^{2}

$\frac{\text{Test area}}{\text{Length of embryo}}$ ±0.004 mm ^{2}/mm

C

	Injected side of embryo			Not injected side of embryo		
	Test area	Length	Test area / Length	Test area	Length	Test area / Length
	mm^2	mm	mm^2/mm	mm^2	mm	mm^2/mm
1	0.02	4.96	0.004	0.021	4.95	0.004
2	0.014	4.46	0.002	0.017	4.50	0.004
3	0.016	4.49	0.004	0.013	4.48	0.003
4	0.008	4.82	0.003	0.009	4.83	0.002
5	0.02	4.79	0.004	0.03	4.75	0.006
Mean	0.016	4.70	0.003	0.018	4.70	0.004

Fig. 2.3 **Example of measurement of test area relative to embryo length.** (**A-B**) The length of the embryo (**red**) and the test area (in this case the glomus, **blue**) were measured using the LUCIA programme (Laboratory Imaging Ltd.). In order to reduce the effect of the size of the embryo on the measurements taken, the ratio of relative test area to length of embryo was used in all statistical analysis not involving left/right comparison of the same embryo. (**C**) An example of raw data obtained from LUCIA measurements.

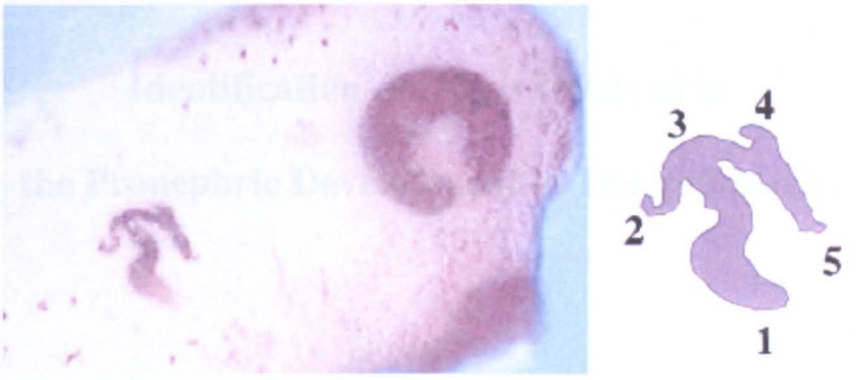

Fig. 2.4 **Pronephric Index (PNI)**. The Pronephric Index is achieved by counting the number of branches/components observed in the pronephric tubules. The PNI of the left and right sides of the same embryo rarely differs by a number greater than 2 (Figure taken from Wallingford, *et al.*, 1998).

Results Part 1

Identification of Genes Involved in the Pronephric Development of *Xenopus laevis*.

Chapter 3

Screening of a stage 13 cDNA phagemid library with a subtracted probe.

Chapter 4

Analysis of potential pronephric UniGene cluster genes.

Chapter 5

Pod 1 and *Darmin r* are expressed in the developing pronephros.

Introduction

The structural development of the pronephros is well documented and several genes have been identified to have specific roles in initiation and development of the pronephros (Introduction). However such information is limited, both by the number of known pronephric genes and the nature of their exact interactions. The first aim of this thesis is therefore, to identify genes that are involved in pronephric initiation and development. Genes with a potential role in pronephric development were identified using three different but complementary approaches:

1. Screening of a stage 13 cDNA phagemid library with a subtracted probe, designed to identify genes expressed in the early development of the pronephros.
2. Analysis of a set of UniGene cluster genes that have previously been shown to be expressed in the pronephros by *in situ* hybridisation.
3. Data mining to identify *Xenopus laevis* homologues of vertebrate genes with a known function in kidney development.

Once these genes had been identified, two genes were chosen for further study based on their spatial and temporal expression, to elucidate their role in pronephric development.

Chapter 3

Screening of a stage 13 cDNA phagemid library with a subtracted probe.

3.1. Introduction

The first method employed to identify potential pronephric development genes was to screen a stage 13 cDNA phagemid library using a subtracted probe. The probe was made from mRNA extracted from animal caps treated with retinoic acid and activin A in combination, a condition known to induce pronephric tissues, subtracted from mRNA extracted from animal caps treated with retinoic acid and activin A individually. This screen would potentially highlight genes that are involved in pronephros initiation and would include known and unknown *Xenopus* genes (Taira, *et al.*, 1994; Brennan, *et al.*, 1999 and Osafune, *et al.*, 2002).

Animal cap experiments with activin A

The animal cap assay was first described in 1961 by Yamada and Takata. An animal cap is the region of tissue that forms the blastocoelic roof within the animal pole of the blastula stage embryo. This tissue comprises two layers of ectodermal cells that are fated to form either epidermal or neural tissues. When left to develop after dissection, the animal cap will produce atypical epidermis. Where, however, the tissue is incubated in saline containing an inducer, the ectodermal cells will differentiate into different cell types, depending on the nature of the inducing factor. A refinement of this technique was added in 1990, where the animal cap cells were dispersed before treatment with an inducing factor, then gently pelleted for longer incubation (Green, *et al.*, 1990). This technique established the importance of cell contacts in the developmental system being studied. The multi or pluripotency of animal cap cells is an invaluable tool in developmental biology (Green and Smith, 1990; Ariizumi and Asashima, 2001 and Okabayashi and Asashima, 2003).

Activin A, thought of as a dorsal inducer, is a TGF-β family protein. Almost all types of mesodermal and endodermal tissues can be induced in amphibian animal caps by activin A in varying concentrations and with different modifiers. In fact, activin A will

induce more dorsal mesodermal structures as concentration of activin A treatment increases, suggesting a role in establishing axial organization in the embryo (Ariizumi, *et al.*, 1991).

With low concentrations of activin A. animal caps differentiate into mildly elongated structures containing blood-like cells (Table 3.1). Some of these cells exhibit erythrocyte morphology, and some are recognised by a leukocyte antibody. However, these cells do not react to anti *Xenopus* globin antibody, indicating that these cells may be primitive blood cells that are not terminally differentiated (Green, *et al.*, 1990 and Miyanaga, *et al.*, 1999).

Muscle tissue is obtained from animal caps following treatment with slightly higher concentrations of activin A (Table 3.1). During this treatment the animal caps elongate, a process involving convergent extension, which is observed in gastrulation. During convergent extension, the organisation of actin filaments was found to be critical for muscle differentiation as treatment with cytochalasin B resulted in a reduction of muscle markers expressed (Tamai, *et al.*, 1999). The induction of cardiac muscle, however, requires higher concentrations of activin A, (Table 3.1) (Logan and Mohun, 1993).

There is a sharp threshold response to activin A induction of muscle tissue or notochord. Antibody 12/101 positive (muscle) cells are found after treatment with low levels of activin A, and notochord cells, detected with MZ15 antibody, are found with medium levels (Table 3.1) (Green, *et al.*, 1997). Neural tissue can also be found in the same dose range as notochord, (Table 3.1) (Smith, *et al.*, 1988). Interestingly, activin A is able to induce 'head' neural tissue, expressing *goosecoid*, at higher concentrations and more posterior neural tissue, expressing *Xbra*, at lower concentrations (Table 3.1) (Green, *et al.*, 1997). This suggests that not only does activin A have a role in dorso-ventral patterning, but also anterior-posterior axis patterning.

In addition to tissue induction, activin A can induce more sophisticated organ structures. The induced cardiac tissue mentioned previously is able to contract, producing beating explants (Logan and Mohun, 1993). Sequential activin A and retinoic acid treatment can produce both pancreatic and pronephric tissue (Moriya, *et al.*, 2000 and Taira, *et al.*,

	Activin A	
Induced tissue type	**ng/ml**	**units/ml**
Blood-like cells	**0.1-1**	**-**
Muscle tissue	**5-10**	**4-8**
Anterior neural tissue	**-**	**4-16**
Notochord	**10-50**	**8-16**
Posterior neural tissue	**-**	**8-32**
Cardiac muscle	**100**	**80**

Table 3.1 **Relative concentrations of Activin A used to induce different tissues in animal cap assays**. Low concentrations are highlighted in blue, medium in green and high in purple. Adapted from Green and Smith, 1990; Ariizumi and Asashima, 2001 and Okabayashi and Asashima, 2003.

1994). The pancreatic tissue formed has some rudimentary cell structures and can produce insulin and glucagon (Moriya, *et al.*, 2000).

An early pronephric marker, *xLim 1*, was identified in retinoic acid and activin A treated animal caps (Taira, *et al.*, 1994). These caps were later found to contain all three components of the pronephros, the tubules, duct and glomus, (Brennan, *et al.*, 1999 and Osafune, *et al.*, 2002). Surprisingly, these three pronephric structures were shown to be functional after transplantation where the host pronephric rudiments had been removed, (Asashima, *et al.*, 2000).

Investigating the gene expression resulting from the activin A and retinoic acid treatment of animal caps has identified many genes. The identification of these genes relies on the requirement for the double treatment of animal caps. That is, genes are selectively expressed during the treatment with both activin A and retinoic acid and are not expressed during the treatment with either activin A or retinoic acid alone. Probes containing cDNA of these enriched genes have been used to screen various libraries and resulted in the isolation of pronephric specific genes. For example, *Annexin IV* (Seville, *et al.*, 2002), *XSMP-30* (Sato, *et al.*, 2000) and *X-CypA* (Massé, *et al.*, 2004) were found to be expressed in the pronephros. I have used probes designed in this way to screen a stage 13 cDNA library. Stage 13 was chosen as it is close to the point which all the elements of the pronephros are induced (Brennan, *et al.*, 1998). The screen would therefore identify genes that are involved in early pronephric development.

Clontech PCR-Select™ Subtraction Hybridisation

The subtraction probes used in this screen were made using the Clontech PCR-Select cDNA subtraction kit. The basic principle of this subtractive hybridisation is the PCR amplification of cDNA fragments that are unique to one experimental sample, the tester, but not the other, the driver, resulting in an enrichment of desired sequences. In this case enrichment of sequences induced by a combination of retinoic acid and activin A (tester) that are not induced by either treatment alone (driver), was desired.

cDNA was synthesised from poly A+ mRNA from all experimental samples and digested using *Rsa I*, yielding blunt ends. The experimental sample containing desired cDNA, called the tester, was halved and ligated to either of two adaptors. The adaptors

were designed without a phosphate group, allowing for only one strand of each adaptor to attach to the 5' end of the cDNA. The cDNA sample to be excluded was left as excess driver cDNA. In the first of the hybridisations, the excess driver cDNA was added to each individual tester cDNA sample. The samples were then heat denatured and allowed to anneal. In the first hybridisation, commonly expressed sequences hybridised and differentially expressed sequences remain unhybridised. Also, the concentrations of sequences are equalised due to the more abundant sequences annealing faster then less abundant sequences. In the second hybridisation, the two cDNA samples are mixed without denaturing. This allowed for the differentially expressed unhybridised tester cDNA with different adaptors to hybridise. More excess driver cDNA was added to further enrich these differentially expressed sequences. The ends were filled in with DNA polymerase and PCR was conducted using nested primers within the tester adaptors. Only the differentially expressed tester cDNA ligated with different adaptors should be amplified.

This method was used to create four probes. Two forward probes that would identify sequences that were expressed with the treatment of animal caps with retinoic acid and activin A, one subtracted with cDNA isolated from retinoic acid treated animal caps, and the other from cDNA from activin A treated animal caps. Two reverse control probes which contained genes that were only induced by retinoic acid or activin A individually were also made (Massé, *et al.*, 2004)

3.2 Results

3.2.1 Preparation of probes and initial screening

This section describes work previously conducted in our laboratory by Dr K Massé. The four probes were generated using animal caps taken at stage 9 and incubated in either 10^{-5} M retinoic acid and 10ng/ml activin A, 10ng/ml activin A alone, or 10^{-5}M retinoic acid alone. At stage 13, most of the animal caps were harvested (retinoic acid and activin A combined treatment ≈ 1200, each individual treatment ≈ 600) and mRNA extracted (retinoic acid and activin A combined treatment ≈ 4μg, each individual treatment ≈ 2μg per sample). Some were allowed to develop until stage 38, after which, pronephric tubules induced were identified using antibody staining with 3G8.

Pronephric tissues were observed only in the animal caps treated with retinoic acid and activin A (Fig. 3.2) (Massé, *et al.*, 2004).

cDNA was generated from extracted RNA using reverse transcription. Two test probes and two control probes were generated using the Clontech PCR-Select cDNA Subtraction hybridisation kit (Fig. 3.1 and 3.3). The probes were as follows:

- **(RA + A)/RA** - forward probe containing cDNAs that are up regulated by treatment with both retinoic acid and activin A, and not retinoic acid alone.
- **(RA + A)/A** - forward probe containing cDNAs that are up regulated by treatment with both retinoic acid and activin A, and not activin A alone.
- **RA/(RA + A)** - reverse control probe containing cDNAs that are up regulated by treatment with retinoic acid alone and not retinoic acid and activin A in combination.
- **A/(RA + A)** - reverse control probe containing cDNAs that are up regulated by treatment with activin A alone and not retinoic acid and activin A in combination.

The four probes were initially used to screen an adult kidney cDNA library (Massé, *et al.*, 2004), which identified kidney specific genes switched on later in development. In this study, the same probes were used to screen a stage 13 library, the point at which the pronephros is initially specified. Consequently, this screen would therefore isolate genes that are involved in early pronephric development.

The stage 13 library had previously been constructed in our laboratory. cDNAs from stage 13 *Xenopus* embryos were cloned into the pBluescript SK(+/-) phagemid using the STRATAGENE cDNA Synthesis and Gold Cloning kit to create a stage 13 cDNA library (Seville and Barnett, unpublished). The phagemids were spread onto 20 LB agar plates after infection with XLI-Blue MRF' at a concentration of 50,000 colonies per plate and duplicate plaque lifts were performed per plate (Methods 2.9.1 Infection of the XLI-Blue MRF'). The plaque lifts underwent hybridisation using either the (RA + A)/A or the (RA + A)/RA forward probes (Methods 2.9.4 Southern Hybridisation). The plaque lifts probed using the (RA + A)/RA forward probe gave 22 positive plaques, and

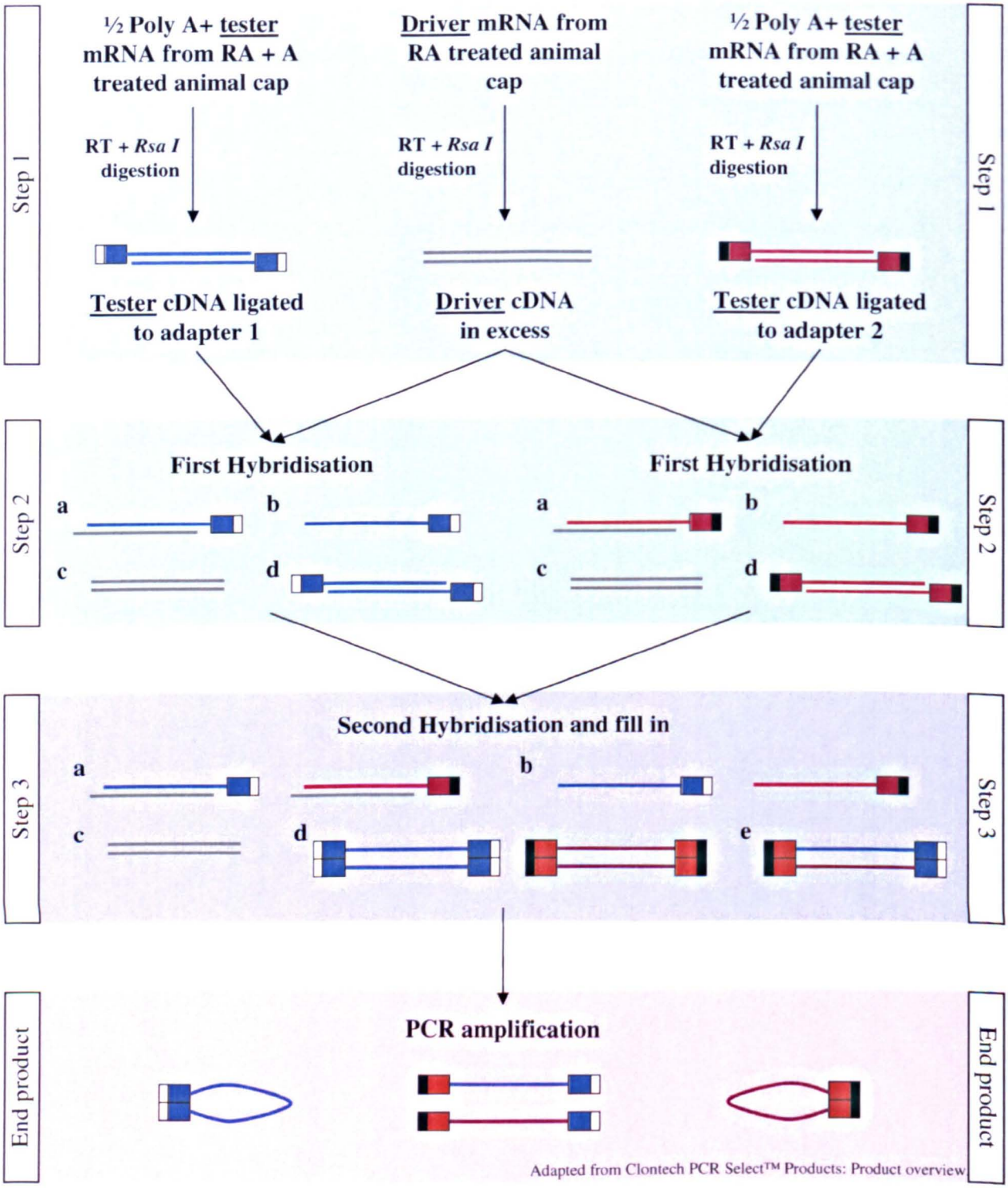
Step 1
½ Poly A+ tester mRNA from RA + A treated animal cap
RT + Rsa I digestion
Tester cDNA ligated to adapter 1
Driver mRNA from RA treated animal cap
RT + Rsa I digestion
Driver cDNA in excess
½ Poly A+ tester mRNA from RA + A treated animal cap
RT + Rsa I digestion
Tester cDNA ligated to adapter 2
Step 1
Step 2
First Hybridisation
a
b
c
d
First Hybridisation
a
b
c
d
Step 2
Step 3
Second Hybridisation and fill in
a
b
c
d
e
Step 3
End product
PCR amplification
End product
Adapted from Clontech PCR Select™ Products: Product overview

Fig. 3.1 **Clontech PCR-Select™ cDNA Subtraction Hybridisation.** The subtraction probes used in this screen were made using the Clontech PCR-Select™ cDNA subtraction kit. **Step 1**; cDNA was synthesised from poly A+ mRNA from all experimental samples and digested using *Rsa I.* The experimental sample containing desired cDNA, called the tester, was halved and ligated to either of two adaptors. The cDNA sample to be excluded was left as excess driver cDNA. **Step 2**; in first of the hybridisations, the excess driver cDNA was added to each individual tester cDNA sample. The samples were then heat denatured and allowed to anneal. The hybridisation gave the following products; (**a**) Commonly expressed tester cDNA hybridised to excess driver cDNA; (**b**) Unhybridised differentially expressed tester cDNA; (**c**) Excess driver cDNA hybridised to excess driver cDNA; (**d**) Abundantly expressed tester cDNA hybridised to abundantly expressed tester cDNA. **Step 3,4**; in the second hybridisation, the two cDNA samples are mixed without denaturing and more excess driver cDNA was added. The ends were filled in with DNA polymerase and PCR was conducted using nested primers within the tester adaptors. The PCR gave the following products; (**a**) Commonly expressed tester cDNA hybridised to excess driver cDNA – not amplified; (**b**) Unhybridised differentially expressed tester cDNA – not amplified; (**c**) Excess driver cDNA hybridised to excess driver cDNA – not amplified; (**d,e**) Tester cDNA hybridised to tester cDNA – only amplified where adaptors are different. The resulting amplified probe contains cDNA fragments that are present with the treatment of animal caps with retinoic acid and activin in combination (tester), but not retinoic acid alone (driver).

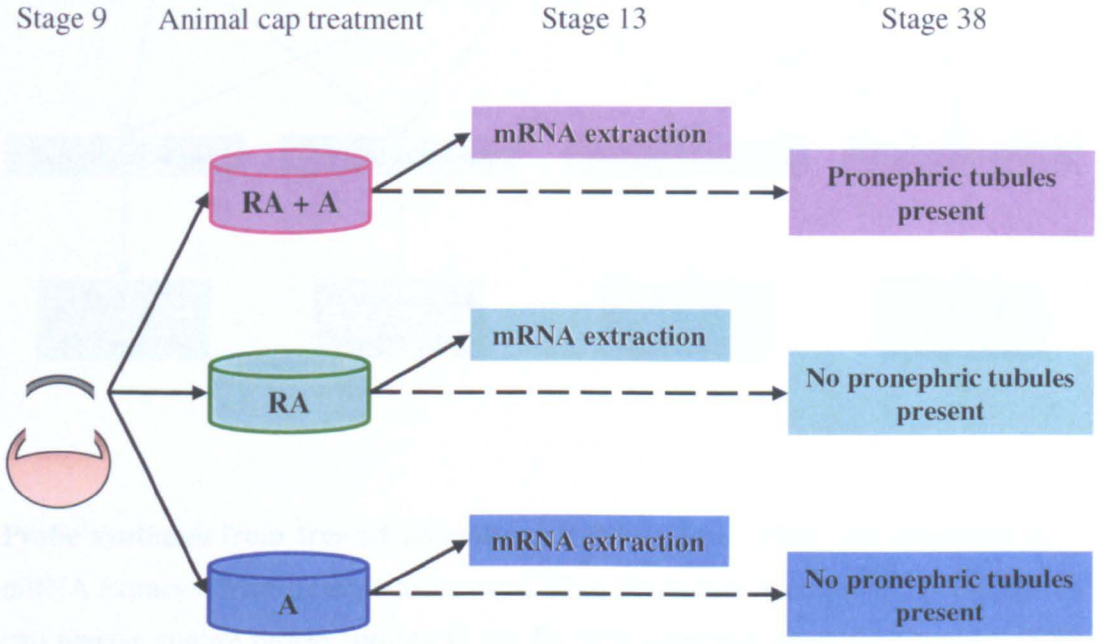

Fig. 3.2 ***In vitro* induction of pronephric tubules.** Animal caps were taken at stage 9 and incubated overnight in either 10^{-5}M retinoic acid (**RA**), 10ng/ml activin (**A**) or both (**RA + A**). At stage 13, the mRNA was extracted from the majority the animal caps. The rest of the animal caps were then incubated until stage 38. The presence of pronephric tubules was identified using antibody staining with 3G8 (tubules).

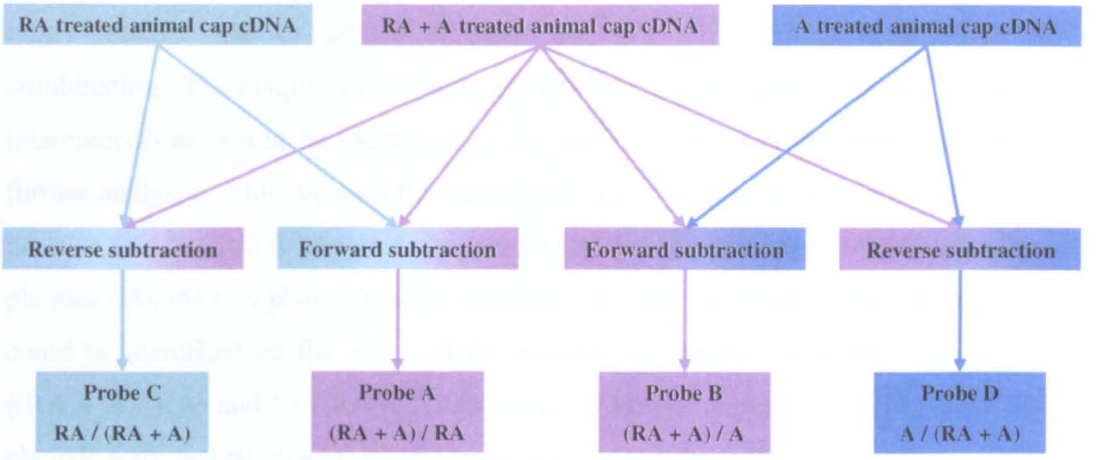

Fig. 3.3 **Probe synthesis from treated animal cap mRNA**. The cDNA was generated from mRNA extracted from treated animal caps. Two forward probes (probes **A** and **B**) and two reverse control probes (probes **C** and **D**) were generated using the Clontech PCR-Select cDNA Subtraction hybridisation kit. **Forward probe A** contained cDNA of genes that were up regulated by animal cap treatment with retinoic acid and activin, but not retinoic acid alone. To make **forward probe A**, the cDNA from animal caps treated with retinoic acid alone was taken as the "excess driver cDNA" and the tester cDNA from animal caps treated with both retinoic acid and activin was the cDNA ligated to the adaptors (See fig. 3.1). This was a **forward subtraction**. In a **reverse subtraction**, **probe C**, the cDNA from animal caps treated with both retinoic acid and activin was taken as the "excess driver cDNA" and the tester cDNA from animal caps treated with retinoic acid alone was ligated to the adaptors. **Reverse probe C** therefore contained cDNA of genes that were up regulated by animal cap treatment with retinoic acid alone, but not retinoic acid and activin together. The probes **B** and **D** were made in a similar manner, with the exception that the treatment was with activin alone instead of retinoic acid alone.

the plaque lifts probed using the (RA + A)/A forward probe gave 57 positive plaques. The filters were subsequently stripped and re-hybridised with the reverse control probes. The reverse control probes contain cDNAs that are up-regulated by treatment with either retinoic acid or activin A alone and not retinoic acid and activin A in combination. The plaques that contain cDNAs that are up-regulated by the single factor treatment alone would be identified by the reverse control probes and excluded from further analysis. This reduced the number of positive plaques of interest to 21 for the positive (RA + A)/RA screened plaques and 53 for the positive (RA + A)/A screened plaques. As the two plate lifts were identical, the false positives identified on one plate could be identified on the other. This reduced the number of positive plaques to 19 ((RA + A)/ RA) and 52 ((RA + A)/A) plaques (Massé, unpublished) (Fig. 3.4). These plaques were picked, plated out and rescreened during this project.

3.2.2 Selection of clones within positive plaques

PCR and Southern hybridisation of positive plaques

PCR was used to determine the degree of clonality of the 71 plaques. The stage 13 cDNA library had been cloned into pBluescript SK(+), flanked by T3 and T7 polymerase binding sites (Appendix). Primers complimentary to T3 and T7 were used to amplify the cDNA fragments within the plaques. The PCR products were run on a 1% agarose gel and observed using UV light. The number of PCR products was used as an indication of clonality of the plaques and the relative band intensity an indication of clone proportions within the plaque (Fig. 3.5). The migration distance of each PCR product was determined before Southern blotting and hybridisation with the same initial probe used to screen the library ((RA + A)/ RA or (RA + A)/A) (Fig. 3.6). Positive clones were identified by matching the PCR products from the X-ray film to those on the UV digital image. 24 plaques were chosen using these data on the basis of:

- Size - plaques with larger PCR products/cDNA fragments were chosen as the genes would be easier to identify with more sequence.
- Intensity - plaques with more intense PCR products/cDNA fragments were chosen as it was likely that the clone containing that cDNA fragment was more abundant within the sample.
- Clonality - plaques with fewer PCR products/cDNA fragments were chosen to facilitate isolating clones.

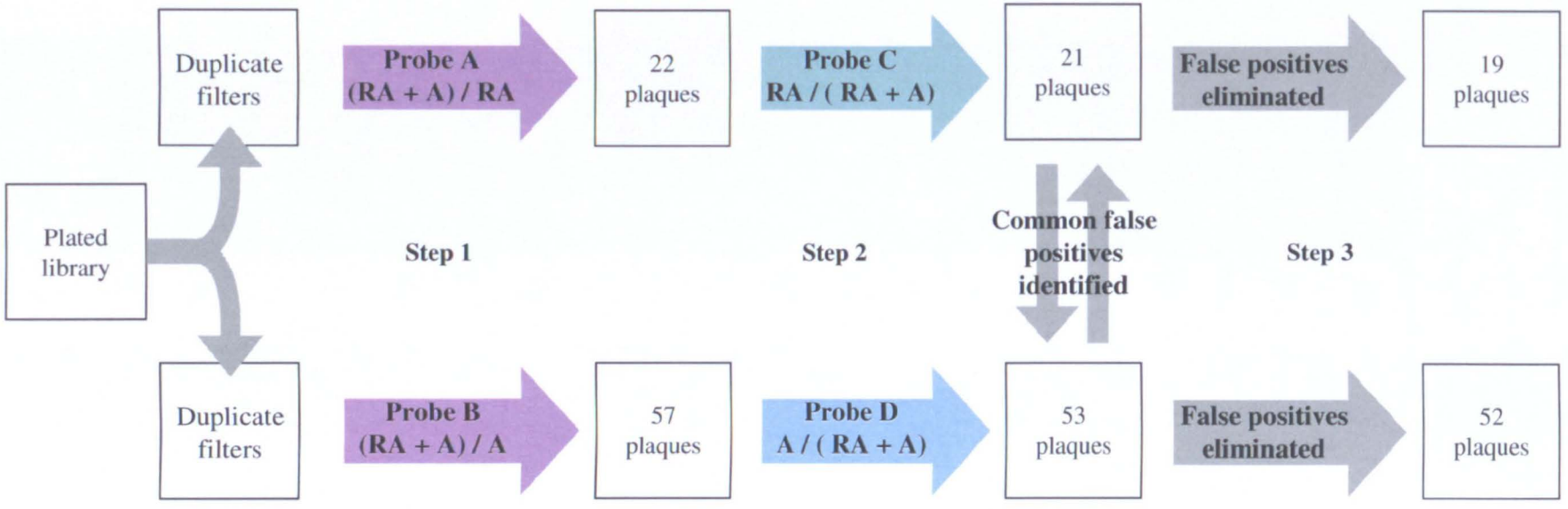

Fig. 3.4 **Stage 13 phagemid cDNA library screening**. Plaque lifts were taken of the phagemid cDNA library and analysed by hybridisation using the subtracted probes. **Step 1** identified all the plaques that contained cDNA up regulated in the animal caps treated with both retinoic acid and activin, but not activin (**forward probe B**) or retinoic acid (**forward probe A**) alone. **Step 2** used the control probes generated by the reverse subtraction. This identified false positives by indicating samples containing cDNA up regulated in animal caps treated with either activin (**reverse probe D**) or retinoic acid (**reverse probe C**) alone and not the combined treatment of retinoic acid and activin. **Step 3** compared false positive plaques, identified in step 2, between the duplicate filters and eliminated them. The **numbers** within the boxes refer to the number of positive plaques at each stage.

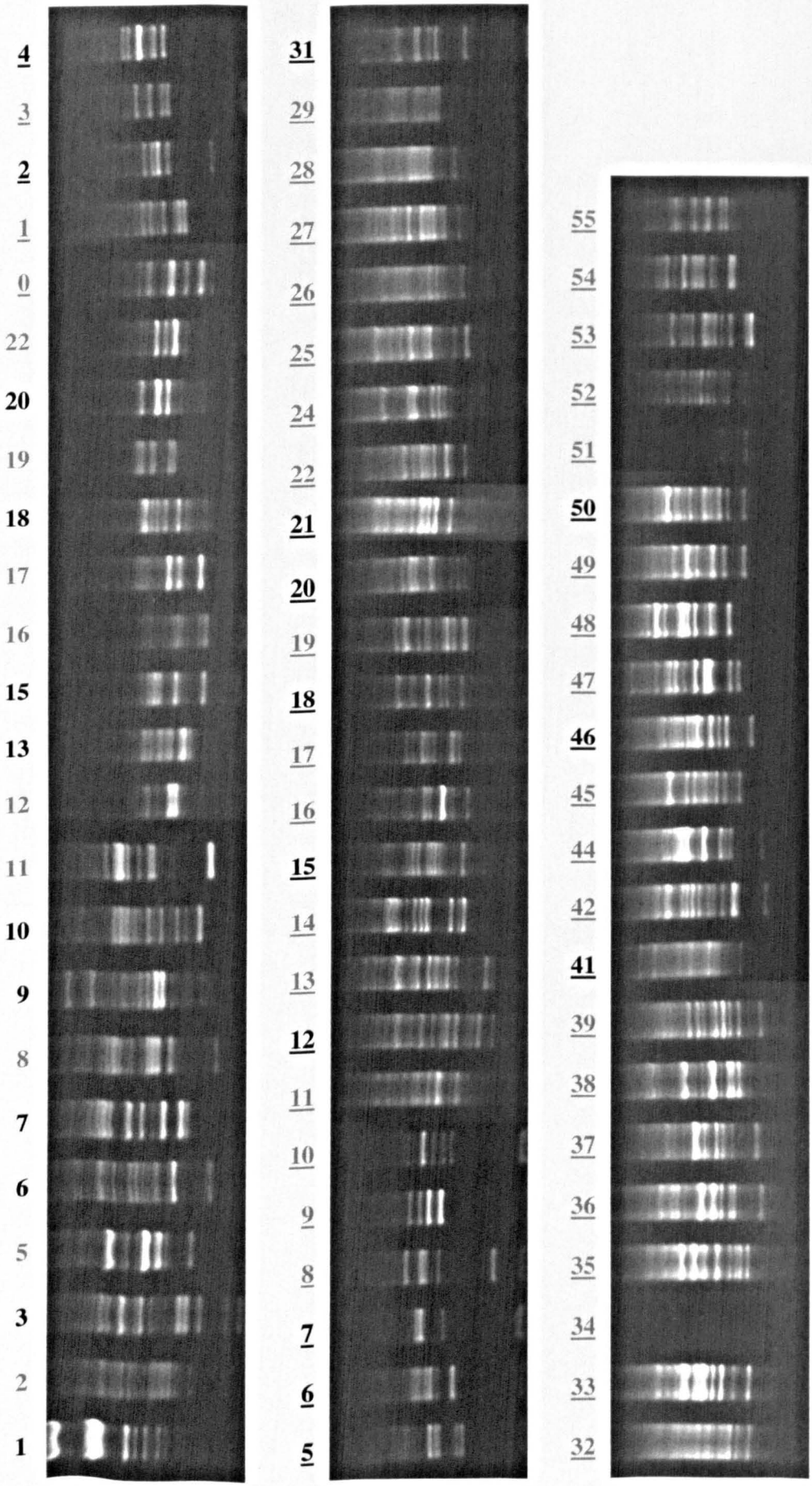
4
3
2
1
0
22
20
19
18
17
16
15
13
12
11
10
9
8
7
6
5
3
2
1
31
29
28
27
26
25
24
22
21
20
19
18
17
16
15
14
13
12
11
10
9
8
7
6
5
55
54
53
52
51
50
49
48
47
46
45
44
42
41
39
38
37
36
35
34
33
32

Fig. 3.5 **First round PCR of positive samples identified in initial screen.** PCR was performed using primers complementary to T3 and T7 polymerase binding sites (positioned on either side of the insert) and a standard programme cycle (annealing temperature of 55°C with 30 cycles). The PCR products were then run on a 1% agarose gel with ethidium bromide. The gel was photographed using UV light with a ruler adjacent to the ladder for quantification of DNA migration. The samples were graded on the basis of signal intensity and clonality. Black numbering indicates selected samples. Underlined numbering represents probe used in screening (Number = (RA + A)/RA, Number = (RA + A)/A).

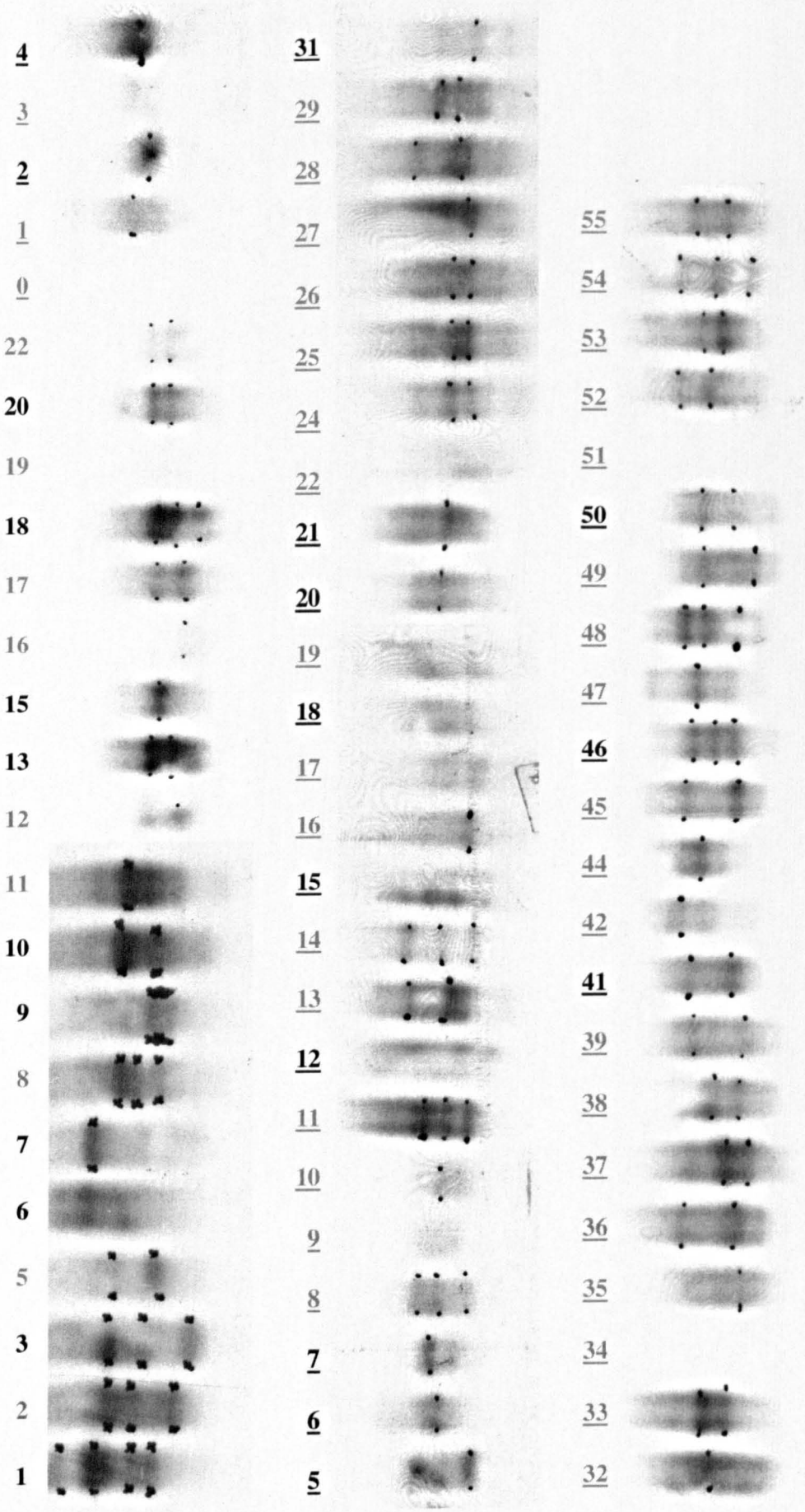
4
3
2
1
0
22
20
19
18
17
16
15
13
12
11
10
9
8
7
6
5
3
2
1
31
29
28
27
26
25
24
22
21
20
19
18
17
16
15
14
13
12
11
10
9
8
7
6
5
55
54
53
52
51
50
49
48
47
46
45
44
42
41
39
38
37
36
35
34
33
32

Fig. 3.6 **Southern hybridisation of first round PCR of positive samples identified in initial screen.** Southern blotting and hybridisation of sample PCR (Fig. 3.5). Underlined numbering represents probe used in hybridisation (Number = (RA + A)/RA = Probe A, Number = (RA + A)/A = Probe B). Positively hybridised PCR products (indicated using black dots) were aligned with the original PCR (Fig. 3.5) using distance migrated to identify them. Again, the samples were graded on the basis of signal intensity and clonality. The data from the PCR and the Southern blot were compared and 24 samples were selected (numbered in black) for further analysis.

Selection of specific positive clones within chosen plaques

The chosen plaques were plated out onto LB agar dishes following infection with XLI-Blue MRF' and plaque lifts were performed, marking the edges of the dish to ensure correct orientation (Methods 2.9.1 Infection of the XLI-Blue MRF'). Hybridisation was performed using the same test probes that were used initially (Results 3.2). Using the markers for orientation, positive phage plaques were chosen on the basis of signal intensity and isolation on the plate, for ease of removal to obtain a pure clone (Fig. 3.7). For each sample, 3-6 phagemid picks were taken, resulting in 78 individual phagemid picks. PCR, using T3 and T7 primers, and Southern hybridisation of the phagemid picks, ensured the correct picks had been chosen, reducing the number of phagemid picks to 30 (Table 3.2).

Sequencing of PCR products

The PCR products from the 30 phagemid picks were sequenced in house using the T3 primer (Table 3.2). The sequences were analysed with the BLAST on the NCBI website (www.ncbi.nlm.nih.gov/BLAST/) (Basic Local Alignment Search Tool, Altschul, *et al.*, 1990) programs, using both direct cDNA sequence and conceptual translated amino acid sequences ("Traduc" using standard genetic code, www.infobiogen.fr). The resulting homologous genes and EST data allowed for the reduction of clone numbers. This was on the basis of ubiquitous expression, for example clone 15d encodes *Elongation Factor 1α*, a *Xenopus* gene known to be expressed ubiquitously, or recognised *Xenopus* kidney genes, such as clone 13D encodes *Cold Inducible RNA Binding Protein 2*, already known to be involved in *Xenopus* kidney development. From this investigation, 19 phagemid picks were chosen for further investigation.

3.2.3 Characterisation of identified clones

Plasmid recovery

To recover the pBluescript SK (+) plasmids and allow for RNA *in situ* hybridisation probes to be made and complete sequencing, the plasmid was excised from the UNI-ZAP XR vector and transfected into the SOLR strain (Methods 2.4 Bacterial Strains). The plasmid was obtained from the SOLR strain by miniprep protocols, with 6 randomly chosen clones for each phagemid pick. As the phagemid picks were already

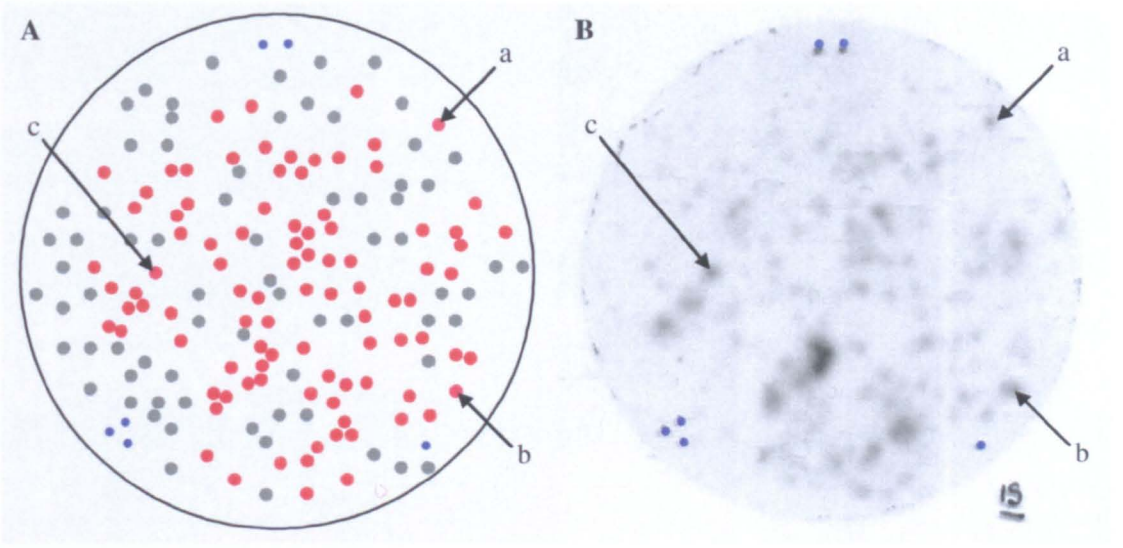

Fig. 3.7 **Hybridisation of plaque lift showing typical clones chosen.** (**A**) Depiction of a typical phage plate. (**B**) Auto-radiograph of plate lift hybridised using (RA +A)/A ^{32}P labelled probe. Blue dots (•) indicate a code, created by pricking the agar, which allows the phage plate to be directly lined up with the radiograph. Red circles (•) denote phage plaques that align with positive signals from the radiograph. Grey circles (•) represent phage plaques that do not align with the radiograph. The black arrows labelled **a**, **b** and **c** symbolise the plaques that were subsequently removed for further screening (Phage picks).

Sample	Phage Pick	Second Southern hybridisation	Size (bp)	Sequencing and BLAST analysis
1	1B	Positive	650	*Xenopus laevis Mitochondrial gene*
3	3A	Positive	701	*Xenopus laevis Cytoskeletal actin Type S*
	3B	Positive	547	97% identity to Human *Sec 23*
6	6C	Positive	559	77% identity to Human Selenoprotein W
7	7C	Negative	-	-
9	9C	Positive	643	*Xenopus laevis Mitochondrial gene*
10	10A	Positive	808	*Xenopus laevis Gene 6720465F12*
	10C	Positive	789	Mouse Ubiquitous protein kinase-like
13	13D	Positive	710	*Xenopus laevis CIRP2*
15	15B	Positive	607	*Xenopus laevis Cytokeratin type II*
	15C	Positive	752	*Xenopus laevis Rack 1/ Xenopus laevis Guanine nucleotide binding protein β2*
18	18B	Positive	800	97% identity to Mouse *VPS28*
	18C	Positive	575	BQ732066 UniGene cluster xl.8071 – unidentified
20	20B	Positive	846	*Xenopus laevis Mitochondrial gene*
2	2b	Positive	851	*Xenopus laevis Neuronal pentatraxin 1*
4	4c	Positive	1003	*Xenopus laevis Rho A*
5	5f	Positive	786	*Xenopus laevis Skp 1*
6	6a	Positive	1044	*Xenopus laevis* Hypothetical protein LOC398467
	6c	Positive	982	*Xenopus laevis* Ribosomal protein S22
7	7d	Negative	-	-
12	12a	Positive	828	JC7 protein, UniGene cluster xl.15910
	12b	Positive	710	BJ038813 UniGene cluster xl.53737 – unidentified
15	15a	Positive	807	*Xenopus laevis HMG-X*
	15b	Positive	864	61% identity to *Bos taurus* *Similar to NADH dehydrogenase*
	15c	Positive	912	MGC80798 protein UniGene cluster xl.24149
	15d	Positive	955	*Xenopus laevis Ef1α*
18	18c	Positive	771	*Xenopus laevis Carnitine acetyltransferase*
20	20b	Positive	871	85% identity to *Rana sylvatica* *Mitochondrial phosphate transporter*
	20c	Positive	900	Unknown
21	21a	Negative	-	-
31	31b	Positive	635	AW766078
41	41b	Positive	1004	*Xenopus laevis FRGY 1*
46	46c	Positive	1385	BJ066388 UniGene cluster xl.53638 – unidentified
50	50a	Negative	-	-

Table 3.2 **Summary of results of PCR and Southern hybridisation of phage picks and sequencing of PCR products.** 3 to 6 phage picks (second column) were taken from each sample (first column) (only those resulting in a PCR product of the correct size are included). PCR and subsequent Southern hybridisation of the phage picks was performed. The result of this "second" Southern hybridisation is indicated in the third column. The resulting PCR products were also sequenced (fourth column) using the T3 primer. Sequences that corresponded to mitochondrial, other ubiquitously expressed genes or already known *Xenopus* kidney genes were not analysed further. Where the outcome of the Southern hybridisation is negative, no further analysis was done. The phage picks that were eliminated from the study are shaded in grey.

clonal, one clone exhibiting the correct fragment sizes after restriction enzyme treatment was selected per phagemid pick.

Initial wholemount *in situ* hybridisation

Initial analysis of the spatial expression patterns of the 19 clones was completed by wholemount *in situ* hybridisation using antisense RNA DIG-labelled probes and the *Xenopus* albino (homozygous and heterozygous) embryo stages 13, 21 and 35 (Methods 2.6.4 Wholemount *in situ* hybridisation). Stage 13 is the stage at which the pronephros is initiated, 21 is the stage at which the pronephric anlargen is formed and elongates and at stage 35 the pronephros is functional. Only the antisense RNA DIG-labelled probes were used for the initial wholemount *in situ* hybridisation to enable the faster screening of clones. The probes were made by digesting the pBluescript SK (+) plasmids at the 5' end of the cDNA fragment insert and transcribing with either T3 or T7 (Table 3.3).

Staining in the pronephros was observed in 9 (3B5, 6C5, 18B1, 5f6, 6a4, 12a1, 15b2, 15c7, 41b2) of the 19 clones investigated (Table 3.4). The expression patterns of these clones were only apparent later in development, stage 27, and hybridisation was not exclusive to the pronephros. The lack of early staining may be due to the inability of the wholemount *in situ* hybridisation technique to detect low levels of expression. Later in this screen RT-PCR was used to detect lower levels of expression.

Probes derived from 7 clones (10A7, 15B7, 4c1, 12b3, 18c1, 31b4, 46c9) did not indicate expression in the pronephros (Table 3.4). The genes identified in this screen should be up regulated by retinoic acid and activin A treatment in animal caps although false positives are possible. The combined treatment of retinoic acid and activin A in animal caps not only induces pronephric tissues, but also has the potential to induce anterior and posterior neural tissue, cardiac tissue and pancreatic tissues (Haldin, *et al.*, 2003 and Moriya, *et al.*, 2000). Therefore, although it is expected that a high proportion of the genes isolated in this screen are expressed in the pronephros, not all genes will be.

Probes from a small number of clones, 18C2, 2b5 and 20c1, failed to reveal staining patterns by wholemount *in situ* hybridisation. It is undetermined whether this was due to low levels of expression, or experimental error. The clones that did not indicate

	Antisense		Sense	
Clone	Restriction enzyme	RNA polymerase	Restriction enzyme	RNA polymerase
3B5	*Bam H1*	T7	-	-
6C5	*Bam H1*	T7	*Xho 1*	T3
10A7	*Pst 1*	T7	-	-
15B7	*Bam H1*	T7	-	-
18B1	*Hind III*	T3	*Bam H1*	T7
18C2	*Bam H1*	T7	-	-
2b5	*Xba 1*	T7	-	-
4c1	*Xba 1*	T7	-	-
5f6	*Eco R1*	T7	*Kpn 1*	T3
6a4	*Xba 1*	T7	*Kpn 1*	T3
12a1	*Bam H1*	T7	*Kpn 1*	T3
12b3	*Xba 1*	T7	-	-
15b2	*Xba 1*	T7	*Kpn 1*	T3
15c7	*Sac 1*	T7	*Kpn 1*	T3
18c1	*Xba 1*	T7	-	-
20c1	*Sac 1*	T7	-	-
31b4	*Xba 1*	T7	-	-
41b2	*Sac 1*	T7	*Kpn 1*	T3
46c9	*Sac 1*	T7	-	-

Table 3.3 **Preparation of antisense DIG-labelled RNA probes for initial whole mount *in situ* hybridisation.** Whole mount *in situ* hybridisation was performed using antisense DIG-labelled RNA probe. The probes were made by digesting the pBluescript SK (+) plasmids at the 5' end of the cDNA fragment insert and transcribing with either T3 or T7 as shown.

Clone	Neurula (Stg. 13)	Early tailbud (Stg. 21)	Late tailbud (Stg. 35)
3B5	No staining.	Neural folds.	Somites, head, possible staining in the pronephros.
6C5	No staining.	Anterior neural folds and eye placodes.	Pronephric duct, head and somites.
10A7	No staining.	Somites, neural folds, migrating neural crest and eye placodes.	Head.
15B7	Epidermis, notably clear in the neural plate.	Epidermis.	Epidermis and growth tip of the tail.
18B1	No staining.	No staining.	Pronephric tubules and head
18C2	No staining.	No staining.	No staining.
2b5	No staining.	No staining.	No staining.
4c1	Neural plate, especially neural groove.	Somites, eye placodes and adhesive organ.	Possible weak staining in the pronephros, area between somites and head.
5f6	No staining.	Brain.	Pronephric tubules, head, lens and spinal cord.
6a4	Anterior and posterior ends of the neural folds.	Eye placodes and migrating neural crest.	Brain, eye and anterior duct.
12a1	Neural plate.	Neural folds.	Pronephric tubules, somites and head.
12b3	Neural plate.	Neural folds.	Spinal cord, eye and adhesive organ.
15b2	Neural groove.	Neural folds, migrating neural crest and eye placodes.	Pronephros, eye components and head.
15c7	Anterior neural plate.	Blood islands.	Pronephric tubules and head.
18c1	Neural plate.	Neural folds.	Head and somites.
20c1	No staining.	No staining.	No staining.
31b4	Anterior and posterior ends of the neural folds.	Neural folds, migrating neural crest and eye placodes.	Area between somites and head.
41b2	Ectoderm.	Ectoderm.	Pronephros and endoderm.
46c9	Anterior neural plate.	No staining.	Head and somites.

Table 3.4 **First round *in situ* hybridisation of the 19 clones chosen in screening**. *Xenopus laevis* embryos were taken at stage 13, 21 and 35 for expression analysis. *In situ* hybridisation was performed using antisense DIG-labelled RNA probe. Areas of clone expression are indicated. The clones that do not show expression in the pronephros or have unclear expression patterns were not included in further analysis and are highlighted in grey.

pronephric expression, or had ambiguous expression patterns were not included in further screening. There were 9 clones continued in the screen (Table 3.4).

Sequencing of cDNA from plasmid

The full cDNA fragments from these 9 clones were sequenced, using the T3 and T7 flanking primers by the Molecular Biology Service, Biological Sciences, University of Warwick. Again, the sequences were analysed with the BLAST on the NCBI website (www.ncbi.nlm.nih.gov/BLAST/) (Basic Local Alignment Search Tool, Altschul, *et al.*, 1990) programs, using direct cDNA sequence and the conceptual amino acid sequences ('Traduc' using standard genetic code, www.infobiogen.fr). One of the clones, 3B5, appeared to consist of two fused cDNA fragments, *Sec 23* and *xCIRP*. As any further study of this clone would require recloning, no more work was carried out at this stage. A total of 8 clones were therefore carried on for further investigation (Table 3.5).

Temporal expression patterns of clones

To analyse the expression patterns of the selected target genes, RT-PCR and wholemount *in situ* hybridisation were used to elucidate the temporal and spatial expression patterns. The temporal expression pattern, given by RT-PCR, was cross-referenced with important stages during the development of the pronephros. For each clone primers were designed to give a PCR product of between 150-400bp (Methods 2.5.4 PCR). The RT-PCR was performed using cDNA prepared from *Xenopus laevis* embryos grown to stages 9, 13, 16½, 21, 26½, 30, 35 and unfertilised eggs (Methods 2.6.2 Reverse Transcription PCR). Furthermore, the relative expression of the clones within the pronephros, or the presumptive pronephric region, compared to the whole embryo was analysed. This was carried out by performing RT-PCR with the cDNA isolated from dissected pronephric tissue along with the whole embryo at stages 12½, 15, 20, 28 and 35 (Methods 2.6.2 Reverse Transcription PCR).

Expression levels in unfertilised eggs represented maternal expression. Of the 9 clones, 5f6, 12a1, 15c7, 41b2 and 18B1 are expressed maternally (Fig. 3.8). In early *Xenopus* development, the majority of zygotic transcription does not occur until the mid-blastula transition. Maternally expressed mRNA therefore plays a critical role in early development until stage 8. This suggests that these clones have a role in early *Xenopus* development.

Clone	T3 sequencing	T7 sequencing
3B5	Human *Sec 23*	*X. laevis CIRP*
6C5	Human *Selenoprotein W*	
18B1	Mouse *VPS28*	
5f6	*X. laevis Skp 1*	
6a4	*X. tropicalis* Vitamin K epoxide reductase complex subunit	
12a1	*X. laevis* Hypothetical protein JC7	
15b2	*X. laevis* NADH dehydrogenase1 alpha subcomplex	
15c7	Human Lysosome-associated membrane glycoprotein 1 precursor	
41b2	*X. laevis FRGY 1*	

Table 3.5 **Complete sequencing of chosen clones.** The clones were sequenced with both the T3 and T7 primers that lay on either end of the cDNA insert. Sequencing of clone 3B5 resulted in 2 different cDNA sequences, suggesting the clone contained two fused cDNA fragments. This clone was not analysed further and is shaded in grey.

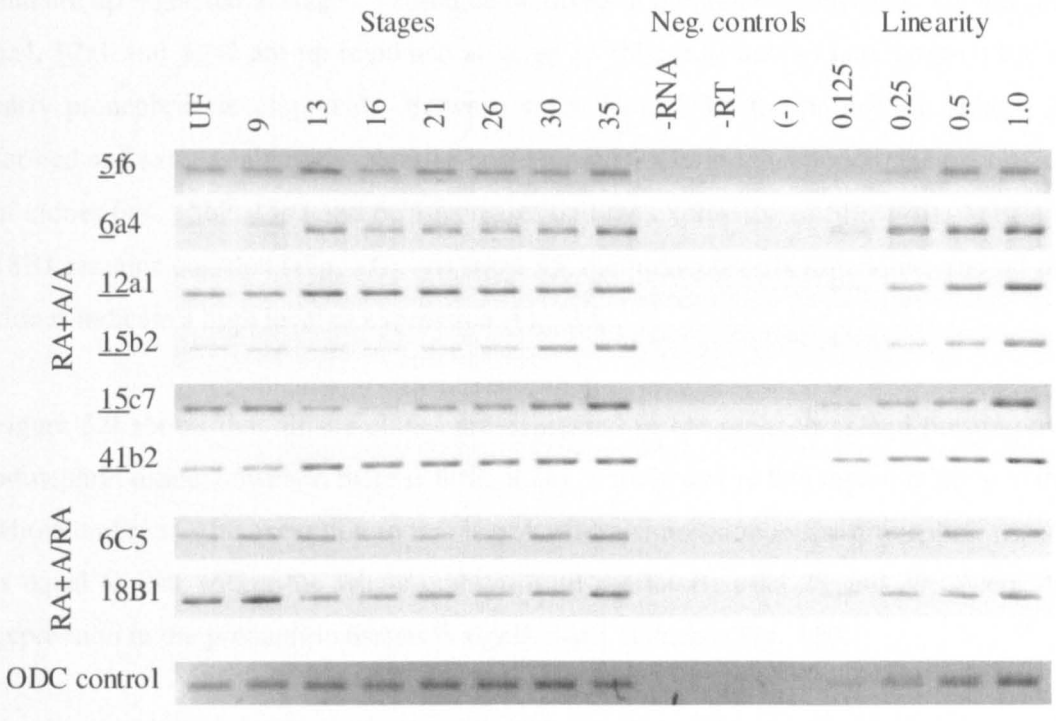

Fig. 3.8 **Temporal expression patterns of clones identified in screens.** RT-PCR analysis of clones identified in the screen. RT-PCR was carried out on embryos of stages from unfertilised eggs to stage 35. Clones are labelled vertically and embryo stages with controls are labelled horizontally. Input cDNA was approximately equalised using the ubiquitously expressed gene *ODC*, and a linearity using doubling dilutions of stage 35 cDNA was performed. Negative controls were (**-RNA**) no RNA in the sample during RT reaction, (**-RT**) no reverse transcriptase in sample during RT reaction and (**-**) no cDNA in PCR reaction.

The specification of the pronephric anlagen has been shown to occur at stage 13. Genes that are up regulated at stage 13 could be involved in pronephros initiation. Clones 5f6, 6a4, 12a1 and 41b2 are up regulated at stage 13 (Fig. 3.8) and so may be involved in early pronephric development. Between stage 16 and 30, the pronephric anlagen is formed and extends along the anterior-posterior axis. During this period, the expression of clones 6a4, 15b2, 15c7 and 6C5 increases and the expression of 5f6, 12a1, 41b2 and 18B1 remains constant (Fig. 3.8). At stage 35, the pronephros is functional, and all the clones indicate a high level of expression (Fig. 3.8).

Figure 3.9 shows that all the clones are expressed in the pronephros and presumptive pronephric tissue, however, there is little, if any, enrichment in this region relative to the whole embryo. The exception to this is 6a4 whose expression in the pronephric tissues is equal to that within the whole embryo until the later stages 28 and 35, where the expression in the pronephric tissues is significantly reduced (Fig. 3.9).

Confirmation of the spatial expression pattern of clones, fully controlled with sense probes

The spatial expression pattern was revealed by wholemount *in situ* hybridisation of an antisense DIG-labelled RNA probe. In addition, a control sense DIG-labelled RNA probe was used to define the amount of non-specific staining present. The sense DIG-labelled RNA probe was made by digesting the plasmid at the 3' end of the insert and transcribing with either T3 or T7 polymerase (Table 3.3). The probes were used for wholemount *in situ* hybridisation with albino (homozygous and heterozygous) *Xenopus laevis* between stages 10 and 42 (Methods).

In situ hybridisation of clone 5f6 shows expression in the neural folds, migrating neural crest and the eye placodes at stages 21 and 25. mRNA expression is first seen in the pronephric tubules at stage 27 and is maintained until stages 35 and 42 (data not shown for stage 42). Other head structures, such as the branchial arches, eye, auditory vesicle and the brain are also stained. The sense control treated embryos are unstained throughout the stages tested and are a good indication of the specificity of the staining observed (Fig. 3.10A).

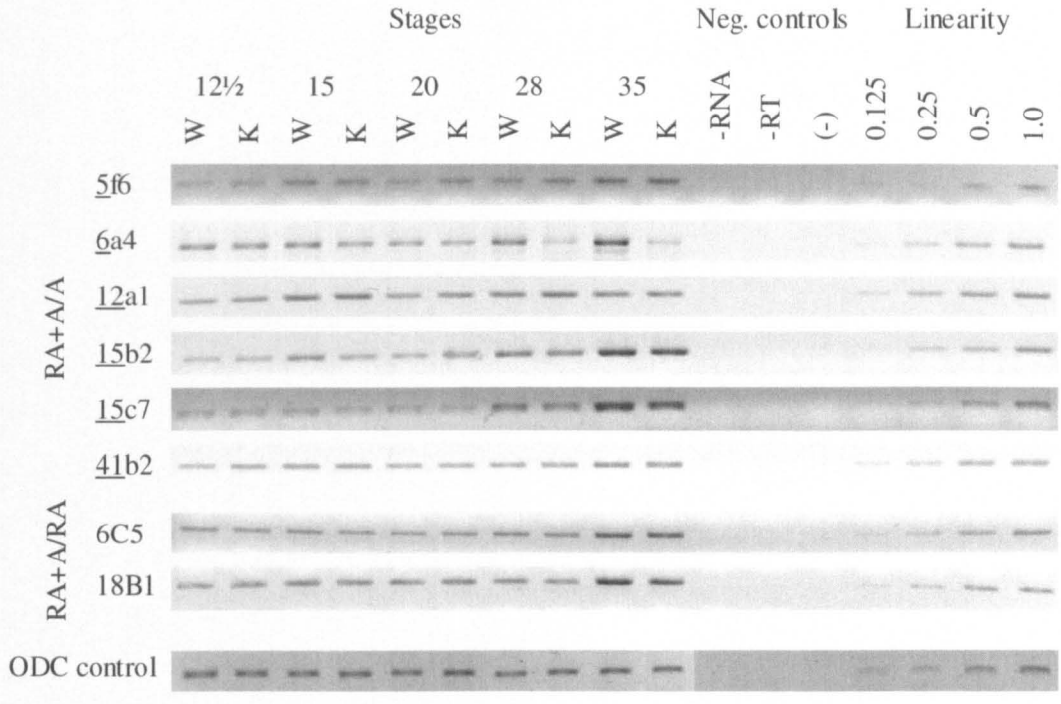

Fig. 3.9 **Comparison of whole embryo and pronephric temporal expression patterns of clones identified in screens.** RT-PCR analysis of identified clones in dissected presumptive pronephros compared to whole embryo. mRNA was extracted from whole embryo (**w**), or dissected pronephric or presumptive pronephric tissue (**k**). Clones are labelled vertically and embryo stages with controls are labelled horizontally. Input cDNA was approximately equalised using the ubiquitously expressed gene *ODC*, and a linearity using doubling dilutions of stage 35 cDNA was performed. Negative controls were (**-RNA**) no RNA in the sample during RT reaction, (**-RT**) no reverse transcriptase in sample during RT reaction and (**-**) no cDNA in PCR reaction.

(A) **5f6**

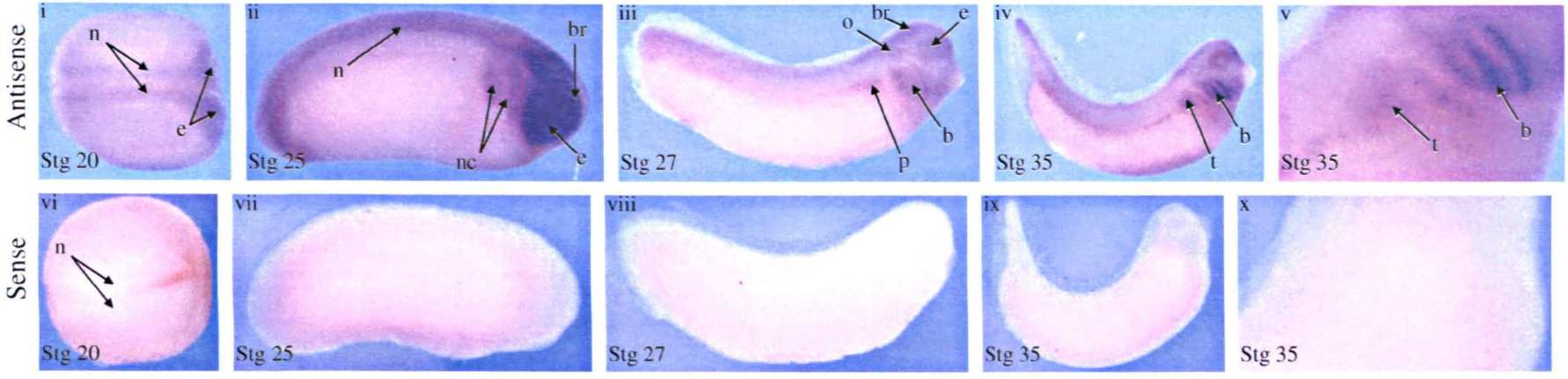
Antisense
Sense
i
n
e
Stg 20
ii
n
br
nc
e
Stg 25
iii
o
br
e
b
p
Stg 27
iv
b
t
Stg 35
v
t
b
Stg 35
vi
n
Stg 20
vii
Stg 25
viii
Stg 27
ix
Stg 35
x
Stg 35

(B) **6a4**

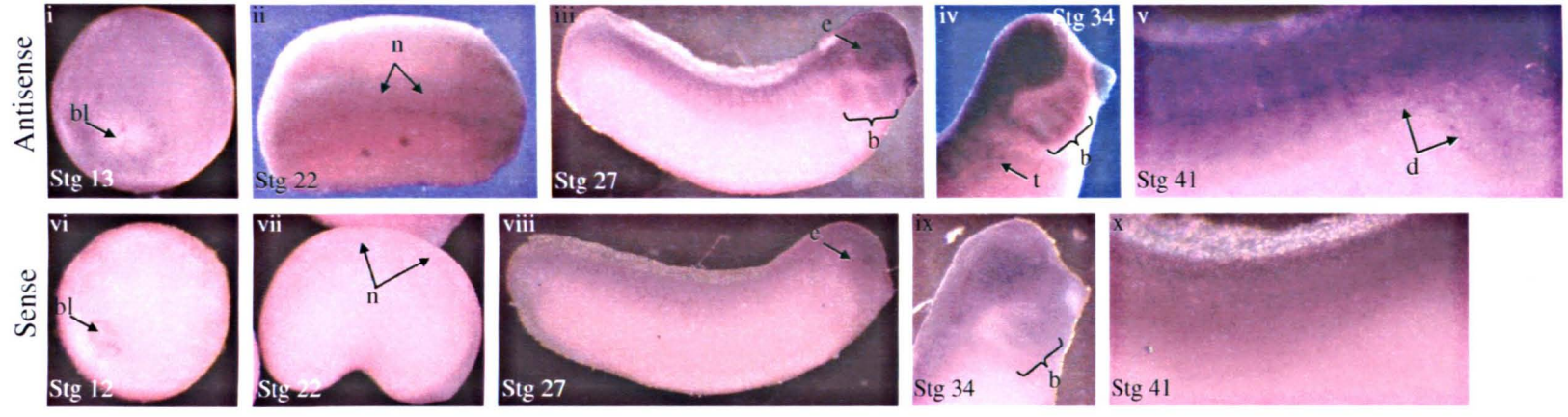
Antisense
Sense
i
bl
Stg 13
ii
n
Stg 22
iii
e
b
Stg 27
iv
Stg 34
b
t
v
d
Stg 41
vi
bl
Stg 12
vii
n
Stg 22
viii
e
Stg 27
ix
b
Stg 34
x
Stg 41

Fig. 3.10 ***In situ* hybridisation analysis of clones 5f6 and 6a4.** *In situ* hybridisation using clones that were identified using the (RA + A/A) probe. Clones were analysed with both antisense and sense RNA probes as indicated. (**A**) Spatial expression of mRNA corresponding to the transcript of the clone **5f6**; (**i**) stage 20 embryos show RNA expression in the eye placodes (**e**) and neural folds (**n**). (**ii**) antisense treated stage 25 embryos with intense staining along the neural folds (**n**), migrating neural crest (**nc**), brain (**br**) and in the eye (**e**). (**iii**) RNA expression seen in the pronephric area (**p**), the branchial arches (**b**), eye (**e**), brain (**br**) and the otic vesicle (**o**) of stage 27 embryos. At stage 35 (**iv** and magnified **v**) it is clear by morphology that the pronephric region stained is the tubules (**t**). The branchial arches (**b**) also show expression. Sense control embryos (**vi, vii, viii, ix** and **x**) are clear throughout all the stages analysed. (**B**) Spatial expression of mRNA corresponding to the transcript of the clone **6a4**; (**i**) RNA expression is present on the whole surface of the stage 13 embryo, except for the blastopore (**bl**). There is no sense control staining at stage 12 (**vi**). At stage 22 there is antisense probe staining along the neural folds (**n**) and the anterior region of the embryo, which are not present with the sense probe treated embryos (**vii**). Stage 27 embryos (**iii**) reveal staining in the branchial arches (**b**) and the eye (**e**), although the eye staining (**e**) is not distinct from the sense control embryo (**viii**). The 6a4 RNA is clearly visible in the tubules (**t**) at stage 34 (**iv**). The branchial arch (**b**) staining visible at stage 34 is present both in the antisense (**iv**) and sense (**ix**) treated embryos. Stage 41 (**v**) reveals RNA expression in the duct (**d**), not seen in the sense embryos (**x**).

Clone 6a4 expression is present on the whole surface of the stage 13 embryo, except for the blastopore corresponding to ectodermal structures. There is no sense control staining at stage 12. At stage 22 there is antisense probe staining along the neural folds and the anterior region of the embryo, which is not present with the sense probe treated embryos. Stage 27 embryos reveal staining in the branchial arches and the eye, although the eye staining is not distinct from the sense control embryo. The 6a4 RNA is clearly visible in the tubules at stage 34. The branchial arch staining visible at stage 34 and is present both in the antisense and sense treated embryos. Stage 41 reveals RNA expression in the duct which is not seen in the sense control embryos (Fig. 3.10B).

Clone 12a1 has strong expression in the eye placodes and in the migrating neural crest cells which are not visible in the sense control embryos. At stage 28 there is a high level of expression in the head, branchial arches and the pronephric region. The pronephric expression is still present at stage 36, but not stage 41. The sense treated embryos are unstained at stages 28, 36 and 41 (Fig. 3.11A).

In situ hybridisation using clone 15b2 gives little staining until stage 21-25, where the migrating neural crest cells, the eye placode and the somites are stained (data not shown). Pronephric expression is first identified at stage 27 and is apparent throughout the whole pronephric region. All three components of the pronephros are stained in late tadpole stages. The head region and the somites are strongly stained in all the stages tested. The sense control embryos are unstained suggesting there is little unspecific background staining (Fig. 3.11B).

Clone 15c7 RNA expression is present in the blood islands at stage 21-29. Expression is also seen in the pronephric tubules from stage 29 to stage 42, the last stage tested (data not shown). The sense control embryos are clear, suggesting high probe specificity (Fig. 3.12A).

In situ hybridisation of clone 41b2 illustrates expression in the ectoderm in all the stages analysed before stage 35 where expression is seen in the endoderm. Pronephric expression is seen between stages 25 and 29, although it is unclear what region within the pronephros is stained. Other areas of expression include the migrating neural crest

(A) **12a1**

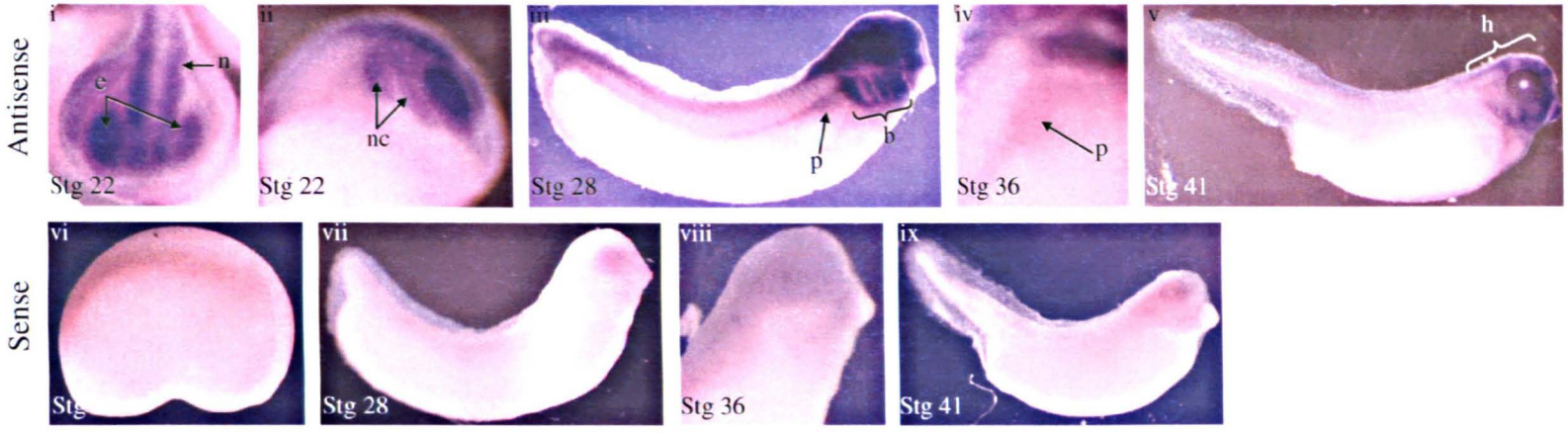
Antisense
i
e
n
Stg 22
ii
nc
Stg 22
iii
p
b
Stg 28
iv
p
Stg 36
v
h
Stg 41
Sense
vi
Stg
vii
Stg 28
viii
Stg 36
ix
Stg 41

(B) **15b2**

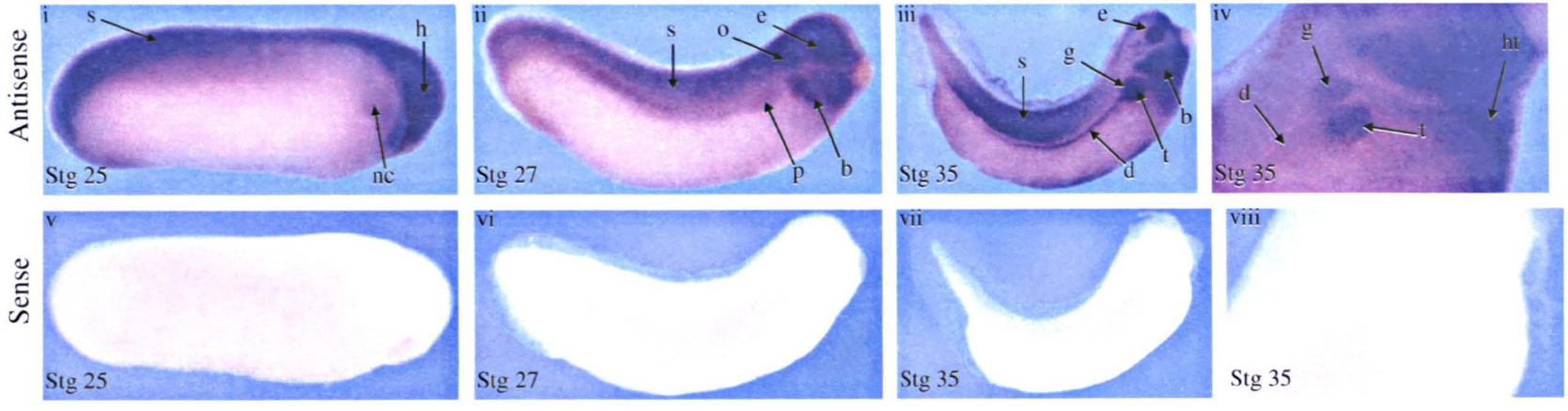
Antisense
i
s
h
nc
Stg 25
ii
s
o
e
p
b
Stg 27
iii
e
s
g
b
t
d
Stg 35
iv
g
ht
d
t
Stg 35
Sense
v
Stg 25
vi
Stg 27
vii
Stg 35
viii
Stg 35

Fig. 3.11 ***In situ* hybridisation analysis of clones 12a1 and 15b2.** *In situ* hybridisation using clones that were identified using the (RA + A/A) probe. Clones were analysed with both antisense and sense RNA probes as indicated. (**A**) Spatial expression of mRNA corresponding to the transcript of the clone **12a1**; (**i** and **ii**) there is strong expression in the eye placodes (**e**) and in the migrating neural crest cells (**nc**) which is not visible in the sense control embryos (**vi**). At stage 28 (**iii**) there is a high level of expression in the head (**h**), branchial arches (**b**) and the pronephric region (**p**). The pronephric expression is still present at stage 36 (**iv**), but not stage (**v**). The sense treated embryos are clear at stages 28, 36 and 41 (**vii, viii, ix**). (**B**) Spatial expression of mRNA corresponding to the transcript of the clone **15b2**; At stage 25 (**i**) there is staining in the migrating neural crest cells (**nc**), the head (**h**) and the somites (**s**). Expression is seen in the pronephros (**p**), branchial arches (**b**), somites (**s**), eye (**e**) and otic vesicle (**o**) in stage 27 embryos (**ii**). Later tailbud staining (**iii** and magnified **iv**) reveals continued strong expression in all three components of the pronephros, the glomus (**g**), the tubules (**t**) and the duct (**d**) and in the heart (**ht**). The sense embryos are completely clear in all the stages analysed (**v, vi, vii** and **viii**).

(A) **15c7**

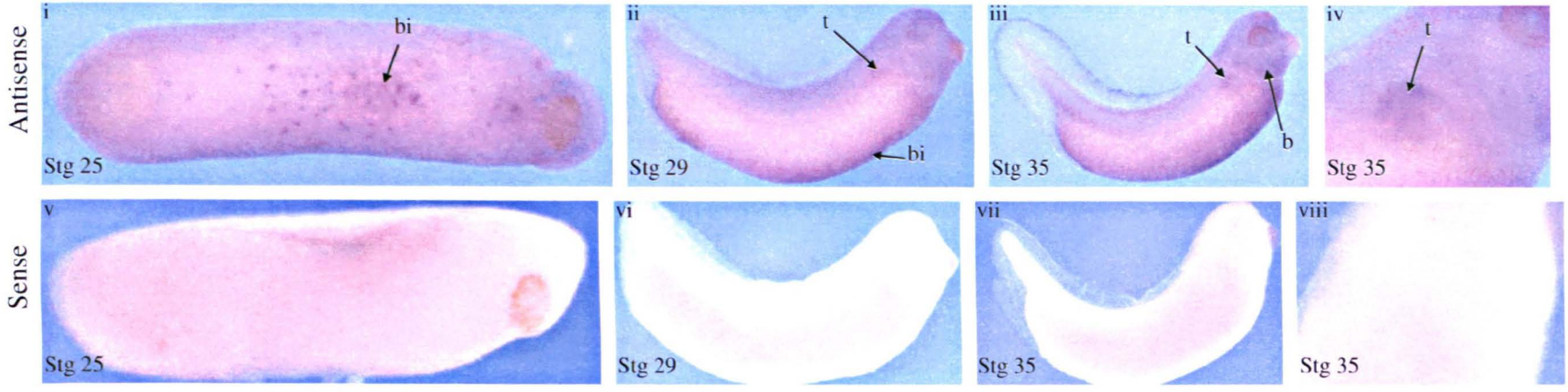
Antisense
Sense
i
bi
Stg 25
ii
t
bi
Stg 29
iii
t
b
Stg 35
iv
t
Stg 35
v
Stg 25
vi
Stg 29
vii
Stg 35
viii
Stg 35

(B) **41b2**

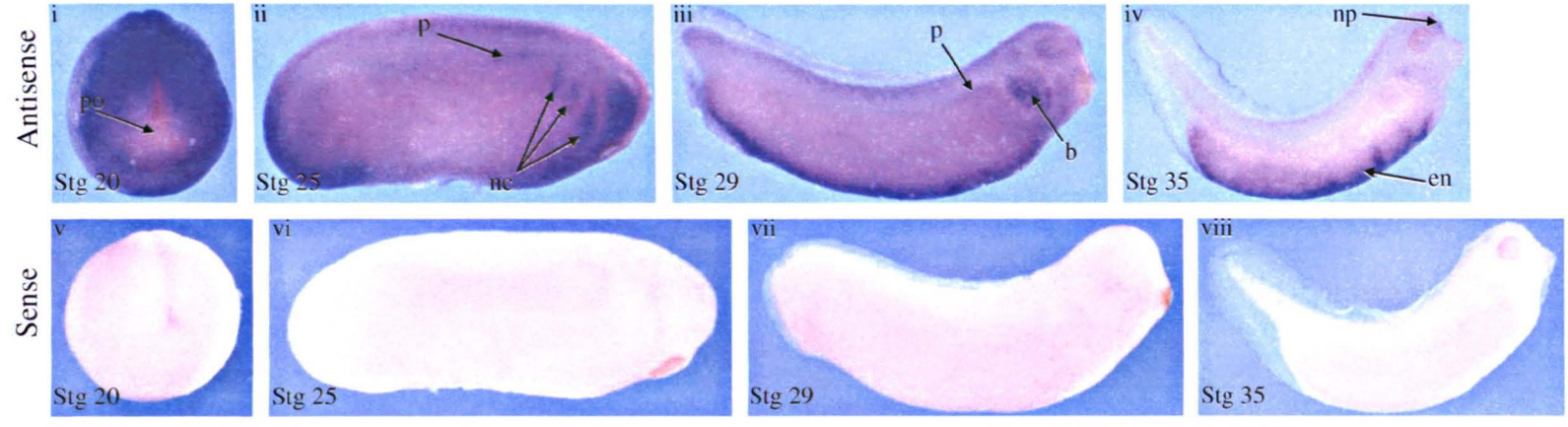
Antisense
Sense
i
po
Stg 20
ii
p
nc
Stg 25
iii
p
b
Stg 29
iv
np
en
Stg 35
v
Stg 20
vi
Stg 25
vii
Stg 29
viii
Stg 35

Fig. 3.12 ***In situ* hybridisation analysis of clones 15c7 and 41b2.** *In situ* hybridisation using clones that were identified using the (RA + A/A) probe. Clones were analysed with both antisense and sense RNA probes as indicated. (**A**) Spatial expression of mRNA corresponding to the transcript of the clone **15c7**; (**i,** ventral view) stage 25 antisense treated embryos show RNA expression in the blood islands (**bi**), not present in the sense control treated embryos (**v,** ventral view). At stage 29 (**ii**) RNA expression is seen in the pronephric tubules (**t**) and the blood islands (**b**). Stage 35 embryos (**iii** and magnified **iv**) indicate RNA expression in the tubules (**t**) and the branchial arches (**b**). No staining was observed in the sense control treated embryos (**v, vi, vii** and **viii**). (**B**) Spatial expression of mRNA corresponding to the transcript of the clone **41b2**; Stage 11 embryos have staining visible around the whole embryo, excluding the blastopore (data not shown). (**i**) this ectoderm patterning is continued at stage 20, where the whole embryo appears stained, with the exception of the posterior most point (**po**). Stage 25 (**ii**) embryos show RNA expression in the pronephric area (**p**) and migrating neural crest cells (**nc**) as well as a general expression all over the embryo. The antisense probe at stage 29 (**iii**) has labelled the pronephric area (**p**), and the branchial arches (**b**) and the epidermis. Expression is observed in the endoderm (**en**) and the nasal pit (**np**) of stage 35 embryos (**iv**). The sense embryos are completely clear in all the stages analysed (**v, vi, vii** and **viii**).

and in late tail bud stages, the nasal pit. There is no apparent sense control staining in any of the stages tested (Fig. 3.12B).

The spatial expression pattern of clone 6C5, as determined by *in situ* hybridisation, is in the brain and the eye from stages 27 to 31. At stage 39, there is no unique staining on the antisense treated embryos that is not also seen in the sense treated embryos (Fig. 3.13A).

In situ hybridisation with antisense clone 18B1 reveals little expression until stage 25 where embryos indicate expression in the head. Antisense probe treated embryos staged 28 to 42 (data not shown for stage 42) show staining in the pronephric tubules, the head region and the notochord. The sense treated embryos do not have any staining and so suggest the antisense probe is highly specific (Fig. 3.13B).

3.3. Discussion: Screening of a stage 13 cDNA phagemid library with a subtracted probe

The aim of this work was to identify new genes with a potential role in pronephros development. The work in this chapter describes a screen of a stage 13 cDNA phagemid library using subtracted probes made from animal caps treated with retinoic acid and activin A individually and in combination.

From the 71 preliminary positive plaques (Massé, unpublished), 8 positive clones were chosen for further analysis. Clone 5f6, identified as *Skp 1*, is a transcription factor specifically involved in the RNA polymerase II transcription complex. Knock down analysis by RNA inhibition results in early embryonic arrest in *C. elegans* (Kostrouchova, *et al.*, 2002), suggesting a critical role in development. The RT-PCR findings are therefore unsurprising, showing a constant level of expression at all stages tested. The spatial expression pattern revealed by wholemount *in situ* hybridisation suggests expression in the pronephric tubules from stage 27. The specificity of *Skp 1* expression in the pronephric tubules, together with an identified developmental role in *C. elegans*, suggests a possible role in development which would make it an attractive gene for further analysis.

(A) **6C5**

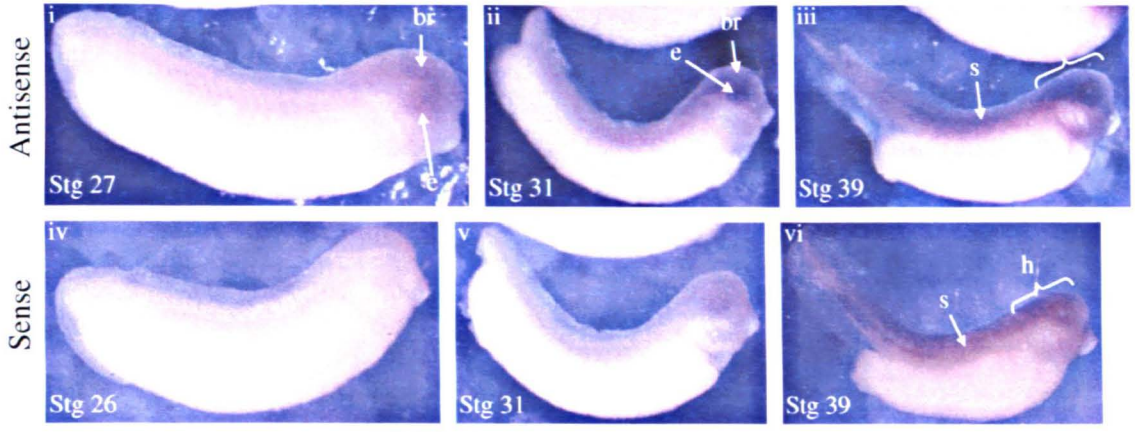
Antisense
Sense
i
br
e
Stg 27
ii
br
e
Stg 31
iii
s
h
Stg 39
iv
Stg 26
v
Stg 31
vi
s
h
Stg 39

(B) **18B1**

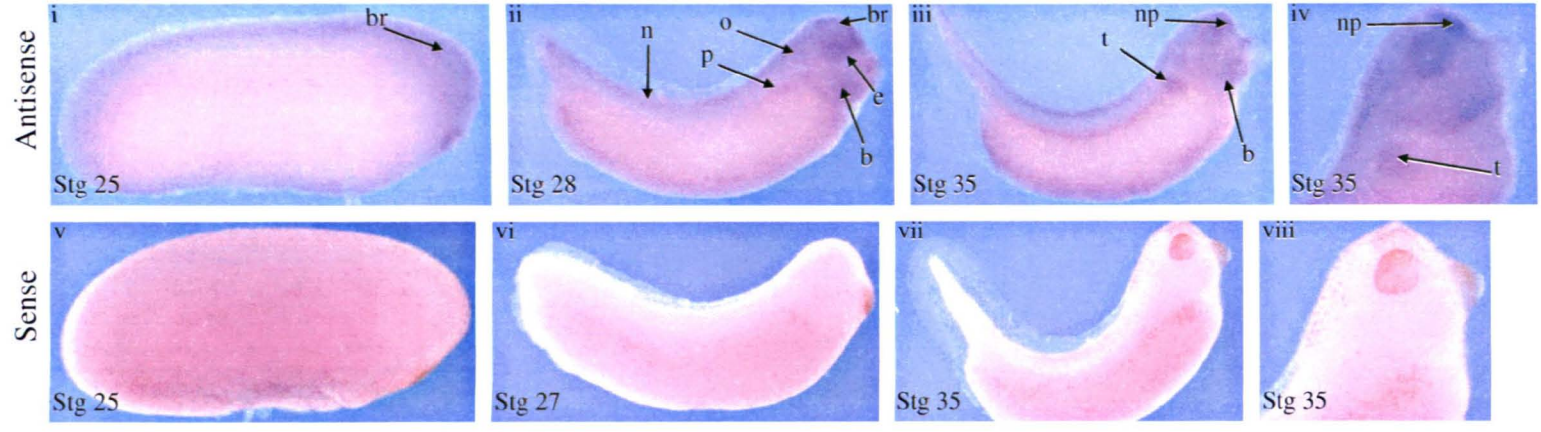
Antisense
Sense
i
br
Stg 25
ii
n
o
p
br
e
b
Stg 28
iii
np
t
b
Stg 35
iv
np
t
Stg 35
v
Stg 25
vi
Stg 27
vii
Stg 35
viii
Stg 35

Fig. 3.13 ***In situ* hybridisation analysis of clones 6C5 and 18B1.** *In situ* hybridisation using clones that were identified using the (RA + A/A) probe. Clones were analysed with both antisense and sense RNA probes as indicated. (**A**) Spatial expression of mRNA corresponding to the transcript of the clone **6C5**; From stages 27 to 31 (**i, ii**), there is staining with the antisense probe in the brain (**br**) and the eye (**e**) which is not present in the sense control embryos (**iv, v**). At stage 39 staining is present in the somites (**s**) and the head (**h**) of both antisense, **iii**, and sense probe, **vi**, treated embryos. (**B**) Spatial expression of mRNA corresponding to the transcript of the clone **18B1**; The brain (**b**) is highlighted in stage 25 antisense embryos (**i**). Stage 28 (**ii**) antisense probe treated embryos show expression in the pronephros (**p**), notochord (**n**), brain, (**br**), otic vesicle (**o**), eye (**e**) and the branchial arches (**b**). Later tail bud embryos (**iii** and magnified **iv**) show RNA expression in the tubules (**t**), branchial arches (**b**) and the nasal pit (**np**). Sense control embryos are clear in all the stages tested (**v, vi, vii** and magnified **viii**).

Clone 6a4 encodes a hypothetical protein, LOC398467, UniGene xl.21907. A revised BLAST on the NCBI website (www.ncbi.nlm.nih.gov/BLAST/) (Basic Local Alignment Search Tool, Altschul, *et al.*, 1990) search revealed 83% identity to the *X. tropicalis vitamin K epoxide reductase complex, subunit 1.* Vitamin K epoxide reductase complex is the enzyme responsible for reducing and so activating vitamin K 2,3-epoxide in blood clotting. It is found predominantly in the liver, but can also be found in the kidney (Thijssen, *et al.*, 1986). Kidney, liver and blood tissues of *Xenopus laevis* originate from the mesodermal layer of the embryo. It is therefore surprising that expression is seen in the ectodermal layer of the gastrula. Pronephric expression of this gene is detected around the time the kidney first begins to function, in late tail bud embryos. Expression may therefore be induced as the tissue begins to function. If this is the case, expression within the liver would be expected from stage 42 as the liver bud grows.

Clone 12a1 encodes a sequence identified as the *Xenopus* UniGene cluster xl.15910 coding for the hypothetical protein JC7. A revised search of this UniGene cluster revealed a 56.08% amino acid identity to the rat nuclear ubiquitous casein kinase 2. Nuclear ubiquitous casein kinase 2 is involved in cell growth, proliferation and survival (Yu, *et al.*, 2001). The high level of expression, therefore, observed during the embryo stages tested could be due to the high level of cell growth and proliferation during *Xenopus* development. Nuclear ubiquitous casein kinase 2 may also have a role in neural crest cell development as the strong expression seen in the migrating neural crest cells was followed through to some neural crest containing tissues, the branchial arches, brain and pronephros.

Searches using the clone 15b2 sequence identified the clone as the *Xenopus NADH dehydrogenase 1 alpha subcomplex*, rather than the *Bos taurus similar to NADH dehydrogenase*. Although an important respiratory mitochondrial protein, and therefore expected to be ubiquitous, wholemount *in situ* hybridisation show strong expression in the developing tail bud pronephros. Expression is seen, however, in many actively developing tissues and is relatively absent from the undeveloped endoderm until later stages. Expression appears to be only present in tissues undergoing high energy requiring processes as anticipated of a respiratory mitochondrial protein.

A revised search using clone 15c7 sequence identified hypothetical protein MGC80798, UniGene xl.24149. The hypothetical protein has approximately 40% amino acid similarity with lysosome-associated membrane glycoprotein 1 precursor, a protein involved in intracellular transport and spermatogenesis (Falcon-Perez, *et al.*, 2005 and Moreno, 2003). Wholemount *in situ* hybridisation indicates specific expression in the blood islands and the pronephric tubules. The temporal expression pattern does not align with pronephric development and so is unlikely to play any role in the development of this organ.

Clone 41b2 encodes *Xenopus FRGY1*, an activational Y box transcription factor. *FRGY1* is believed to be a ubiquitous transcription factor providing basal levels of transcriptional activity for the transcription factor IIIA gene in somatic cells (Tafuri and Wolffe, 1990 and Ranjan, *et al.*, 1993). Northern analysis demonstrated up-regulation of mRNA in developing oocytes, however translation was repressed. *FRGY1* mRNA was found to be stored in mRNP storage particles and then transported to the ribosomes prior to transcriptional activation of the zygotic genome (Tafuri and Wolffe, 1993). Northern analysis also showed up-regulation during gastrulation, which was confirmed in this study by RT-PCR analysis, however there was no enrichment in the pronephric tissues. Northern analysis of adult *Xenopus* organs indicated high expression in the metanephros (Tafuri and Wolffe, 1990), although in this work pronephric expression was only seen in the mid tail bud stages, not later, by whole-mount *in situ* hybridisation.

Clone 6C5, human *Selenoprotein W*, is a selenium incorporated protein important in muscle metabolism and immune response (Brown and Arthur, 2001). Wholemount *in situ* hybridisation reveals little staining suggesting that this gene plays little role in development and may be a false positive from the screen.

Clone 18B1 encodes VPS28, a class E vacuolar sorting protein involved in intracellular transport (Rieder, 1996). Of the clones resulting from the screen, clone 18B1 is the only clone to down regulate at stage 13, making it unlikely to be involved in pronephric induction. Wholemount *in situ* hybridisation analysis however, indicates very specific late expression in the pronephric tubules which could indicate a role in development or tubule function.

Despite the clones originating from a stage 13 cDNA library, wholemount *in situ* hybridisation analysis suggested few of the clones were expressed at stage 13 at significant levels (data not shown). The RT-PCR data indicates that all clones are expressed at stage 13. This demonstrates the relative insensitivity of the wholemount *in situ* hybridisation to RT-PCR, as a method of detecting mRNA transcripts.

Not all clones identified in the screen were expressed in the pronephros. The clones resulting from the screen were expressed during retinoic acid and activin A treatment in animal caps. This combined treatment of retinoic acid and activin A in animal caps does not only induces pronephric tissues, but also anterior and posterior neural tissue, cardiac tissue and pancreatic tissues (Haldin, *et al.*, 2003 and Moriya, *et al.*, 2000). Therefore, although it is expected that a high proportion of these genes are expressed in the pronephros, not all genes identified in such a screen will be. Furthermore, the screen does not account for the down regulation of genes. If any of the animal cap treatments were to down regulate a gene, then it may be picked up by the probes as a false positive.

None of the clones in the screen were expressed uniquely in the pronephros, as revealed by wholemount *in situ* hybridisation analysis. However, all the clones were expressed in the pronephros, shown by RT-PCR, and, except 18B1, were up regulated at stage 13. The pronephric expression, however, was not enriched, as compared to the whole embryo. For these reasons, it is unlikely that the clones resulting from the screen are specific pronephric development genes and were not analysed further by mis-expression experiments in this work.

During the course of this work the wholemount *in situ* hybridisation protocol was refined. Earlier methods (Methods 2.6.4 Wholemount *in situ* hybridisation) resulted in a high level of background staining as indicated by the hybridisation of control sense DIG-labelled RNA probe. The clones highlighted in this screen were all analysed using the original whole-mount *in situ* hybridisation protocol. The high level of background masked the true expression pattern of some of these clones. *In situ* hybridisation was repeated using the new protocol and for some of the clones (18B1, 5f6, 15b2, 15c7 and 41b2) the expression patterns were greatly improved. The expression patterns shown in this work include the improved data. Therefore, although some of the clones, 18B1 and

5f6, appear to be ideal candidates for further analysis, they were not chosen in the early stages of this work based on the information available at the time.

Chapter 4

Analysis of potential pronephric UniGene cluster genes

4.1 Introduction

The second method of identifying potential pronephric development genes was to analyse four UniGene cluster genes that had previously been found to be expressed in the pronephros. These UniGene cluster genes were selected using wholemount *in situ* hybridisation on stage 27 *Xenopus laevis* embryos using an EST from the cluster (Personal communication from Pollet, N.).

The NCBI UniGene site

The UniGene site, part of the National Center for Biotechnology Information service (www.ncbi.nlm.nih.gov), automatically groups submitted EST sequences into a non-redundant set of gene-oriented clusters (Wheeler, *et al.*, 2005). The system was used to find unique genes by aligning EST sequences using statistically significant sequence similarity in the 3' UTR and identifying gene sequence characteristics. Related EST sequences were classed under one UniGene cluster. UniGene clusters were also generated containing EST sequences that contain possible homologous genes across organisms. Today, more than 26,980 3'-anchored *Xenopus* UniGene clusters exist, a number which is updated every 2 months. The UniGene sets are put into a public searchable database (www.ncbi.nlm.nih.gov), which contains other relevant gene centred information, such as homologies and expression profiles.

UniGene cluster gene analysis

4 UniGene cluster genes were identified by N. Pollet (Faculte de Medicine, Universite de Rennes, Rennes, France) as having a distribution that included the pronephros. We were kindly given the UniGene cluster numbers for these clones. The spatial expression pattern of the UniGene cluster genes was analysed using wholemount *in situ* hybridisation with a representative EST, at a variety of embryonic stages using both antisense and control sense DIG-labelled RNA probes. In addition, the temporal expression pattern was elucidated by RT-PCR using RNA from various stages of whole embryo and pronephric tissue.

4.2 Results: Temporal and Spatial expression patterns of UniGene cluster genes

The UniGene cluster genes whose expression included the pronephros (Personal correspondence from Pollet, N.), are numbered xl.5110, xl.5983, xl.12848 and xl.16795. The preliminary wholemount *in situ* hybridisation data carried out in France showed that UniGene cluster genes xl.5110 and xl.5983 are expressed in the pronephric tubules and xl.12848 and xl.16795 are expressed in the glomus of early tail bud embryos. In this study, the temporal and spatial expression patterns of the UniGene cluster genes were analysed by RT-PCR and wholemount *in situ* hybridisation, using a representative EST, to confirm and further elucidate their roles in pronephric development.

Temporal expression patterns of UniGene cluster genes

RT-PCR was used to investigate the expression of UniGene cluster genes during important stages in the development of the pronephros. Primers were designed to give PCR products of between 150-400bp using a representative EST for each UniGene cluster gene (Methods Table 2.1). The ESTs representing the UniGene cluster genes were chosen to cover the whole coding sequence and the maximum amount of 3' UTR. Primers were designed to incorporate 3' UTR where possible to increase PCR specificity. The cDNA used in the RT-PCR was prepared from *Xenopus laevis* embryos grown to stages 9, 13, 16, 21, 26, 30, 35 and unfertilised eggs (Methods 2.6.2 RT-PCR). The relative expression of the UniGene cluster genes within the pronephros, or the presumptive pronephric region, compared to the whole embryo was analysed. This was carried out by performing RT-PCR with the cDNA isolated from dissected pronephric tissue along with the whole embryo at stages 12½, 15, 20, 28 and 35 (Methods 2.6.2 RT-PCR).

All of the selected UniGene cluster genes were found to be expressed in unfertilised eggs and were therefore maternally expressed (Fig. 4.1). As the majority of transcription does not occur until the mid-blastula transition, maternal expression plays a critical role in early development until stage 7-8. This suggests that these UniGene cluster genes may have a role in directing the earliest stages of *Xenopus* development. Development of the three components of the pronephros are initiated at stage 13-14. Genes that are up regulated in this region at stage 13 may be involved in pronephros

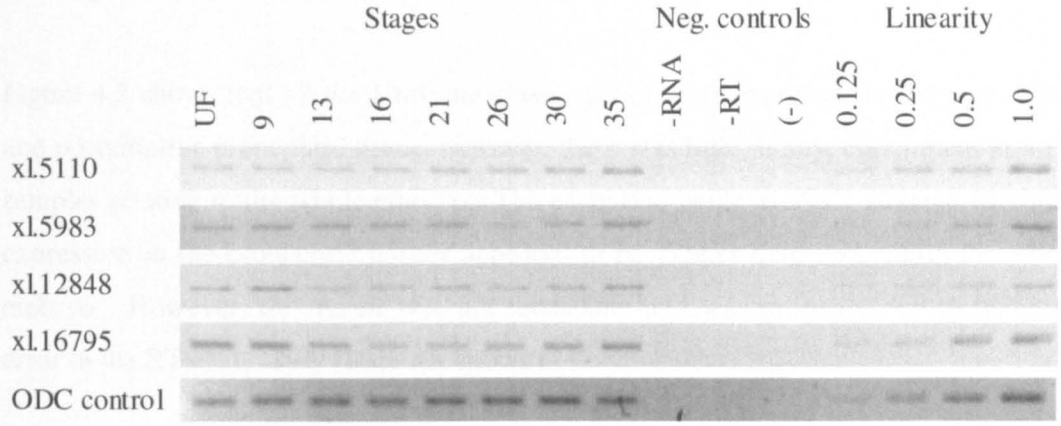

Fig. 4.1 **Temporal expression patterns of selected UniGene cluster genes.** RT-PCR analysis of UniGene cluster gene expression in an embryo stage series. RT-PCR was carried out on embryos of stages from unfertilised eggs to stage 35. UniGene cluster genes are labelled vertically and embryo stages with controls are labelled horizontally. Input cDNA was approximately equalised using the ubiquitously expressed gene *ODC*, and a linearity using doubling dilutions of stage 35 cDNA was performed. Negative controls were (**-RNA**) no RNA in the sample during RT reaction, (**-RT**) no reverse transcriptase in sample during RT reaction and (-) no cDNA in PCR reaction.

initiation. Between stages 16 and 30, the pronephric anlagen is formed and extends along the anterior-posterior axis and at stage 35, the pronephros is functional. It is expected that the temporal expression pattern of a gene involved in pronephric development would alter at these stages. The temporal expression of the 4 UniGene cluster genes, however, remained constant throughout the stages tested (Fig. 4.1).

Figure 4.2 shows that all the UniGene cluster genes were expressed in the pronephros and presumptive pronephric tissue, however, there was little, if any, enrichment in these samples relative to the whole embryo. The exception being xl.5983, at stage 28 where expression in the pronephric tissues appeared to be greater than that within the whole embryo. However, this result was not repeatable and was probably due to pipetting error in the RT-PCR assay (Data not shown).

Spatial expression patterns of UniGene clusters

An EST from the database was chosen for each of the UniGene cluster genes which included a ATG and a stop sequence, thus including the full length coding region. This EST was then acquired from the IMAGE consortium (http://image.llnl.gov/). Table 4.1 includes the details of the clones ordered.

Wholemount *in situ* hybridisation was used to analyse the spatial expression patterns of the selected UniGene cluster genes. Both antisense and sense RNA DIG labelled probes were used on *Xenopus* albino (homozygous and heterozygous) embryo stages 10 to 41 (Methods 2.6.4 Wholemount *in situ* hybridisation). The antisense probes were made by digesting the IMAGE plasmids at the 5' end of the EST insert and transcribing with either SP6, T3 or T7 polymerase (Table 4.1). Similarly, the sense probes were made by digesting the IMAGE plasmids at the 3' end of the EST insert and transcribing with either SP6, T3 or T7 polymerase (Table 4.1).

Wholemount *in situ* hybridisation investigation of UniGene cluster gene xl.5110 (represented by EST BE508547) revealed expression in the neural folds and the eye placodes of stage 20 embryos. In mid tail bud stages, expression was seen in the somites, the eye and the adhesive organ. The first indication of pronephric expression was in the tubules at stage 31 and continued to stage 39. The control sense probe

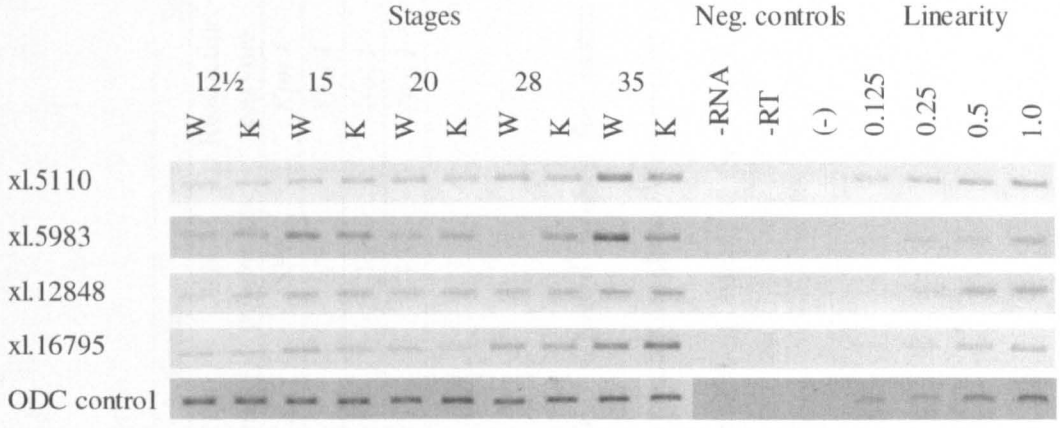

Fig. 4.2 **Temporal expression patterns of selected UniGene clusters genes in dissected kidney anlagen.** RT-PCR analysis of UniGene cluster gene expression in dissected presumptive pronephros compared to whole embryo. mRNA was extracted from whole embryo (**w**), or dissected pronephric or presumptive pronephric tissue (**k**). UniGene cluster genes are labelled vertically and embryo stages with controls are labelled horizontally. Input cDNA was approximately equalised using the ubiquitously expressed gene *ODC,* and a linearity using doubling dilutions of stage 35 cDNA was performed. Negative controls were (**-RNA**) no RNA in the sample during RT reaction, (**-RT**) no reverse transcriptase in sample during RT reaction and (-) no cDNA in PCR reaction.

				Antisense		Sense	
UniGene Cluster	GenBank EST	IMAGE number	Plasmid	Restriction enzyme	RNA polymerase	Restriction enzyme	RNA polymerase
xl.5110	BE508547	3397387	pCMV-SPORT6	*Spe I*	SP6	*Kpn I*	T7
xl.5983	BC043955	5571335	pCMV-SPORT6	*Kpn I*	T7	*Xho I*	SP6
xl.12848	CA974150	6326648	pBLUESCRIPT SK	*Kpn I*	T3	*Not I*	T7
xl.16795	CA981992	6870563	pBLUESCRIPT SK	*Kpn I*	T3	*Not I*	T7

Table 4.1 **IMAGE consortium data and preparation of antisense and sense RNA DIG labelled probes for initial wholemount *in situ* hybridisation**. UniGene clusters, chosen representative EST sequences and IMAGE consortium data. Wholemount *in situ* hybridisation was performed using antisense DIG labelled RNA probe. The probes were made by digesting the plasmids at the 5' or 3' end of the EST insert and transcribing with either SP6, T3 or T7 polymerase as shown.

treated embryos showed little staining, implying minimal background colouring (Fig. 4.3A).

The expression of UniGene cluster gene xl.5983 (represented by EST BC043955) was not visible by wholemount *in situ* hybridisation until stage 30, where it was observed in the glomus, eye socket, and adhesive organ. Later tail bud embryos displayed continued expression in the glomus and eye with additional expression in the branchial arches. Background, indicated by control sense probe analysis, was present in the eye, suggesting the eye staining may be unspecfic (Fig. 4.3B).

Spatial expression pattern analysis of UniGene cluster gene xl.12848 (represented by EST CA974150) revealed expression in the tubules, eye, auditory vesicle and branchial arches of stage 28 embryos when cleared. Pronephric tubule expression is continued to stage 39 where low level expression is also seen in the pronephric duct. Control sense probe treated embryos showed staining in the eye, suggesting that the eye staining is non-specific (Fig. 4.4A).

Wholemount *in situ* hybridisation using UniGene cluster gene xl.16795 (represented by EST CA981992) revealed expression in the eye placodes and neural folds of stage 20 embryos. Expression was seen in the brain and eye of tail bud embryos. Pronephric staining was only weakly present in late tail bud embryos. Background staining was minimal, as indicated by control sense probe staining (Fig. 4.4B).

4.3 Discussion: Potential future analysis of UniGene cluster genes

The UniGene cluster numbered xl.5110 consists of one EST, BE508547, that has homology to the *Arabidopsis* extensin-like protein (32.45 % amino acid similarity) (www.ncbi.nlm.nih.gov). The initial wholemount *in situ* hybridisation indicated expression in the pronephric tubules and brain in early tail bud embryos. The pronephric tubule expression was confirmed and appears between stage 25 and 30 (Fig. 4.3A). The temporal expression of the UniGene cluster gene remained constant throughout the stages tested and was unchanged during important events in pronephric development (Fig. 4.1). Comparative pronephric and whole embryo RT-PCR indicated

(A) **xl.5110**

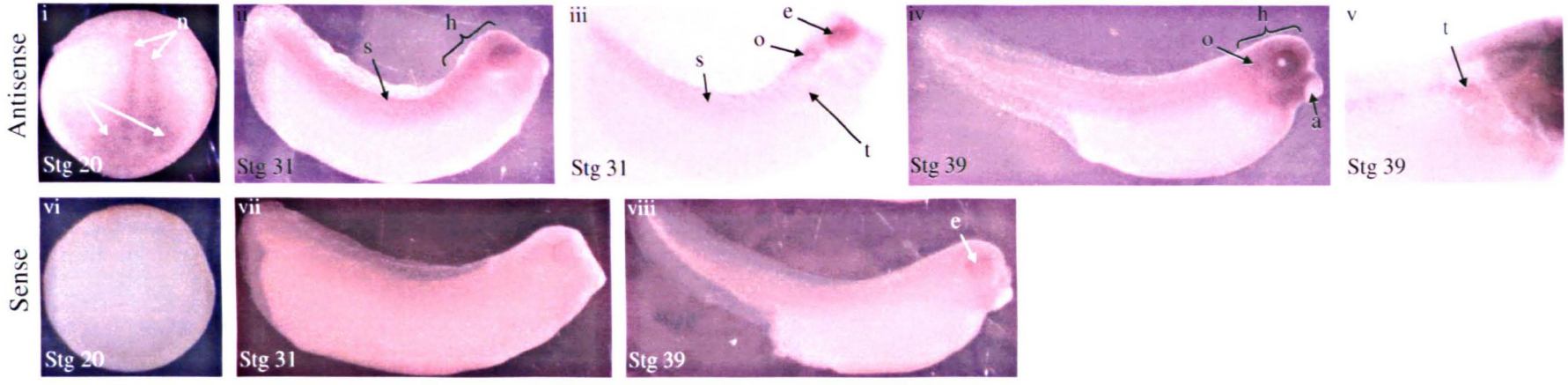

(B) **xl.5983**

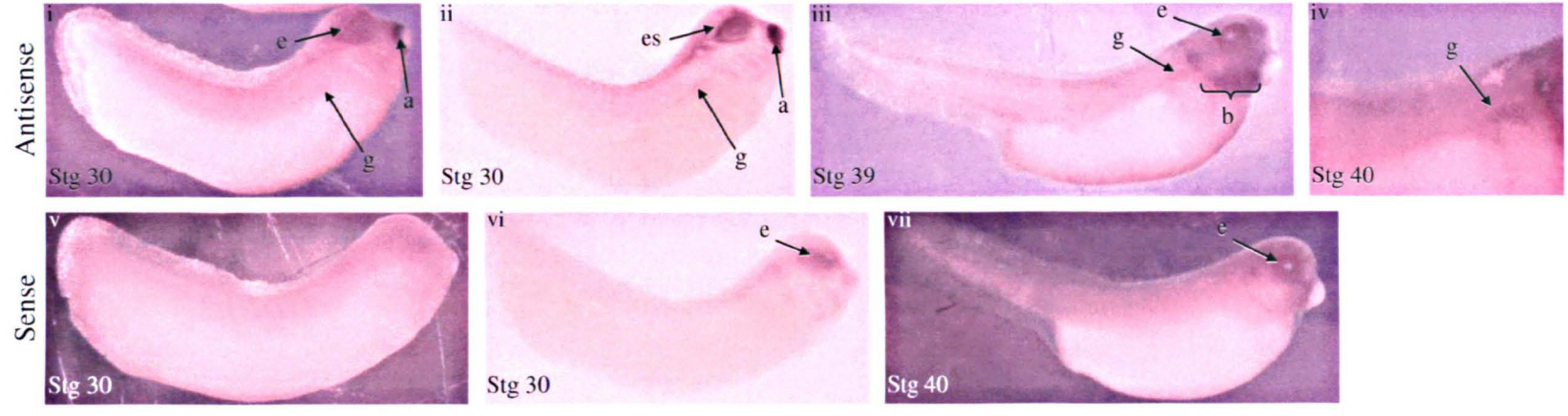

Fig. 4.3 ***In situ* hybridisation analysis of UniGene cluster genes xl.5110 and xl.5983.** *In situ* hybridisation of UniGene cluster genes. DIG-labelled RNA probes were made using representative ESTs and were either antisense or sense as indicated. (**A**) Spatial expression of mRNA transcribed from EST BE508547 representing UniGene cluster gene **xl.5110**; Antisense probe staining is observed in the neural folds, **n** and the eye placodes, **e**, of stage 20 embryos (**i**). At stage 31, uncleared embryos (**ii**) show expression in the somites, **s** and the head region, **h**, including the eye and the brain (**ii**). Cleared stage 31 embryos (**iii**) indicate additional expression in the tubules, **t** and the otic vesicle, **o**. Later at stage 39 (**iv**, magnified and cleared **v**), embryos continue to have staining in the head region, **h**, including the otic vesicle, **o**, and the eye, but excludes the adhesive organ, **a**. Again, the cleared embryos, (**v**) reveal expression in the tubules, **t**. Sense probe treated embryos (**vi**, **vii** and **viii**) are unstained, with some colouring in the eye, **e**, at stage 39. (**B**) Spatial expression of mRNA transcribed from EST BC043955 representing UniGene cluster gene **xl.5983**; There is little expression until stage 30 (**i** and cleared **ii**), where there is staining in the glomus, **g**, eye, **e**, and surrounding the adhesive organ, **a**. When cleared (**ii**) the expression in the eye includes the eye socket, **es**. Stage 39 antisense treated embryos (**iii**, magnified **iv**) indicates continued expression in the glomus, **g**, and some staining in the eye, **e**, and branchial arches, **b**. Sense control embryos (**v**, cleared **vi**, and **vii**) have some low level background staining in the eye, **e**.

no enrichment in pronephric tissue, where expression was reduced compared to whole embryo beyond stage 20 (Fig. 4.2).

The UniGene Cluster numbered xl.5983 contains 122 EST sequences, 2 of which include the start site and the poly-adenylation signal. Conceptual translation revealed 60-90% protein sequence similarity with GDP dissociation inhibitor of various organisms (www.ncbi.nlm.nih.gov). GDP dissociation inhibitors regulate rad GTP-binding proteins by inhibiting GDP-GTP conversion during intracellular transport. Expression was not found in the *Xenopus* adult kidney of 7719 ESTs tested, but was found in the adult human, in 101 of 180994 ESTs, and in the adult mouse, in 82 of 117542 ESTs (www.ncbi.nlm.nih.gov). Although the preliminary wholemount *in situ* hybridisation (Personal correspondence from Pollet, N.), showed expression in the pronephric tubules, the UniGene cluster gene xl.5983 expression was found only in the glomus (Fig. 4.3B). This discrepancy is due to the difficulty in separating these two structures at stage 27. The staining in the glomus appeared to be very weak, especially when contrasted to the signal in the eye. The temporal expression decreased during the period of pronephric anlagen elongation, stages 20-30, and increased as the pronephros began to function (Fig. 4.1). Furthermore pronephric expression was reduced compared to the whole embryo in the stages analysed (Fig. 4.2). This expressional behaviour is not indicative of a pronephric development gene.

The UniGene cluster numbered xl.12848 (previously numbered xl.4229) consists of 85 EST sequences, one of which includes the start site and the poly-adenylation signal. Hypothetical translation indicated 85-90% amino acid sequence similarity to human and mouse alpha 3 type IV collagen binding protein, a major constituent of the basement membrane (www.ncbi.nlm.nih.gov). Introductory wholemount *in situ* hybridisation (Personal correspondence from Pollet, N.), showed expression in the glomus in early tail bud embryos. Wholemount *in situ* hybridisation performed in this study revealed expression in the tubules, not the glomus (Fig. 4.4A). As before, this inconsistency could be due to difficulty in distinguishing tubules and glomus tissue at stage 26. The glomus was only visible when the stage 30 embryo had been cleared, however, RT-PCR analysis indicates pronephric expression in all stages tested (Fig. 4.2). Since the initial analysis, alpha 3 type IV collagen binding protein has been implicated in podocyte function, specifically in diabetes (Chen, *et al.*, 2004).

(A) **xl.12848**

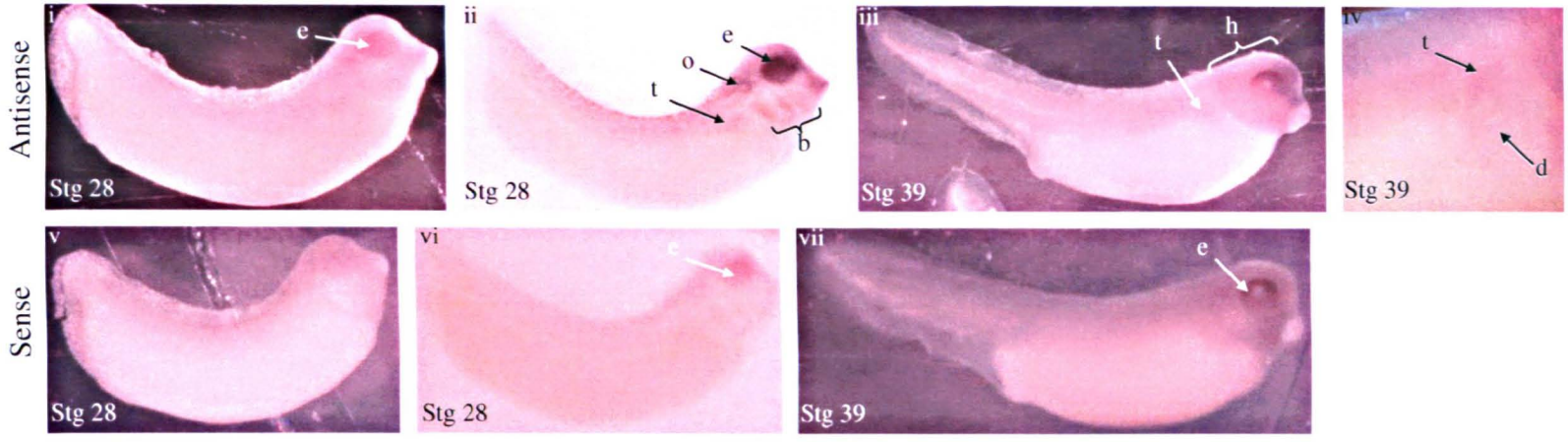

(B) **xl.16795**

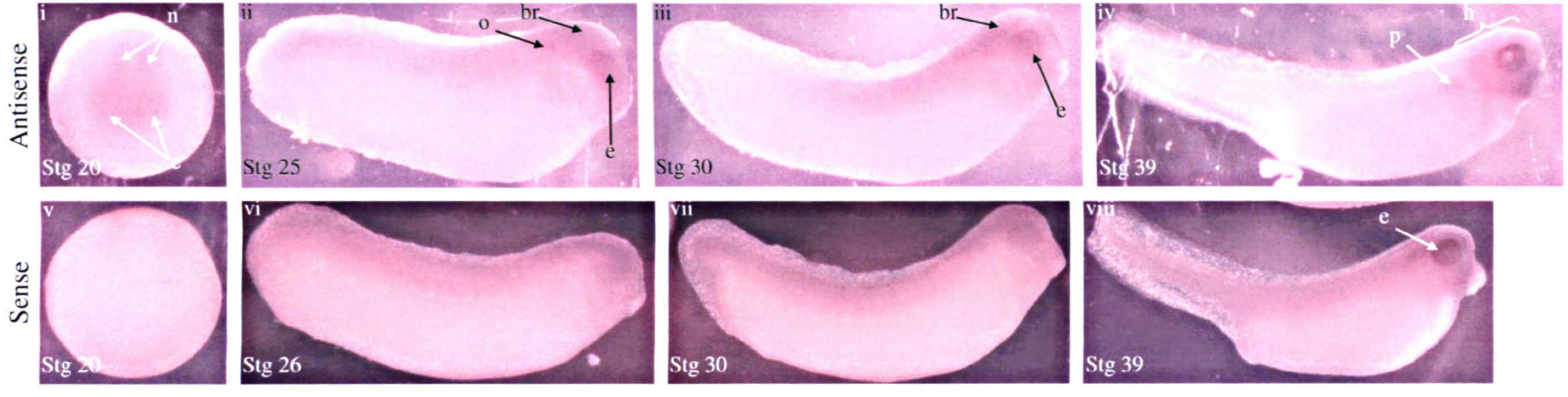

Fig. 4.4 ***In situ* hybridisation analysis of UniGene cluster genes xl.12848 and xl.16795.** *In situ* hybridisation of UniGene cluster genes. DIG-labelled RNA probes were made using representative ESTs and were either antisense or sense as indicated. (**A**) Spatial expression of mRNA transcribed from EST CA974150 representing UniGene cluster gene **xl.12848**; Little staining is seen in uncleared antisense treated embryos at stage 28 (**i**), except in the eye, **e**. Cleared stage 28 embryos (**ii**), show expression in the glomus, **g**, eye, **e**, otic vesicle, **o**, and the branchial arches, **b**. Some staining is seen in the pronephros at stage 39 (**iii**, magnified **iv**), specifically in the tubules, **t**, and faintly in the anterior duct, **d**. Control sense probe treated embryos (**v**, cleared **vi** and **vii**) indicate little background staining, with the exception of the eye, **e**. (**B**) Spatial expression of mRNA transcribed from EST CA981992 representing UniGene cluster gene **xl.16795**; Expression is first seen at stage 20 (**i**), in the anterior neural folds, **n**, and the eye placodes, **e**. Early tailbud embryos (**ii**), reveal expression in the brain, **br**, otic vesicle, **o**, and eye, **e**. The brain, **br**, and eye, **e**, expression continues in stage 29 embryos, (**iii**). Stage 39 antisense probe treated embryos (**iv**), display colouring in the head, **h**, and faintly in the pronephric region, **p**. Sense probe treated embryos (**v**, **vi**, **vii** and **viii**) are clear, except for some non specific eye, **e**, staining.

The UniGene cluster numbered xl.16795 was renamed xl.2936 during the course of this study and although no homologies have been found, the hypothetical translation is known as protein LOC496295 (www.ncbi.nlm.nih.gov). Initial wholemount *in situ* hybridisation (Personal correspondence from Pollet, N.), showed expression in the glomus in early tail bud embryos. Unfortunately the wholemount *in situ* hybridisation performed in this study was unable to confirm this observation. The data indicated that the UniGene cluster gene xl.16795 was expressed very weakly in the pronephros at stage 39, however, due to the weak staining, it is unclear whether the glomus or the tubules was stained (Fig. 4.4A). The temporal expression was constant throughout the stages tested and there was no enrichment of expression within the dissected pronephric tissue (Fig. 4.1 and Fig. 4.2). The low level of pronephric expression and temporal expression behaviour are not consistent with a pronephric development gene.

These UniGene cluster genes were investigated after showing highly specific wholemount *in situ* patterns, identified by N. Pollet (Faculte de Medicine, Universite de Rennes, Rennes, France). However, since publication of other UniGene cluster gene expression patterns, an issue of UniGene cluster numbering has led to considerable confusion (Pollet, *et al.*, 2005). This may explain why that although all UniGene cluster genes were found to be expressed in the pronephros, they were not all expressed in the regions expected.

Wholemount *in situ* hybridisation analysis of the 4 UniGene cluster genes indicated specific, though weak, expression in the pronephros (Fig. 4.3A-B and Fig. 4.4A-B). These data contrasted with the high level of specificity which originally led to the acquisition of these clones. Furthermore, RT-PCR data revealed that the 4 UniGene cluster genes were expressed in the pronephros (Fig. 4.2). The pronephric expression, however, was not enriched, as compared to the whole embryo and temporally, the expression did not alter with respect to pronephric development (Fig. 4.1 and Fig. 4.2). For these reasons, the UniGene cluster genes were not investigated further by mis-expression experiments in this work.

Chapter 5

Pod 1 and *Darmin r* are expressed in the developing pronephros

5.1 Introduction

The first two methods of identifying potential pronephric development genes were to screen a stage 13 cDNA phagemid library using a subtracted probe and to analyse four cDNA sequences that had previously been found to be expressed in the pronephros. The third method was to review the current literature and select potential genes of interest. The genes were chosen on the basis of their expression pattern and functional analysis in either *Xenopus* or mouse. Two genes were chosen after consideration of the literature and were subjected to further temporal and spatial expression analysis by RT-PCR. Clones were obtained for the two chosen genes from existing NCBI EST databases (www.ncbi.nlm.nih.gov).

5.1.1 *Pod 1*

During development, basic helix-loop-helix transcription factors are involved in cell lineage commitment and organogenesis. They bind to E box regions (CANNTG) (Murre, *et al.*, 1989) and are classified into two groups, ubiquitous class A and tissue specific class B (Lassar, *et al.*, 1991). *Pod 1*, also known as *Epicardin*, *Capsulin*, *Transcription factor 21*, is a class B basic helix-loop-helix transcription factor (Hidai, *et al.*, 1998, Quaggin, *et al.*, 1998, Robb, *et al.*, 1998).

Mouse *Pod 1* expression

In murine development, wholemount *in situ* hybridisation suggests *Pod 1* is first expressed 8.5 dpc in the heart (Lu, *et al.*, 1998). Detailed analysis was carried out using wholemount *in situ* hybridised and sectioned 13.5 dpc mouse embryos. This showed expression in the proepicardial organ of the heart and the mesenchymal cells surrounding epithelium of the gut, lungs and metanephros (Hidai, *et al.*, 1998, Lu, *et al.*, 1998 and Robb, *et al.*, 1998).

In the analysis of adult mouse tissues, RT-PCR revealed highest expression in the lung then the ovary, spleen, kidney, intestine, uterus and heart (in order of expression levels)

(Hidai, *et al.*, 1998). Wholemount *in situ* hybridisation analysis, however, indicated that expression was restricted to the podocytes lining the glomerulus, interstitial cells of the heart, interstitial cells within the alveolar wall, the submucosa of the gut and urinary bladder and the stroma of the uterus (Lu, *et al.*, 1998).

Role of *Pod 1* in mouse development

Pod 1 has been shown to have multiple roles in vertebrate development. The *Pod 1* null mouse died from multiple organ failure with hypoplastic lungs and kidneys and aspleenism. The post mortem analysis revealed failure of the lung epithelium to undergo branching morphogenesis, resulting in the absence of alveoli. The kidneys also had severe branching defects and lacked mature glomeruli and the splenic area was devoid of cells (Quaggin, *et al.*, 1999 and Lu, *et al.*, 2000).

From studying neonatal knock-out mice, *Pod 1* appeared to have a role in ureteric bud branching and the differentiation of cell groups within the nephron (Quaggin, *et al.*, 1999). During development, ureteric branching was reduced both in the number of branches and the number of ureteric branch tips (Quaggin, *et al.*, 1999), suggesting a critical role in branching morphogenesis.

Pod 1 may also have a role in the conversion of condensing mesenchyme into nephric epithelium. The loss of *Pod 1* resulted in the increase of metanephric condensing mesenchyme (Quaggin, *et al.*, 1999 and Cui, *et al.*, 2003). Differentiation of the condensing mesenchyme, specifically into S-shaped bodies and capillary loop glomeruli, was delayed in chimeric mice (chimeric mice were generated by combining null Pod 1 and heterozygous Pod 1 ES cells with wild type embryos) (Quaggin, *et al.*, 1999). Differentiation was delayed rather than blocked, as at birth, a small number of capillary loop glomeruli were found that were formed from null *Pod 1* cells (Quaggin, *et al.*, 1999).

Pod 1 is involved in the terminal differentiation of specialised cell types in the kidney. In chimeric mice, a few nephrons were formed from null *Pod 1* cells that have normal tubular structures, however, their proximal tubular cells lacked the specialised brush border (Quaggin, *et al.*, 1999). In the glomerulus, podocytes were specified but failed to undergo terminal differentiation and formed no foot processes (Quaggin, *et al.*, 1999

and Cui, *et al.*, 2003). Spindle-shaped cells were missing from null *Pod 1* mice kidneys and in chimeric mice kidneys were only formed by GFP wild type cells, implying a cell automonous role in spindle-shaped cell development. The condensing mesenchyme of null *Pod 1* mice kidneys does not develop, whereas in chimeric mice kidneys the condensing mesenchyme will develop in the presence of GFP wild type stromal cells. This indicates a non cell automonous role of *Pod 1*. Therefore the role of *Pod 1* in differentiation may be both cell autonomous and non cell automonous (Cui, *et al.*, 2003).

It has been proposed that Pod 1 has a role in patterning the airways of the lungs (Quaggin, *et al.*, 1999). Knock-out studies have shown that structurally, there are abnormal bronchi, reduced primordial tubules, a lack of acinar tubules and no terminal alveoli. RT-PCR analysis has indicated an increased expression of early lung specification markers and a reduced expression of terminal differentiation markers in null *Pod 1* embryos. Compromised lung function due to missing alveoli and type II pneumocytes is the primary cause of neonatal fatality.

Early markers of spleen specification were present in null *Pod 1* embryos at 12.5 dpc. However, at birth null *Pod 1* mice lacked any spleen tissue. Analysis of TUNEL staining revealed an increase in apoptotic cell death in the splenic lineage-forming-region of null *Pod 1* embryos. *Pod 1* may therefore be required for the proliferation and survival of the splenic lineage (Lu, *et al.*, 2000).

In skeletal muscle, exogenous expression of *Pod 1* has been shown to inhibit the terminal differentiation of C2C12 myoblasts (Funato, *et al.*, 2003). Myo $R^{-/-}$ and Pod $1^{-/-}$ mice, however, lose mastication muscles originating from the primary branchial arch and possess a cleft palate and a defective diaphragm (Lu, *et al.*, 2002). The role of *Pod 1* in skeletal muscle development is therefore unclear.

Pod 1 is also involved in gonadogenesis. At 13.5 dpc *Pod 1* was strongly expressed in the male and weakly expressed in the female mouse. Later, at 3 months, high expression was seen in the female and low expression was seen in the male mouse. This suggested a role in male/female specification. *Pod 1* and *SF 1*, a regulator of sexual differentiation, have complementary expression patterns (Tamura, *et al.*, 2001).

Null *Pod 1* male mice were externally feminised. The testes failed to descend, lacked testicular cords and were in some cases attached to the adrenal glands. Similarly, in female mice the ovaries were also attached to the adrenal gland and remained close to the kidneys (Cui, *et al.*, 2004). *Pod 1* has been shown to transcriptionally repress steroidogenic factor 1 in Leydig derived cells (Tamura, *et al.*, 2001, Cui, *et al.*, 2004). However, over-expression of *SF 1* does not phenocopy the *Pod 1* knock-out animal (Cui, *et al.*, 2004).

Pod 1 is also required for capillary remodelling, chimeric null *Pod 1* mice have large, dilated and poorly organised vascular structures (Cui, *et al.*, 2003). *Pod 1* knock-down using antisense oligonucleotides, inhibited the differentiation of stratified cells to differentiated epithelia in stomach tissue cultures in the presence of 1 μM hydrocortisone. Furthermore, gland formation and mucin granule formation were inhibited using *Pod 1* morpholino oligonucleotides (Andersson, *et al.*, 2001). This indicated that *Pod 1* may also play a role in stomach epithelium development.

Dimerisation of Pod 1

As a group/class B basic helix-loop-helix transcription factor, *Pod 1* is expected to either form homodimers or heterodimerise with group A basic helix-loop-helix transcription factors. Although a number of studies have been carried out, it is unclear which is the case *in vivo*. Gel mobility shift assays using E-box sequences as the probe have shown that *Pod 1* alone does not bind to DNA, but a heterodimer of *Pod 1* and *E12* does bind to DNA (Lu, *et al.*, 1998). Yeast two-hybrid screens have identified other possible Pod 1 heterodimer complexes, HEB, HEB-s and ITF-2 (Miyagishi, *et al.*, 2000a, Miyagishi, *et al.*, 2000b). However, sequence analysis and *in vitro* experiments have shown that *Pod 1* alone is capable of binding cognate E-box consensus sequences and activating transcription (Hidai, *et al.*, 1998).

***Pod 1* and transcription**

Using Gal4-fused *Pod 1* deletion mutants, *Pod 1* has been shown to exhibit both activational and repressor activities, depending on cell line. The C-terminal region of Pod 1 was able to activate transcription in HT1080 and HeLa cells and the C-terminus and N-terminus were able to repress transcription in HepG2 cells. The bHLH region was unable to affect transcription (Miyagishi, *et al.*, 2000).

To identify the *Xenopus Pod 1* homologue, the human Pod 1 protein sequence (O43680) was used to search the translated NCBI database by using the tBLASTn software (Basic Local Alignment Search Tool, Altschul, *et al.*, 1990). Conceptual translation of the *Xenopus* EST CF270487 gave 82.3% identity with the human Pod 1 protein sequence and was chosen for further investigation.

5.1.2 *Darmin r*

Darmin-related was identified by a direct secretion screen (Pera, *et al.*, 2003). The technique involved transfecting human 293T cells with pools of cDNA from a *Xenopus* expression library. The newly translated proteins were labelled using ^{35}S methionine or cysteine and were isolated using SDS PAGE and autoradiography. Single positive clones were selected in a second cycle of screening and partially sequenced (Pera and De Robertis, 2000).

Analysis of *Xenopus Darmin r* showed expression in the glomus and the eye of stage 32 embryos. Temporal RT-PCR revealed high levels of maternal expression and later zygotic expression in late tail bud embryos. Over expression of *Darmin r* did not indicate any endodermal phenotype, no morpholino knock-down was carried out and there was no specific analysis of pronephric structures (Pera, *et al.*, 2003).

Darmin r, registered as EST BU993920, showed 99% identity to *Xenopus laevis cytosolic non-specific dipeptidase*, UniGene cluster xl.10218. *Cytosolic non-specific dipeptidase* has a broad specificity and is inhibited by bestatin, a known peptidase inhibitor (Lenney, 1985). Optimum degradation of carnosine by human *Cytosolic non-specific dipeptidase* was found to be at pH 9.5 in the presence of 0.1mM Mn^{2+}. The presence of magnesium ions was found to be critical for activity. The enzyme has a specific activity of 1.0 μmol^{-min}/mg of histidine formed as obtained at pH 9.5 from 1.8×10^9 transiently transfected CHO cells. Human *Cytosolic non-specific* dipeptidase has a molecular mass of 52.8 kDa and forms a homodimer of 90 kDa.

Cytosolic non-specific dipeptidase (also known as *tissue carnosinase* and *carnosine dipeptidase II*) is in the metallopeptidase family M20, specifically M20.005, which are

generally involved in the hydrolysis of dipeptides in the cytosol of mammalian cells (*MEROPS*: Rawlings, *et al.*, 2006).

The first isolations by Hanson and Smith, of cytosolic non-specific dipeptidase in 1949 were contaminated with the related serum carnosinase (also known as *carnosine dipeptidase II, carnosinease I, glutamate carboxypeptidase-like protein 2*) therefore much early work was subject to confusion. It was not until 1990 that the two dipeptidases were individually characterised by Lenney and colleagues (1990).

Human *cytosolic non-specific dipeptidase* is ubiquitously expressed throughout adult tissues, with high expression in the kidney and liver (Teufel, *et al.*, 2003 and Janssen, *et al.*, 2005) and in the pig and rat, expression can be found in the kidney, brain and liver (Lenney, 1990). The enzymatic properties and spatial expression suggest that it acts as a non-selective cytosolic dipeptidase rather than a selective carnosinase and therefore may function as a housekeeping enzyme in the catabolism of dipeptidic substrates (Teufel, et al., 2003).

5.2 Results

In this study, the temporal and spatial expression patterns of *Pod 1* and *Darmin r* were analysed by RT-PCR and wholemount *in situ* hybridisation to further elucidate their potential roles in pronephric development.

5.2.1 Temporal expression patterns of *Pod 1* and *Darmin r*

To analyse the temporal expression patterns of the selected genes, RT-PCR was used. Important stages during the development of the pronephros were chosen to provide appropriate samples for RT-PCR analysis. For each clone, primers were designed using the EST sequences (*Pod 1*, CF270487 and *Darmin r*, BU993920) to give a PCR product of between 150-400bp (Methods Table 2.1). The RT-PCR was performed using cDNA prepared from *Xenopus laevis* embryos grown to stages 9, 13, 16, 21, 26, 30, 35 and unfertilised eggs (Methods 2.6.2 RT-PCR). Furthermore, the relative expression of the two genes within the pronephros, or the presumptive pronephric region, compared to a whole embryo at the same stage was analysed. This was carried out by performing RT-PCR with the cDNA isolated from dissected pronephric tissue along with the whole

embryo at stages 12½, 15, 20, 28 and 35 (Methods 2.6.2 RT-PCR). The input cDNA was approximately equalised using ODC which is ubiquitously expressed, and a linearity using doubling dilutions of stage 35 cDNA was performed to ensure amplification was in the linear phase.

Pod 1

This temporal RT-PCR analysis indicated that *Pod 1* expression was initiated by stage 13 after which there was a gradual increase in *Pod 1* expression from stages 16 to 26 and maintenance at this concentration through to stages 30 and 35 (Fig. 5.1A). The temporal RT-PCR of whole embryo and kidney dissections revealed an increased expression of *Pod 1* in the developing pronephros compared to the whole embryo (Fig. 5.1B). No expression was seen in stage 12.5 whole embryos or dissected pronephros, thus confirming the initiation of *Pod 1* expression at stage 13, the start of neurulation and the start of kidney specification.

Darmin r

Consistent with published work, *Darmin r* has been shown to have a high level of maternal expression (Pera, *et al.*, 2003). This expression decreased to negligible levels at stage 16 and subsequently increased at stage 26 until stage 35 (Fig. 5.1A). This patterning corresponds to the initial high level of maternal expression followed by zygotic expression during tail bud stages. *Darmin r* expression was observed within the pronephric tissue dissections, however no elevation in expression in the dissected kidney anlagen relative to the whole embryo samples was observed (Fig. 5.1B).

5.2.2 Spatial expression patterns of *Pod 1* and *Darmin r*

The ESTs identified for *Pod 1* (CF270487) and *Darmin r* (BU993920) from Pera, *et al.*, 2003 were obtained from the IMAGE consortium (http://image.llnl.gov/). *Pod 1* antisense DIG-labelled RNA probe was made by digesting the pCMV SPORT 6 plasmid containing the *Pod 1* insert with *Eco RI* (5' end of insert) and transcribing with T7 RNA polymerase. The control sense probe was made by digesting with *Not I* (3'end of insert) and transcribing with SP6 RNA polymerase. Similarly, the *Darmin r* antisense DIG-labelled RNA probe was made by digesting the pCMV SPORT 6 plasmid containing the *Darmin r* insert with *Eco RI* and transcribing with T7 RNA

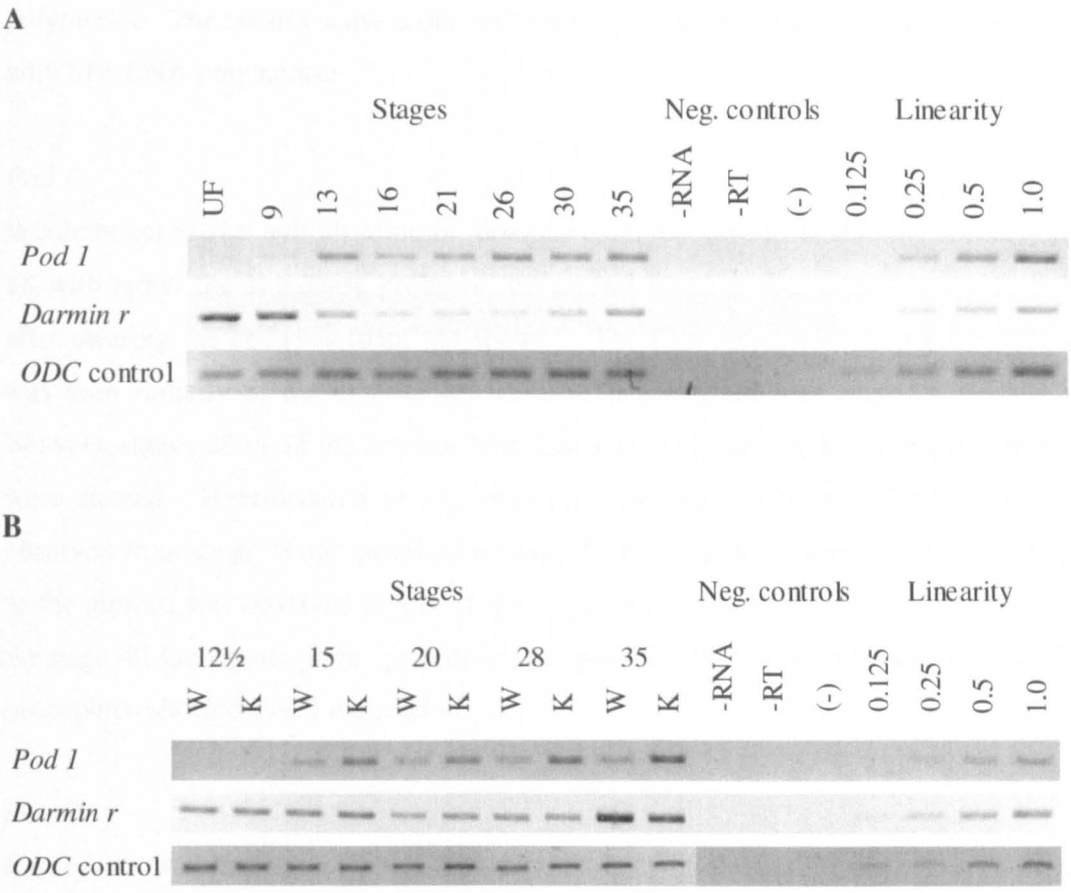

Fig. 5.1 **Temporal expression patterns of *Pod 1* and *Darmin r*.** (**A**) RT-PCR analysis of *Pod 1* and *Darmin r* expression in an embryo stage series. RT-PCR was carried out on embryos of stages from unfertilised eggs to stage 35. (**B**) RT-PCR analysis of *Pod 1* and *Darmin r* in dissected presumptive pronephros and isolated pronephric regions. RT-PCR of genes comparing the whole embryo to the kidney or presumptive kidney dissections (Embryo dissections; (**w**) indicates whole embryo and (**k**) indicates pronephric or presumptive pronephric tissue) shows enrichment of *Pod 1*, but not *Darmin r* in the pronephric regions. Genes are labelled vertically and embryo stages with controls are labelled horizontally. Input cDNA was approximately equalised using the ubiquitously expressed gene *ODC*, and a linearity using doubling dilutions of stage 35 cDNA was performed.

polymerase. The control sense probe was made by digesting with *Not I* and transcribing with SP6 RNA polymerase

Pod 1

Wholemount *in situ* hybridisation of *Xenopus* embryos gave little staining before stage 28 with either the anti-sense probe or the control sense probe, even when visualised after clearing the embryos (data not shown). The first indication of specific staining was seen initially in the anterior branchial arch and glomus at stage 28 (Fig. 5.2). Between stages 28 to 32 the anterior branchial arch, followed by the remaining arches, were stained. Hybridisation of antisense probe to the developing glomus was first observed from stage 28 and persisted to stage 40, the last stage tested. No hybridisation to the glomus was observed in any of the negative control, sense hybridised, embryos. At stage 40 the presumptive epicardium, the posterior end of the forming gut and the pronephros showed *Pod 1* expression.

Darmin r

Expression was first seen by wholemount *in situ* hybridisation in the adhesive organ (cement gland) at stage 21 (Fig. 5.3). Pronephric expression was observed in the tubules at stage 32, and continued to stage 42, the last stage analysed. Non-specific staining was not observed in the pronephros in any of the stages tested on sense embryos. This was not consistent with published work (Pera, *et al.*, 2003), that stated that *Darmin r* was expressed in the glomus. By clearing the stained embryos, tubular structures could be identified, confirming that it is the pronephric tubules that are stained. Darmin r expression was also present in the eye, auditory vesicle and the adhesive organ. The latest stage tested, stage 42, showed antisense probe hybridisation in the tubules, not the glomus, and in the pigmented cells of the epidermis. Sense-probed embryos suggest the staining seen in the head and eye was non-specific, a problem with late stage embryos (Fig. 5.3).

5.3 Discussion: Potential future analysis of selected genes

Pod 1 has been shown to have a well established role in mammalian kidney development. However, the role of the *Xenopus Pod 1* homologue remains unknown. The *Xenopus* temporal expression pattern is comparable to that observed in mouse

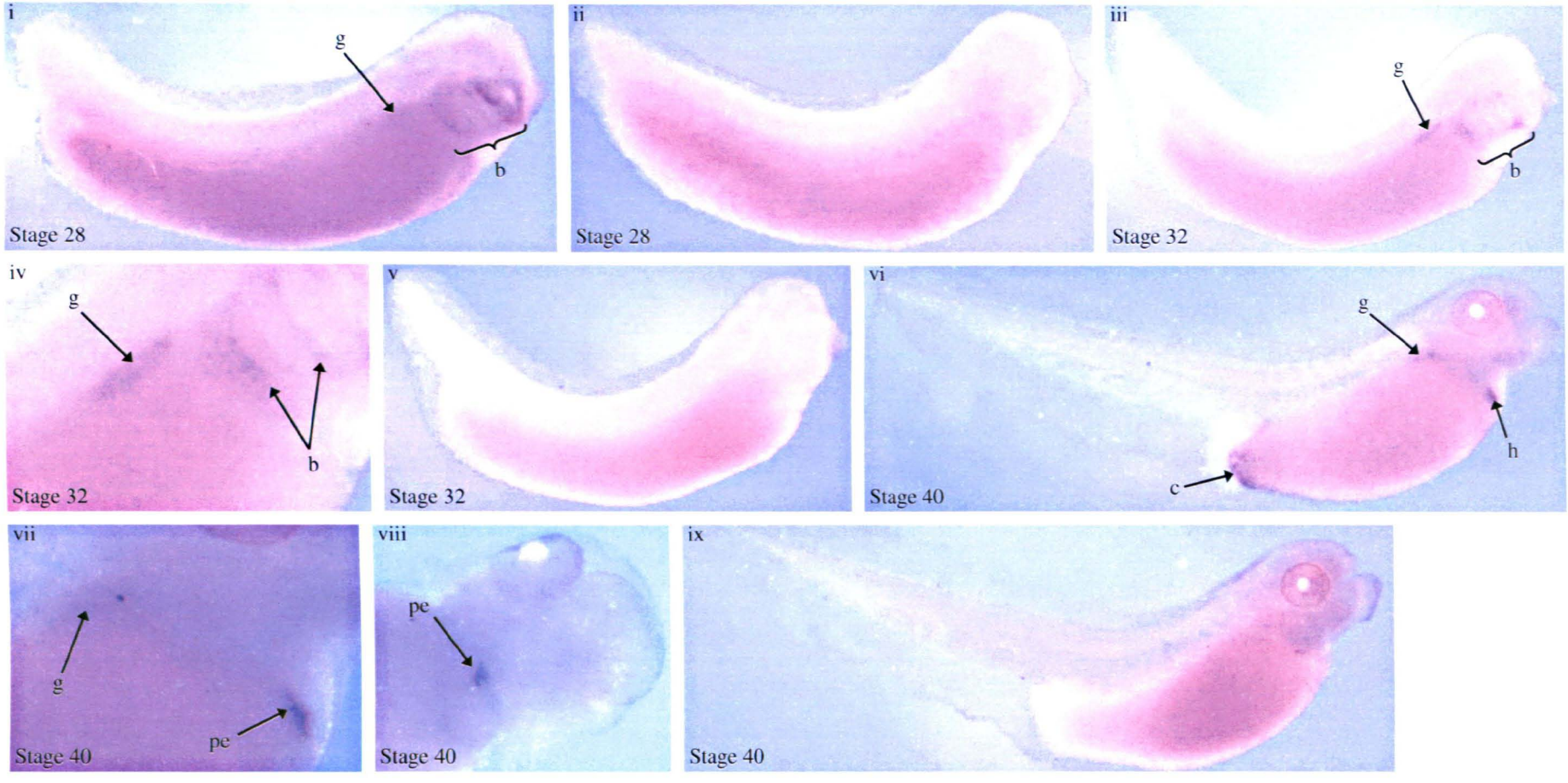
i
g
b
Stage 28
ii
Stage 28
iii
g
b
Stage 32
iv
g
b
Stage 32
v
Stage 32
vi
g
h
c
Stage 40
vii
g
pe
Stage 40
viii
pe
Stage 40
ix
Stage 40

Fig.5.2 ***Pod 1* is expressed in the developing pronephros.** Wholemount *in situ* hybridisation with a *Pod 1* DIG-labelled antisense (**i, iii, iv, vi, vii** and **viii**) and sense (**ii, v** and **ix**) RNA probe was performed on embryos at the stage indicated. No staining above background was present in embryos between stages 9 and 22 (data not shown). First observable expression is seen in the glomus, **g**, and predominantly the anterior branchial arch, **b**, at stage 28 (**i**). Stage 28 sense RNA probed embryos do not show staining in the branchial arch or the glomus. Continued expression is found in the glomus, **g**, and the branchial arches, **b**, of stage 32 embryos (**iii**, magnified **iv**). Sense probe treated embryos at stage 32 are unstained (**v**). Late tail bud antisense treated embryos, stage 40 (**vi**, magnified **vii** and **viii**), are stained in the glomus, **g**, proepicardium within the heart, **pe**, and the coelum, **c**. No non specific staining is seen in the late stage sense control embryos, (**ix**).

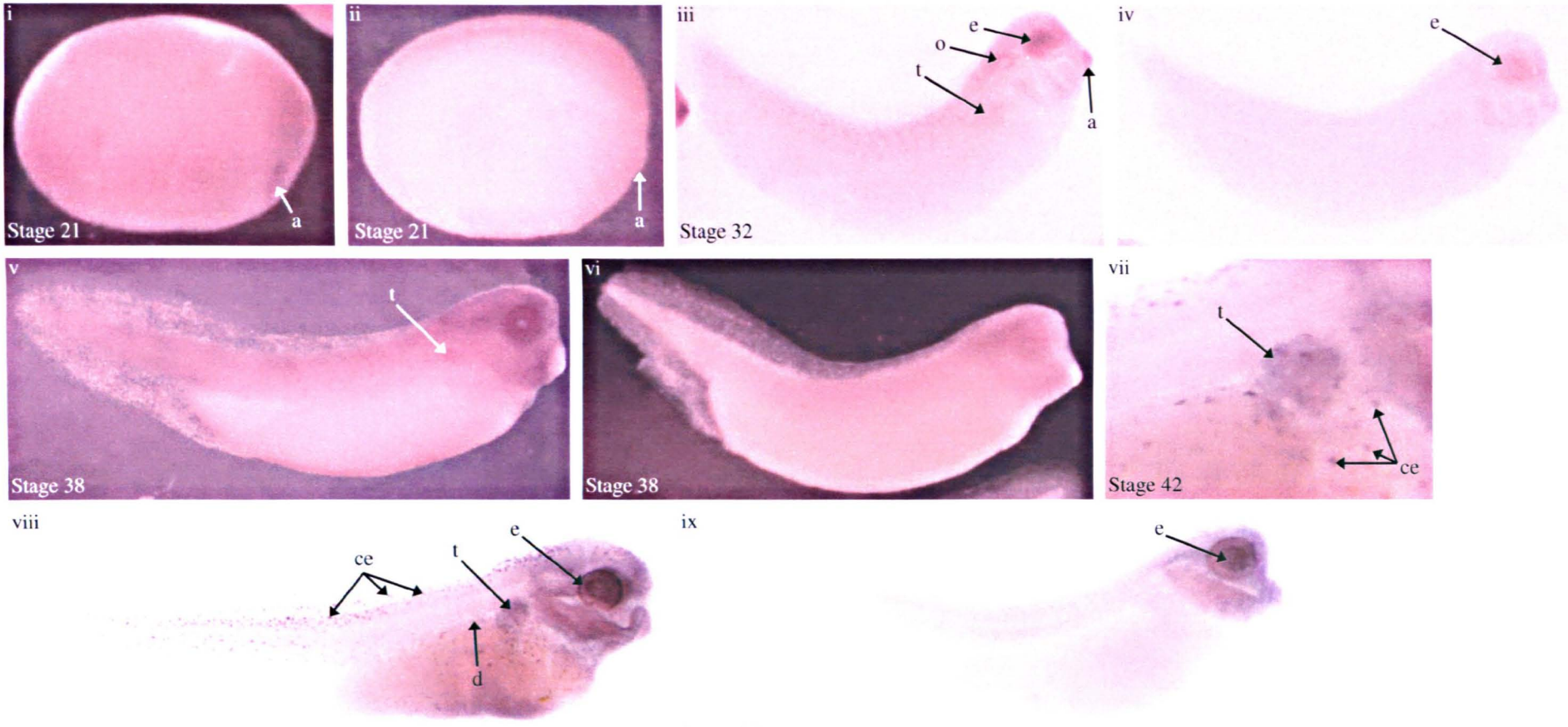
i
Stage 21
a
ii
Stage 21
a
iii
e
o
t
a
Stage 32
iv
e
v
t
Stage 38
vi
Stage 38
vii
t
ce
Stage 42
viii
ce
t
e
d
Stage 42
ix
e
Stage 42

Fig.5.3 ***Darmin r* is expressed in the developing pronephros.** Wholemount *in situ* hybridisation with a *Darmin r* DIG-labelled antisense (**i, iii, v, vii** and **viii**) and sense (**ii, iv** and **ix**) RNA probe was performed on embryos at the stage indicated. Embryos **iii**, **iv**, **vii**, **viii** and **ix** were cleared using Murray's solution. No staining was observed in embryos between stages 9 and 20 (data not shown). Expression is first seen in the adhesive organ at stage 21 (**i**). Expression in the pronephros is identifiable at stage 32 (**iii**) where the tubules, **t**, appear to be stained. In addition, stage 32 antisense RNA probed embryos (**iii**) have staining in the eye, **e**, otic vesicle, **o**, and the adhesive organ, **a**. Pronephric tubule expression, **t**, is continued in stage 38 (**v**) embryos. Late tail bud antisense treated embryos, stage 42 (magnified **vii** and **viii**), are stained in the tubules, **t**, duct, **d** and in the ciliated cells of the epidermis, **ce**. No non specific staining is seen in the sense control embryos, (**ii, iv** and **ix**), except in the eye, **e**.

embryos. Detection of *Pod 1* in mouse embryos by Northern blot analysis showed first expression at 8.5 dpc in the branchial arches, after which there was an increase to 15.5 dpc where it peaked at and persisted to 17.5 dpc (Hidai, *et al.*, 1998). By comparing the developmental stages at the start of neurulation, stage 13 in *Xenopus laevis*, 8-9 dpc in mouse, the onset of *Pod 1* expression is temporally similar. The increased *Xenopus Pod 1* expression in the kidney, compared to the whole embryo was also observed in the mouse, where Northern blot analysis at 15.5 dpc revealed higher expression in the kidney, lung and intestine than in the whole embryo (Hidai, *et al.*, 1998). In murine development *in situ* hybridisation has revealed expression from 9.5dpc with high levels in the presumptive epicardium and the mesenchymal cells surrounding the gut, lung and kidney (Hidai, *et al.*, 1998). This may be comparable to the staining pattern in the *Xenopus laevis* stage 40 embryos where expression is observed in the heart, gut and kidney, although anterior branchial arch expression is identified earlier.

In summary, the results from the initial analysis indicated that *Pod 1* had a high level of expression in the kidney by both RT-PCR and wholemount *in situ* hybridisation. In addition, this expression was early, around initiation, in the development of the pronephros. The early expression also appeared to be restricted to the glomus. To conclude, the data implied that *Pod 1* might be involved in early glomus initiation and may be an important developmental gene.

The role of *Pod 1* in development has mainly been studied within the metanephros, the most complicated of the three progressive kidney structures. This has meant that much of the data has involved the analysis of sophisticated structural phenotypes or highly specialised individual cells. The pronephros, however, is the simplest and the earliest of the three progressive kidney structures, comprising just one nephron. It is difficult to study the pronephros in mammals due to the inaccessibility of the embryo at early stages and the speed at which it is formed and degraded. The pronephros is the only kidney structure of the larval stages of *Xenopus laevis*, and forms just under the epidermal layer. Therefore, although the role of *Pod 1* in mammalian kidneys has been well researched, important information may still be gathered from studying the behaviour of the gene in *Xenopus* at the earliest stages of kidney development.

The role of *Darmin r* or *cytosolic non-specific dipeptidase*, in development is unknown. Hypothetically, a dipeptidase may be involved in signalling, metabolism, and the regulation of biologically active peptides. Even though the developmental function of *Darmin r* is unclear, high expression has been identified in the adult kidneys of the rat, pig and human (Lenney, 1990, Teufel, *et al.*, 2003 and Janssen, *et al.*, 2005). Initial analysis indicated high pronephric tubule expression in the mid to late tail bud stages by wholemount *in situ* hybridisation, and continued expression within the kidney region throughout the stages tested by RT-PCR. The high level tubule expression makes this an appealing gene to manipulate due to the exclusivity within one nephron subunit and the relative selectivity within the embryo. The high maternal expression, followed by mid tailbud zygotic expression is not clearly aligned with the developmental stages of the pronephros, but does suggest an important role in development.

To conclude the wholemount *in situ* hybridisation analysis of the genes indicated specific expression within the pronephros and RT-PCR data revealed expression within the developing pronephros. Furthermore, published literature indicated important roles in development for both genes. For these reasons, *Pod 1* and *Darmin r* were chosen for further investigation by mis-expression experiments in this work.

Part 1 Conclusion

The first aim of this study was to identify genes that are involved in pronephric initiation and development. This was to be done by using three different but complementary approaches:

1. Screening of a stage 13 cDNA phagemid library with a subtracted probe, designed to identify genes expressed in the early development of the pronephros (Chapter 3).
2. Analysis of a set of UniGene cluster genes that have previously been shown to be expressed in the pronephros by *in situ* hybridisation (Chapter 4).
3. Data mining to identify *Xenopus laevis* homologues of vertebrate genes with a known function in kidney development (Chapter 5).

Screening of a stage 13 cDNA phagemid library with a subtracted probe did identify genes that are expressed in the pronephros and whose expression was up-regulated during pronephric initiation. However, their expression within the pronephros did not appear to be unique, nor enriched. For these reasons, the clones identified in the screen were not chosen for further analysis. Since this decision was made, the data has been re-examined and 2 of the 13 clones could prove interesting if examined further.

The second approach was to analyse four UniGene cluster genes that had previously been found to be expressed in the pronephros by wholemount *in situ* hybridisation on stage 27 *Xenopus laevis* embryos (Personal correspondence from Pollet, N.). The UniGene cluster genes were found to be mainly expressed within the pronephros. Although, expression was not enriched within the pronephros and it did not alter with respect to pronephric development. The UniGene cluster genes were therefore not investigated further.

The two genes chosen for further study were *Pod 1* and *Darmin r.* The two genes were chosen after consideration of the literature and the data obtained from the temporal and spatial expression analysis. The genes were then investigated further, looking at homologue protein sequence similarity, adult spatial expression, and mis-expression. Some of the data presented in Chapter 5 has been published (Simrick, *et al.*, 2005).

Results Part 2

The Developmental Role of *Pod 1* in *Xenopus laevis*.

Chapter 6

Pronephric lineage targeted *Pod 1* over-expression results in a reduced glomus.

Chapter 7

Pod 1 expression is required for glomus development.

Introduction

The second aim of this thesis was to elucidate the role of the chosen genes in the development of the pronephros. The first gene chosen for further investigation was *Pod 1*. Initial analysis indicated that *Pod 1* might play a role in early glomus development (Chapter 5). In order to further elucidate the role of *Pod 1* in pronephric development, the following were investigated:

Chapter 6

- Comparison of amino acid sequences of vertebrate *Pod 1* homologues to establish the degree of evolutionary conservation.
- Establish the spatial expression pattern within adult organs by RT-PCR which might indicate functional roles in the adult.
- Carry out over-expression studies in developing embryos, using targeted micro-injected mRNA.

Chapter 7

- Carry out knock-down analysis of Pod 1 translation using morpholino oligonucleotides.
- Initiate a gene network investigation to try to establish the position of *Pod 1* in the regulatory network controlling pronephric glomus development using animal cap assays and RT-PCR.

Chapter 6

Pronephric lineage targeted *Pod 1* over-expression results in a reduced glomus.

6.1 Introduction

Pod 1, also known as *Capsulin, Epicardin* and *Transcription factor 21* is a class B basic helix-loop-helix transcription factor. *Pod 1* has been shown to be expressed in the podocytes lining the glomerulus of mice kidneys as well as the ovary, spleen, intestine, uterus and heart (Lu, *et al.*, 1998 and Hidai, *et al.*, 1998). From studying null and chimeric *Pod 1* mice, *Pod 1* appeared to have a role in branching morphogenesis and/or differentiation in the kidney, lungs, spleen, gut and skeletal muscle (Quaggin, *et al.*, 1999, Lu, *et al.*, 2000, Andersson, *et al.*, 2001, Lu, *et al.*, 2002, Cui, *et al.*, 2003 and Funato, *et al.*, 2003). *Pod 1* also has been shown to have a role in gonadogenesis, possibly in sex determination (Tamura, *et al.*, 2001, Cui, *et al.*, 2004) (Chapter 5 Background).

Previous analysis of the developmental role of *Pod 1* in the kidney has focused on the mouse metanephros. By studying the role of *Pod 1* in the pronephros of *Xenopus laevis*, the effect of *Pod 1* on the nephron and early initiation events can be more easily investigated. The *Xenopus Pod 1* homologue, EST CF270487, was identified using the translated NCBI database, tBLASTn (Basic Local Alignment Search Tool, Altschul, *et al.*, 1990). We have previously shown by wholemount *in situ* hybridisation and RT-PCR analysis (Chapter 5) that *Pod 1* expression is initiated at the same time as the developing pronephros and is enriched in the pronephros compared to the whole embryo.

In this chapter, the evolutionary conservation of *Pod 1* was investigated by comparing the amino acid sequences of the mouse, rat and human Pod 1 homologues. The region of *Pod 1* expression within the pronephros was determined using RT-PCR with mRNA extracted from a dissected stage 42 pronephros. The *Xenopus* adult spatial expression pattern of *Pod 1* transcript was elucidated using RT-PCR analysis of adult tissues. These data gave an indication of the possible functional role of *Pod 1* in adult tissues.

The importance of *Pod 1* in pronephric development was investigated using over-expression analysis.

6.2 Results

6.2.1 Pod 1 is evolutionarily conserved through a number of vertebrate species

The full length *Xenopus Pod 1* EST, CF270487, was obtained from the IMAGE consortium (http://image.llnl.gov, IMAGE No. 5512805) and sequenced in house. The published NCBI nucleotide sequence (http://mgc.nci.nih.gov/) of this clone fails to identify a translational start site. In house sequencing corrected the sequencing error by identification of the translational start site at an equivalent point to that of the mouse sequence (EST AF029753). The open reading frame runs from 23bp to 560bp, encoding a 179 amino acid protein that is approximately 25kDa when separated on a 10% SDS polyacrylamide gel (Fig. 6.4).

The conceptual translation of the *Xenopus Pod 1* sequence was performed using the INFOBIOGEN web site (www.infobiogen.fr). The *Xenopus* Pod 1 amino acid sequence was compared with the *H. sapiens*, NP_003197, *M. musculus*, NP_035675 and *R. norvegicus* Corl, XP_341738, Pod 1 homologues. The alignment showed 100% conserved identity in the basic helix-loop-helix region between the vertebrate Pod 1 homologues of the mouse, rat and human (Fig. 6.1A). A similarity of approximately 85% among the Pod 1 vertebrate homologues was identified over the whole length of the protein (Fig. 6.1B).

6.2.2 *Pod 1* expression is concentrated in the pronephric glomus

The pronephros from a *Xenopus laevis* stage 42 embryo was dissected into the glomus, tubules and duct regions, and RT-PCR was performed on mRNA extracted from the dissected pieces. The input cDNA was approximately equalised using *EF1α* and a linearity using doubling dilutions of whole embryo cDNA was performed. The purity of the pronephric dissections were ascertained by Dr Caroline Haldin using *WT1* for the glomus, *Pax8* for the tubules and *X c-ret* for the duct. The pronephric dissection RT-PCR suggested a greater expression of *Pod 1* in the glomus compared to the tubules and duct (Fig. 6.2).

A

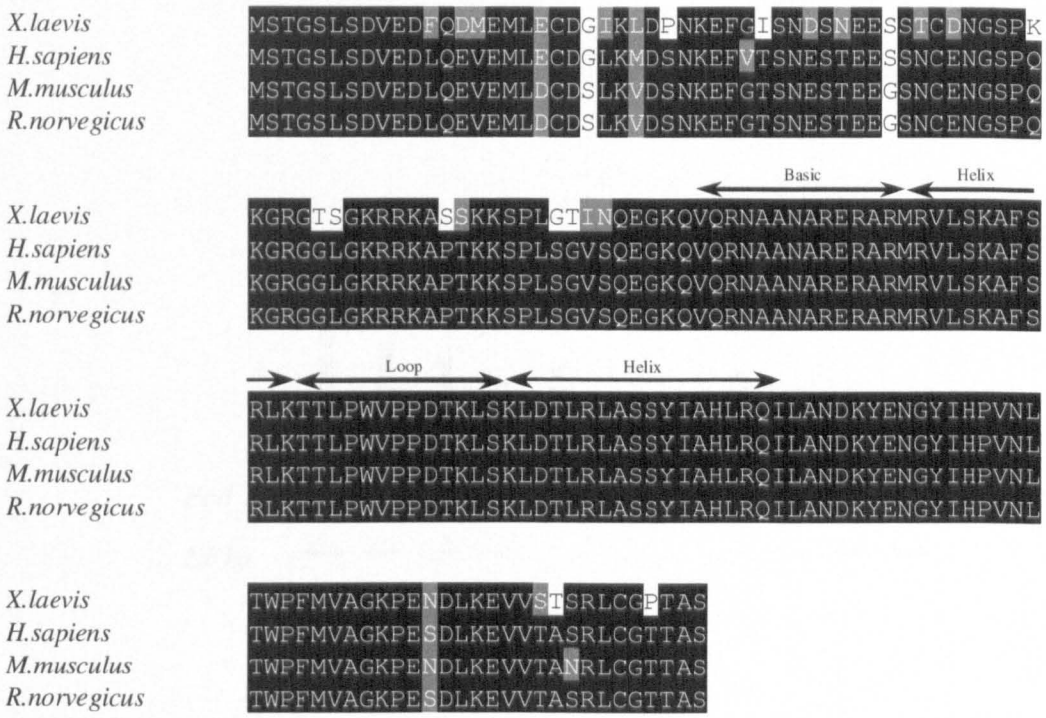

B

	X.laevis	*H.sapiens*	*M.musculus*	*R.norvegicus*
X.laevis	-	-	-	-
H.sapiens	87	-	-	-
M.musculus	85	96	-	-
R.norvegicus	85	97	99	-

Fig. 6.1 **Alignment of homologous Pod 1 amino acid sequences.** **(A)** Alignment of the predicted *X. laevis* amino acid sequence (conceptually translated from CF270487), *H. sapiens* Pod1 (NP_003197), *M. musculus* Pod 1 (NP_035675) and potential *R. norvegicus* homologue Cor1 (XP_341738). Black shading indicates identical amino acids, whereas the gray shading specifies the same amino acid family. **(B)** Percentage identity (%). The table indicates paired percentage identity as given by BLAST (Basic Local Alignment Search Tool, Altschul *et al.*, 1990).

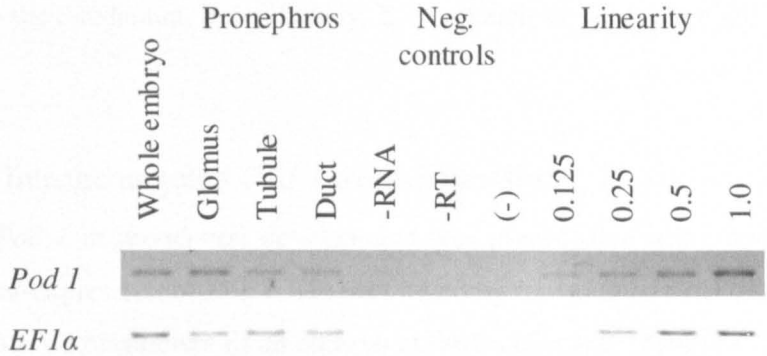

Fig. 6.2 **Spatial pronephric expression of *Pod 1* in stage 42 *X. laevis*.** The pronephros from a *Xenopus laevis* stage 42 embryo was dissected into the glomus, tubules and duct tissues, and an RT-PCR using *Pod 1* primers was carried out. Equalisation was carried out using *EF1α* and linearity and negative controls carried out as described in the methods. A fine dissection of the pronephros of a stage 42 *X. laevis* tadpole reveals the spatial expression of *Pod1* within the pronephros. *Pod 1* appears to be most expressed in the glomus, less in the tubules and weakest in the duct.

6.2.3 *Pod 1* is expressed highly in a number of adult tissues

The *Xenopus* adult spatial expression was elucidated using RT-PCR analysis on mRNA isolated from adult tissues. These data gave an indication of any potential role of *Pod 1* in adult tissues. The input cDNA was approximately equalised using *EF1α* and a linearity using doubling dilutions of kidney cDNA was performed. The RT-PCR indicated that *Pod 1* expression is highest in the rectum and the spleen, with significant expression in the duodenum, heart, kidney, lungs, pancreas, skin, liver and muscle (Fig. 6.3).

6.2.4 Pronephric lineage targeted *Pod 1* over-expression

The role of *Pod 1* in pronephric development was investigated using over-expression analysis. Over-expression of *Pod 1* was performed by injecting *in vitro* transcribed *Pod 1* mRNA into a V2 blastomere of an embryo at the 8 cell stage. *Xenopus Pod 1* mRNA was synthesised using SP6 mMessage mMachine kit (Ambion). Pod 1 cDNA from the IMAGE clone (http://image.llnl.gov, IMAGE No. 5512805) was cloned into the pCS2+ plasmid using *Eco RI* and *Xba I* (Appendix). Mouse *Pod 1* mRNA was also synthesised for over-expression analysis, to indicate the degree of functional conservation. The mouse *Pod 1* mRNA was also synthesised using SP6 mMessage mMachine kit (Ambion). Mouse *Pod 1* cDNA from the IMAGE clone (http://image.llnl.gov, IMAGE No. 6529241) was cloned into the pCS2+ plasmid using *Eco RI* and *Xba I* (Appendix).

The translation of *Pod 1* mRNA was analysed using *in vivo* translation within *Xenopus* oocytes. *Xenopus* oocytes were injected with either *Xenopus Pod 1* mRNA, mouse *Pod 1* mRNA or water and incubated in Barth X containing ^{35}S methionine and cysteine. This radioactively labelled any new proteins synthesised after oocytes were injected. The mRNA-injected oocytes and the water-injected oocytes were compared. Both *Pod 1* homologues were translated, giving proteins of approximately 25kDa (Fig. 6.4). The human Pod 1 protein had been previously found to be 26kDa (Miyagishi, *et al.*, 2000a).

The *in vitro* transcribed *Pod 1* mRNAs were injected into the embryos at the 8 cell stage (Methods Fig. 2.3). The mRNA was immediately translated in the embryo, yielding higher levels of *Pod 1* expression at an earlier stage than that observed during endogenous expression. The *Pod 1* mRNA was injected into one V2 cell of an 8 cell

Fig. 6.3 **Expression pattern of *Pod 1* in the adult organs of *X. laevis*.** RT-PCR was performed on mRNA isolated from the organs of an adult *Xenopus laevis*. The RT-PCR was equalised using *EF1α* and linearity and negative controls performed as described in the methods. *Pod 1* expression in adult *X. laevis* organs appears to be greatest in the spleen and rectum. Other, more moderate expression is seen in the duodenum, heart, kidney, lungs, pancreas and skin. There are also low levels in the liver, muscle, spinal cord and stomach.

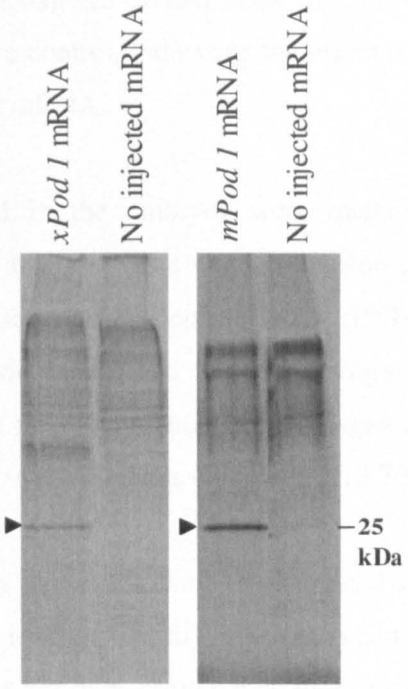

Fig. 6.4 **Oocyte translation of *Xenopus* and mouse *Pod 1* mRNA**. Oocytes were injected and incubated overnight in full strength Barth X containing ^{35}S labelled methionine and cysteine. The protein from the oocytes was extracted and run on a 10% SDS PAGE gel and exposed for autoradiography. Oocytes were injected and lanes were loaded as indicated. Protein product of the injected *Pod 1* mRNA transcripts are highlighted by the black arrow. As indicated, the size of both *Xenopus* and mouse Pod 1 protein is approximately 25kDa. The lanes labelled "No injected mRNA" are negative controls were no mRNA was injected and no Pod 1 protein is observed.

embryo to target the effect of exogenous *Pod 1* to the pronephric region. Lineage tracing was performed by co-injecting with GFP and sorting the embryos for pronephric left or right fluorescence at stage 25-30 (Methods 2.10.3 Micro-injection). *GFP* mRNA was also used as a negative control, indicating the effect of injecting an embryo with a developmentally irrelevant mRNA.

The phenotypes observed in the embryos were quantified by measurements and validated using statistical analysis. The over-expression phenotype of the pronephric tubules was determined using the Pronephric Index (PNI) (Wallingford, *et al.*, 1998) (Methods 2.10.8 Pronephric Index) and the morphology of the pronephric duct was scored by eye. The size of the glomus/pronephric anlagen and the length of the embryo were measured as detailed in the methods (Methods 2.10.7 Measurement of tissue area).

Where the comparison was within the same experimental set, left and right comparison of the same embryo was used to identify potential phenotypes. The significance of difference within the same set of measurements or Pronephric Index (PNI) (Methods 2.10.8 Pronephric Index) was validated using either the paired t-test, if the data were normal, or the Wilcoxon paired test, if the data were not normal.

Where the comparison was between different sets of embryos, the ratio of glomus/pronephric anlagen area to embryo length of each set was used in the analysis. The statistical analysis of measurements or Pronephric Index (PNI) involved a Kruskal Wallis test, and a Dunn's post test to indicate the significant differences between the groups of test subjects. All statistical analysis was performed using the InSTAT 3 programme, (GraphPad Software Inc).

6.2.4.1 Pronephric lineage targeted *Pod 1* over-expression results in a reduced glomus phenotype as indicated by *WT1* and *xlmx1b in situ* analysis

In vitro transcribed mRNA was injected into one V2 cell of an 8 cell embryo. Embryos were injected with either 0.6ng *Xenopus Pod 1* mRNA and *GFP* mRNA, 0.6ng mouse *Pod 1* mRNA and *GFP* mRNA or *GFP* mRNA alone. The embryos were sorted using GFP fluorescence to indicate targeting of the left or right side of the embryo. Wholemount *in situ* hybridisation using a *WT1* antisense DIG-labelled RNA probe was

performed on stage 33-35 embryos. The glomus area on each side of the embryo and the length of the embryo was measured as detailed in the methods (Methods 2.10.7 Measurement of tissue area).

Comparison of the 0.6ng *Xenopus Pod 1* mRNA and *GFP* mRNA injected side of the embryo and the not injected side of the embryo revealed a reduction in glomus area, as indicated by *WT1* expression (Fig. 6.5A). The mean area of glomus of the injected side of the embryos was $0.020mm^2$, and the not injected side of the embryo was $0.027mm^2$ (N = 38). These measurements are actual sizes of the glomus and are not relative sizes of glomus, that is, they have not been divided by the embryo length to give ratio of glomus area to embryo length. The measurements were found to be significantly different using a two-tailed paired t-test, $p < 0.0001$.

In experiments comparing the *GFP* alone injected embryos, the mean area of the glomus on the injected side was 0.030 mm^2, and the mean area of the glomus on the not injected side was 0.029 mm^2. The glomus areas of the embryo did not reveal any significant difference in the measurements, $p = 0.04348$ (number of embryos = 36) (Fig. 6.5B). Again, these measurements are actual sizes of the glomus and are not relative sizes of glomus, that is, they have not been divided by the embryo length to give ratio of glomus area to embryo length

Comparison of the mean relative areas of the glomus on the injected side of the embryo injected with 0.6ng *Xenopus Pod 1* mRNA and *GFP* mRNA with the equivalent side of the *GFP* mRNA alone embryos, further confirmed that the reduction of glomus area was due to exogenous *Pod 1*. In order to remove any distortion in data caused by variation in the length of the tadpole, the ratio of area of glomus (mm^2) to length of tadpole (mm) was calculated (Methods 2.10.7 Measurement of tissue area). The following data are therefore a ratio of area of glomus (mm^2) to length of tadpole (mm), and mean values are from all embryos injected with the stated mRNA. The mean of the ratio of glomus area (mm^2) to tadpole length (mm) of the 0.6ng *Xenopus Pod 1* mRNA and *GFP* mRNA injected embryos on the injected side was $0.004mm^2/mm$, and the *GFP* mRNA alone injected equivalent was $0.005mm^2/mm$. The mean values indicated a reduction in mean area due to *Pod 1* over expression. These measurements were significantly different according to Kruskal Wallis test, and had a Dunn's post test p

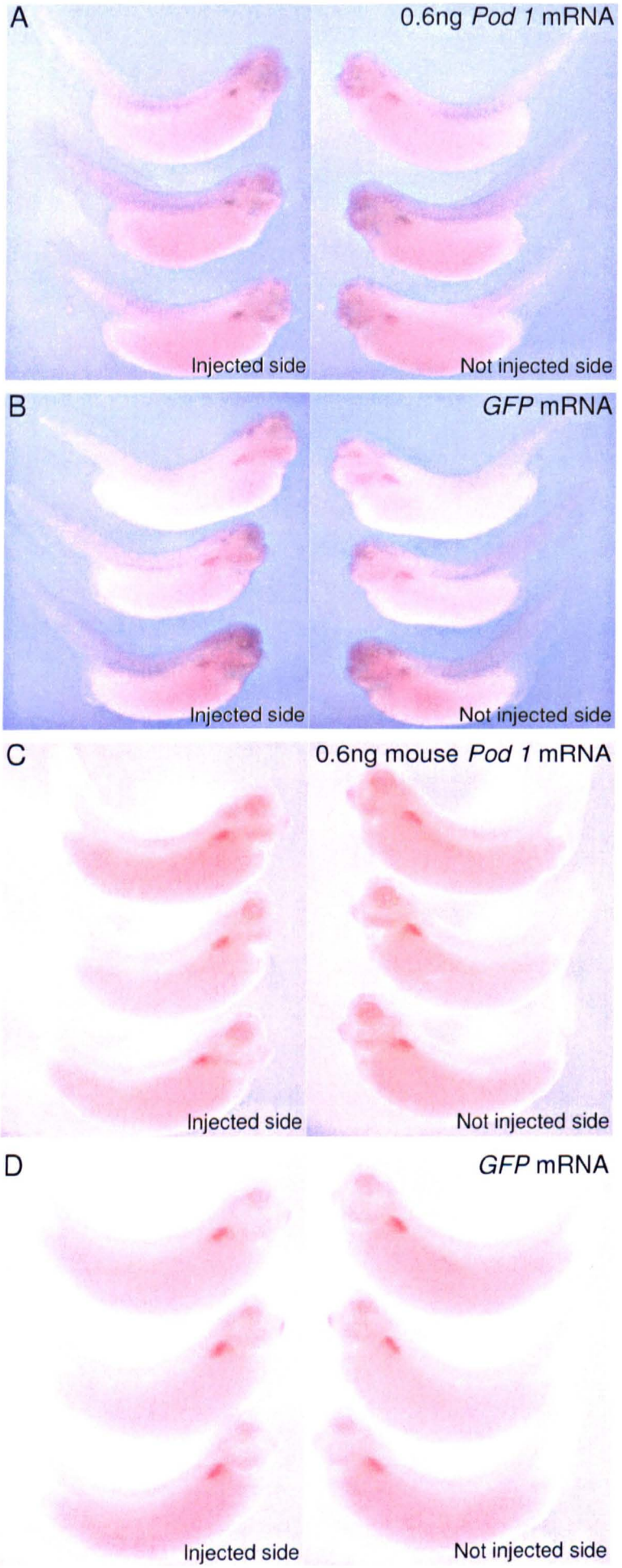
A
0.6ng *Pod 1* mRNA
Injected side
Not injected side
B
GFP mRNA
Injected side
Not injected side
C
0.6ng mouse *Pod 1* mRNA
Injected side
Not injected side
D
GFP mRNA
Injected side
Not injected side

Fig. 6.5 ***Xenopus* and mouse *Pod 1* show the same over-expression phenotype demonstrated by *WT1 in situ* indicating the size of the glomus.** Embryos were injected with either; 0.6ng *Xenopus Pod 1* mRNA and *GFP* mRNA (**A**), *GFP* mRNA (**B**), 0.6ng mouse *Pod 1* mRNA and *GFP* mRNA (**C**) or *GFP* mRNA (**D**). Injections were done at the 8 cell stage into one V2 cell to target the pronephros. Embryos were sorted using GFP fluorescence, checking for left or right pronephric targeting. Not injected sides and injected sides of the same embryos are as indicated. Wholemount *in situ* hybridisation was preformed with a *WT1* DIG-labelled antisense RNA probe on stage 33-35 embryos. (**A**) *Xenopus Pod 1* over expression decreases the size of the glomus as indicated by *WT1* expression. (**C**) Embryos injected with mouse *Pod 1* also have a decreased glomus. (**B, D**) *GFP*, used as an injected mRNA control, does not affect the size of the glomus.

value of less than 0.01. These tests also indicated that no significant differences were measured between the GFP injected embryos and the uninjected embryos ($p > 0.05$).

This *Xenopus Pod 1* over-expression experiment was repeated 3 times and consistently resulted in a reduction of glomus area, as indicated by *WT1* expression. The result was also statistically significant in each case.

Comparison of the 0.6ng mouse *Pod 1* mRNA and *GFP* mRNA injected side of the embryo and the not injected side of the embryo also revealed a reduction in glomus area, as indicated by *WT1* expression (Fig. 6.5C). The mean area of the injected side of the embryos was $0.019mm^2$, and the not injected side of the embryo was $0.023mm^2$ ($N = 31$). The measurements were found to have a significant difference using a Wilcoxon paired test, $p = 0.0083$. As before, the *GFP* alone injected embryos (injected side $0.025mm^2$, not injected side $0.027mm^2$), did not show a significant difference in the measurements, $p = 0.1294$ ($N = 22$) (Fig. 6.5D).

Comparison of the injected sides of the embryos did reveal a significant difference between 0.6ng mouse *Pod 1* mRNA and *GFP* mRNA injected embryos, $0.004mm^2/mm$, and *GFP* mRNA alone injected embryos, $0.005mm^2/mm$. The Kruskal Wallis test indicated significant variation among the medians and the Dunn's post test had a p value of less than 0.05. These tests were also used to indicate no significant differences between the GFP injected embryos and the uninjected embryos ($p > 0.05$).

The mouse *Pod 1* over-expression experiment was repeated 4 times and consistently resulted in a reduction of glomus area, as indicated by *WT1* expression. However, this result was not statistically significant in each case (data not shown). This may be due to subtle differences in the mouse Pod 1 protein structure making it less functionally efficient in *X. laevis*. It may also reflect the difficulty of being able to inject sufficiently high amounts of mRNA without generating gross developmental abnormalities.

The *Xenopus* Pod 1 over-expression experiment was repeated and 3 embryos from both sets (0.6ng *Xenopus Pod 1* mRNA and *GFP* mRNA; *GFP* mRNA alone) were wax embedded and transverse sections collected across the glomus region (All sections were performed by Mr Surinder Bhamra) (Methods 2.10.6 Wax Sections and Fig. 6.6D).

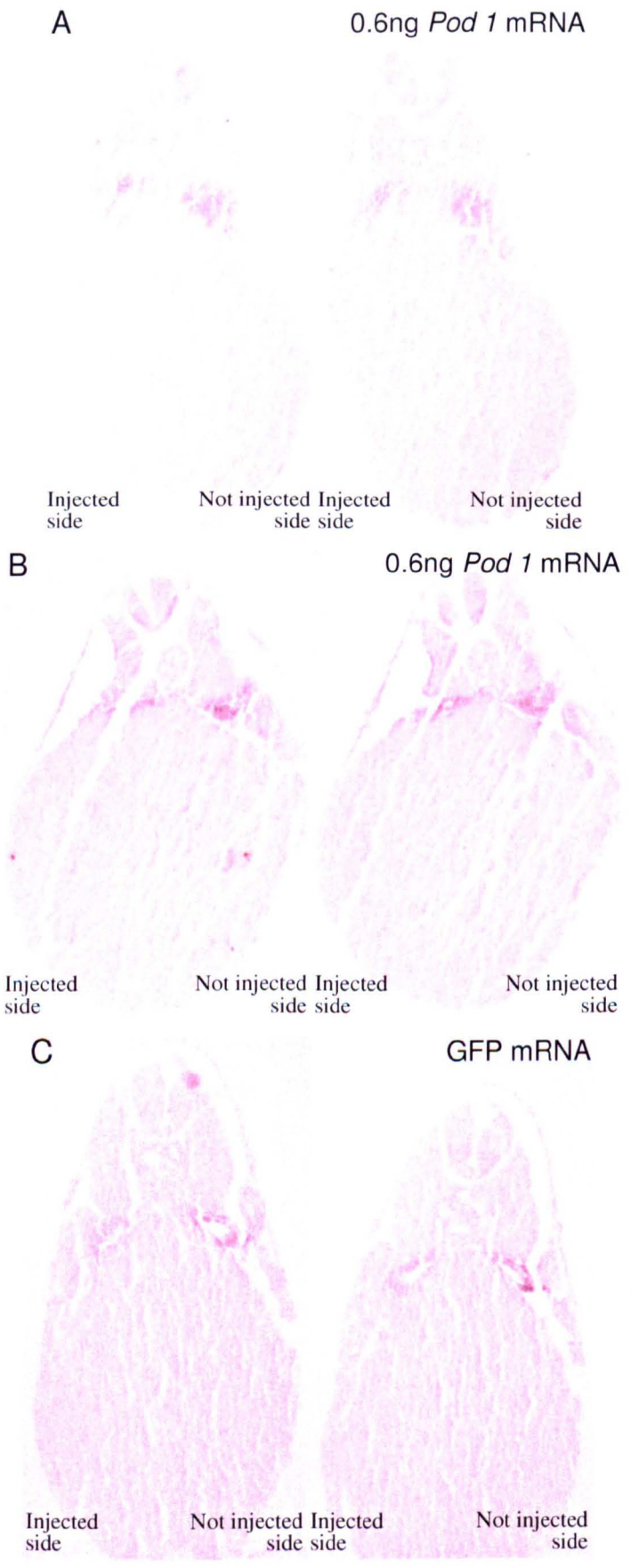
A
0.6ng *Pod 1* mRNA
Injected side
Not injected side
Injected side
Not injected side
B
0.6ng *Pod 1* mRNA
Injected side
Not injected side
Injected side
Not injected side
C
GFP mRNA
Injected side
Not injected side
Injected side
Not injected side

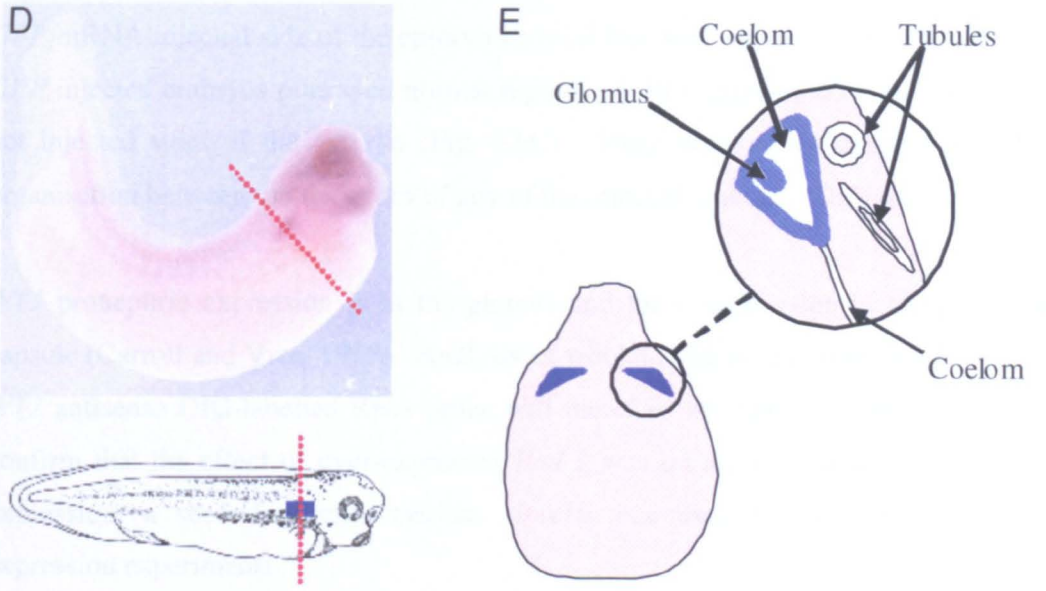

Adapted from Carroll, T.J. and Vize, P.D. (1996)

Fig. 6.6 **Sections of *Xenopus Pod 1* over-expression analysis in embryos confirms a reduction in glomus size**. Injections were done at the 8 cell stage into one V2 cell to target the pronephros. Embryos were injected with either; 0.6ng *Pod 1* mRNA and *GFP* mRNA (**A, B**) or *GFP* mRNA (**C**). Embryos were sorted using GFP fluorescence, checking for left or right pronephric targeting. Not injected sides and injected sides of the same embryos were as indicated. The embryos were fixed at stage 33-35 and wholemount *in situ* hybridisation with a *WT1* DIG-labelled antisense RNA probe followed by wax sections were performed. Two sequential sections are shown per embryo. (**D**) Images of embryos indicating plane of section (Cartoon from Nieuwkoop and Faber, 1994). (**E**) Cartoon diagram of area stained during whole mount *in situ* hybridisation using a *WT1* DIG-labelled antisense RNA probe. (**A, B**) *Pod 1* over expression decreases the size of the glomus as indicated by area stained, although no observable difference in cellular organisation was observed (data not shown). *GFP* injected tadpoles have a normal glomus on the not injected and injected sides of the embryo.

Consistent with the glomus area measurements, the 0.6ng *Xenopus Pod 1* mRNA and *GFP* mRNA injected side of the embryo showed less *WT1* staining (Fig. 6.6A-B). The *GFP* injected embryos portrayed normal regions of *WT1* expression in the injected and not injected sides of the embryo (Fig. 6.6C). There were no differences in cellular organisation between the two sides of any of the injected embryos (Data not shown).

WT1 pronephric expression is in the glomus and the coelom edge of the pronephric capsule (Carroll and Vize, 1996). Analysis of wholemount *in situ* hybridisation using a *WT1* antisense DIG-labelled RNA probe will therefore not only stain the glomus. To confirm that the effect of over-expressed *Pod 1* was on the glomus and not just *WT1* expression, a second glomus marker, *xlmx1b* was used to analyse further over-expression experiments.

Xenopus Pod 1 mRNA and *GFP* mRNA was injected and the embryos were left/right sorted as before. The embryos were fixed at stage 33-35 and wholemount *in situ* hybridisation using an *xlmx1b* antisense DIG-labelled RNA probe was performed. The glomus area was measured and statistical analysis was conducted.

The 0.6ng *Xenopus Pod 1* mRNA and *GFP* mRNA injected side of the embryo had a reduced glomus compared to the not injected side of the embryo, as indicated by *xlmx1b* expression (Fig. 6.7A). The mean area of the injected side of the embryos was $0.01mm^2$, and the not injected side of the embryo was $0.012mm^2$ (N = 28). These measurements are actual sizes of the glomus and are not relative sizes of glomus, that is, they have not been divided by the embryo length to give ratio of glomus area to embryo length. The measurements were significantly different according to the Wilcoxon paired test, p = 0.0393. The control *GFP* injected embryos did not show a significant difference between the injected side, 0.019 mm^2, and the not injected side, $0.017mm^2$, (p = 0.5789, N = 14) (Fig. 6.7B).

Reduction of the glomus by exogenous pronephric *Pod 1* expression is therefore confirmed using two glomus markers, *WT1* and *xlmx1b*.

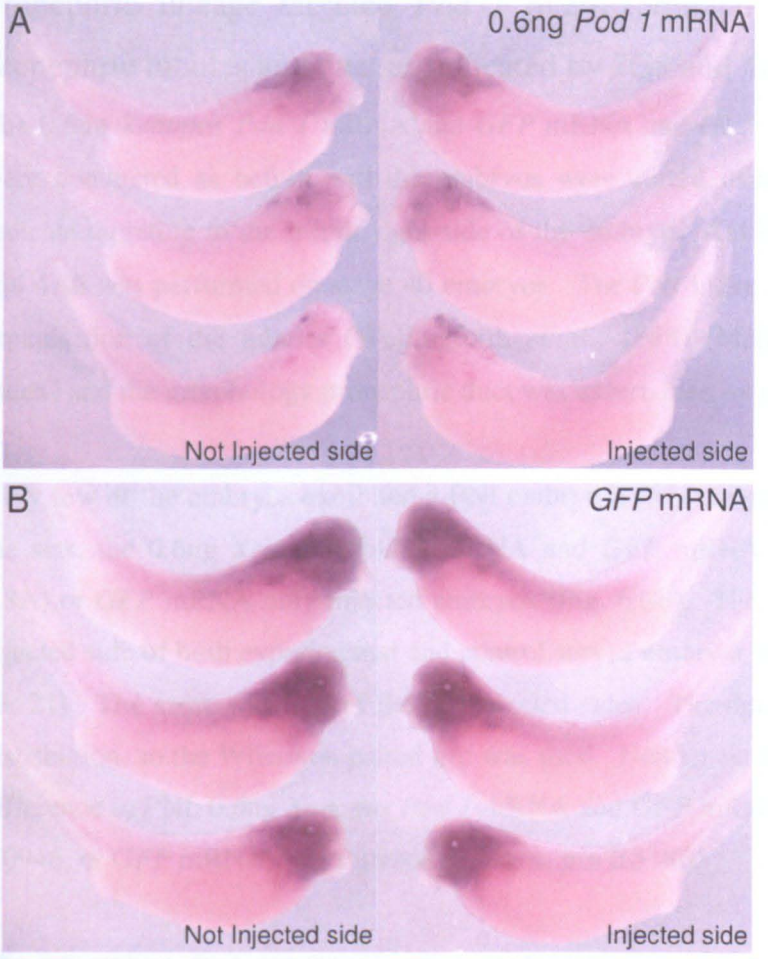

Fig. 6.7 ***Xenopus Pod 1* over-expression glomus phenotype confirmed by *xlmx1b* expression analysis**. Embryos were been injected with either; 0.6ng *Pod 1* mRNA and *GFP* mRNA (**A**) or *GFP* mRNA (**B**). Injections were done at the 8 cell stage into one V2 cell to target the pronephros. Embryos were sorted using GFP fluorescence, checking for left or right pronephric targeting. Not injected sides and injected sides of the same embryos are as indicated. Wholemount *in situ* hybridisation with a *xlmx1b* DIG-labelled antisense RNA probe was performed on stage 33-35 embryos. (**A**) *Pod 1* over expression decreases the size of the glomus as indicated by *xlmx1b* expression. (**B**) *GFP*, used as an injected mRNA control, does not affect the size of the glomus.

6.2.4.2 Pronephric lineage targeted *Pod 1* over-expression does not effect the pronephric tubules and duct as indicated by 3G8 and 4A6 antibody staining

The 0.6ng *Xenopus Pod 1* mRNA and *GFP* mRNA and *GFP* mRNA alone injections were conducted as before and the embryos were sorted using GFP fluorescence to indicate targeting to the left or right side of the embryo. Antibody staining using 3G8 and 4A6 was performed on stage 40 embryos. The PNI index was used to analyse the organisation of the tubules (Wallingford, *et al.*, 1998) (Methods 2.10.8 Pronephric Index) and the morphology pronephric duct was ascertained by eye.

Very few of the embryos exhibited a PNI embryo difference greater than 2 in either of the sets, the 0.6ng *Xenopus Pod 1* mRNA and *GFP* mRNA injected embryos (Fig. 6.8A) or *GFP* mRNA only injected embryos (Fig. 6.8B). The median values from the injected side of both experimental and control sets of embryos were 4 in each case (N = 23, 21). The same was true of the not injected sides. The data did not have a normal distribution, so the Wilcoxon paired test was used. Neither set indicated any significant difference in PNI, 0.6ng *Xenopus Pod 1* mRNA and *GFP* mRNA injected embryos, $p = 0.0946$, or *GFP* mRNA only injected embryos, $p = 0.5186$.

The pronephric duct appeared similar on the injected and not injected sides of the embryo of both the 0.6ng *Xenopus Pod 1* mRNA and *GFP* mRNA injected embryos and the *GFP* mRNA only injected embryos (Fig. 6.8A-B).

6.2.4.3 Pronephric lineage targeted *Pod 1* over-expression does not effect the pronephric anlagen as indicated by *Xlim1 in situ* hybridisation

The mRNA injections were performed as before and the embryos were sorted and fixed at stage 20-25. Wholemount *in situ* hybridisation using a *Xlim1* antisense DIG-labelled RNA probe was conducted and the pronephric anlagen each side of the embryo and the length of the embryo was measured (Methods 2.10.7 Measurement of tissue area).

Exogenous *Xenopus Pod 1* expression did not have an effect on the area of the pronephric anlagen, as indicated by *Xlim1* expression (Fig. 6.9A). The mean areas of the injected and not sides of the *Xenopus Pod 1* mRNA and *GFP* mRNA injected embryos was $0.044mm^2$ (N = 28). The mean area of *GFP* mRNA only injected side of

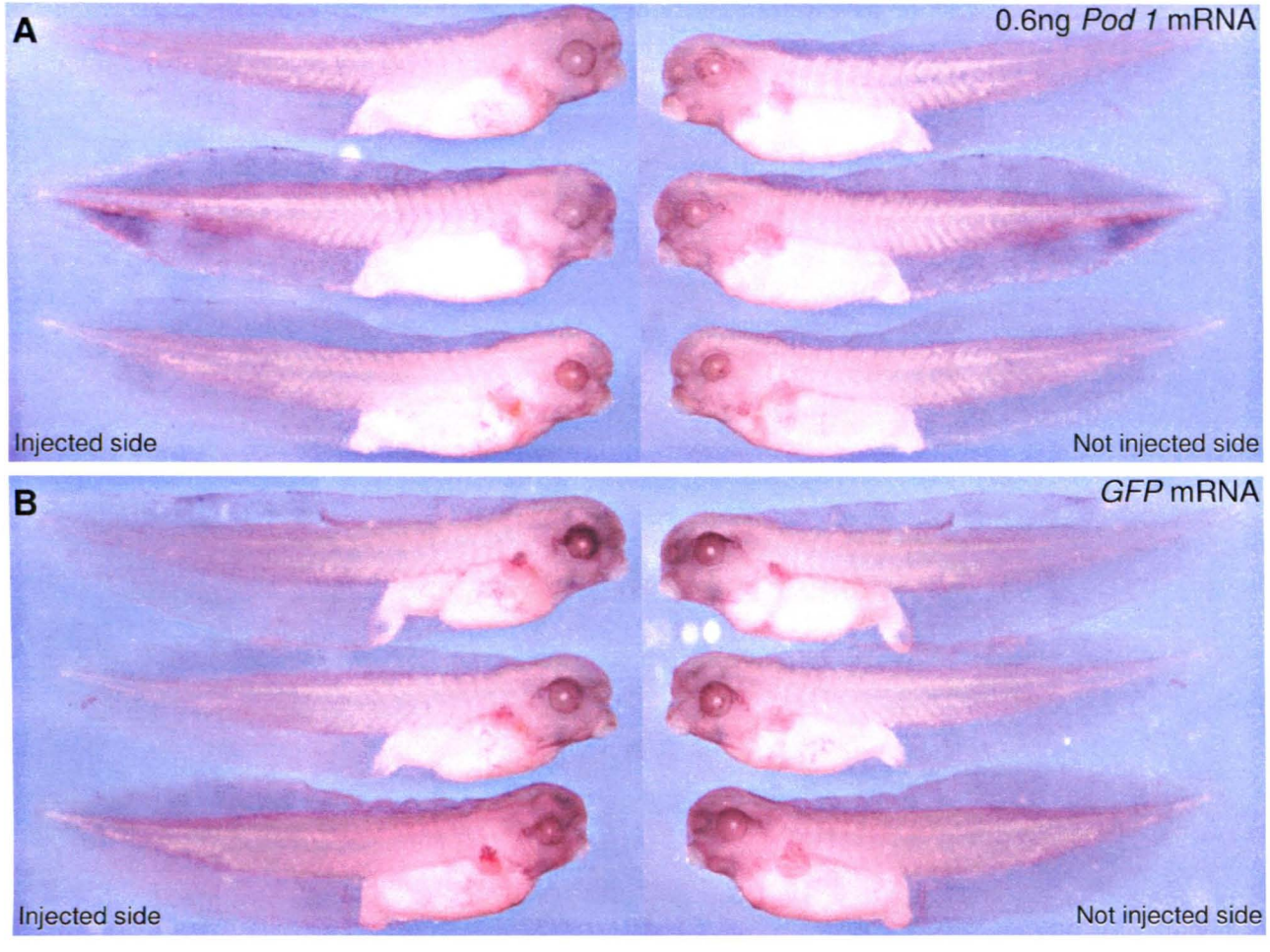
A
0.6ng *Pod 1* mRNA
Injected side
Not injected side
B
GFP mRNA
Injected side
Not injected side

Fig. 6.8 **Histochemical analysis of the *Xenopus Pod 1* over expression phenotype showed no observable effect on either pronephric tubule or duct.** Embryos were injected with either; 0.6ng *Pod 1* mRNA and *GFP* mRNA (**A**) or *GFP* mRNA (**B**). Injections were done at the 8 cell stage into one V2 cell to target the pronephros. Embryos were sorted using GFP fluorescence, checking for left or right pronephric targeting. Not injected sides and injected sides of the same embryos are as indicated. Embryos underwent antibody staining with 3G8, to detect the pronephric tubules and 4A6, to detect the pronephric duct performed on stage 40 embryos. (**A**) *Xenopus Pod 1* over expression does not effect the structure of the pronephric tubules or duct. (**B**) *GFP*, used as an injected mRNA control, does not have an effect on the tubules or duct.

the embryos was 0.063mm^2, and the not injected side of the embryo was 0.069mm^2 (N = 18) (Fig. 6.9B). These measurements were found to have no significant differences using a Wilcoxon paired test and a two-tailed paired t-test; *Xenopus Pod 1* mRNA and *GFP* mRNA injected embryos p = 0.7998, *GFP* mRNA only injected embryos p = 0.3922.

6.2.5 *Pod 1* over-expression has no clear effect on heart development

Wholemount *in situ* hybridisation using a *Pod 1* antisense DIG-labelled RNA probe was conducted on stage 40.5 embryos using the enhanced *in situ* protocol. The embryos were photographed (Fig. 6.10i-iv) then wax sectioned to show the area of expression within the heart (All sections were performed by Mr Surinder Bhamra) (Fig. 6.10v-viii).

The area of *Xenopus Pod 1* expression within the heart was confirmed to be the proepicardium. The region of *Pod 1* expression was below the truncus arteriosis in a ventral-posterior direction, between the heart and the endoderm (Kolker, 2000) (Fig. 6.10i-iv). In amphibian embryos, proepicardium cells form ventrally to the sinus venosus (Fransen and Lemanski, 1990). The region of *Pod 1* expression was therefore believed to be the proepicardium (Horb and Thomsen, 1999). Wax sections of the heart also confirm location of the *Pod 1* expression to the left ventral region of the heart, consistent with the proepicardium (Fig. 6.10vi-viii).

6.2.5.1 *Pod 1* over-expression fails to result in a clear heart phenotype although may result in an altered heart position.

The role of *Pod 1* in heart development was investigated using over-expression analysis. *Xenopus Pod 1* and *GFP* mRNA were *in vitro* transcribed and injected into both V1 cells of an 8 cell embryo to target the heart. 0.6ng of *Xenopus Pod 1* mRNA and *GFP* mRNA was injected into both V1 cells, giving a total of 1.2ng of injected *Xenopus Pod 1* mRNA. *GFP* mRNA was also injected as a negative control, indicating any effect of injecting an embryo with mRNA. Lineage tracing was performed using the co-injected *GFP* mRNA and sorting the embryos for heart region fluorescence at stage 25-30 (Methods 2.10.3 Micro-injection).

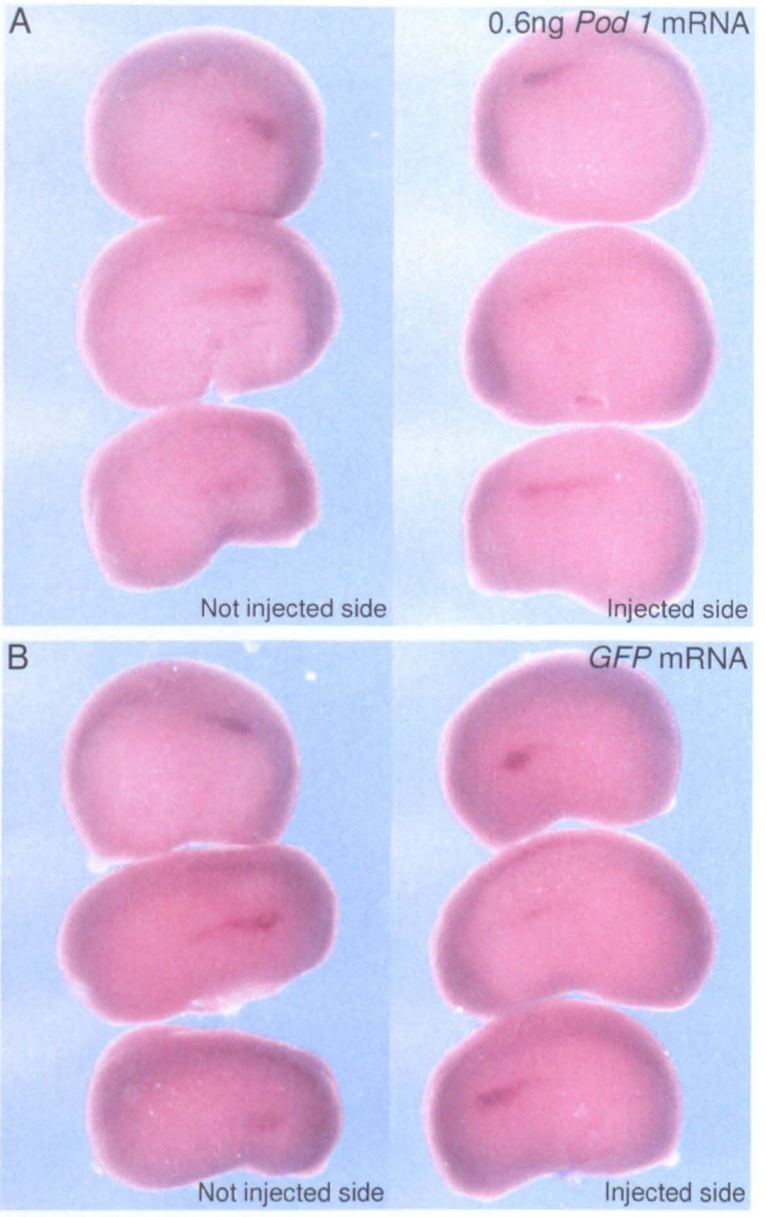

Fig. 6.9 ***Xenopus Pod 1* over expression analysis with *Xlim 1* does not indicate a pronephric anlagen phenotype**. Embryos were injected with either; 0.6ng *Xenopus Pod 1* mRNA and *GFP* mRNA (**A**) or *GFP* mRNA (**B**). Injections were done at the 8 cell stage into one V2 cell to target the pronephros. Embryos were sorted using GFP fluorescence, checking for left or right pronephric targeting. Not injected sides and injected sides of the same embryos are as indicated. Wholemount *in situ* hybridisation with a *Xlim 1* DIG-labelled antisense RNA probe was performed on stage 20-25 embryos. (**A**) *Pod 1* over expression does not have an effect on the size of the pronephric anlagen as indicated by *Xlim 1* expression. (**B**) GFP, used as an injected mRNA control, does not affect the size of the pronephric anlagen.


i

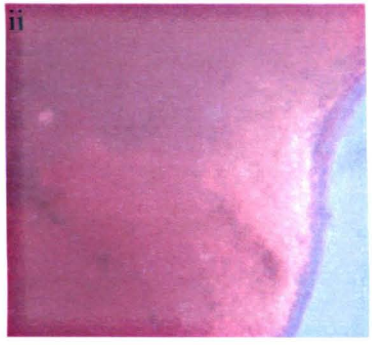
ii


iii

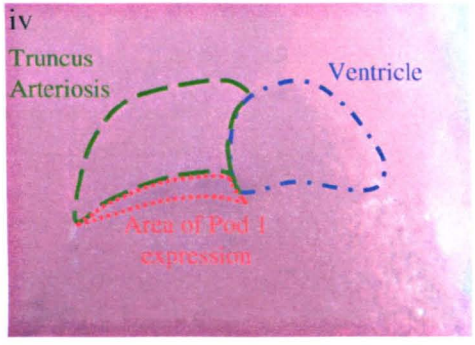
iv
Truncus
Arteriosis
Ventricle
Area of Pod 1
expression

v

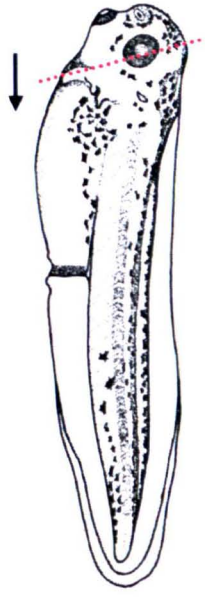

vi

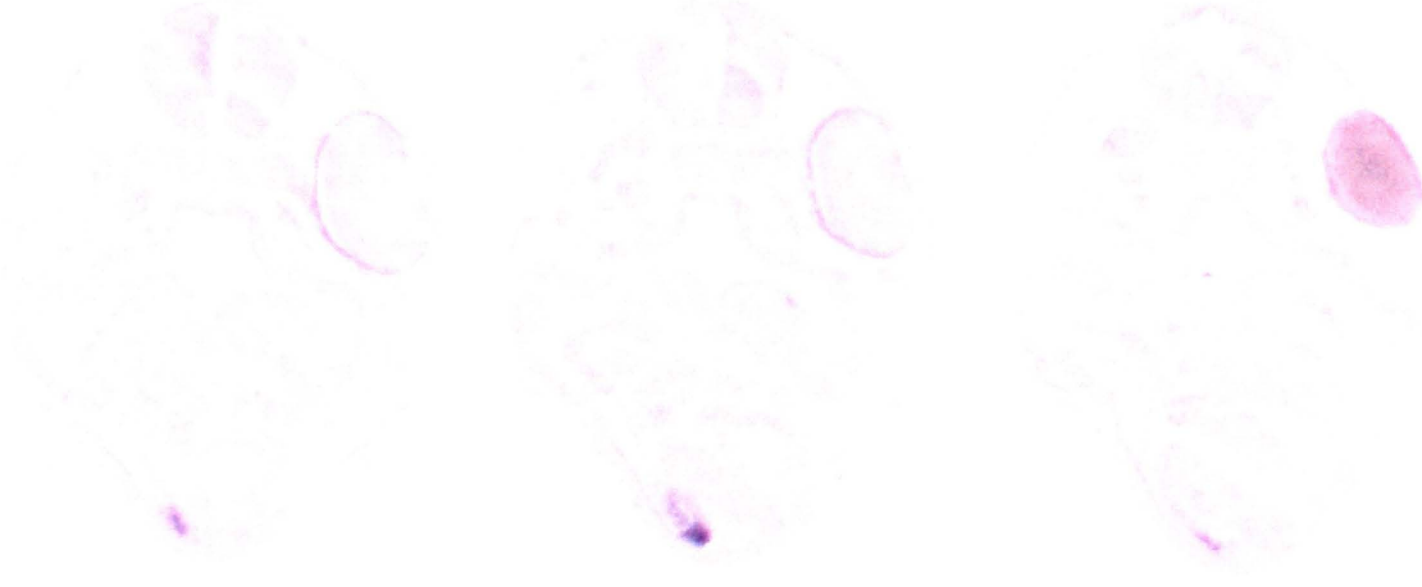

vii

viii

Fig. 6.10 **Analysis of the *Xenopus Pod 1* heart expression pattern by wholemount *in situ* hybridisation and sectioning.** Wholemount *in situ* hybridisation with a *Pod 1* DIG-labelled antisense RNA probe performed on stage 40 embryos (**i-iv**) which are later sectioned (**vi-viii**). Image of stage 40 embryo indicating plane and direction of sections (**v**) (Nieuwkoop and Faber, 1994). Areas of heart observed are shown relative to *Pod 1* expression (**iv**). *Pod 1* expression appears to be below the truncus arteriosis, between the truncus arteriosis and the endoderm, an area considered to be the proepicardium (**i-iv**). Sections indicate that *Pod 1* is expressed in the proepicardium (**vi-viii**).

Wholemount *in situ* hybridisation with a *Cardiac troponin I* antisense DIG-labelled RNA probe was used to reveal the heart morphology. The heart phenotypes observed in the embryos were quantified by measurements and validated using statistical analysis. The size of the heart was measured on both sides using the LUCIA programme (Laboratory Imaging Ltd.). The length of the embryo was measured to eliminate the factor of the size of the embryo on the area of the heart (Methods 2.10.7 Measurement of tissue area). The ratio of heart area to embryo length was compared across sets of embryos using a Kruskal Wallis test, and a Dunn's post test to indicate the significant differences between the sets. All statistical analysis was performed using the InSTAT 3 programme, (GraphPad Software Inc).

Embryos injected with 1.2ng *Xenopus Pod 1* mRNA and *GFP* mRNA did not show any difference in heart area compared to the *GFP* mRNA alone injected embryos (Fig. 6.11). The mean areas of hearts were 0.024 mm^2, left and 0.025 mm^2, right for 1.2ng *Xenopus Pod 1* mRNA and *GFP* mRNA injected embryos (N = 35), and 0.034 mm^2, left and 0.024mm^2, right for 1 *GFP* mRNA alone injected embryos (N = 30). There was no significant variation between the sets with the Kruskal Wallis test ($p = 0.0965$) and so the Dunn's post test was not performed.

In order to maximise any possible effects the embryos were injected with 1.2ng *Xenopus Pod 1* mRNA and *GFP* mRNA, double the concentrations used previously and wholemount in situ hybridisation with a *Cardiac troponin I* antisense DIG-labelled RNA probe was conducted. 3 embryos from each set (1.2ng *Xenopus Pod 1* mRNA and *GFP* mRNA; *GFP* mRNA alone) were then wax embedded and transverse sections were cut across the heart (Fig. 6.12C).

Exogenous *Pod 1* expression does not appear to effect the morphology of the heart, but may have an effect on the positioning of the heart. Comparison of the wax sections from 1.2ng *Xenopus Pod 1* mRNA and *GFP* mRNA injected embryo with the *GFP* mRNA alone injected embryos indicated no overall difference in heart morphology (Fig. 6.12A-B). The ventricle chamber was observed in both embryo sections (Fig. 6.12A iii and Fig. 6.12B iii). The 3 chambers, atrium, ventricle and truncus arteriosis are also present in both embryo sections (Fig. 6.12A iv and Fig. 6.12B iv). The atrium

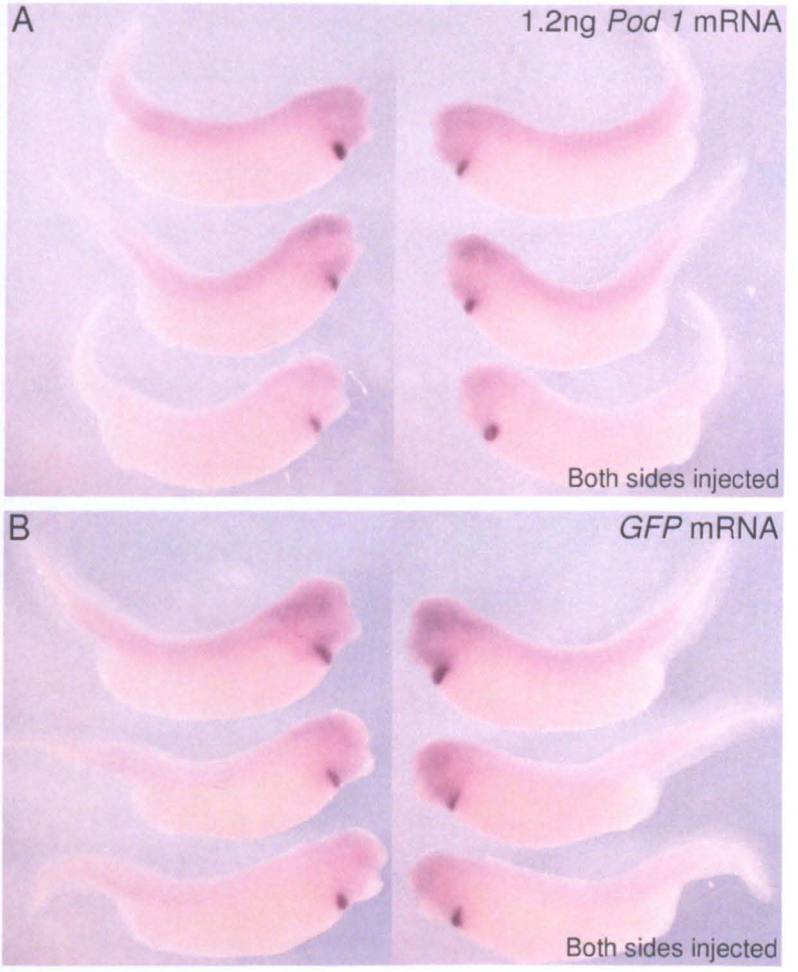

Fig 6.11 ***Xenopus Pod 1* over expression does not have an effect on the heart, as indicated with *Cardiac troponin I* expression**. Embryos were injected with either; 1.2ng *Pod 1* mRNA and *GFP* mRNA (**A**) or *GFP* mRNA (**B**). Injections were done at the 8 cell stage into both V1 cells to target the heart. Embryos were sorted using GFP fluorescence, checking for heart targeting. Wholemount *in situ* hybridisation with a *Cardiac troponin I* DIG-labelled antisense RNA probe was performed on stage 35-37 embryos. (**A**) *Pod 1* over expression does not appear to have an effect on the heart as indicated by *Cardiac troponin I* expression. (**B**) *GFP*, used as an injected mRNA control, does not affect the heart.

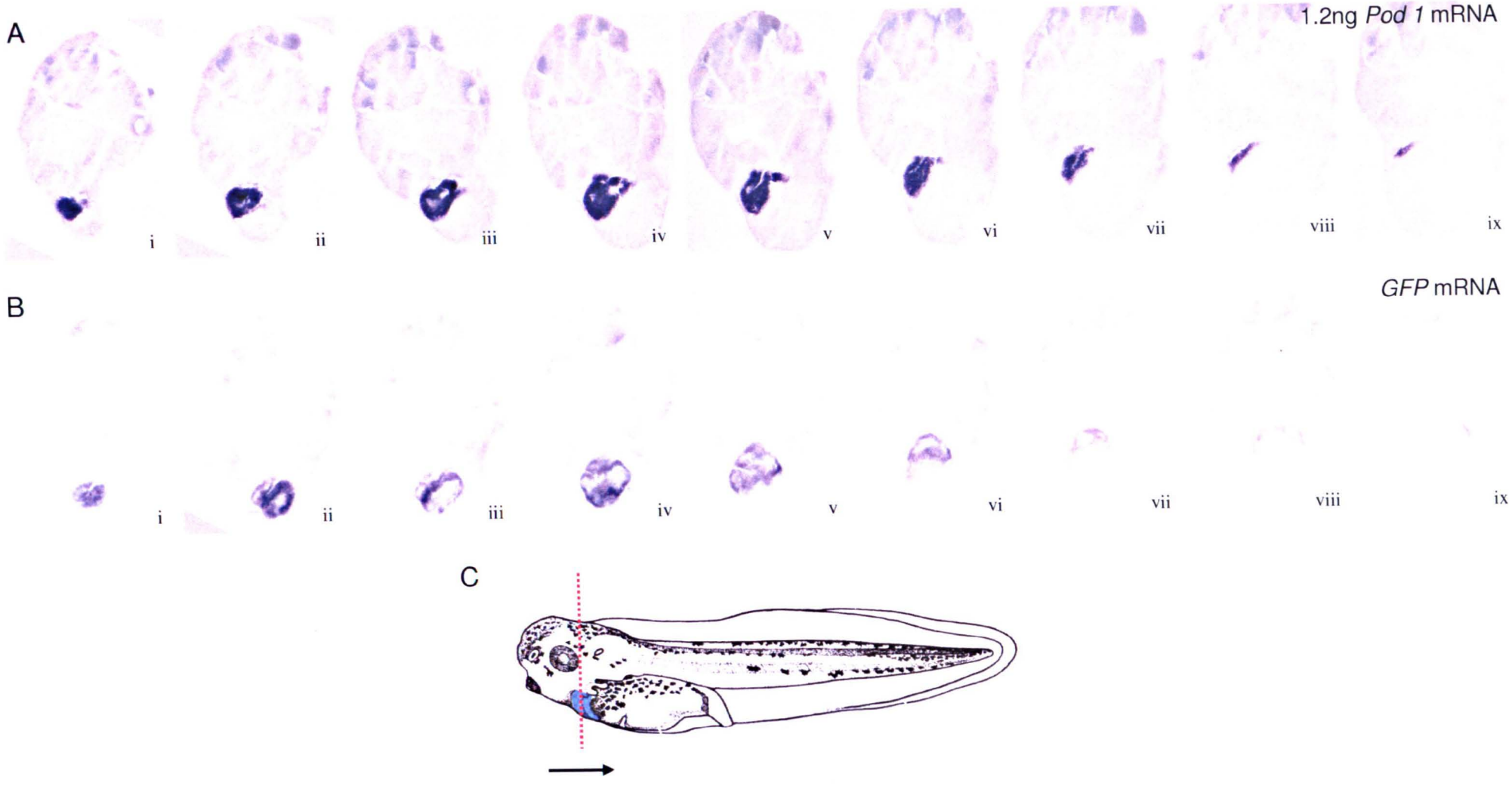
A
1.2ng *Pod 1* mRNA
i
ii
iii
iv
v
vi
vii
viii
ix
B
GFP mRNA
i
ii
iii
iv
v
vi
vii
viii
ix
C

Fig. 6.12 **Transverse sections of wax embedded embryos over-expressing *Pod 1* suggest a possible heart phenotype**. Embryos were injected with either; 1.2ng *Pod 1* mRNA and *GFP* mRNA (**A**) or *GFP* mRNA (**B**). Injections were done at the 8 cell stage into both V1 cells to target the heart. Embryos were sorted using GFP fluorescence, checking for heart tissue targeting. Wholemount *in situ* hybridisation with a *Cardiac troponin I* DIG-labelled antisense RNA probe was performed on stage 42 embryos and which were then wax sectioned. The **black** arrow indicates direction of sequential sections and the **red** dotted line shows the sectioning plane (**C**) (Image from Nieuwkoop and Faber, 1994). (**A**) *Pod 1* over expression effects the positioning of the heart as indicated by area stained. The heart appears to have formed displaced to the left of the embryo. The *GFP* injected tadpoles have a normally positioned heart (**B**).

(Fig. 6.12A vi and Fig. 6.12B vi) and the sinus venosus (Fig. 6.12A viii and Fig. 6.12B viii) structures are also apparent.

The position of the heart in the 1.2ng *Xenopus Pod 1* mRNA and *GFP* mRNA injected embryo wax sections appears to be displaced to the left. In each case, sectioned *Pod 1* over-expression embryos showed this displacement to the left with the corresponding area to the right filled with cells similar to the endodermal cells found more ventral and posterior to the heart. This phenomenon was observed in all three *Pod 1* over-expression sectioned embryos. However, further analysis is required to ascertain whether this was a result of variation in the plane of embryo sections, or a *Pod 1* over-expression phenotype.

6.3 Discussion

There was a high percentage of protein sequence similarity of the hypothetically translated *Xenopus laevis Pod 1* homologue with other vertebrates, especially within the basic helix-loop-helix region suggesting a conserved DNA binding function. Further more, mouse *Pod 1* over-expression was able to induce the same phenotype as *Xenopus laevis Pod 1* over-expression, strongly suggesting that there is a conserved developmental function.

The pronephric dissection RT-PCR indicated *Pod 1* expression in the three components of the pronephros with high expression in the glomus. This is comparable to mouse kidney expression, where *Pod 1* is expressed in several differentiated cell types within all three main components of the nephron, particularly the glomerulus and the tubules (Cui, *et al.*, 2003). The *Xenopus* adult organ RT-PCR also indicated a similar expression pattern to the mouse, where Northern blot analysis have shown *Pod 1* expression in the lung, kidney, heart liver, spleen and testis (Lu, *et al.*, 1998 and Miyagishi, *et al.*, 2000). However, unlike the *Pod 1* expression in *Xenopus laevis*, there is no expression in the muscle (Lu, *et al.*, 1998 and Miyagishi, *et al.*, 2000).

Xenopus Pod 1 over-expression in the pronephros resulted in a reduction of glomus area. The effect was observed using two glomus markers, *WT1* and *xlmx1b* and was found to be statistically significant. A further significant difference was found between

embryos with exogenous *Pod 1* and *GFP* expression, indicating that the glomus phenotype observed was not due to the mechanics of injecting mRNA into an embryo. *Pod 1* is known to promote differentiation, and in some cases inhibit proliferation (Andersson, *et al.*, 2001, Lu, *et al.*, 2000, Cui, *et al.*, 2003 and Funato, *et al.*, 2003). Exogenous *Pod 1* expression in the pronephros may reduce the size of the glomus directly, by inhibiting glomus competent cells from proliferating, or indirectly, by advancing the development of the glomus before critical cell numbers are achieved or recruited.

In accordant with the whole embryo measurements, sectioned *Pod 1* over-expression embryos also showed a reduction in glomus, as revealed by *WT1* expression. However, sections also indicated no difference in cell organisation between a pronephros with *Pod 1* or *GFP* over-expression (data not shown). This suggests the phenotype was not a result of compacted glomus cells.

The exogenous *Pod 1* expression did not appear to have an effect on the pronephric anlagen. The reduced glomus was therefore not due to an overall reduced cell number forming the pronephros. The pronephric tubules and duct were also unaffected by *Pod 1* over expression, which would suggest that the tubules and duct were not amassing pronephric anlagen cells at the expense of the glomus. Accordingly, it is improbable that the reduced glomus was a specific effect due to a reduced number of pronephric glomus competent cells available.

The reduced glomus may have been formed by glomus competent cells undergoing apoptosis. This is unlikely as the sectioned *Pod 1* over-expression embryos do not show any lesions or obvious spaces left by missing cells. However, this could be looked into by further analysis using TUNEL staining.

The reduced glomus may have also been formed by later differentiation events occurring earlier due to the presence of *Pod 1*. *Pod 1* is known to be involved in the terminal differentiation of specialised kidney cells (Quaggin, *et al.*, 1999 and Cui, *et al.*, 2003). The pronephric anlagen may develop into the three component subunits sequentially, for example later glomus differentiation events could trigger the onset of tubule formation which in turn trigger duct formation. If this was the case, *Pod 1* could

be differentiating pronephric anlagen competent cells into glomus competent cells earlier, which triggers tubule formation before enough pronephric anlagen cells have been recruited into glomus formation. The later pronephric tubule and duct events would carry on as normal. This would explain why the pronephric anlagen, pronephric tubules and duct remain unchanged by *Pod 1* over-expression, and yet the glomus is reduced.

The lack of pronephric anlagen, tubule and duct over-expression phenotype may be due to the absence of an appropriate Pod 1 binding partner. This is unlikely as a glomus phenotype was observed. Thus there would be a requirement for a separate binding partner for tubule and duct tissues from the glomus.

Pod 1 expression in the heart was found to be within the proepicardium, consistent with the mouse *Pod 1* expression (Hidai, *et al.*, 1998). The proepicardium is the region from which epicardial cells originate before migrating into and over the heart (Horb and Thomsen, 1999). Proepicardium cells are found mainly in the visceral pericardium surrounding the heart. By transplanting a quail donor proepicardial serosa into chick hearts, Männer (1999) also found proepicardial cells in the myocardium of the ventricles, outflow tract and the atria and the atrioventricular cushions. Some proepicardial cells go through an epithelial-mesenchymal transition and are found in connective tissue and coronary vascular elements (Münoz-Chapuli, *et al.*, 2002). This transition occurs just before cell migration (Morabito, *et al.*, 2001). *Pod 1* proepicardium expression was only visible briefly at stage 40.5. As *Pod 1* is known to be expressed in mesenchymal cells and involved in epithelial and mesenchymal interactions (Hidai, *et al.*, 1998, Lu, *et al.*, 1998, Lu, *et al.*, 2000, Robb, *et al.*, 1998, Quaggin, *et al.*, 1999 and Andersson, *et al.*, 2001), the brief expression of *Pod 1* in the *Xenopus* proepicardium may therefore be involved with, or a result of the epithelial-mesenchymal transition.

Although significantly contributing to the heart structure, the proepicardium does not derive from the cardiac loop (Fransen and Lemanski, 1990). This could explain why no structural phenotype was observed in the heart with exogenous *Pod 1* expression. The positioning of the heart to the left has not been analysed fully with repeat sections and

markers identifying the different regions of the heart, however, it is interesting that the heart lies to the left, similar to the proepicardium.

Further analysis of the heart phenotype would include observation of the proepicardium in *Pod 1* over-expression embryos. A lack of proepicardium markers in *Xenopus* have so far hindered this line of investigation. Looking into a *Xenopus* homologue of a mouse proepicardial marker such as *Tbx18* (Kraus, *et al.*, 2001) may resolve this issue.

Chapter 7

Pod 1 expression is required for glomus development.

7.1 Introduction

The potential role of *Pod 1* in pronephric development, suggested in Chapter 5, was strengthened in Chapter 6, by a reduction in glomus size resulting from *Pod 1* over-expression. To further investigate the function of *Pod 1* during pronephric development, *Pod 1* knock-down phenotypes were investigated and an attempt to place *Pod 1* in a genetic hierarchy by network analysis using animal caps was performed.

7.2 Results

7.2.1 *Pod 1* knock-down

Conventional knock-out experiments are impossible to perform in *Xenopus laevis* due to the tetraploid nature of the organism and lack of embryonic stem cell lines. However, knock-down experiments are possible with the use of morpholino oligonucleotides. A morpholino oligonucleotide is typically 18 to 25 bases in length, differing from DNA by the backbone consisting of 6-membered morpholino rings joined by non-ionic phosphorodiamidate links compared to DNA which has 5-membered deoxyribose rings. For knock-down properties, the morpholino oligonucleotide is usually designed to be complementary to a selected mRNA across the start site of the coding region. The morpholino oligonucleotide binds directly to the selected mRNA after transcription, preventing the assembly of ribosome on the mRNA. Without ribosome assembly, the selected mRNA will not be translated and no protein product will be formed. The morpholino oligonucleotide can therefore specifically knock-down the translation of a selected mRNA by inhibiting translation (Fig. 7.1).

The 6-membered morpholino ring backbone of the morpholino oligonucleotide is not recognised by cell nucleases and is so not degraded. The molecules are therefore stable in the cells for up to seven days after delivery into embryos, with activity only diminishing due to dilution by cell division. The backbone is also non-ionic, minimising interactions with proteins, and so reducing non-specific effects. Morpholino

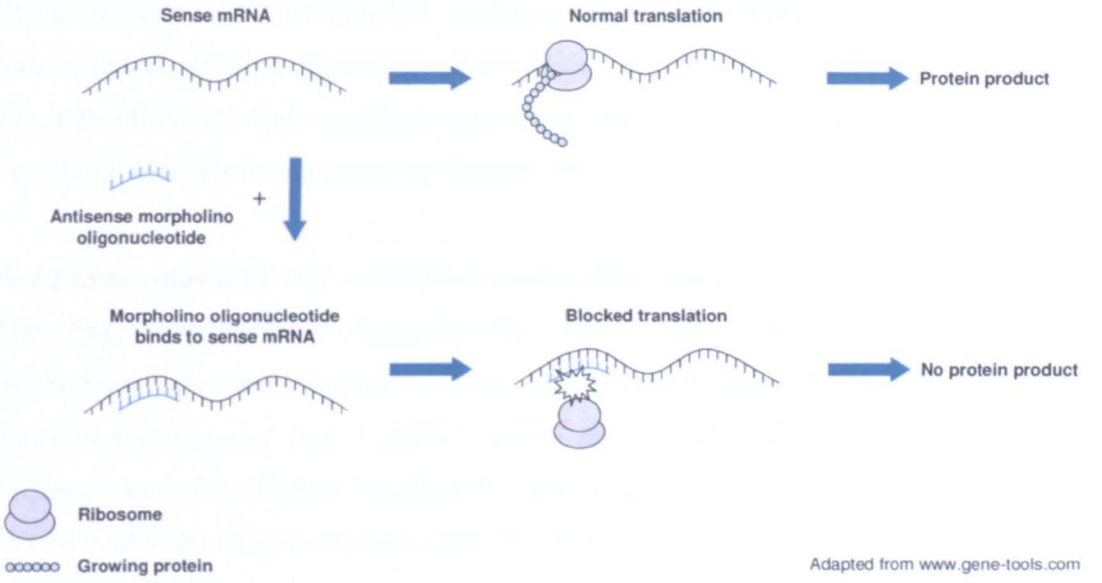

Fig. 7.1 **Morpholino oligonucleotides bind to mRNA inhibiting translation**. Sense mRNA is transcribed by the cell. During normal translation, ribosomes bind to the mRNA and translate the mRNA into the protein product. A morpholino oligonucleotide is typically 18-25 bases long and is designed to be complementary to a specific mRNA sequence over the translation start site of the coding region. In the presence of a morpholino oligonucleotide, the morpholino oligonucleotide binds to the mRNA and inhibits the assembly of ribosome on the mRNA. As the ribosome cannot bind to the mRNA, translation is inhibited and no protein product is formed.

oligonucleotides have a high affinity for mRNA, similar to that of DNA, and a minimum inactivating length of 14 (based on the minimum length sufficient to avoid attack on essentially all non-target sequences in a human RNA pool). They are also water soluble, allowing for embryo micro-injection (www.gene-tools.com). Together this high efficiency and specificity means that these molecules can decrease protein expression to levels undetectable by Western blot.

Pod 1 knock-down by *Pod 1* morpholino oligonucleotide

The *Pod 1* morpholino oligonucleotide (PMO) was designed by Gene Tools (www.gene-tools.com) using the *Xenopus Pod 1* sequence (EST CF270487). The PMO binds to the *Xenopus Pod 1* mRNA across the translational start site (Fig. 7.2A). Sequence analysis using the NCBI EST database indicated that the designed PMO is able to bind to *Pod 1* pseudoalleles (data not shown, www.ncbi.nlm.nih.gov). The PMO was able to specifically knock-down exogenous *Pod 1* expression in vivo (Fig. 7.2B) as indicated by an autoradiograph showing translation of *Pod 1* mRNA in oocytes in the presence of radioactive amino acids. *Xenopus Pod 1* mRNA, synthesised using SP6 mMessage mMachine kit (Ambion), was injected alone, with the PMO and with the control morpholino oligonucleotide (CMO). The oocytes were incubated in Barth X containing ^{35}S methionine and cysteine. This radioactively labelled any new proteins synthesised after oocytes were injected. The *Xenopus* Pod 1 protein, identified by size (25kDa) and absence from the water injected oocytes, was present only in oocytes injected with *Xenopus Pod 1* mRNA alone and with the CMO. The lack of Pod 1 protein in the *Xenopus Pod 1* mRNA and PMO co-injected oocytes indicated that the morpholino oligonucleotide inhibited translation of the mRNA.

The ability of PMO to inhibit *xPod 1* translation was further confirmed by western analysis using c-myc tagged *xPod 1* mRNA injected into oocytes (Fig. 7.2C). The injections were performed as previously, except c-myc tagged *xPod 1* mRNA was used and the oocytes were not radioactively labelled. Instead, Western analysis using anti-myc antibody (MAB 9E10) followed by an anti-mouse alkaline phosphatase secondary antibody (SIGMA) was performed. The *Xenopus* Pod 1 protein was absent from the PMO injected oocytes.

The effect of the PMO on the translation of mouse *Pod 1* mRNA, transcribed from BC053525 (previously cloned into pCS2+ and synthesised using SP6 mMessage mMachine kit), was also analysed using radioactively labelled oocytes. Translation of the mouse *Pod 1* mRNA was not effected by the presence of the PMO or CMO, as indicated by the presence of the protein in the injected oocytes (Fig. 7.2B). Mouse *Pod 1* mRNA was therefore used to rescue the *Pod 1* knock-down phenotypes.

Phenotyping of PMO knock-down

The morpholino oligonucleotides were injected into one V2 cell of an 8 cell embryo to target the effect of *Pod 1* knock-down to the pronephric region. GFP was also co-injected for lineage tracing and the embryos were sorted for left or right pronephric fluorescence at stage 25-30 (Methods 2.10.3 Micro-injection). The phenotypes observed in the embryos were quantified by measurements and validated using statistical analysis similarly to the over-expression experiments.

The morphology of the pronephric tubules was determined using the Pronephric Index (PNI) (Wallingford, *et al.*, 1998) (Methods 2.10.8 Pronephric Index). The morphology of the pronephric duct and presence of the glomus/pronephric anlagen was scored by eye. The size of the pronephric anlagen was measured in accordance with the methods (Methods 2.10.7 Measurement of tissue area).

Comparisons within the same experimental set involved left and right comparison of the same embryo to identify potential phenotypes. For PNI and pronephric anlagen measurements, this involved using the paired t-test, if the data were normal, or the Wilcoxon paired test, if the data were not normal. Where the data were categorical (presence or absence of the glomus/pronephric anlagen), the data were analysed using the Fisher's exact test. Fisher's exact test was used rather than the better known Chi Square test due to the table producing 1 degree of freedom, and the low values within the table. All statistical analysis was performed using the InSTAT 3 programme, (GraphPad Software Inc).

A

...5′ GGAGCAGCATAACAGATCATGTCCACCGGTTCTCTC 3′ ... *xPod 1* sequence

3′ CGTCGTATTGTCTAGTACAGGTGGC 5′ *xPod 1* morpholino (reverse)

...5′ CCCTCCACCTCTCTAAACATGTCCACTGGCTCCCTC 3′ ... *mPod 1* sequence

B

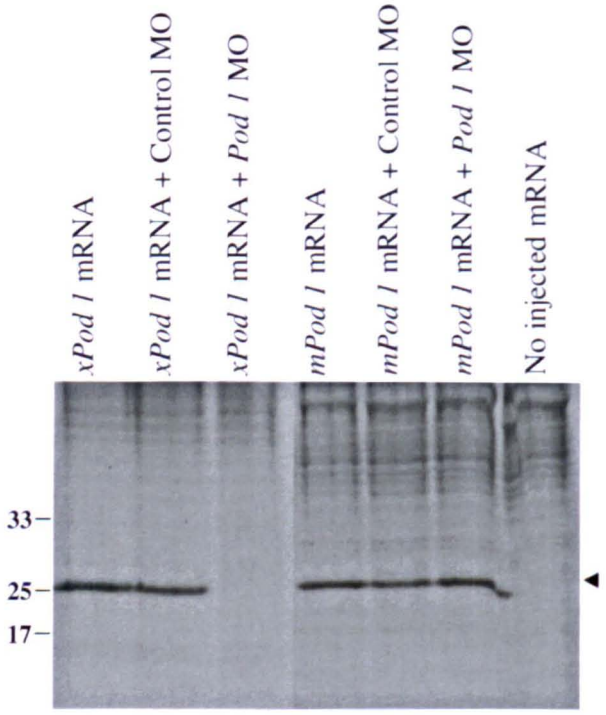

C

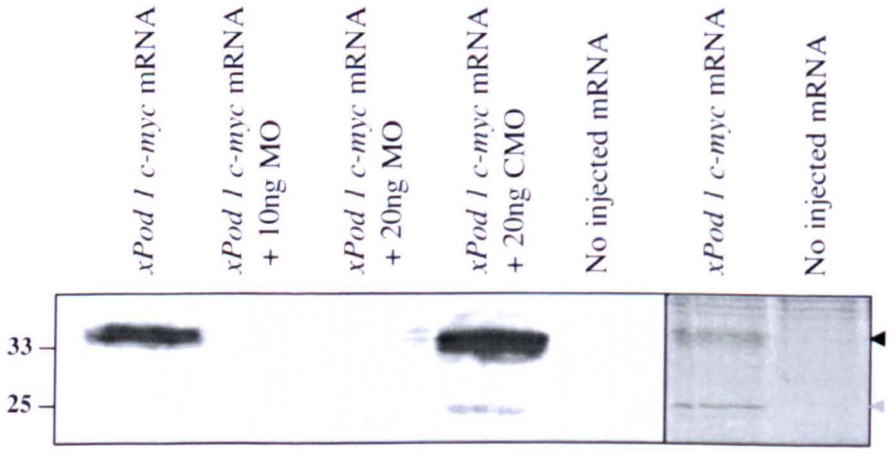

Fig. 7.2 ***Pod 1* morpholino specifically knocks-down *Xenopus Pod 1* mRNA translation *in vivo*.**

(**A**) The *Xenopus Pod 1* sequence (EST CF270487, www.ncbi.nlm.nih.gov) was used to design the *Pod 1* morpholino oligonucleotide by Gene Tools (www.gene-tools.com). The *Pod 1* morpholino oligonucleotide binds to the *Xenopus Pod 1* mRNA across the translational **start site**, inhibiting translation. The *Pod 1* morpholino oligonucleotide ($^{5'}$CGG TGG ACA TGA TCT GTT ATG CTG C$^{3'}$) is shown in reverse to indicate **binding region**. Mouse *Pod 1* mRNA (BC053525) was used to rescue the *Pod 1* knock-down phenotype as it will not anneal to the morpholino oligonucleotide. (**B**) Autoradiograph showing *in vivo* translation of *Xenopus* and mouse *Pod 1* mRNA in *Xenopus* oocytes in the presence and absence of morpholino oligonucleotides. The oocytes were injected and incubated overnight in full strength Barth X containing ^{35}S labelled methionine and cysteine (10μCi). The protein from the oocytes was extracted and run on a 10% SDS PAGE gel and exposed for autoradiography. The protein products from injected *Xenopus* and Mouse *Pod 1* mRNA are highlighted by the **black arrow** and protein size is shown in kDa. The oocytes were injected and lanes were loaded as indicated, with the "No injected mRNA" as the negative control. *xPod 1* translation was knocked-down specifically by the *Pod 1* morpholino oligonucleotide and not by the control morpholino oligonucleotide. However, mouse *Pod 1* translation was not affected by the presence of either of the morpholino oligonucleotides. (**C**) Western blot and autoradiograph showing *in vivo* translation of c-myc tagged *Xenopus Pod 1* mRNA in the presence of morpholino oligonucleotides. As previously, the oocytes were injected and lanes were loaded as indicated. The western blot (to the left) using anti-myc antibody, shows the translated Pod 1 protein (**black arrow**) was knocked-down by the *Pod 1* morpholino oligonucleotide and not by the control morpholino oligonucleotide. An autoradiograph (to the right) is also shown to verify the size, approximately 35kDa, of the c-myc tagged Pod 1 protein. A smaller band (grey arrow) was also apparent in the western and the autoradiograph which may be a degradation product of the c-myc tagged Pod 1 protein.

7.2.1.1 *Pod 1* expression is required for glomus development

***Pod 1* knock-down obliterates expression of the glomus marker *WT1*.**

The 8 cell embryos were injected into one V2 cell with either; 40ng PMO and *GFP* mRNA to indicate the effect of *Pod 1* knock-down; 40ng PMO, 0.6ng mouse *Pod 1* mRNA and *GFP* mRNA to rescue the effect of the *Pod 1* knock-down, confirming that a reduction in *Pod 1* expression caused any phenotype observed; or 40ng CMO and *GFP* mRNA to show the non-specific consequences of injecting an embryo with a morpholino oligonucleotide. GFP fluorescence was used to indicate left or right pronephric targeting between stages 25 to 30. The embryos were fixed at stage 33 to 35 and wholemount *in situ* hybridisation was performed with a *WT1* DIG-labelled antisense RNA probe.

Pod 1 expression was found to be required for *WT1* expression in the glomus (Fig. 7.3). The 40ng PMO and *GFP* mRNA injected embryos showed a complete reduction of *WT1* expression in the glomus on the injected side of 13 out of 22 embryos tested (Appendix). Comparing the presence of *WT1* expression in the glomus on the injected and not injected sides of the embryo with the Fisher's exact test, indicated a significant correlation between whether the side of the embryo was injected and the observed down regulation of the *WT1* expression domain ($p < 0.0001$). The rescued embryo injected with 40ng PMO, 0.6ng *mPod 1* mRNA and *GFP* mRNA did not show a correlation using Fisher's exact test ($p = 0.0557$) with only 7 out of 35 embryos missing *WT1* expression. The PMO phenotype was therefore partially rescued using mouse *Pod 1* mRNA, which confirms that the specificity of the phenotype was caused by *Pod 1* knock-down. The 40ng CMO and *GFP* mRNA injected embryos also did not show a glomus phenotype by the Fisher's exact test ($p = 1$, $N = 32$) suggesting that the phenotype was not a product of injecting the embryos with any morpholino oligonucleotide or an injection artefact.

***Pod 1* knock-down prevents expression of *Xlmx1b* in the glomus**

In order to observe whether *Pod 1* knock-down had an effect on the glomus, not just *WT1* expression, a second glomus marker, *xlmx1b*, was used to analyse the *Pod 1* knock-down phenotype. The 8 cell embryos were injected as previously into one V2 cell, using GFP as a lineage marker. The embryos were sorted for left/right pronephric

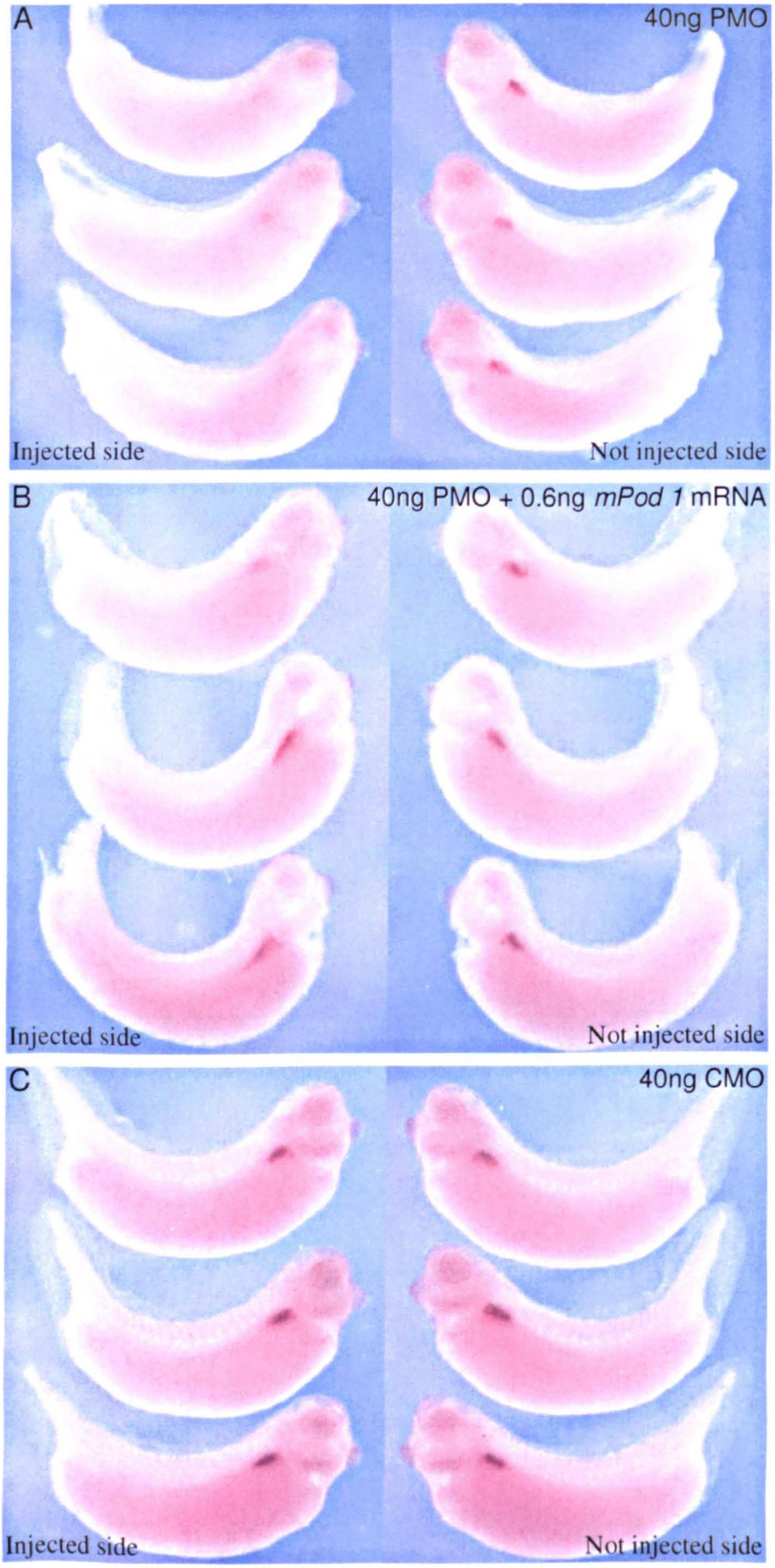
A
40ng PMO
Injected side
Not injected side
B
40ng PMO + 0.6ng *mPod 1* mRNA
Injected side
Not injected side
C
40ng CMO
Injected side
Not injected side

Fig. 7.3 ***Pod 1* expression is required for *WT1* expression in the glomus.** Embryos were injected into one V2 cell of an 8 cell embryo. The injections were; 40ng *Pod 1* morpholino oligonucleotide and *GFP* mRNA (**A**), 40ng *Pod 1* morpholino oligonucleotide, 0.6ng *mPod 1* mRNA and *GFP* mRNA (**B**) and 40ng control morpholino oligonucleotide and *GFP* mRNA (**C**). GFP fluorescence was used as a lineage trace, checking for left or right pronephric targeting. Not injected sides and injected sides of the same embryos were as indicated. Wholemount *in situ* hybridisation was performed with a *WT1* DIG-labelled antisense RNA probe on stage 33-35 embryos. *Pod 1* expression is required for *WT1* expression in the glomus, as indicated by the lack of WT1 expression in the *Pod 1* morpholino oligonucleotide injected side of the embryo (**A**). This phenotype was rescued using mouse *Pod 1* mRNA which does not bind to the *Pod 1* morpholino oligonucleotide (**B**). The control morpholino oligonucleotide injected embryos have normal *WT1* expression in the glomus (**C**).

targeting using GFP fluorescence and fixed at stage 35 to 38. Wholemount *in situ* hybridisation was performed with an *xlmx1b* DIG-labelled antisense RNA probe to highlight expression.

The data confirmed that *Pod 1* expression is also required for *xlmx1b* expression (Fig. 7.4). The glomus, indicated by *xlmx1b* expression, was missing on the injected side of the 40ng PMO and *GFP* mRNA injected embryos in 11 out of 22 embryos (Appendix). The Fisher's exact test gave a p value of 0.0002, showing a significant correlation between whether the side of the embryo was injected and the presence of the glomus. The phenotype was rescued in embryos injected with 0.6ng mouse *Pod 1* mRNA with the Fisher's exact test implying no significant correlation in injected or not injected side of the embryo with the presence of the glomus (N = 20, p = 0.1818). The embryos injected with the CMO also indicated no significant correlation (N = 23, p = 1). The phenotype observed was therefore from the knock-down of *Pod 1* expression and not from the mechanics of injecting a non-specific morpholino oligonucleotide.

These experiments studying the effect of *Pod 1* knock-down on the glomus, were repeated 6 times, each time with the phenotype being observed.

Histological analysis of *Pod 1* knock-down embryos shows a lack of any glomus structure.

The embryos were injected as before, and wholemount *in situ* hybridisation was performed on embryos staged 33 to 35, with a *WT1* DIG-labelled antisense RNA probe. To observe the effect of *Pod 1* knock-down in the glomus at the cellular level, 3 embryos from the 3 injection sets (40ng PMO and *GFP* mRNA; 40ng PMO, 0.6ng mouse *Pod 1* mRNA and *GFP* mRNA; 40ng CMO and *GFP* mRNA – data not shown) were wax embedded and transverse sections were collected across the glomus region (All sections were performed by Mr Surinder Bhamra) (Methods 2.10.6 Wax-sectioning and Fig. 7.5). As expected from the earlier whole embryo analysis, the embryo injected with PMO did not appear to have any *WT1* expressing cells in the glomus region. Furthermore, there did not appear to be any cells in the glomus region, when compared to the other not injected side of the embryo. The rescued embryo, injected with PMO and mouse *Pod 1* mRNA, had a normal glomus on the injected and not injected sides of

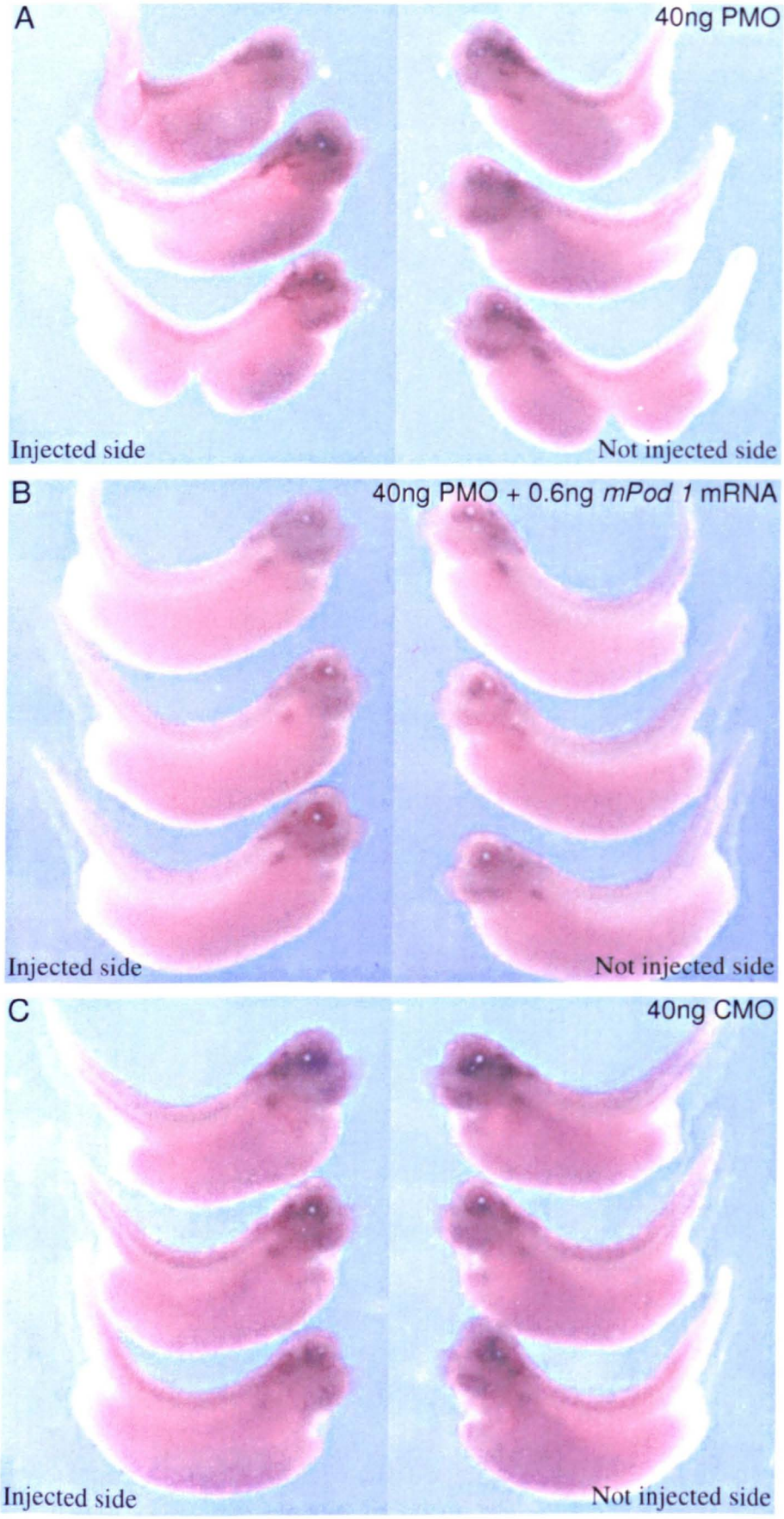
A
40ng PMO
Injected side
Not injected side
B
40ng PMO + 0.6ng *mPod 1* mRNA
Injected side
Not injected side
C
40ng CMO
Injected side
Not injected side

Fig. 7.4 ***Pod 1* expression is required for glomus development.** 8 cell stage embryos were injected into one V2 cell. The embryos were injected with; 40ng *Pod 1* morpholino oligonucleotide and *GFP* mRNA (**A**), 40ng *Pod 1* morpholino oligonucleotide, 0.6ng *mPod 1* mRNA and *GFP* mRNA (**B**) and 40ng control morpholino oligonucleotide and *GFP* mRNA (**C**). Left or right pronephric targeting was identified using GFP fluorescence. The not injected sides and injected sides of the same embryos were as indicated. Wholemount *in situ* hybridisation was performed with an *xlmx1b* DIG-labelled antisense RNA probe on stage 35-38 embryos. Pod 1 knock-down results in the complete reduction of the glomus, as shown by xlmx1b expression (**A**). The phenotype was rescued using mouse *Pod 1* mRNA which will not bind to the *Pod 1* morpholino oligonucleotide (**B**). The control morpholino oligonucleotide injected embryos have normal glomus development (**C**).

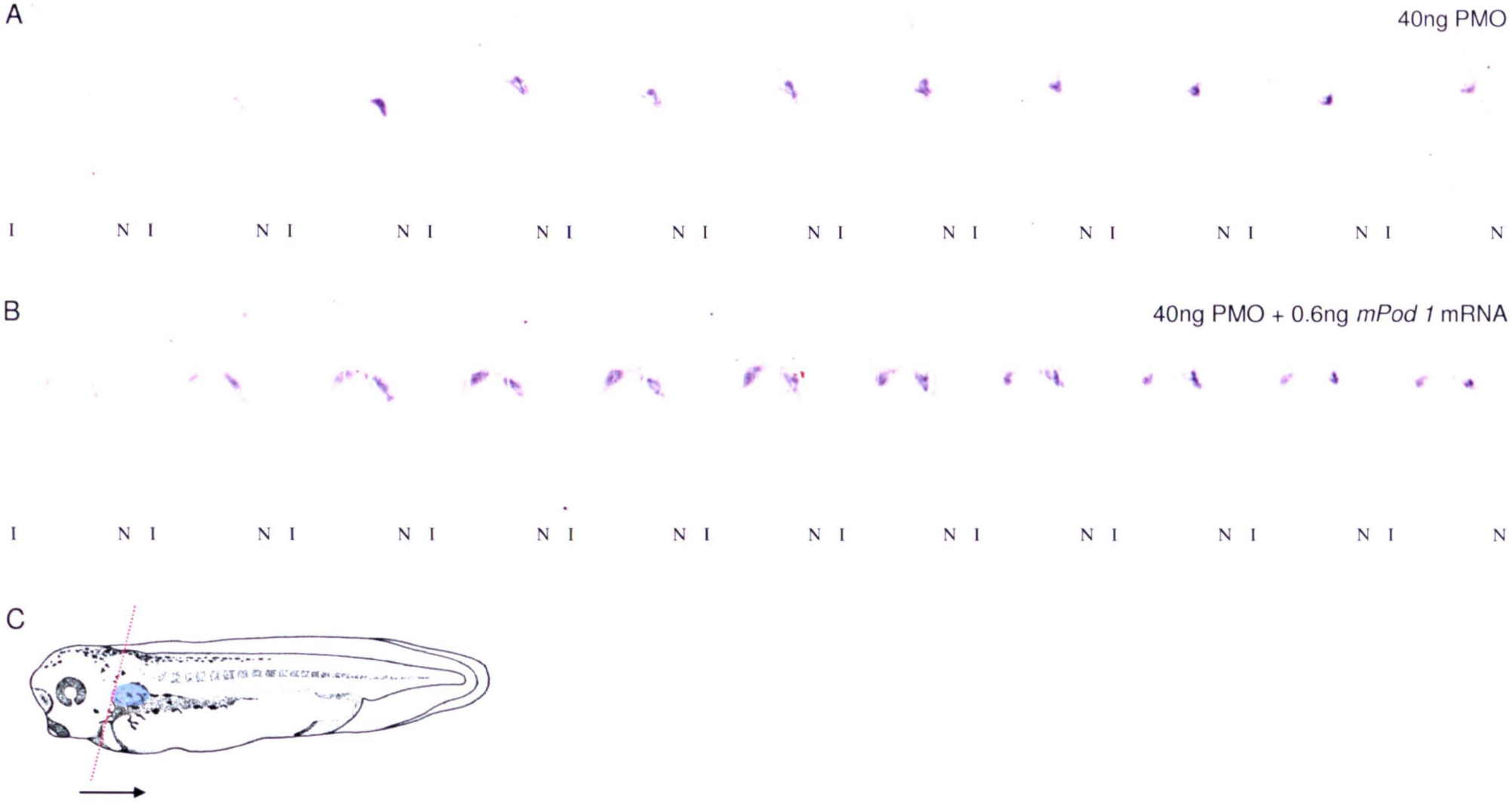
A
40ng PMO
I N I N I N I N I N I N I N I N I N I N
B
40ng PMO + 0.6ng *mPod 1* mRNA
I N I N I N I N I N I N I N I N I N I N
C

Fig. 7.5 **Pod 1 knock-down may reduce survival of glomus cells.** The embryos were injected at the 8 cell stage into one V2 cell, with; 40ng *Pod 1* morpholino oligonucleotide and *GFP* mRNA (**A**) or 40ng *Pod 1* morpholino oligonucleotide, 0.6ng *mPod 1* mRNA and *GFP* mRNA (**B**). Embryos were sorted using GFP fluorescence, checking for left or right pronephric targeting. The injected side (**I**) and the not injected side (**N**) of the embryo are indicated. Wholemount *in situ* hybridisation was performed with a *WT1* DIG-labelled antisense RNA probe on stage 33-35 embryos. The embryos were then wax-sectioned. The **black** arrow indicates the anterior to posterior direction of sequential wax sections and the **red** dotted line shows the sectioning plane (**C**) (Image from Nieuwkoop and Faber, 1994). (**A**) Embryos injected with *Pod 1* morpholino oligonucleotide appear to be missing WT1 expressing cells on the injected side of the embryo. Embryos that have been rescued by co-injecting *mPod 1* mRNA have a normal glomus on the injected and not injected sides of the embryo (**B**). In addition, pronephric tubule tissue also appears to be missing in the *Pod 1* morpholino oligonucleotide injected embryos (**A**).

the embryo, further evidence that the mouse *Pod 1* mRNA is able to rescue the *Pod 1* knock-down phenotype and restore the glomus structure.

7.2.1.2 *Pod 1* knock-down disrupts tubule morphology

In order to establish whether other components of the kidney were effected, the experiment was repeated and the embryos fixed at stage 38 to 42. Wholemount immuno-histochemistry analysis was performed and the monoclonal antibodies, 3G8 to highlight the pronephric tubules, and 4A6 to show the duct, were used. The PNI was used to analyse the morphology of the tubules (Wallingford, *et al.*, 1998) (Methods 2.10.8 Pronephric Index) and the structure of the pronephric duct was scored by eye. As slight differences between embryo sets could not be discounted, the embryos were analysed by comparison of the injected side to not injected side only.

The pronephric tubules on the injected side of the *Pod 1* knock-down embryos were disorganised, having a PNI median of 2, compared to the not injected side, with a PNI median of 4 (Fig. 7.6) (Appendix). A Wilcoxon paired test revealed the difference in PNI between the injected and not injected sides of the embryo to be significant, $p = 0.0004$. Furthermore, a PNI difference of 2 or more was observed in 13 of the 17 embryos. The tubules themselves were larger and appeared to consist of just one tubule branch.

The phenotype was rescued in mouse *Pod 1* mRNA co-injected embryos which have relatively normal pronephric tubules on both sides of the embryo, each with a PNI median of 4. There was no significant difference observed in the data after analysis with the Wilcoxon paired test, $p = 0.0730$ ($N = 23$). The effect on the pronephric tubules could therefore be attributed to the knock-down effect of *Pod 1*, and not a by-product of injecting the PMO. The CMO injected embryos also had normal pronephric tubule morphology, with PNI of 4 for the injected side of the embryo and 5 for the not injected side of the embryo ($N = 24$). Again, the Wilcoxon paired test revealed no significant differences, $p = 0.0897$.

Differences in the pronephric duct structure were difficult to ascertain due to a lack of staining in the pronephric duct region. This could either be due to abnormal staining or

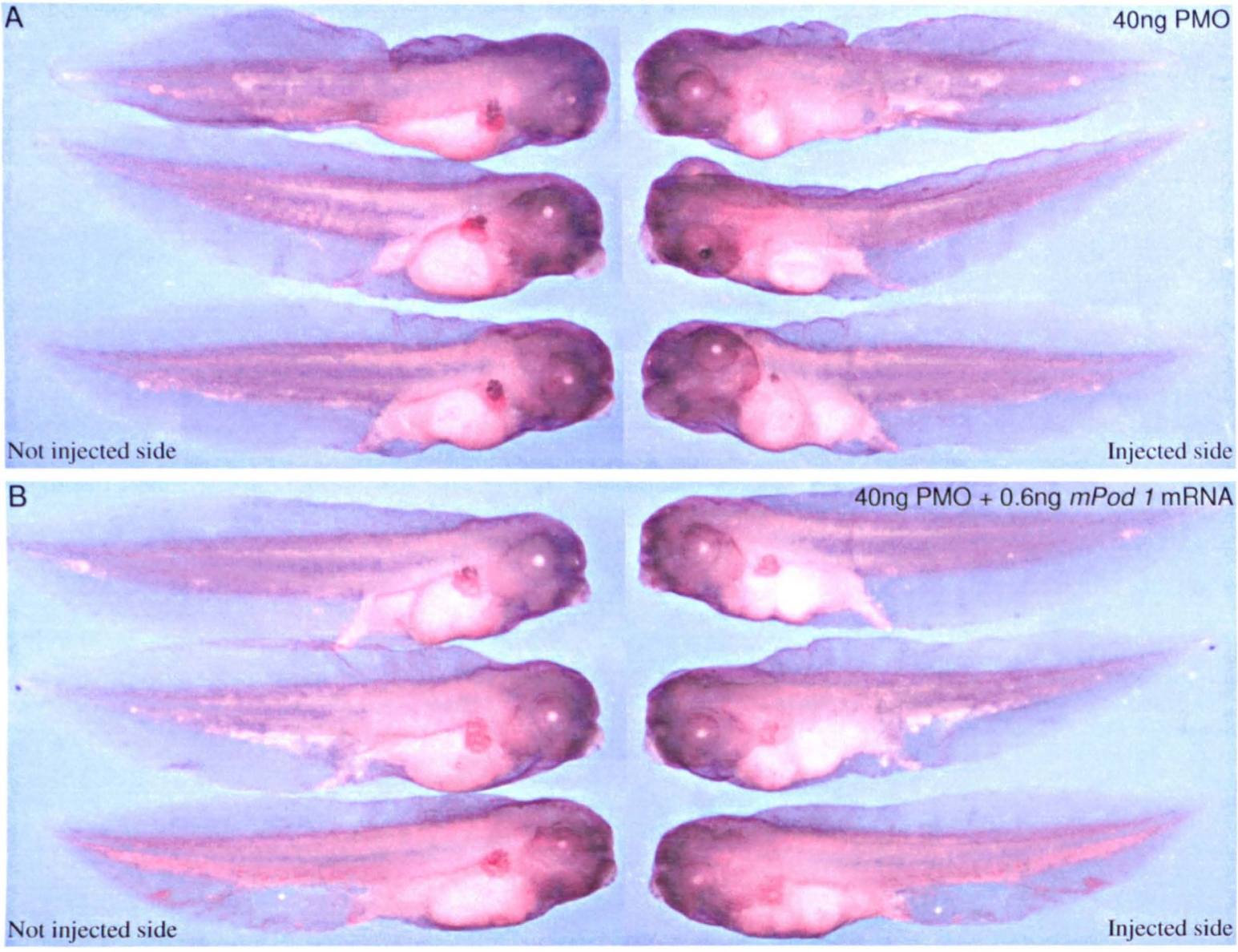
A
40ng PMO
Not injected side
Injected side
B
40ng PMO + 0.6ng *mPod 1* mRNA
Not injected side
Injected side

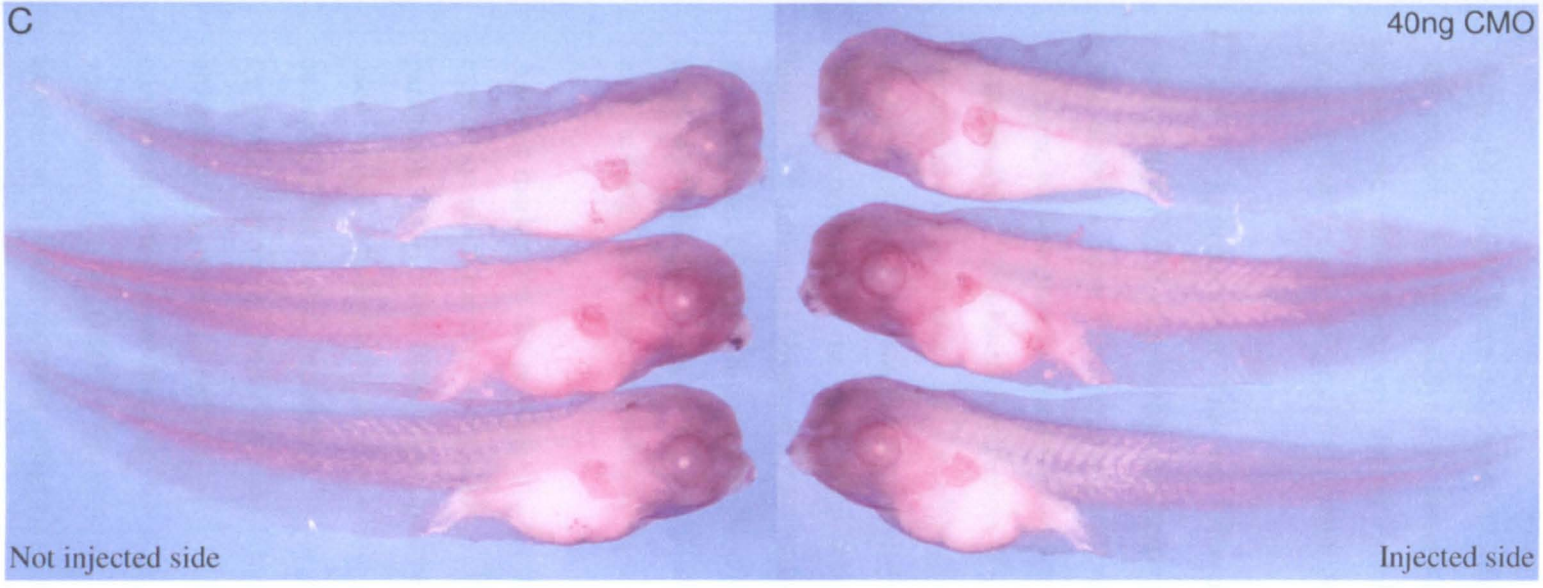

Fig. 7.6 ***Pod 1* knock-down disrupts tubule morphology.** Embryos were injected at the 8 cell stage into one V2 cell. The injections included; 40ng *Pod 1* morpholino oligonucleotide and *GFP* mRNA (**A**), 40ng *Pod 1* morpholino oligonucleotide, 0.6ng *mPod 1* mRNA and *GFP* mRNA (**B**) and 40ng control morpholino oligonucleotide and *GFP* mRNA (**C**). The left or right pronephric targeting was indicated using GFP fluorescence. Not injected sides and injected sides of the same embryos are as shown. Wholemount immunohistochemistry was performed stage 39 to 42 embryos, identifying the pronephric tubules, 3G8 (purple), and the duct, 4A6 (red). The pronephric tubules of Pod 1 knock-down pronephroi were disorganised compared to the not injected side of the same embryo (**A**). The phenotype was rescued in mouse *Pod 1* mRNA injected embryos which have a normal pronephros (**B**). The control morpholino oligonucleotide injected embryos have normal pronephric tubule morphology (**C**).

a phenotypic difference. Further repeat experiments and section analysis will resolve this issue.

Although striking, these data have not been repeated, since they were achieved late in the project. Further analysis is therefore required to clarify the true nature of the pronephric tubule phenotype during *Pod 1* knock-down. However, the success of the mouse *Pod 1* rescue suggests the phenotype discovered was genuine.

7.2.1.3 *Pod 1* knock-down has no obvious effect on *Xlim1* expression, but abrogates *Pax 8* expression in the pronephric anlagen

The embryos were injected and sorted as previously. To visualise the pronephric anlagen, wholemount *in situ* hybridisation was performed on embryos staged 20 to 25, with an *Xlim1* DIG-labelled antisense RNA probe. The area of *Xlim1* expression was measured on both sides of the embryo using the LUCIA programme (Laboratory Imaging Ltd.). The data indicated that *Pod 1* knock-down did not have an effect on *Xlim1* expression in the pronephric anlagen (Fig. 7.7) (Appendix). There was no significant difference observed by the Wilcoxon paired test between the injected and not injected sides of the embryo in the 40ng PMO injected embryos ($N = 31$, $p = 0.1042$), the 40ng PMO and 0.6ng mouse *Pod 1* mRNA injected embryos ($N = 26$, $p = 0.8117$) and the 40ng CMO injected embryos ($N = 28$, $p = 0.6556$).

Another marker for the pronephric anlagen is *Pax 8* (Carroll and Vize, 1999). *Pod 1* expression in animal caps was shown to effect *Pax 8* expression by RT-PCR (Chapter 7, paragraph 7.2.3). The PMO experiment was repeated with the exception that the probe used in the wholemount *in situ* hybridisation analysis was a *Pax 8* DIG-labelled antisense RNA probe. In addition, 1.2ng of mouse *Pod 1* mRNA was required to rescue the PMO phenotype. *Pod 1* knock-down eliminated *Pax 8* expression in the pronephric anlagen of 12 out of 25 embryos (Fig. 7.8). Fisher's exact test indicated a significant correlation in the observation of *Pax 8* expression and whether the side of the embryo was injected, $p < 0.0001$. Co-injection with mouse *Pod 1* mRNA restored *Pax 8* expression in the pronephric anlagen of 16 out of 21 embryos, and no correlation with the presence of expression domain in the injected and not injected side of the embryos, was found after Fisher's exact test, $p = 1836$. The control morpholino oligonucleotide

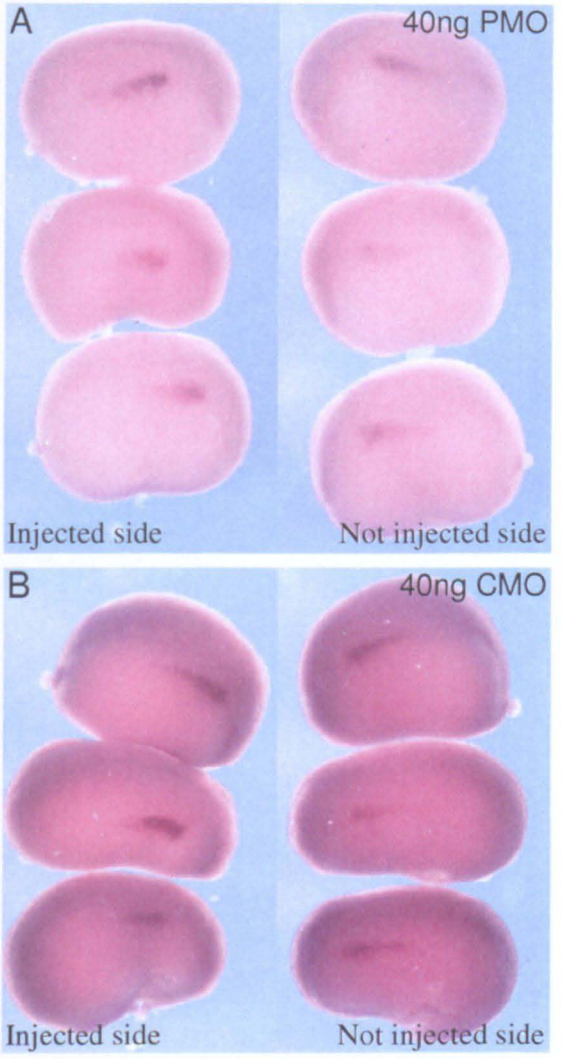

Fig. 7.7 ***Pod 1* knock-down has no effect on early *Xlim1* expression**. The 8 cell embryos were injected into one V2 cell with either; 40ng *Pod 1* morpholino oligonucleotide and *GFP* mRNA (**A**) or 40ng control morpholino oligonucleotide and *GFP* mRNA (**B**). Left or right pronephric targeting was identified using GFP fluorescence. The injected and not injected sides of the same embryo are as shown. Wholemount *in situ* hybridisation was performed with an *Xlim 1* DIG-labelled antisense RNA probe on stage 20 to 25 embryos to indicate the pronephric anlagen. Pod 1 knock-down did not appear to have an effect on early *Xlim 1* expression (**A**). The control morpholino oligonucleotide injected embryos also had normal *Xlim 1* expression (**B**).

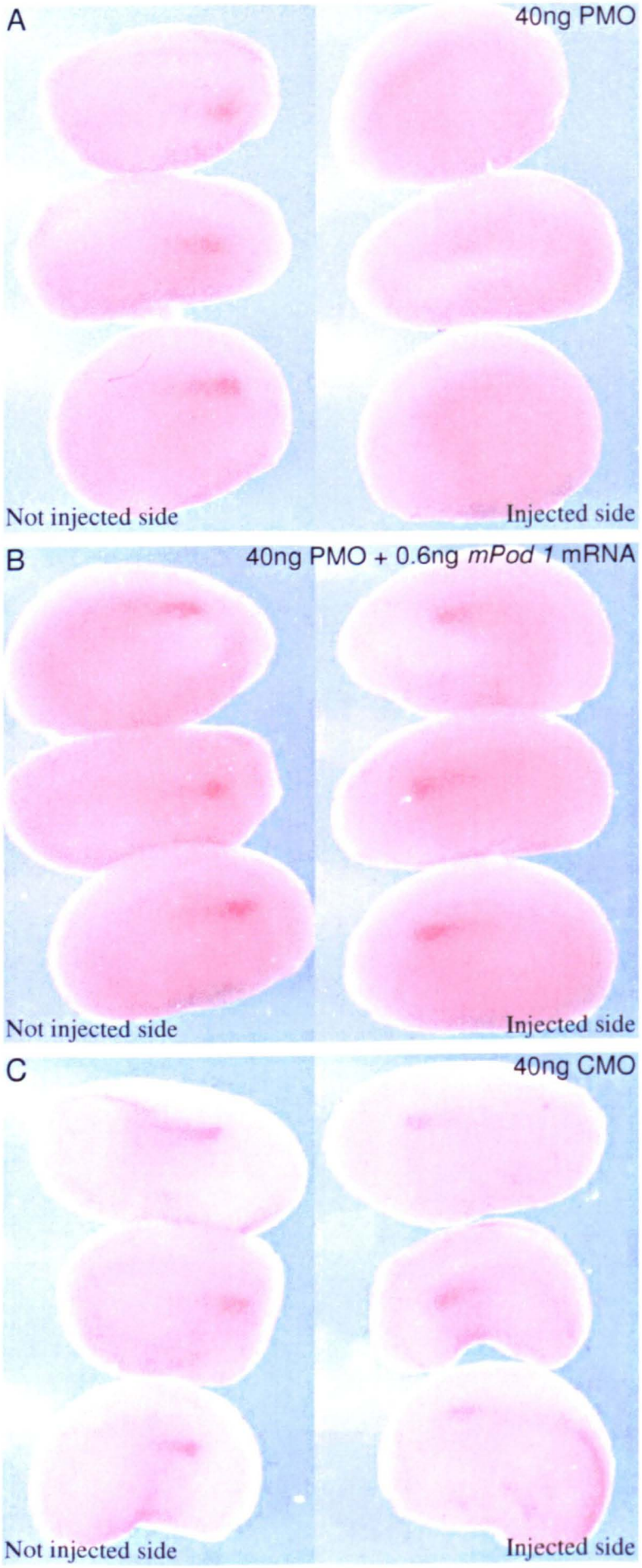
A
40ng PMO
Not injected side
Injected side
B
40ng PMO + 0.6ng *mPod 1* mRNA
Not injected side
Injected side
C
40ng CMO
Not injected side
Injected side

Fig. 7.8 ***Pod 1* expression is required for *Pax 8* expression.** The embryos were injected at the 8 cell stage into one V2 cell, with; 40ng *Pod 1* morpholino oligonucleotide and *GFP* mRNA (**A**), 40ng *Pod 1* morpholino oligonucleotide, 0.6ng *mPod 1* mRNA and *GFP* mRNA (**B**) and 40ng control morpholino oligonucleotide and *GFP* mRNA (**C**). GFP fluorescence was used to identify left or right pronephric targeting. The not injected sides and injected sides of the same embryos were as shown. Wholemount *in situ* hybridisation was performed with a *Pax 8* DIG-labelled antisense RNA probe on stage 20-25 embryos. *Pod 1* knock-down eliminated *Pax 8* expression in the pronephric anlagen (**A**). *Pax 8* expression was restored by co-injecting mouse *Pod 1* mRNA, as it does not bind to the *Pod 1* morpholino oligonucleotide (**B**). The control morpholino oligonucleotide injected embryos showed normal *Pax 8* expression (**C**).

injected embryos showed normal *Pax 8* expression on both sides of the embryo and also gave no correlation with Fisher's exact test, p = 1 (N = 20).

7.2.2 *Pod 1* expression was initiated at the same stage as other pronephric development genes

The temporal expression pattern of *Pod 1* was determined using RT-PCR in Chapter 5. The same method was used to compare the temporal expression patterns of other pronephric development genes and class A basic helix-loop-helix transcription factors to that of *Pod 1*. This might indicate which genes *Pod 1* expression might influence during pronephric development. RT-PCR was performed using primers designed for *E12*, *E47*, *ITF2b*, *Lim 1*, *Pax 2*, *Pax 8*, *WT1* and *xlmx1b* (Methods Table 2.1). The mRNA was extracted from stages 9, 13, 16, 21, 26, 30, 35 and unfertilised eggs and cDNA was generated. As previously, the input cDNA was equalised using *ODC* and a linearity was produced using doubling dilutions of stage 35 cDNA. The class A basic helix-loop-helix transcription factors, *E12*, *E47*, and *ITF2b* were expressed in unfertilised eggs or early in the blastula and did not have similar temporal expression patterns to *Pod 1* (Fig. 7.9). The pronephric development genes, however, were all up regulated at stage 13, pronephros initiation, except for *WT1* expression which was initiated at stage 21.

7.2.3 *Pod 1* expression in animal caps can up-regulate other pronephric development genes

Pod 1 is a basic helix-loop-helix transcription factor and is, therefore likely to be involved in a transcriptional network of genes resulting in the formation of the pronephros. It may be possible, using an animal cap system, to investigate the genetic pathway within which *Pod 1* acts. As described previously (Chapter 3), an animal cap is dissected from the animal pole region of the embryo at stage 8/9. This region of the embryo is multipotent and under the influence of 'differentiating factors', can form different tissues (Okabayashi and Asashima, 2003). The response of an animal cap to an injected mRNA could be interpreted as a simplification of events that occur in the whole embryo. Therefore, by analysing dissected animal caps injected with *Pod 1* mRNA the *Pod 1* or other pronephric development genes down stream in the genetic network could be revealed.

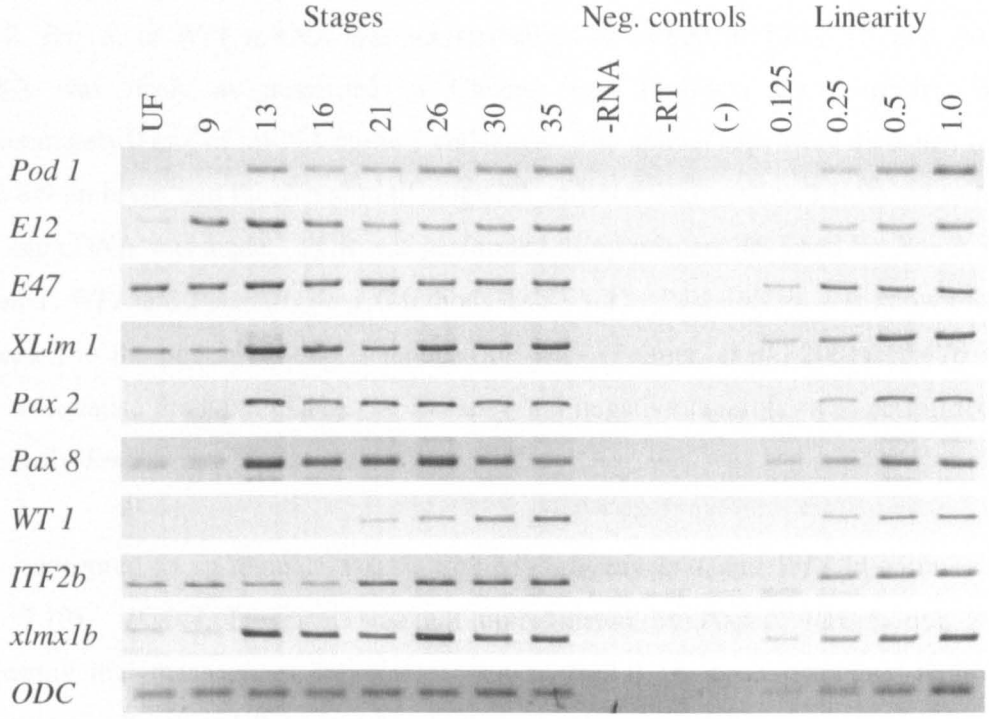

Fig. 7.9 ***Pod 1* temporal expression compared to a selection of pronephric development genes and class A basic helix-loop-helix transcription factors.** RT-PCR was performed on unfertilised *Xenopus laevis* eggs (UF) and whole *Xenopus laevis* embryos at stages 9, 13, 16, 21, 26, 30 and 35, using *Pod 1*, E12, *E47, Lim 1, Pax 2, Pax 8, Wt 1, ITF2b, xlmx1b* primers. Equalisation was carried out using *ODC* as a loading control and linearity was performed with doubling dilutions of input cDNA from stage 35 embryos. Negative controls include (**-RNA**) no RNA in the reverse transcription reaction, (**-RT**) no reverse transcriptase in the reverse transcription reaction and (**-**) no cDNA in the PCR reaction. RT-PCR analysis indicated that the class A basic helix-loop-helix transcription factors, *E12, E47*, and *ITF2b* were expressed in unfertilised eggs or early in the blastula. The pronephric development genes, *Pod 1*, *Lim 1*, *Pax 2*, *Pax 8*, and *xlmx1b* were all up regulated at stage 13, except for *WT 1* expression which was initiated at stage 21.

Pax 2, *Pax 8*, or *WT1* mRNA was transcribed as described in Table 7.1 and *Pod 1* mRNA was made as described in Chapter 6. Embryos were injected with approximately 0.6ng of mRNA at the 1 cell stage. The animal caps were dissected from stage 8/9 embryos and incubated until stage 25. mRNA was extracted from the animal caps and cDNA was made. PCR was performed using primers designed for *Pax 2*, *Pax 8*, *Pod 1*, *WT1* and *Podocalyxin 1* (Methods Table 2.1). *Podocalyxin 1* is known to be expressed in the podocytes and is induced by *WT1* (Palmer, *et al.*, 2001). *EF1α* was used to equalise the input cDNA. A linearity and negative controls were performed as previously described.

Pod 1 appeared to up-regulate *Pax 2*, *Pax 8*, *Podocalyxin 1* and *WT1* in animal caps (Fig. 7.10). *Pod 1*, however, was not up-regulated by *Pax 2*, *Pax 8*, nor *WT1*, suggesting that these genes are downstream of *Pod 1* in the hypothetical pathway. Interestingly, *Pax 8* and *WT1* injected animal caps behaved similarly, and up-regulated *Pax 2* and *Podocalyxin 1*. *Pax 8* and *WT1* injected animal caps were also able to increase the expression of each other, which may indicate a regulatory loop in the pathway.

7.2.4 Co-injection of *Pod 1* with class A basic helix-loop-helix transcription factors *E12*, *E47*, *HEB* and *ITF-2* fails to indicate any potential association

Pod 1 is a class B basic helix-loop-helix transcription factor (Hidai, *et al.*, 1998, Quaggin, *et al.*, 1998, Robb, *et al.*, 1998). Conventionally, class B basic helix-loop-helix transcription factors are expected to either form homodimers or heterodimerise with class A basic helix-loop-helix transcription factors. As detailed in Chapter 5, it is unknown whether Pod 1 homo- or heterodimerises *in vivo*. Possible binding partners include E12, HEB, HEB-s, ITF-2 (Lu, *et al.*, 1998, Miyagishi, *et al.*, 2000a, Miyagishi, *et al.*, 2000b) and there is evidence of homodimerisation (Hidai, *et al.*, 1998). One way to investigate potential binding partners was to inject *Pod 1* and selected class A basic helix-loop-helix transcription factors into embryos alone and in combination, and perform RT-PCR on dissected animal caps for known pronephric development genes. An up-regulation of a pronephric development gene in a co-injection would suggest an

Gene	Plasmid	Digest	mMessage mMachine kit (Ambion)	Source
Xenopus E12	E12 pSP64 Xβm	*Xba I*	SP6	Kindly donated by Prof. Gurdon, (Rashbass, et al., 1992)
Human *E47*	hE47p pGEM Teasy	*Sst II*	SP6	Kindly donated by Dr Caroline Haldin
Mouse *HEB*	HEB pBluescript KS	*Not I*	T3	BC037097, ordered from the IMAGE consortium (http://image.llnl.gov, IMAGE No. 5345693) and cloned into pBluescript KS with *Eco RV* and *Not I.*
Mouse *ITF2b*	ITF2b pBluescript KS	*Not I*	T3	BC043050, ordered from the IMAGE consortium (http://image.llnl.gov, IMAGE No. 5708370) and cloned into pBluescript KS with *Eco RI* and *Not I.*
Xenopus Pax 2	xPax 2 pSP64TS	*Sst I*	SP6	Kindly donated by Dr Tom Carroll
Xenopus Pax 8	xPax 8 pCS2+	*Sst II*	SP6	Kindly donated by Dr Tom Carroll
Xenopus WT 1	xWT1 pSP64TS	*Sst I*	SP6	Kindly donated by Dr Tom Carroll

Table 7.1 **mRNA sources used in animal cap assays**. Details of mRNA preparation for subsequent injection into embryos for animal cap assays. For full plasmid details, please refer to the Appendix.

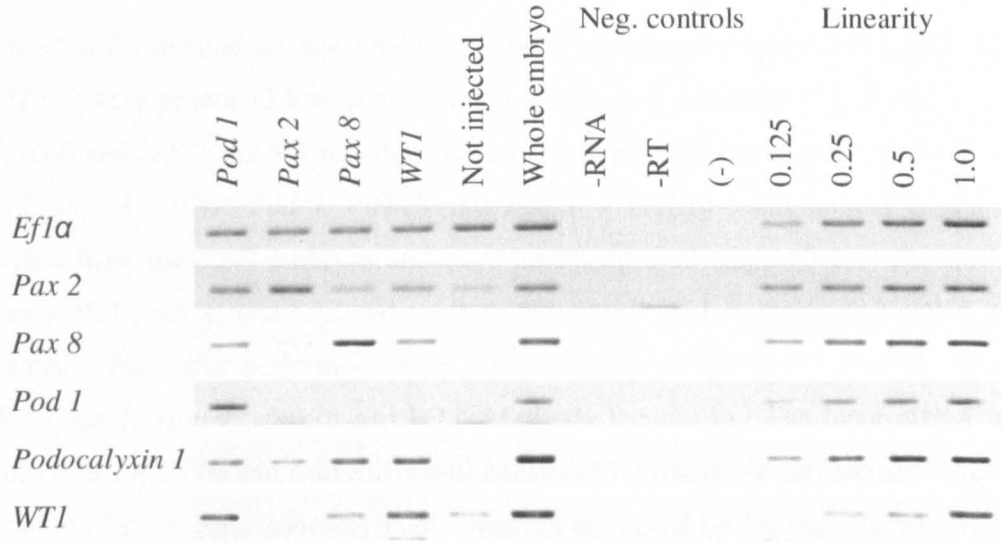

Fig. 7.10 ***Pod 1* may up-regulate other pronephric development genes.** Approximately 0.6ng of either *Pod 1*, *Pax 2*, *Pax 8*, or *WT1* mRNA was injected into embryos at the 1 cell stage (labelled horizontally). Animal caps were taken at stage 8/9 and incubated in ½ strength Barth's X. mRNA was extracted from animal caps and whole embryos when they reached stage 25 and cDNA was generated. PCR was performed using primers designed for *Pax 2*, *Pax 8*, *Pod 1*, *Podocalyxin 1* and *WT1*, as indicated vertically. Negative controls include, (**-RNA**) no RNA in the reverse transcription reaction, (**-RT**) no reverse transcriptase in the reverse transcription reaction and (**-**) no cDNA in the PCR reaction. A linearity control was performed using doubling dilutions of whole embryo cDNA and the loading of cDNA in the PCR reaction was equalised using *EF1α*. Levels of expression were compared with animal caps taken from not injected embryos (**Not injected**). *Pod 1* appeared to up-regulate *Pax 2*, *Pax 8*, *Podocalyxin 1* and *WT1*. *Pax 8* and *WT1* behaved similarly, up-regulating *Pax 2*, *Pax 8*, *Podocalyxin 1* and *WT1*. *Pax 2* weakly up-regulated *Podocalyxin 1*. Pod 1, however, is not up-regulated by *Pax 2*, *Pax 8*, or *WT1*, suggesting it lies close to the start of the regulatory cascade.

interaction and may be taken as evidence of heterodimerisation with the class A basic helix-loop-helix transcription factor.

The mRNA for the class A basic helix-loop-helix transcription factors, *E12*, *E47*, *HEB* and *ITF2b* were generated according to Table 7.1. Approximately 0.6ng of *Pod 1*, *E12*, *E47*, *HEB* and *ITF2b* mRNA was injected into 1 cell embryos alone and in pairs (*Pod 1* + *E12*, *Pod 1* + *E47*, *Pod 1* + *HEB* and *Pod 1* + *ITF2b*). The animal caps were dissected from stage 8/9 embryos and were incubated until stage 20-25. The mRNA was extracted from animal caps and some stage control whole embryos and cDNA was generated. PCR was performed using primers designed for *Pax 2*, *Pax 8*, *Pod 1*, *Podocalyxin 1*, *Xlim 1*, *xlmx1b* and *WT1* (Methods Table 2.1). The input cDNA was equalised using *EF1α* and a linearity and negative controls were performed. The up-regulation of pronephric genes by Pod 1 was not enhanced by the class A basic helix-loop-helix transcription factors injected, suggesting *Pod 1* may act as a homodimer or at least failed to heterodimerise with the class A transcription factors tested (Fig. 7.11). *E12* alone was able to up-regulate all the pronephric development genes tested, except *Podocalyxin 1*. This was an unexpected property for a class A basic helix-loop-helix transcription factor. E12 may have a role in pronephric development gene regulation or may be binding to a different class B transcription factor involved in pronephric development. The *E12* mRNA injected animal caps were extended, indicating mesoderm formation which could explain the up-regulation of the genes (Data not shown). This intriguing result may benefit from further investigation.

7.2.5 Retinoic acid and activin A effects *Pod 1* expression in treated animal caps

Retinoic acid and activin A can induce many different tissues, including the pronephros (Taira, *et al.*, 1994, Brennan, *et al.*, 1999 and Osafune, *et al.*, 2002), in treated animal caps, as detailed in Chapter 3. It is probable, therefore, that retinoic acid and activin A treatment in animal caps could effect the expression of pronephric development genes. To observe their effects on *Pod 1* expression, *Xenopus* animal caps were treated with different concentrations of retinoic acid and activin A. The animal caps from stage 8/9 embryos were dissected and incubated overnight in a range of 0 to 1 x 10^{-4}M of retinoic acid and 0 to 20ng/ml of activin A, as previously described (Chapter 3). Following treatment, the animal caps were incubated in Barth X until the equivalent of stage 22

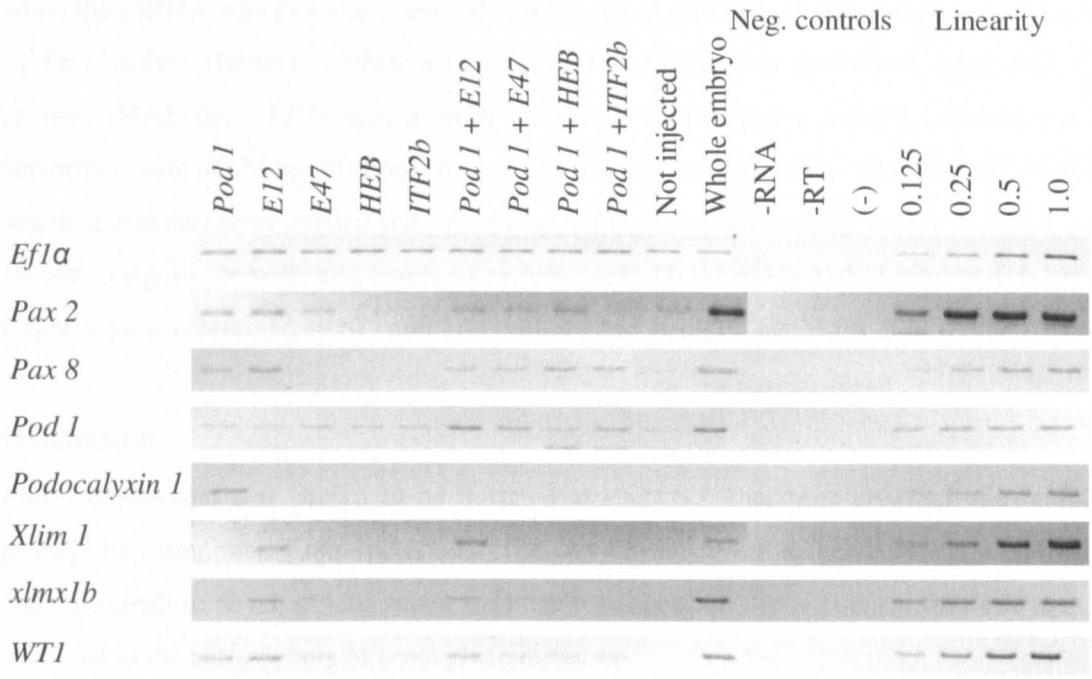

Fig. 7.11 ***Pod 1* pronephric gene up-regulation was not enhanced by the presence of class A basic helix-loop-helix transcription factors *E12, E47, HEB* and *ITF2b*.** Approximately 0.6ng of *Pod 1* mRNA and class A basic helix-loop-helix transcription factor mRNA, *E12*, *E47*, *HEB* and *ITF2b,* were injected into 1 cell embryos, alone and in combination (labelled horizontally). Animal caps were dissected from stage 8/9 embryos and incubated until stage 20-25. The mRNA was extracted from animal caps and stage control whole embryos and cDNA was generated. PCR was performed using primers designed for *Pax 2*, *Pax 8*, *Pod 1*, *Podocalyxin 1, Xlim 1, xlmx1b* and *WT1*, as indicated vertically. Negative controls include, (**-RNA**) no RNA in the reverse transcription reaction, (**-RT**) no reverse transcriptase in the reverse transcription reaction and (**-**) no cDNA in the PCR reaction. A linearity check was performed using doubling dilutions of whole embryo cDNA and the cDNA in the PCR reaction was loading equalised using *EF1α*. Levels of expression were compared with animal caps taken from not injected embryos (**Not injected**). *Pod 1* up-regulation was not enhanced by the class A basic helix-loop-helix transcription factors injected. Interestingly, the class A basic helix-loop-helix transcription factor *E12* was able to up-regulate all the pronephric development genes tested, except *Podocalyxin 1*.

when the mRNA was extracted (animal cap treatment and mRNA extraction carried out by Dr Caroline Haldin). cDNA was generated and PCR was performed using *Pod 1* primers (Methods). *EF1α* was used as a loading control and a linearity control was performed with doubling dilutions of stage 22 whole embryo cDNA. Standard RT-PCR negative controls were carried out. *Pod 1* appeared to be induced by activin A alone at 10 and 20ng/ml, or with low levels of retinoic acid (1 x 10^{-6}M) and 5ng/ml activin A. Expression was retained at 10^{-6} and 10^{-5} with 10 and 20ng/ml activin A (Fig. 7.12).

7.3 Discussion

Pod 1 expression was shown to be initiated at stage 13, the stage at which the main pronephric components are specified. This was also shown to be the same stage as other pronephric development genes were up-regulated, and may suggest that *Pod 1* is involved in the early events of pronephric initiation.

Pod 1 and *WT1* miss-expression

The *Pod 1* knock-down resulted in a complete reduction of *WT1* expression in the glomus. Wax-sectioning revealed a lack of cells in the area of the glomus, which could be the cause of the missing mRNA expression. Injected animal caps showed that *Pod 1* was able to induce the expression of *WT1* and *WT1* was not able to up-regulate *Pod 1* expression. This may suggest that *WT1* is in the same pathway and in fact downstream of *Pod 1*. This places *Pod 1* firmly in an important position with regard to development of the pronephric glomus.

The *WT1* pronephric over-expression phenotype in *Xenopus laevis* was not identical to that of *Pod 1* observed in Chapter 6. *WT1* over-expression results in reduced pronephric tubules and reduced *Xlim1* expression in the pronephric anlagen (Wallingford, *et al.*, 1998). However, there are similarities in the mouse knock-out phenotypes of *Pod 1* and *WT1*. Both show lack of the maturation of specified glomerulus cells, reduced tubules and reduced or absent ureteric bud branching, (Kreidberg, *et al.*, 1993, Quaggin, *et al.*, 1999, Moore, *et al.*, 1999 and Cui, *et al.*, 2003). The mouse *WT1* knock-out phenotypes were, however, more extreme than the null *Pod 1* phenotypes. The loss of *Pod 1* resulted in the increase of metanephric condensing mesenchyme, but a failure to develop (Quaggin, *et al.*, 1999 and Cui, *et al.*, 2003), whereas the null *WT1* phenotype

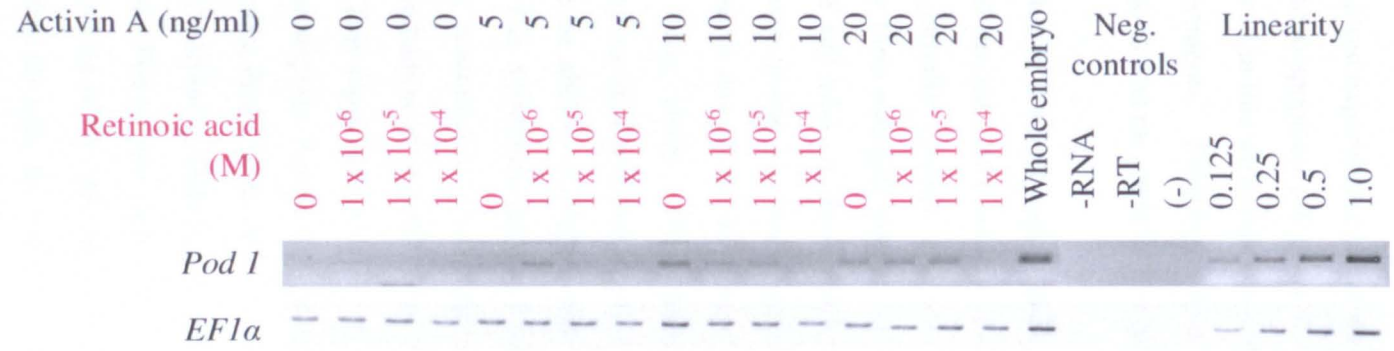

Fig. 7.12 ***Pod 1* expression in animal caps treated with retinoic acid and activin**. Animal caps were dissected from stage 9 embryos and were incubated in a range of concentrations of **retinoic acid** (M) and **activin** (ng/ml) until the equivalent of stage 22. RT-PCR was performed on mRNA extracted from the treated animal caps. *EF1α* was used as a loading control and a linearity of doubling dilutions of whole embryo cDNA was performed. The negative controls are no RNA in the RT reaction (**-RNA**), no reverse transcriptase in the RT reaction (**-RT**) and no cDNA in the PCR (-). *Pod 1* appeared to be up-regulated in animal caps treated with activin A and down-regulated with retinoic acid.

results in apoptosis of the mesenchyme prior to condensation, (Kreidberg, *et al.*, 1993). Interestingly, both *WT1* knock-out and *Pod 1* knock-out results in tubule abnormalities also found in this study with *Xenopus laevis* where the tubules were reduced with little branching morphology.

Separate knock-out experiments in the mouse with *Pod 1* and *WT1* have both resulted in aspleenism due to apoptotic cell death (Lu, *et al.*, 2000 and Herzer, 1999). The lack of glomus observed in this work bears a striking resemblance to the missing spleen tissue in these experiments. Further investigation with TUNEL analysis would indicate whether apoptosis was the cause of glomus absence.

Gene regulation in the early pronephric anlagen

As mentioned in the Introduction, the expression of *Pax 8* and *Xlim1* during development partially overlap, and over-expression of both *Pax 8* and *Xlim1* will synergistically form enlarged ectopic pronephroi. These data indicated a co-operation between *Pax 8* and *Xlim1* in the formation of the pronephric anlagen (Carroll and Vize, 1999). However, it has also been hypothesised that *Pax 8* and *Xlim1* are induced by separate pathways due to the differences in partially overlapping expression patterns (Carroll and Vize, 1999). Interestingly, *Pod 1* knock-down only effects *Pax 8* expression and no measurable difference was observed on *Xlim1* expression. *Pod 1* may therefore be able to transcriptionally regulate Pax 8. Indeed, E box motifs are present in the *Pax 8* promoter region (Murre, *et al.*, 1989 and ENSEMBLE, Hubbard, *et al.*, 2005). In contradiction to this hypothesis, *Pod 1* over-expression alone does not result in the induction of the *Pax 8* over-expression phenotype of ectopic pronephroi (Chapter 6). This suggests one of two possibilities, either that although *Pod 1* may be required for pronephric *Pax 8* expression, it is not sufficient in itself to induce *Pax 8* expression; or that *Pod 1* both induces *Pax 8* expression and regulates *Pax 8* expression levels. Animal cap assay analysis performed in this chapter has shown that *Pod 1* alone can up-regulate *Pax 8* expression, but *Pax 8* cannot up-regulate *Pod 1* expression, eliminating the first of the two possibilities. *Pod 1* may therefore be regulating *Pax 8* expression either directly, as *Pod 1* is known to have both activational and inhibitory transcription properties (Miyagishi, *et al.*, 2000), or indirectly through an intermediate transcription factor. The mouse *Pod 1* knock-out phenotype cannot be completely explained by a loss in *Pax 8* expression as mice lacking *Pax 8* expression do not have

kidney phenotype (Mansouri, *et al.*, 1998). *Pod 1* therefore may be involved in a number of different pathways. This is perhaps supported by its identification in multiple roles during development.

***Pod 1* pathway analysis**

Pax 8 has been shown to induce *WT1* expression (Dehbi and Pelletier, 1996), supporting the hypothesised pathway in this study of *Pod 1* → *Pax 8* → *WT1* (Fig 7.13). As may be anticipated due to the role of *Pod 1* in mouse podocyte development, *Pod 1* was able to induce *Podocalyxin 1* expression in the animal cap assay. Furthermore, *Podocalyxin 1* transcription has been shown to be activated by *WT1* (Palmer, *et al.*, 2001). The pathway may therefore be extended; *Pod 1* → *Pax 8* → *WT1* → *Podocalyxin 1* (Fig 7.13). *Podocalyxin 1* knock-out studies in mice have shown severe kidney defects including the absence of foot processes (Doyonnas, *et al.*, 2001). Although similar, the expression patterns and mouse knock-out phenotypes of the genes in the hypothetical pathway do not match exactly, suggesting that other factors are involved.

One of these factors could be *Pax 2*, which was also induced by *Pod 1* expression in animal caps. *WT1* and *Pax 2* are believed to be in a regulatory cycle, whereby *WT1* down regulates *Pax 2* expression and *Pax 2* induces *WT1* expression (Ryan, *et al.*, 1995 and Dehbi, *et al.*, 1996). Mouse knock-out analysis has show that *WT1* expression was found to be required for *Pax 2* expression in the condensing mesenchyme (Kreidberg, *et al.*, 1993) and *Pax 2* down regulation was found to be required for podocyte maturation, (Quaggin, 2002). In addition, *Pax 8* and *Pax 2* are believed to be redundant in pronephric development, through their ability to rescue knock-out phenotypes (Bouchard, *et al.*, 2002). The hypothetical pathway could be further developed to include *Pax 2*, although further analysis is required to support this hypothesis (Fig 7.13).

In this study, the relationships of *Pod 1* with *Xlim1* and *xlmx1b* were also investigated. Neither *Xlim1* nor *xlmx1b* up-regulated *Pod 1* or were up-regulated by *Pod 1* in the animal cap assays (Data not shown). Furthermore, in *Pod 1* knock-down embryos, there was no measurable effect on *Xlim1* expression. This indicates that *Pod 1* and *Xlim1* are on different genetic pathways in the development of the kidney. The phenotypic effect on *xlmx1b* expression observed in *Pod 1* knock-down embryos could be due to the lack

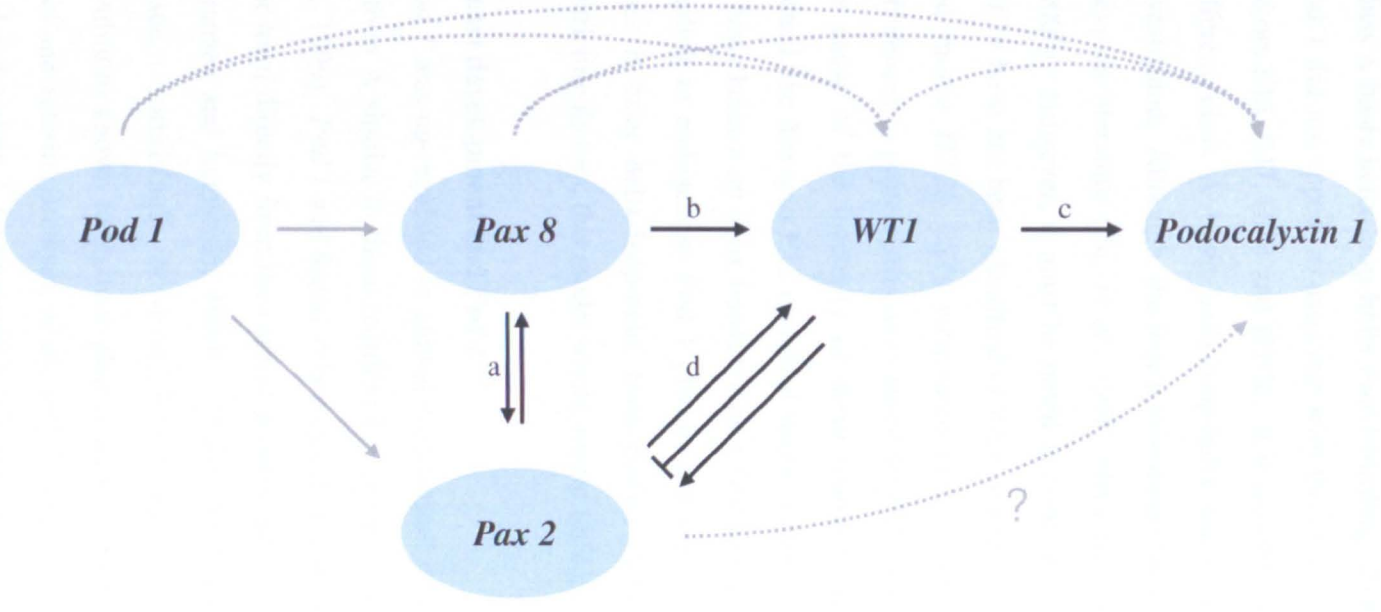

Fig. 7.13 **Hypothetical *Pod 1* gene network**. Summary of results from animal cap network analysis (Fig. 7.10) and literature search. Grey shaded arrows indicate results from the animal cap analysis performed in this study. **Black shaded** arrows are established from published data. (**a**) Bouchard, *et al.*, (2002); (**b**) Dehbi and Pelletier (1996); (**c**) Palmer, *et al.*, (2001) and (**d**) Jordan, *et al.*, (1993), Ryan, *et al.*, (1995) and Dehbi, *et al.*, (1996). (?) Does not fit with the hypothesis that down-regulation of *Pax 2* required for podocyte maturation (Quaggin, 2002).

of glomus tissue present, rather than a direct down-regulation of gene expression. Therefore *xlmx1b* also seems unlikely to be on the same gene pathway as *Pod 1*.

Class A basic helix-loop-helix *Pod 1* binding partners

Pod 1 did not appear to associate with the class A basic helix-loop-helix transcription factors E12, E47, HEB and ITF2b. It is possible that Pod 1 forms heterodimers with a different class A basic helix-loop-helix transcription factor that has not yet been investigated. Although, the four transcription factors were chosen on the evidence from previous literature (Lu, *et al.*, 1998, Miyagishi, *et al.*, 2000a and Miyagishi, *et al.*, 2000b). However, it must be noted that the *Xenopus* homologues for *E47*, *HEB* and *ITF2b* have not been identified or were unattainable, and the human *E47*, mouse *HEB* and mouse *ITF2b* ESTs were used in this study (www.ncbi.nlm.nih.gov). Subtle differences in protein structure caused by differences in amino acid sequences could be the cause of the inactivity of these transcription factors in the *Xenopus* embryos. Indeed, the *Xenopus* E12 indicated strong mesoderm inducing properties, the only class A basic helix-loop-helix transcription factor activity observed. It is possible that E12 is binding to endogenous Pod 1 protein and inducing pronephric tissues. However, as class B basic helix-loop-helix transcription factors are typically the rate and tissue restricting factors, this model would appear unlikely.

Heart development and *Pod 1*

Pod 1 was up-regulated in animal caps treated with concentrations of retinoic acid and activin A similar to those required for an up-regulation of *Cardiac actin* (Brennan, *et al.*, 1999). *Pod 1* was found to be expressed in the proepicardium, which although does not form directly from the cardiac primordium, does develop to form part of the heart (Fransen and Lemanski, 1990). These conditions could therefore be forming heart tissue. Surprisingly, however, *Pod 1* was not induced in animal caps treated in conditions known to produce glomus tissue, which are higher concentrations of retinoic acid and activin (Brennan, *et al.*, 1999). The induction of *Pod 1* expression by retinoic acid and activin A treatment was however, similar to that of *Pax 8* (Heller and Brandli, 1999), a known pronephric development gene (Introduction).

Both *Pod 1* and *WT1* were found to be expressed in the epicardium and have been implicated by expression patterns in the epithelial/mesenchymal transition of

proepicardial cells, (Hidai, *et al.*, 1998, Lu, *et al.*, 1998, Robb, *et al.*, 1998, Lu, *et al.*, 1999, Moore, *et al.*, 1999, Quaggin, *et al.*, 1999, Andersson, *et al.*, 2001 and Munoz-Chapuli, *et al.*, 2002). The null *WT1* mouse heart is severely disrupted and does not have many epicardial cells (Moore, *et al.*, 1999). Unfortunately, the null *Pod 1* mouse phenotype has not been analysed in detail, except for observed hemopericardium (Quaggin, *et al.*, 1999). *Pod 1* and *WT1* are both expressed during the terminal development of mouse podocytes in the kidney before they terminally differentiate from epithelial cells to partially mesenchymal cells during normal development (Moore, *et al.*, 1999). Again, this implies a role for both genes in the epithelial/mesenchymal transition of specialised heart and kidney cells.

Part 2 Conclusion

Pod 1 over-expression experiments from chapter 6 indicated that *Pod 1* has a role in glomus and heart development. This role appears to be a conserved developmental function in the mouse. Further analysis in chapter 7 has shown that *Pod 1* may have a regulatory role in early pronephric development and was required for normal glomus and pronephric tubule development. Wax-sectioning has further highlighted a possible role in glomus cell survival. In addition, *Pod 1* was expressed in animal caps treated with concentrations of retinoic acid and activin A similar to that required to produce pronephric tissue. The animal cap assay also demonstrated that Pod 1 does not associate with class A basic helix-loop-helix transcription factors E12, E47, HEB and ITF-2 which have previously been implicated as potential binding partners, (Lu, *et al.*, 1998, Miyagishi, *et al.*, 2000a, Miyagishi, *et al.*, 2000b).

Pod 1 network analysis has led to the following hypothetical *Pod 1* pathway, although further analysis is required.

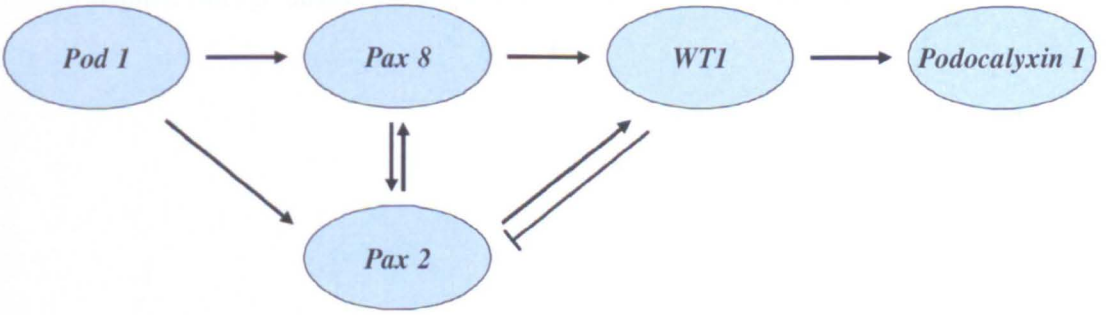

Results Part 3

The Role of *Darmin r* in the Development of the Pronephros.

Chapter 8

Pronephric lineage targeted *Darmin r* over-expression disrupts pronephric tubule formation.

Introduction

This thesis aimed to elucidate the role of two chosen genes in the development of the pronephros. The second gene chosen for further investigation was *Darmin r*. Preliminary analysis of *Darmin r* suggested a role in pronephric tubule development (Chapter 5). In order to further elucidate the role of *Darmin r* in pronephric development, the following were investigated:

Chapter 8

- Comparison of amino acid sequences of Darmin r homologues to establish the degree of evolutionary conservation.
- Clarify the spatial expression pattern within the pronephros by RT-PCR.
- Investigate the effects of Retinoic acid and Activin A on *Darmin r* expression.
- Carry out over-expression studies in developing embryos, using targeted micro-injected mRNA.

Chapter 8

Pronephric lineage targeted *Darmin r* over-expression disrupts pronephric tubule formation.

8.1 Introduction

Darmin-related was identified by in a direct secretion screen (Pera, *et al.*, 2003). *Darmin r* (EST BU993920) has 99% identity to *Xenopus laevis cytosolic non-specific dipeptidase*, UniGene cluster xl.10218. *Cytosolic non-specific dipeptidase* is also known as *tissue carnosinase* and *carnosine dipeptidase II* and is in the metallopeptidase family M20, specifically M20.005. Members of the metallopeptidase family M20.005 are generally involved in the hydrolysis of dipeptides in the cytosol of mammalian cells (*MEROPS*: Rawlings, *et al.*, 2006).

Early analysis of *Xenopus Darmin r* by Pera and colleagues (2003) indicated expression in the glomus and the lens of stage 32 embryos. However in this study, expression was observed in the pronephric tubules, not the glomus by wholemount *in situ* hybridisation. In order to resolve this issue, a stage 42 pronephric dissection RT-PCR was performed and is detailed in this Chapter. The temporal expression of *Darmin r* detailed by Pera and colleagues (2003) was confirmed in this work by RT-PCR (Chapter 5) and indicated high levels of maternal expression followed by late tail bud zygotic expression.

In this chapter, the evolutionary conservation of *Darmin r* was established by comparing the amino acid sequences of the human, mouse, fly, worm and yeast Darmin r homologues. The region of *Darmin r* expression within the pronephros was determined using RT-PCR with mRNA extracted from a dissected stage 42 pronephros. The *Xenopus* adult spatial expression was elucidated using RT-PCR of adult tissues. These data gave an indication of the role of *Darmin r* in adult tissues. The role of *Darmin r* in pronephric development was investigated using over-expression analysis.

8.2 Results

8.2.1 Darmin r amino acid sequence is evolutionarily conserved

The full length *Xenopus Darmin r* EST, BU993920 (Pera, *et al.*, 2003), was obtained from the IMAGE consortium (http://image.llnl.gov, IMAGE No. 5512805) and fully sequenced in house. The open reading frame runs from 35bp to 1459bp, encoding a 474 amino acid protein that is approximately 56kDa when separated on a 10% SDS polyacrylamide gel (Fig. 8.5). The EST has recently been linked to the UniGene cluster xl.10218, encoding *Cytosolic nonspecific dipeptidase.*

The *Xenopus* Darmin r amino acid sequence was aligned with the *H. sapiens* Cytosolic nonspecific dipeptidase (NP_060705), *M. musculus* Cytosolic nonspecific dipeptidase (NP_075638), *D. melanogaster* CG17337 protein (NP_610181), *C. elegans* Glutamate carboxypeptidase-like protein 1 (NP_506610) and potential homologue *S. cerevisiae* Hypothetical protein (YFR044C) (Fig. 8.1A). Percentage similarity values were obtained using the NCBI BLAST program (Basic Local Alignment Search Tool, Altschul *et al.*, 1990). The alignment indicated a high percentage similarity of approximately 80% with the mouse and human homologues, across the whole protein (Fig. 8.1B). Lower levels of percentage similarity were observed with *D. melanogaster*, *C. elegans* and *S. cerevisiae*, however, this was expected due to a greater evolutionary distance between these species.

8.2.2 *Darmin r* is expressed in the pronephric tubules

The pronephros and individual components, the glomus, pronephric tubules and duct, were dissected from a stage 42 *Xenopus laevis* embryo. The RT-PCR was performed as previously described in Chapter 7.

Darmin r exhibits highest levels of expression within the pronephric tubules and lower expression in the glomus (Fig. 8.2). This is in agreement with the wholemount *in situ* hybridisation analysis performed in Chapter 5, where strong expression was observed in the pronephric tubules in stages 32 to 42.

A

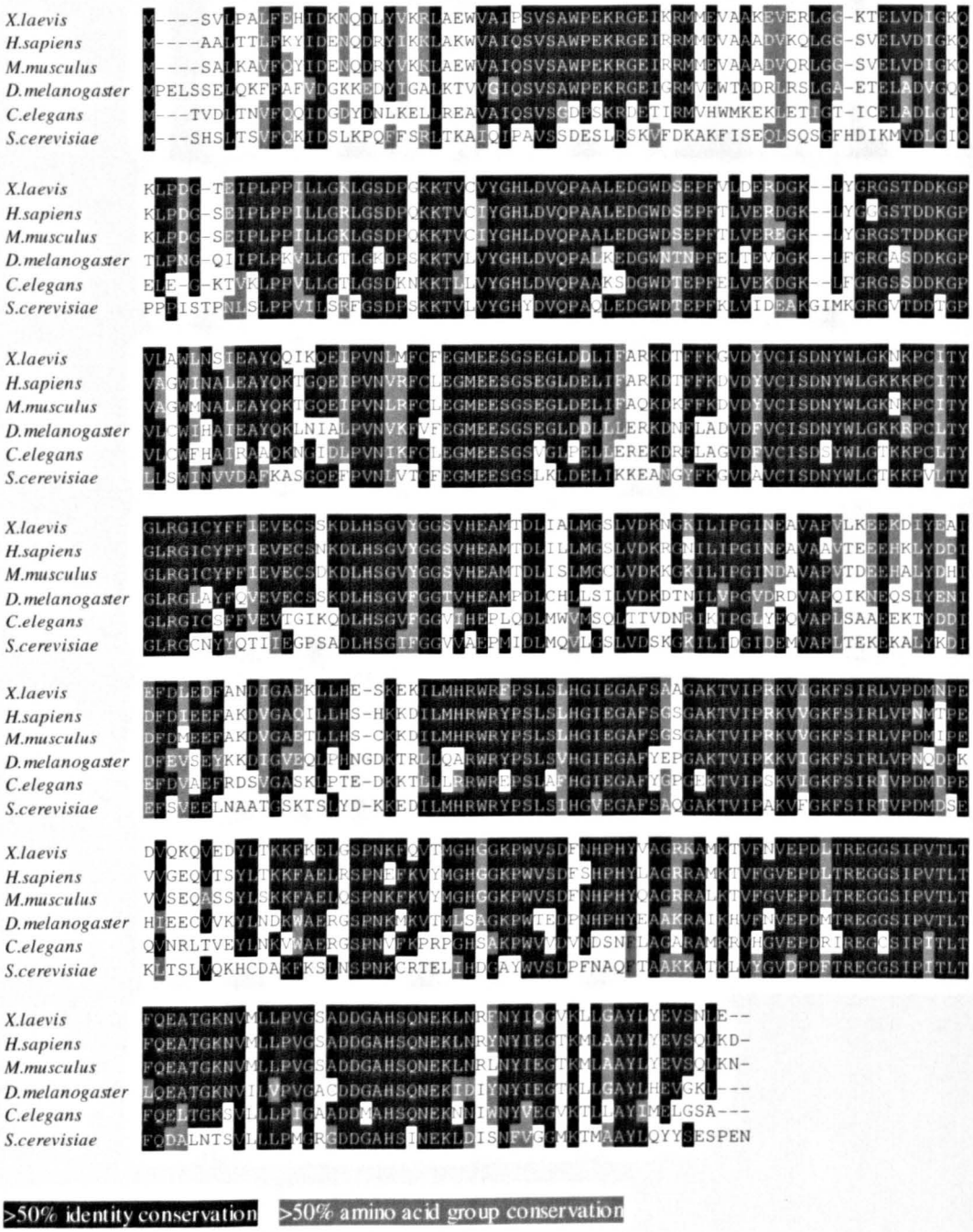

>50% identity conservation >50% amino acid group conservation

B

	X. laevis	*H. sapiens*	*M. musculus*	*D. melanogaster*	*C. elegans*	*S. cerevisiae*
X. laevis	-	-	-	-	-	-
H. sapiens	79	-	-	-	-	-
M. musculus	80	86	-	-	-	-
D. melanogaster	63	62	61	-	-	-
C. elegans	55	53	53	57	-	-
S. cerevisiae	51	48	48	45	47	-

Fig. 8.1 **Alignment of homologous Darmin r amino acid sequences.** (**A**) Alignment of Darmin r amino acid sequence (AAH56069), *H. sapiens* Cytosolic nonspecific dipeptidase (NP_060705), *M. musculus* Cytosolic nonspecific dipeptidase (NP_075638), *D. melanogaster* CG17337 protein (NP_610181), *C. elegans* Glutamate carboxypeptidase-like protein 1 (NP_506610) and potential homologue *S. cerevisiae* Hypothetical protein (YFR044C). **Black shading** indicates identical amino acids in all sequences compared with a frequency greater than 50%, whereas the **grey shading** specifies the same amino acid family frequency greater than 50%. (**B**) Percentage identity (%). The table indicates paired percentage identity as given by BLAST (Basic Local Alignment Search Tool, Altschul *et al.*, 1990).

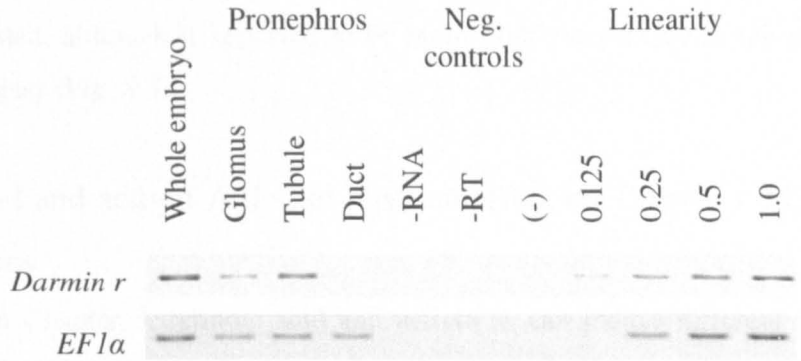

Fig. 8.2 **Spatial pronephric expression of *Darmin r* in stage 42 *X. laevis*.** The pronephros from a *Xenopus laevis* stage 42 embryo was dissected into the glomus, tubules and duct tissues, and an RT-PCR using *Darmin r* primers was carried out. Equalisation was carried out using *EF1α*, and linearity and negative controls carried out as described in the methods. A fine dissection of the pronephros of a stage 42 *X. laevis* tadpole reveals the spatial expression of *Darmin r* within the pronephros. *Darmin r* appears to be most expressed in the tubules, less in the glomus and weakest in the duct.

8.2.3 *Darmin r* is expressed ubiquitously in *Xenopus* adult tissues

The *Xenopus* adult spatial expression of *Darmin r* was elucidated using RT-PCR analysis on mRNA isolated from adult tissues. The RT-PCR analysis might indicate whether *Darmin r* had a particular role in the adult organs. The input cDNA was approximately equalised using *EF1α* and a linearity check using doubling dilutions of kidney cDNA was performed. *Darmin r* was shown to be ubiquitously expressed in all the tissues tested, although it appeared to be more highly expressed in the ovary and duodenal samples (Fig. 8.3).

8.2.4 Retinoic acid and activin A do not have an effect on *Darmin r* expression in animal caps

As detailed in Chapter 3, retinoic acid and activin A can induce different tissues in treated animal caps, including the pronephros (Taira, *et al.*, 1994, Brennan, *et al.*, 1999 and Osafune, *et al.*, 2002). It may be hypothesised, therefore, that the expression of pronephric development genes could be affected by retinoic acid and activin A treatment in animal caps. To observe their effects on *Darmin r* expression, *Xenopus* animal caps were treated with different concentrations of retinoic acid and activin A.

Animal caps were dissected from stage 8/9 embryos and incubated overnight in a range of 0 to 1 x 10^{-4}M retinoic acid and 0 to 20ng/ml activin A, as previously described (Chapter 3). Following treatment, the animal caps were incubated in Barth X until the equivalent of stage 22 when the mRNA was extracted (animal cap treatment and mRNA extraction carried out by Dr Caroline Haldin). RT-PCR was then performed using *EF1α* as a loading control. *Darmin r* was found to be expressed at a constant level in all the animal caps tested (Fig. 8.4). Retinoic acid and activin A did not appear to effect the expression of *Darmin r* in treated animal caps.

8.2.5 *Darmin r* over-expression gives a pronephric phenotype

Pera and colleagues (2003) observed that *Darmin r* over-expression did not indicate an endodermal phenotype, however, no specific analysis of pronephric structures was performed at this time. To further investigate the role of *Darmin r* in pronephric development, *Darmin r* over-expression was targeted to the pronephros and analysed using pronephric markers.

Fig. 8.3. **Expression pattern of *Darmin r* in the adult organs of *X. laevis*.** RT-PCR was performed on mRNA isolated from the organs of an adult *Xenopus laevis*. The RT-PCR was equalised using *EF1α* and linearity and negative controls performed as described in the methods. *Darmin r* expression is seen in all adult *X. laevis* organs analysed, with a higher expression observed in the ovary and the duodenum.

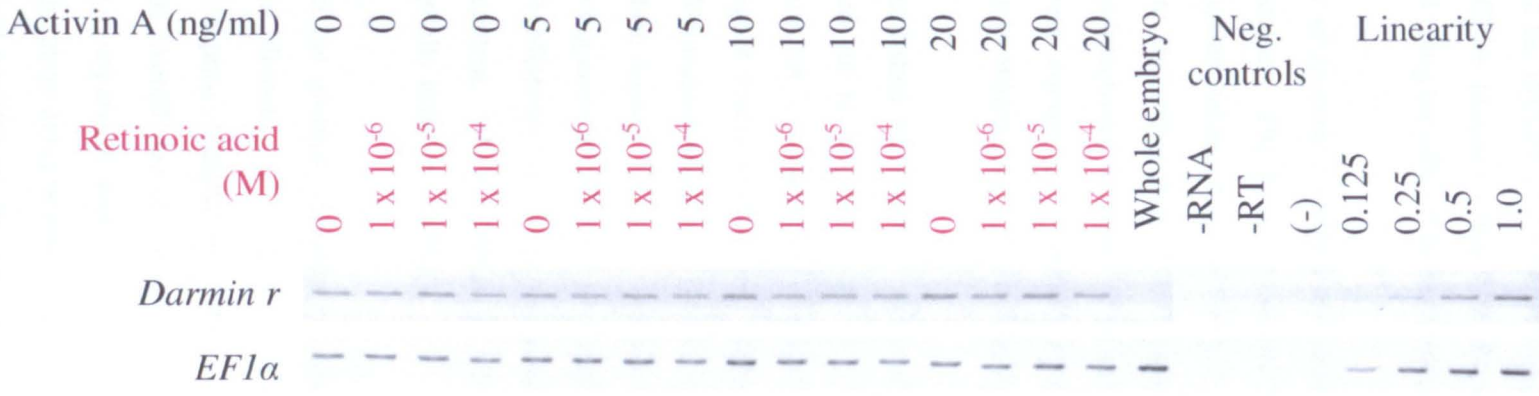

Fig. 8.4 ***Darmin r* expression in animal caps treated with retinoic acid and activin A.** Animal caps taken from stage 9 embryos were incubated in a range of concentrations of **retinoic acid** (M) and **activin A** (ng/ml) until the equivalent of stage 22. RT-PCR was performed on mRNA extracted from the animal caps. *EF1α* was used as a loading control and a linearity of doubling dilutions was performed. The negative controls are no RNA in the RT reaction (**-RNA**), no reverse transcriptase in the RT reaction (**-RT**) and no cDNA in the PCR (-). *Darmin r* was expressed in all the animal caps tested. Retinoic acid and activin do not appear to have an effect on *Darmin r* expression.

Targeted *Darmin r* over-expression was performed by injecting *in vitro* transcribed *Darmin r* mRNA into a V2 blastomere of an embryo at the 8 cell stage. *Darmin r* cDNA from the IMAGE clone (http://image.llnl.gov, IMAGE No. 4965475) was cloned into the pCS2+ plasmid using *Eco RI* and *Xba I* (Appendix), and the mRNA was synthesised using the SP6 mMessage mMachine Kit (Ambion).

The ability of *Darmin r* mRNA to translate was checked using *in vivo* translation in *Xenopus* oocytes. The *Xenopus* oocytes were injected with either *Xenopus Darmin r* mRNA or water and incubated in Barth X containing ^{35}S methionine and cysteine. Any new proteins containing these amino acids synthesised after oocytes were injected, were therefore radioactively labelled. The mRNA-injected oocytes and the water-injected oocytes were compared. *Darmin r* mRNA was translated, giving a protein of approximately 56kDa (Fig. 8.5) consistent with Pera and colleagues (2003).

Having established the ability of the mRNA to translate, over-expression experiments were carried out in *Xenopus* embryos. In these experiments the *in vitro* transcribed *Darmin r* mRNA is immediately available for translation in the embryo after injection, yielding higher levels of *Darmin r* expression at an earlier stage than that observed during endogenous expression. The V2 cell of an 8 cell embryo was injected to target the pronephric region. *Darmin r* mRNA was co-injected with *GFP* mRNA to facilitate lineage tracing and the embryos were sorted for pronephric left or right fluorescence at stage 25-30 (Methods 2.10.3 Micro-injection). *GFP* mRNA was also injected alone as a negative control, which indicated the effect of injecting an embryo with a developmentally irrelevant mRNA.

The size of the glomus, pronephric anlagen and length of embryo was measured as described in Methods 2.10.7 Measurement of tissue area. When analysing the glomus and the pronephric anlagen, the length of the embryo was measured to eliminate the factor of the overall size of the embryo on the size of the glomus/pronephric anlagen. Where the comparison was made between different sets of embryos, the ratio of glomus/pronephric anlagen area to embryo length of each set was used in the analysis. The statistical analysis of measurements involved a Kruskal Wallis test, and a Dunn's post test to indicate the significant differences between the groups of test subjects. All

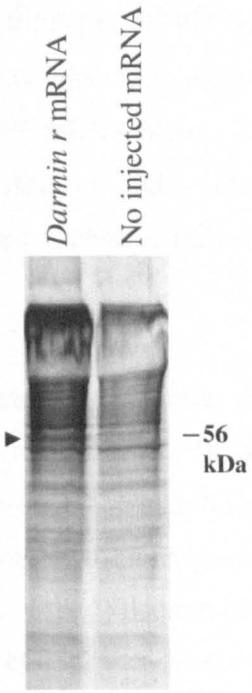

Fig. 8.5 **Oocyte translation of *Darmin r* mRNA**. Oocytes were injected with *Darmin r* mRNA and incubated overnight in full strength Barth X containing ^{35}S labelled methionine and cysteine. The protein from the oocytes was extracted and run on a 10% SDS PAGE gel and exposed for autoradiography. Oocytes were injected and lanes were loaded as indicated. Protein product of the injected *Darmin r* mRNA transcripts are highlighted by the black arrow. As indicated, the size of the *Xenopus* Darmin r protein is approximately 56kDa. The lane labelled "No injected mRNA" is the negative control where no mRNA was injected and no Darmin r over-expression is observed.

statistical analysis was performed using the InSTAT 3 programme, (GraphPad Software Inc).

8.2.5.1 *Darmin r* over-expression disrupts tubule development

One of the V2 blastomeres was injected in each 8 cell embryo with 0.5ng *Darmin r* mRNA and *GFP* mRNA or *GFP* mRNA alone. GFP fluorescence was used to indicate pronephric targeting of the left or right side of the embryo. 3G8 and 4A6 immunohistochemistry was used to observe the pronephric tubule (3G8) and duct (4A6) phenotypes at stage 40.

Similarly to Chapter 6, the pronephric tubule phenotype was determined using the Pronephric Index (PNI) (Wallingford, *et al.*, 1998) (Methods 2.10.8 Pronephric Index) and subsequent statistical analysis. The significant difference of the Pronephric Index (PNI) between the different sides of the embryos were validated using either the paired t-test, if the data were normal, or the Wilcoxon paired test, if the data were not normal. The morphology of the pronephric duct was scored by eye and given a rating of reduced, normal or enlarged.

Injecting the embryos with 0.5ng *Darmin r* mRNA and *GFP* mRNA disrupted tubule development, reducing the PNI on the injected side of the embryo (Fig. 8.6). Half of the 0.5ng *Darmin r* mRNA and *GFP* mRNA injected embryos analysed gave a PNI left/right difference of 2 or more. The 0.5ng *Darmin r* mRNA and *GFP* mRNA injected embryos has a median PNI of 2 on the injected side and 4 on the not injected side (N = 20). The data did not have a normal distribution, so the Wilcoxon paired test was used, which indicated a significant difference in PNI between the injected and the not injected sides, $p < 0.0001$.

The *GFP* mRNA alone injected embryos did not show any tubule phenotype and had a median PNI value of 5 on both the injected and not injected side (N = 43). The Wilcoxon paired test was used as the data was not normal, which did not show a significant difference in PNI, $p = 0.4261$ (Fig. 8.6).

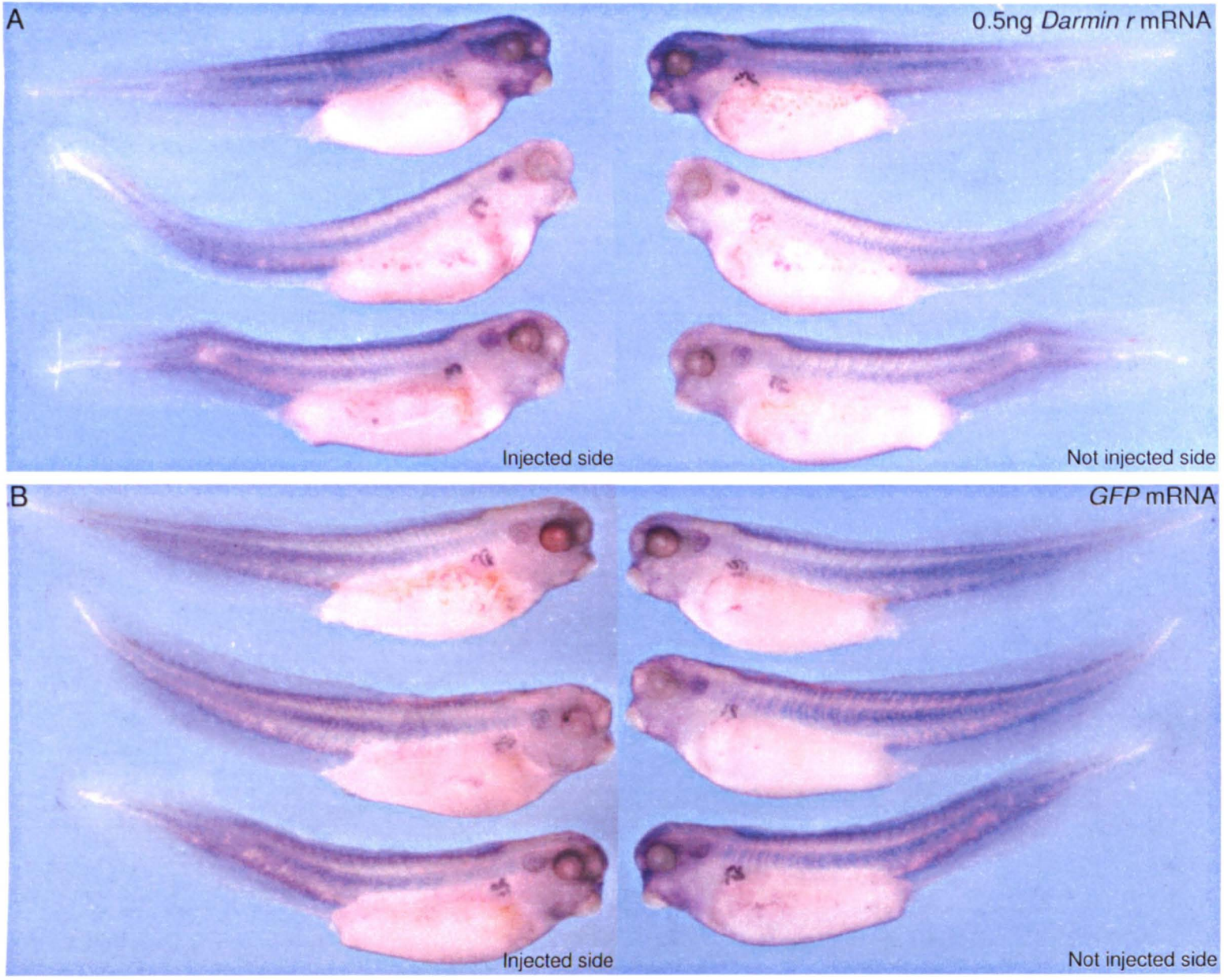
A
0.5ng *Darmin r* mRNA
Injected side
Not injected side
B
GFP mRNA
Injected side
Not injected side

Fig. 8.6 ***Darmin r* over-expression disrupts tubule formation.** Embryos were injected with either; *Darmin r* mRNA and *GFP* mRNA (**A**) or *GFP* mRNA alone (**B**). Injections were done at the 8 cell stage into one V2 cell to target the pronephros. Embryos were sorted using GFP fluorescence, checking for pronephric targeting. Not injected sides and injected sides of the same embryos are as indicated. Antibody staining was performed with 3G8 to highlight the tubules, on stage 39-41 embryos. (**A**) *Darmin r* over-expression disrupts tubule morphology. (**B**) *GFP*, used as an injected mRNA control, does not affect tubule development.

The pronephric duct appeared similar on the injected and not injected sides of the embryo of both the 0.5ng *Darmin r* mRNA and *GFP* mRNA injected embryos and the *GFP* mRNA alone injected embryos (Data not shown, Statistical analysis in Appendix).

8.2.5.2 *Darmin r* over-expression does not effect the size of the glomus

In vitro transcribed 0.5ng *Darmin r* mRNA and *GFP* mRNA or *GFP* mRNA alone was injected into one V2 cell of an 8 cell embryo as before. The pronephric left/right targeting was again, lineage traced using GFP fluorescence. However to observe the size of the glomus, wholemount *in situ* hybridisation using a *WT1* antisense DIG-labelled RNA probe was performed on stage 33-35 embryos. The glomus area on each side of the embryo was measured (Methods 2.10.7 Measurement of tissue area).

There was no observable difference in glomus area on the injected side of the embryo compared to the not injected side of the embryo of 0.5ng *Darmin r* mRNA and *GFP* mRNA or *GFP* mRNA alone injected embryos (Fig. 8.7). The mean areas of glomus were $0.020mm^2$ for the injected side and $0.022mm^2$ for the not injected side (N = 33) of 0.5ng *Darmin r* mRNA and *GFP* mRNA injected embryos. The Wilcoxon paired test was used to analyse the non parametric data. This did not show a significant difference, $p = 0.5477$.

The *GFP* mRNA alone injected embryos also did not indicate a significant difference in glomus area, giving a glomus mean area of $0.024mm^2$ for the injected side, $0.025mm^2$ for the not injected side (N = 34) and a Wilcoxon paired test p value of 0.5958 (Fig. 8.7).

8.2.5.3 *Darmin r* over-expression may effect nephrostome distribution

As previously, 0.5ng *Darmin r* mRNA and *GFP* mRNA or *GFP* mRNA alone was *in vitro* transcribed and injected into one V2 blastomere of an 8 cell embryo. GFP fluorescence was used for lineage tracing left/right pronephric targeting. The nephrostomes were identified by wholemount *in situ* hybridisation with a *β-tubulin* antisense DIG-labelled RNA probe on stage 34 embryos.

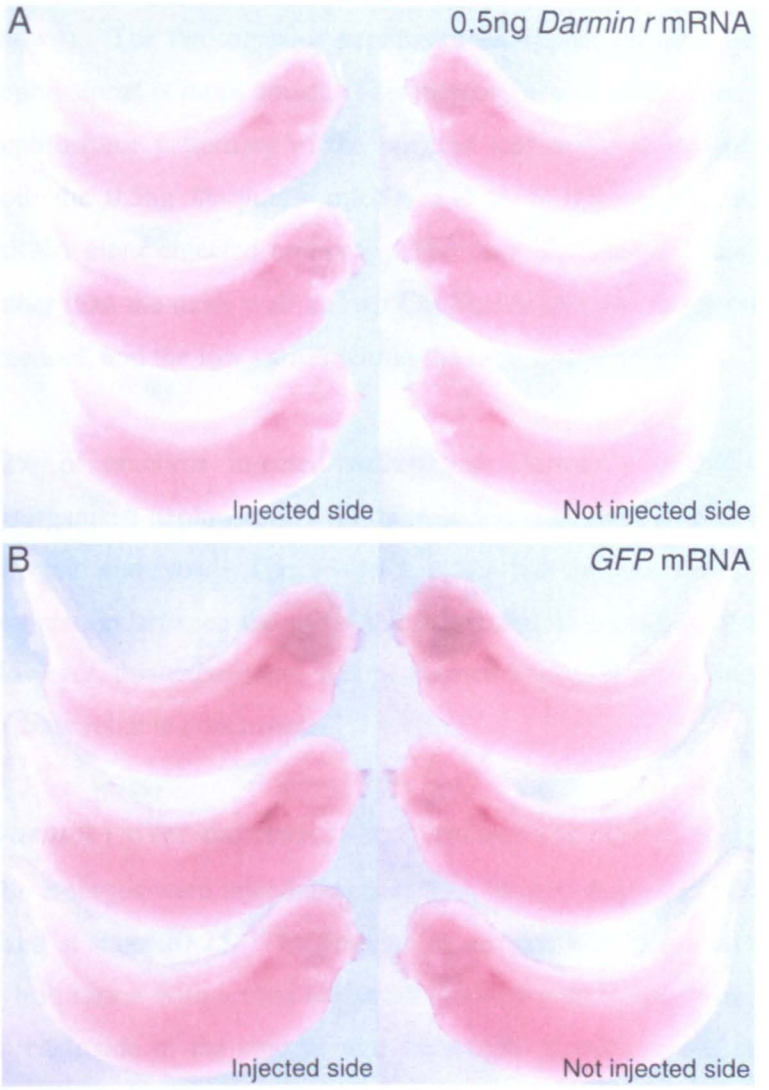

Fig. 8.7 ***Darmin r* over-expression does not have an effect on the glomus**. Embryos were injected with either; 0.48ng *Darmin r* mRNA and *GFP* mRNA (**A**) or *GFP* mRNA alone (**B**). Injections were done at the 8 cell stage into one V2 cell to target the pronephros. Embryos were sorted using GFP fluorescence, checking for left or right pronephric targeting. Not injected sides and injected sides of the same embryos are as indicated. Wholemount *in situ* hybridisation with a *WT1* DIG-labelled antisense RNA probe was performed on stage 33-35 embryos. (**A**) *Darmin r* over-expression does not have an effect on the size of the glomus as indicated by *WT1* expression. (**B**) The *GFP* mRNA control injected embryos also have a normal sized the glomus.

Darmin r over-expression appears to alter the positioning of the nephrostomes (Data not shown). The two anterior nephrostomes appear closer together and the dorsal most nephrostome is more dorsal. This phenotype was categorised by observing whether the nephrostome patterning of the injected side matched that of the not injected side for both the 0.5ng *Darmin r* mRNA and *GFP* mRNA injected embryos and the *GFP* mRNA alone injected embryos. The data was analysed using the Fisher's exact test rather than the more well known Chi Square test due to the table producing 1 degree of freedom, and the low values within the table (Appendix).

32% of embryos injected with 0.5ng *Darmin r* mRNA and *GFP* mRNA have disorganised nephrostomes on the injected side compared to 9% of *GFP* mRNA alone injected embryos. The Fisher's exact test indicates that there was a significant association between the mRNA injected and organisation of nephrostome, $p = 0.0091$. However, this experiment was performed once and would need to be repeated in order to draw reliable conclusions.

8.2.5.4 *Darmin r* over-expression may reduce the size of the pronephric anlagen

The embryos were injected with mRNA as previously and the embryos were sorted and fixed at stage 20-25. The pronephric anlagen was identified using wholemount *in situ* hybridisation with a *lim1* antisense DIG-labelled RNA probe. The pronephric anlagen on each side of the embryo and the length of embryo was measured (Methods 2.10.7 Measurement of tissue area).

Exogenous *Darmin r* expression appears to reduce the area of the pronephric anlagen, as indicated by *lim1* expression (Fig. 8.8). The mean area of the pronephric anlagen on the injected side was $0.032mm^2$ and the not injected side was $0.038mm^2$ of 0.5ng *Darmin r* mRNA and *GFP* mRNA injected embryos, and there was a significant difference with the Wilcoxon paired test, $p = 0.0199$ ($N = 32$). The mean area of *GFP* mRNA only injected side of the embryos was $0.031\ mm^2$, and the not injected side of the embryo was $0.029mm^2$, with no significant difference after the Wilcoxon paired test, $p = 0.3391$ ($N = 36$).

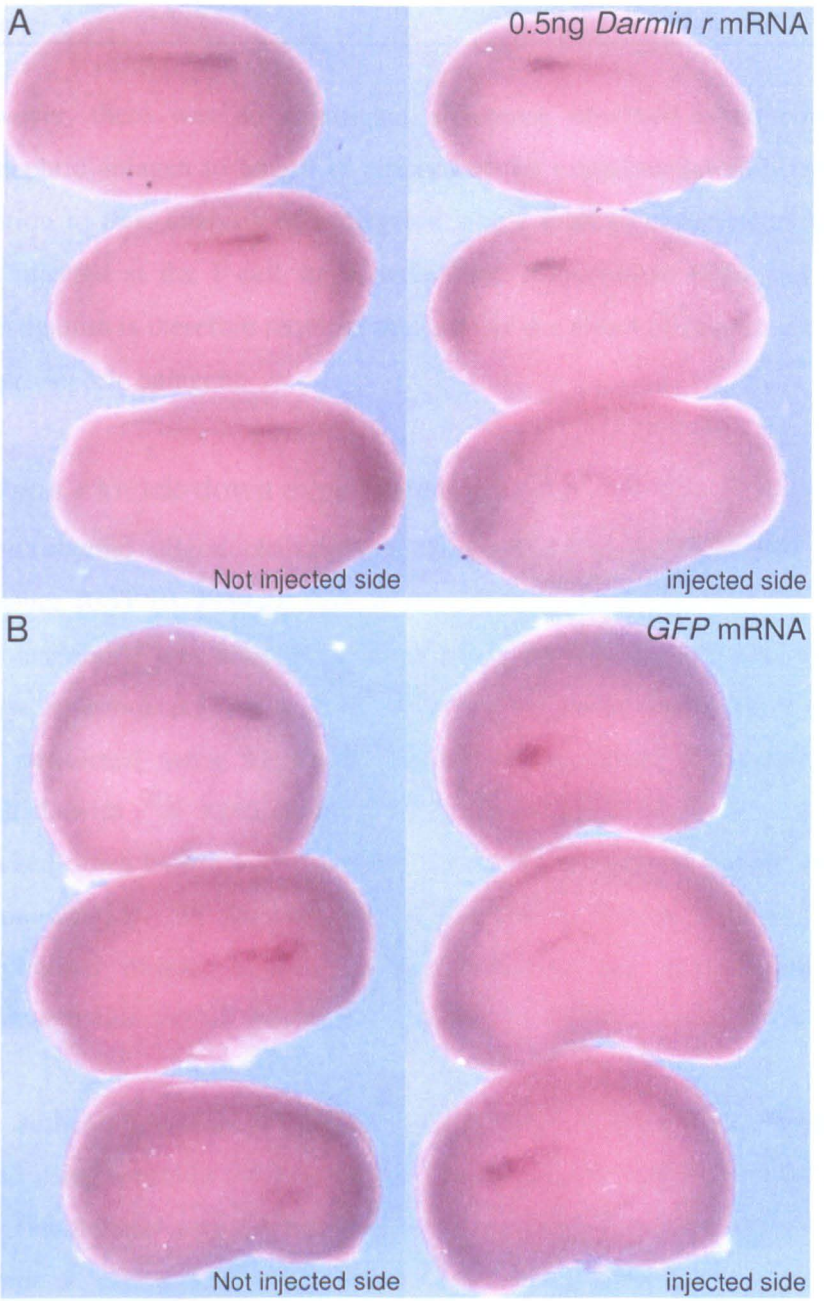

Fig. 8.8 ***Darmin r* over-expression reduces the size of the pronephric anlagen**. Embryos were injected with either; 0.5ng *Darmin r* mRNA and *GFP* mRNA (**A**) or *GFP* mRNA alone (**B**). Injections were done at the 8 cell stage into one V2 cell to target the pronephros. Embryos were sorted using GFP fluorescence, checking for left or right pronephric targeting. Not injected sides and injected sides of the same embryos are as indicated. Wholemount *in situ* hybridisation with a *lim1* DIG-labelled antisense RNA probe was performed on stage 20-25 embryos. (**A**) *Darmin r* over-expression reduces the size of the pronephric anlagen as indicated by *lim1* expression. (**B**) The *GFP* mRNA injected embryos have a normal sized the pronephric anlagen.

However, there was no significant difference observed when comparing ratios of pronephric anlagen to length of embryo of the experimental and control embryos. In addition to this, analysis of untargeted whole embryo experiments where the embryo was injected at the 1 cell stage, have been inconclusive (Data not shown). Further investigation is therefore required to elucidate the effect of *Darmin r* over-expression on the pronephric anlagen.

8.2.6 *Darmin r* knock-down experiments

A morpholino oligonucleotide was designed using the published *Darmin r* cDNA sequence (EST BU993920; Pera, *et al.*, 2003) (Chapter 7). The *Darmin r* morpholino oligonucleotide was designed to bind across the translational start site by Gene Tools (www.gene-tools.com) (Fig. 8.9). *In vitro* translation of *Darmin r* and *Pod 1* mRNA was performed using the Rabbit Reticulolysate system (Promega) and the proteins labelled with ^{35}S methionine. An autoradiograph showed *Darmin r* translation knocked-down by *Darmin r* morpholino oligonucleotide and not by *Pod 1* morpholino oligonucleotide. In addition, *Pod 1* translation was not effected by the *Darmin r* morpholino oligonucleotide. This indicated that the *Darmin r* morpholino oligonucleotide should specifically knock-down *Darmin r* expression (Fig. 8.9).

The authenticity of a morpholino oligonucleotide generated phenotype is typically tested using a rescue mRNA that will not bind to the morpholino oligonucleotide and will functionally replace the activity of the knocked-down gene (Chapter 7). For *Darmin r* knock-down experiments, the mouse homologue, Cytosolic nonspecific dipeptidase (BC005532) (Fig. 8.9), could be used. The *Darmin r* morpholino oligonucleotide should not bind to this mRNA.

Unfortunately there was not enough time investigate *Darmin r* knock-down in *Xenopus* embryos, however with a relatively strong over-expression phenotype, *Darmin r* knock-down analysis would be very interesting to investigate.

8.3 Discussion

The *Xenopus* Darmin r amino acid alignment with Cytosolic nonspecific dipeptidase homologues, indicated a high percentage similarity, 80%, with humans and mice and

A

5′ ...AACATGTCTGTTCTGCCAGCCCTGTTTGAGCACATC... 3′ *xDarmin r* sequence

3′ TACAGACAAGACGGTCGGGACAAAC 5′ *Darmin r* morpholino (reverse)

5′ ...AAGATGTCAGCCCTCAAAGCTGTCTTCCAGTATATC... 3′ *mDarmin r* sequence

B

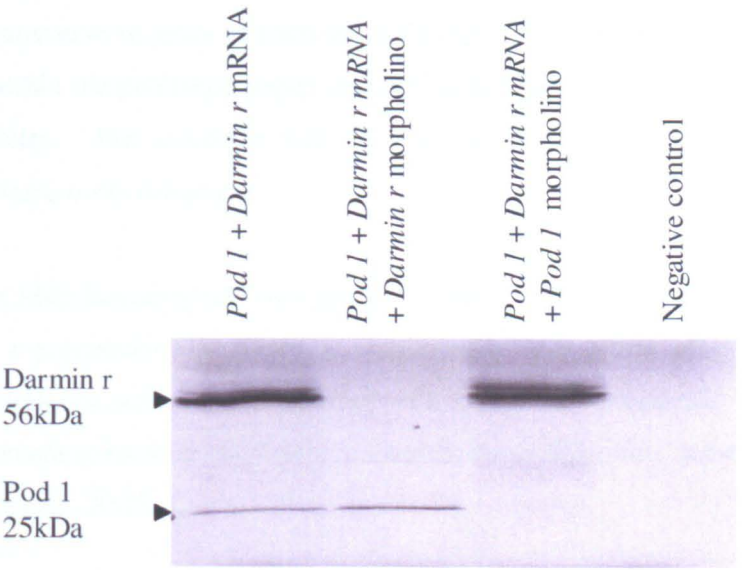

Fig. 8.9 ***In vitro Darmin r* expression is knocked-down by a *Darmin r* morpholino oligonucleotide**. (**A**) A morpholino oligonucleotide was designed using the *Xenopus Darmin r* sequence (EST BU993920, www.ncbi.nlm.nih.gov) to include the tranlational start site by Gene Tools (www.gene-tools.com). By annealing to *Xenopus Darmin r* mRNA, the morpholino oligonucleotide will inhibit translation and knock-down Darmin r protein expression. The *Darmin r* morpholino oligonucleotide (5′CAA ACA GGG CTG GCA GAA CAG ACA T3′) is shown in reverse to indicate **binding region**. To rescue the *Darmin r* knock-down, mouse *Darmin r* (*M. musculus* Cytosolic nonspecific dipeptidase, BC005532) could be used as it will not anneal to the morpholino oligonucleotide. (**B**) Autoradiograph showing *in vitro* translation of *Darmin r* and *Pod 1* mRNA knocked-down by respective morpholino oligonucleotides. Lanes and proteins are labelled accordingly. Negative control does not contain any mRNA, and therefore no protein is observed. *In vitro* translation was performed using the Rabbit Reticulocyte lysate system (Promega).

good percentage similarity with less related organisms, the fly, worm and yeast. This high degree of similarity across the phyla suggests a conserved biological role.

The published *Darmin r* wholemount *in situ* hybridisation indicated expression in the glomus at stage 32. This is in conflict with the wholemount *in situ* hybridisation performed in this study, where expression was observed in the pronephric tubules at stage 32. At stage 32 the glomus and the pronephric tubules are difficult to distinguish, however, the transverse sections of embryos subjected to *Darmin r* wholemount *in situ* hybridisation within the published paper are more consistent with expression within the pronephric tubules. We conclude that the published interpretation of the spatial expression of *Darmin r* is incorrect.

Consistent with adult human expression patterns (Teufel, *et al.*, 2003 and Janssen, *et al.*, 2005), *Darmin r* expression was observed ubiquitously in *Xenopus* adult tissues. The adult organ expression pattern is in keeping with Cytosolic nonspecific dipeptidase's role as a housekeeping enzyme involved the catabolism of dipeptidic substrates in adult tissues (Teufel, *et al.*, 2003).

Darmin r was evenly expressed in all the retinoic acid and activin A treated animal caps. *Darmin r* expression was observed at high level at stage 9 by a temporal RT-PCR. This expression appears to be continued in dissected animal caps from this stage, as indicated by the untreated animal cap. Although retinoic acid and activin A treatment did not appear to have an effect on *Darmin r* expression, it is still possible that *Darmin r* is involved in pronephric development. The mRNA in this experiment was extracted from animal caps at stage 22, the stage at which the pronephric anlagen is elongating. However temporal RT-PCR did not show *Darmin r* expression at this stage. It is conceivable, that *Darmin r* has a role later in pronephric development; especially when considering the over-expression phenotype involved pronephric tubule structure, which is formed later than stage 22.

Darmin r over-expression disrupts the organisation of the pronephric tubules, the region of highest pronephric expression. The pronephric duct and the glomus showed no or low endogenous expression and did not appear to be effected by *Darmin r* over-

expression. The exogenous *Darmin r* pronephric tubules were larger and had less branches/components than the negative controls.

The nephrostomes, ciliated funnels located at the origin of the tubules (1.1.1 Introduction), were disorganised. This would be consistent with the tubule *Darmin r* over-expression phenotype, as nephrostomes are linked to the pronephric tubules. However, exogenous *Darmin r* expression had a reduced effect on the nephrostome positioning, compared to the highly disrupted pronephric tubule coiling. Nephrostome positioning may therefore be more dependant on the position of the coelom than the pronephric tubule structures. Concurrently, the nephrostomes are formed from the tubule primordium, before the coiled tubules develop (Jones, 2005). Furthermore, in zebrafish, transient nephrostomes are formed in the coelom before the tubules develop (Drummond, 1998).

Darmin r over-expression reduced the area of the pronephric anlagen. The reduction of the pronephric anlagen suggests that either there was a reduced number of pronephric competent cells forming the pronephros, or a condensation of these cells to occupy a smaller area. Wholemount *in situ* hybridisation using a DIG-labelled *Xlim1* antisense probe to highlight the cells of the pronephric anlagen and wax-sectioning of the *Darmin r* over-expressed embryos would resolve this issue. If, however, the cells were condensed, then other pronephric morphological differences may be expected. A reduction in pronephric competent cell number could explain the localised effect on the tubules. Considering the previously stated hypothesis, that pronephric anlagen may develop into the three component subunits sequentially, *Darmin r* over-expression could be reducing the available pronephric competent cells to form the pronephric tubules. *Darmin r* is endogenously expressed in the tubules, possibly as a factor of later tubule development. The presence of Darmin r could prematurely signal the end of pronephric tubule development, and so result in a disruption of tubule morphology.

Darmin r is also identified as *Cytosolic nonspecific dipeptidase* which is involved in the breakdown of dipeptides. The kidney has been identified to have a major role in the removal of dipeptides from the blood (Lochs, *et al.*, 1988). *Darmin r* may therefore function as a general dipeptidase, hydrolysing dipeptides in the pronephric tubules for reabsorbtion or excretion. However, this does not explain why *Darmin r* is expressed

during development. *Darmin r* could be regulating biologically active dipeptides, such as carnosine which is associated with cellular oxidative resistance and functional exhaustion (Boldyrev, 2000), neurotransmission (Sassoe-Pognetto, *et al.*, 1993), and ageing (Ferrari, 2004), or similar related dipeptides like carcinine, homocarnosine and ophidine (Pegova, 2000).

Although *Cytosolic nonspecific dipeptidase* may not traditionally be expected to have a developmental role, recent studies have shown that other metabolic or 'house keeping' enzymes do have a role in development. For example, Prolidase, has been implicated in fetal maturation, (Gurdol, *et al.*, 1995), NTPDase has been found to have a critical role in eye development (Massé, *et al.*, Submitted) and membrane-type matrix metalloproteinase 1 has been found to be involved in lung organogenesis (Irie, *et al.*, 2005).

Further investigation into the role of *Darmin r* during development could include the effect of *Darmin r* over-expression and knock-down on the expression of tubule development genes such as, *Pax 2*, *Pax 8* (Carroll and Vize, 1999), and *Annexin IV* (Seville, *et al.*, 2002). In addition, knock-down analysis of the pronephric tubules, nephrostomes, glomus and duct have not been performed. The potential regulatory effect of *Darmin r* in pronephric development could be examined using animal cap assays in the same fashion that has been performed with *Pod 1* (Chapter 7). This may further indicate whether *Darmin r* has a role in the development or function of the pronephros.

Part 3 Conclusion

Darmin r is also identified as *Cytosolic nonspecific dipeptidase* which is involved in the breakdown of dipeptides. As expected of a housekeeping enzyme (Teufel, M., et al., 2003), the *Xenopus* adult organ expression pattern indicated expression throughout the tissues tested. In addition, the *Xenopus* Darmin r amino acid alignment with Cytosolic nonspecific dipeptidase homologues, indicated a high degree of similarity across the phyla suggesting a conserved biological role.

Over-expression analysis disrupted the structure and branching of the pronephric tubules, the region of highest expression in the developing embryo. Unsurprisingly, the nephrostomes, ciliated funnels located at the origin of the tubules (Introduction), were also weakly disorganised. *Darmin r* over-expression was found to reduce the area of the pronephric anlagen indicating that the disruption of pronephric tubule morphology was due to a reduction in pronephric tubule fated cells.

Chapter 9

Discussion

9.1 Potential target gene identification

This thesis had two main aims, the identification of a suitable target gene involved in the development of the pronephros and then to study its role in development. The first aim was addressed by examining the spatial and temporal expression patterns of genes identified from 3 different sources. The effectiveness of the sources of the studied genes is discussed.

9.1.1 Screen of a stage 13 cDNA library with a subtractive hybridisation probe

The formation of pronephric structures can be induced in animal caps with the combined treatment of activin A and retinoic acid, but not by the treatment of the factors alone (Taira, *et al.*, 1994, Brennan, *et al.*, 1999 and Osafune, *et al.*, 2002). This phenomenon was used to create a subtractive hybridisation probe that potentially highlighted the genes involved pronephric organogenesis. The screen was performed on a stage 13 cDNA library, the stage of approximate pronephric initiation, to identify genes that are involved early in pronephric development (Brennan, *et al.*, 1998).

The screening methodology had two weaknesses. Firstly, the subtractive hybridisation probes could detect the down-regulation of a gene in the animal cap treatments as a false positive. Secondly, treatment of retinoic acid and activin A in animal caps can also induce anterior and posterior neural tissue, cardiac tissue and pancreatic tissues (Haldin, *et al.*, 2003 and Moriya, *et al.*, 2000). This combined with the screen being performed using a whole embryo stage 13 cDNA library, meant that not only pronephric development genes were highlighted in the screen.

The screen resulted in the isolation of eight clones from the stage 13 cDNA library. Each of the eight clones were found to be expressed in the pronephros, although expression was not unique, nor enriched. The eight clones were not chosen for further analysis. However, during the course of this work the wholemount *in situ* hybridisation protocol was refined, and some clones now appear to be candidates for further

investigation. This screen was therefore successful in the identification of target genes. This screening methodology or similar screening methodologies, have previously been successful in the isolation of other pronephric genes, for example *Annexin IV*, *XSMP-30* and *X-CypA* (Seville, *et al.*, 2002, Sato, *et al.*, 2000 and Massé, *et al.*, 2004).

9.1.2 UniGene cluster genes

The second source of potential target genes was from the preliminary analysis of a set of UniGene cluster genes that were previously found to be pronephros specific (Personnal correspondence Pollet, N). UniGene cluster genes are formed as part of the National Center for Biotechnology Information service and are in a public searchable database (www.ncbi.nlm.nih.gov). They are created by aligning EST sequences using statistically significant sequence similarity in the 3' UTR, the recognition of gene sequence characteristics and/or by the identification of possible homologous genes across organisms (Wheeler, *et al.*, 2005).

The four UniGene cluster genes were found to be expressed the pronephros, although expression was not augmented in this region and the UniGene cluster genes were not investigated further. In hindsight, the spatial expression analysis could be improved with the enhanced wholemount *in situ* hybridisation protocol, however, the temporal expression data were not promising.

9.1.3 Data mining

The third source of target genes included data mining to identify *Xenopus* homologues of kidney development genes or newly established genes expressed in the pronephros. *Pod 1* and *Darmin r* were selected for further study after consideration of the literature and the preliminary data obtained from the temporal and spatial expression analysis. Further investigation of these two potential pronephric development genes proved promising and some of the initial work on *Pod 1* has been published (Simrick, *et al.*, 2005). A further publication on the functional role of *Pod 1* will be written after completion of this thesis.

9.2 *Pod 1*

Preliminary analysis of *Pod 1*, a basic-helix-loop-helix transcription factor, indicated an early glomus development gene, with enhanced expression in the pronephros. The expression patterns of *Pod 1* strongly matched that of the mouse homologue, implying a conserved evolutionary role (Hidai, *et al.*, 1998). *Pod 1* was therefore chosen as an ideal target gene for further functional investigation.

Functional analysis

Pod 1 targeted over-expression resulted specifically in the reduction of glomus tissue with no alteration in pronephric tubule or duct morphology. The hypothesis was that the reduced glomus resulted from the promotion of later glomus differentiation events at the expense of glomus cell recruitment from the pronephric anlagen. This concurs with data from the mouse, whereby *Pod 1* is involved in the terminal differentiation of specialised kidney cells (Quaggin, *et al.*, 1999 and Cui, *et al.*, 2003), although no gain of function experiments have been published in the mouse. Further evidence could come from the higher order magnification analysis of glomus sections during the course of pronephric organogenesis. The developing glomus cells may have a more differentiated morphology, or express maturation genes such as *podocalyxin* or *nephrin* (Schnabel, *et al.*, 1989 and Gerth, *et al.*, 2005), earlier in the presence of exogenous Pod 1.

Another hypothesis is that the boundary between the glomus and the pronephric tubules may be regulated by the dynamic relationship between *WT1* and *Pax 2*. The expression patterns of *Pax 2* and *WT1* are exclusive at the glomus/pronephric tubule boundary (Carroll, *et al.*, 1999). *WT1* has been shown to inhibit *Pax 2* expression and *Pax 2* down regulation was found to be required for podocyte maturation (Ryan, *et al.*, 1995 and Quaggin, 2002). In addition, mouse knock-out analysis has shown that *WT1* expression was found to be required for *Pax 2* expression in kidney development and *Pax 2* can induce *WT1* expression (Kreidberg, *et al.*, 1993 and Dehbi, *et al.*, 1996). In this work, *Pod 1* has been shown to induce both *WT1* and *Pax 2* expression in injected animal caps. An over-expression of *Pod 1* may therefore lead to an increased expression of these factors, resulting in a disruption of the glomus/pronephric tubule boundary. Inconsistent with this hypothesis, there does not appear to be a pronephric tubule

phenotype with *Pod 1* over-expression. Observation of *Pax 2* expression in targeted *Pod 1* over-expression would indicate whether *Pax 2* expression is increased. Also, the observation of another boundary marker, *xWnt-4*, may also prove interesting (Heller and Brandli, 1997).

The targeted knock-down of *Pod 1* resulted in the absence of cells in the glomus region. Further investigation with TUNEL analysis would show whether this was due to apoptosis, or a failure of cells to proliferate. As mentioned previously, *Pod 1* can induce both *xWT1* and *Pax 2* in injected animal caps. Interestingly, *Pax 2* expression has been linked with protection against apoptosis in mouse kidneys (Porteous, *et al.*, 2000 and Dziarmaga, *et al.*, 2003) and *WT1* was found to be required for *Pax 2* expression in mice (Kreidberg, *et al.*, 1993). *xWT1* expression was found to be reduced in *Pod 1* morpholino oligonucleotide injected embryos. The lack of both *Pod 1* and *xWT1* may severely reduce *Pax 2* expression, which may lead to increased apoptosis in *Pod 1* knock-down pronephroi. To test this hypothesis, *Pax 2* expression could be observed in *Pod 1* knock-down embryos. Also the observation of whether *Pax 2* or *WT1* expression could rescue the ablation of cells in the glomus. However, experiments performed on chimeric null *Pod 1* knock-out mice did not display an altered *Pax 2* expression pattern (Quaggin, *et al.*, 1999).

Pod 1 as a tumour suppressor gene

The human *Pod 1* homologue has been located to chromosome 6q23-24 (Smith, *et al.*, 2006). This chromosomal region has been implicated in head and neck squamous cell carcinomas and non-small-cell lung cancer. By screening for methylation events in these types of carcinomas, a common methylation event was found to be located within the human *Pod 1* gene (Smith, *et al.*, 2006). Hypermethylation was shown to silence the human *Pod 1* gene, and expression was absent in carcinoma cells, despite being present in surrounding epithelial tissues (Smith, *et al.*, 2006). The study goes on to over-express *Pod 1* in a lung cancer cell line, which reduces cell proliferation without visible cell death. The *Pod 1* over-expressing cells also indicated a gain of contact inhibition. These data clearly place *Pod 1* as a tumour suppressor gene and suggest that *Pod 1* mis-expression in carcinoma cells may be due to methylation and not gene mutation.

Pod 1* and *WT1

Pod 1 has similar properties to another tumour suppressor gene involved in kidney development, *WT1*. Mutations in the *WT1* gene are responsible for a number of renal conditions such as Denys-Drash syndrome and Frasier's syndrome (1.2.1 Introduction) (Denys, *et al.*, 1967, Drash, *et al.*, 1970 and Barbaux, *et al.*, 1997). The dominant symptoms linked to these conditions are nephropathy and intersex. The nephropathy mainly effects the glomerulus, specifically the morphology of the podocytes and the glomerulus capillaries (Denys, *et al.*, 1967, Drash, *et al.*, 1970 Barbaux, *et al.*, 1997, Scharnhorst, *et al.*, 2001 and Ito, *et al.*, 2003). Podocytes appear immature with reduced or fused foot processes and glomerulus capillaries are disturbed due to alterations in mesangial cell proliferation. *Pod 1* knock-out experiments result in mice with comparable kidney phenotypes. Podocytes are similarly immature and lack foot processes, and the glomerulus capillary network is highly disorganised, although it is not clear whether the mesangial cells are responsible for this effect (Quaggin, *et al.*, 1999 and Cui, *et al.*, 2003).

WT1 mutations also effect gonad development. Genetically male Denys-Drash syndrome and Frasier's syndrome patients often have female or ambiguous genitalia, streak gonads and develop gonadoblastoma (Little and Wells, 1997). This phenotype was also observed in Frasier's syndrome mice, where *WT1* was shown to activate *SF1*, a sex organogenesis gene (Wilhelm and Englert, 2002). Interestingly, null *Pod 1* male mice are also externally female and have immature gonads (Cui, *et al.*, 2004). However, contrary to *WT1*, *Pod 1* has been shown to repress *SF1* expression (Tamura, *et al.*, 2001 and Cui, *et al.*, 2004).

From these data, a clear link between *Pod 1* and *WT1* may be established. Indeed, in this work, *Pod 1* has been shown to induce *WT1* expression in *Xenopus* animal caps. A potential study would be to analyse *Pod 1* expression in Denys-Drash syndrome and Frasier's syndrome mouse models. In humans, expression analysis could prove more fruitful than sequencing, especially regarding the study of *Pod 1* methylation (Smith, *et al.*, 2006).

9.3 *Darmin r*

Preliminary analysis of *Darmin r*, a cytosolic non-specific dipeptidase, indicated a role later in pronephric tubule development. Targeted over-expression experiments disrupted tubule morphology and reduced the size of the pronephric anlagen. Hypothetically, the over-expression of *Darmin r* could be prematurely signalling the terminal differentiation of pronephric tubule cells, and so reduce the number of pronephric tubule cells recruited via the pronephric anlagen. Observation of the number of cells within the pronephric anlagen contributing to the pronephric tubules by double wholemount *in situ* hybridisation, or analysis of the pronephric anlagen using a second marker, *xPax 8*, could add to the hypothesis. Also, the *Darmin r* knock-down analysis by morpholino oligonucleotide may further elucidate the role of *Darmin r*.

Diabetic nephropathy has been linked to human chromosome 18q and is suggested to be the result of a dominant acting mutation in this locus (Janssen, *et al.*, 2005). Analysis of diabetic patients with and without nephropathy indicated a significant association with mutations in the *CNDP1* gene and 5' of the human *Darmin r* homologue, *CNDP2*. These two genes are positioned at chromosome 18q22.3. The significance of the human *Darmin r* homologue association with diabetic nephropathy is unclear. Darmin r may degrade peptide carnosine, which has been shown to protect against oxidative stress and inhibit the renin-angiotensin system. Inhibition of the renin-angiotensin system can delay disease progression in patients with diabetic nephropathy. However, there is no direct evidence of the involvement of *Darmin r* in these processes.

9.4 Future work

As well as testing the discussed hypothesises arisen in the thesis, future work could also include analysis of the various clones highlighted in the search for target genes. These clones were previously overlooked due to inferior wholemount *in situ* hybridisation methodology, for example screen clones 18B1 and 5f6, or strict selection procedures, for example 15c7. These clones may yet prove important in the development of the pronephros.

9.5 Conclusion

The data obtained in this study with the evidence discussed in this thesis, show a conserved developmental role of genes, not only between the 3 successive kidney forms, but also between species, such as the frog, mouse and even human. It is hoped, that by the functional analysis of developmental genes in lower organisms, steps towards understanding human congenital conditions may be made.

References

Abrahamson D. R. (1986) Recent studies on the structure and pathology of basement membranes. *J Pathol.* **149**, 257-78.

Altschul S. F., Gish W., Miller W., Myers E. W., and Lipman D. J. (1990) Basic local alignment search tool. *J Mol Biol.* **215**, 403-410.

Andersson M., Giraud A. S., Familari M. (2001) The role of capsulin in the morphogenesis and differentiation of fetal rat gastric mucosa. *Int J Dev Biol.* **45**, 887-93.

Ariizumi T., and Asashima M. (2001) *In vitro* induction systems for analyses of amphibian organogenesis and body patterning. *Int J Dev Biol.* **45**, 273-279.

Ariizumi T., Sawamura K., Uchiyama H., and Asashima M. (1991) Dose and time-dependent mesoderm induction and outgrowth formation by activin A in *Xenopus laevis*. *Int J Dev Biol.* **35**, 407-414.

Asashima M., Ariizumi T., and Malacinski G. M. (2000) *In vitro* control of organogenesis and body patterning by activin during early amphibian development. *Comp Biochem Physiol B Biochem Mol Biol.* **126**,169-178.

Barbaux S., Niaudet P., Gubler M. C., Grunfeld J. P., Jaubert F., Kuttenn F., Fekete C. N., Souleyreau-Therville N., Thibaud E., Fellous M., McElreavey K. (1997) Donor splice-site mutations in *WT1* are responsible for Frasier syndrome. *Nat Genet.* **17**, 467-70.

Barnett, M. W., Old, R. W. and Jones, E. A. (1998). Neural induction and patterning by fibroblast growth factor, notochord and somite tissue in Xenopus. *Dev Growth Differ.* **40**, 47-57.

Boldyrev A. A. (2000) Problems and perspectives in studying the biological role of carnosine. *Biochemistry (Mosc).* **65**, 751-6.

Bouchard M., Souabni A., Mandler M., Neubuser A., Busslinger M. (2002) Nephric lineage specification by Pax2 and Pax8. *Genes Dev.* **16**, 2958-70.

Brandli A. W., (1999) Towards a molecular anatomy of the *Xenopus* pronephric kidney. *Int. J. Dev. Biol.* **43**, 381-395.

Breen J. J., Agulnick A. D., Westphali H., and Dawid I. B. (1998) Interactions between LIM Domains and the LIM Domain-binding Protein Ldb1. *J. Biol. Chem.* **273**, 4712–4717.

Brennan H. C., Nijjar S., and Jones E. A. (1998) The specification of the pronephric tubules and duct in *Xenopus laevis*. *Mech Dev.* **75**, 127-137.

Brennan, H. C., Nijjar, S. and Jones, E. A. (1999). The specification and growth factor inducibility of the pronephric glomus in *Xenopus laevis*. *Development.* **126**, 5847-56.

Breslow N. E., Takashima J. R., Ritchey M. L., Strong L. C., Green D. M. (2000) Renal failure in the Denys-Drash and Wilms' tumor-aniridia syndromes. *Cancer Res.* **60**, 4030-2.

Brown K.M., and Arthur J.R. (2001) Selenium, selenoproteins and human health: a review. *Public Health Nutr.* **4**, 593-599.

Burtey S., Leclerc C., Nabais E., Munch P., Gohory C., Moreau M., Fontes M. (2005) Cloning and expression of the amphibian homologue of the human PKD1 gene. *Gene.* **357**, 29-36.

Buttiglieri S., Deregibus M. C., Bravo S., Cassoni P., Chiarle R., Bussolati B., Camussi G. (2002) Role of *Pax2* in apoptosis resistance and proinvasive phenotype of Kaposi's sarcoma cells. *J Biol Chem.* **279**, 4136-43.

Call K. M., Glaser T., Ito C. Y., Buckler A. J., Pelletier J., Haber D. A., Rose E. A., Kral A., Yeger H., Lewis W. H. (1990) Isolation and characterization of a zinc finger polypeptide gene at the human chromosome 11 Wilms' tumor locus. *Cell.* **60**, 509-20.

Carmona R., Gonzalez-Iriarte M., Perez-Pomares J. M., Munoz-Chapuli R. (2001) Localization of the Wilm's tumour protein WT1 in avian embryos. *Cell Tissue Res.* **303**, 173-86.

Carroll, T. J. and Vize, P. D. (1996). Wilms' tumor suppressor gene is involved in the development of disparate kidney forms: evidence from expression in the *Xenopus* pronephros. *Dev Dyn.* **206**, 131-8.

Carroll, T. J. and Vize, P. D. (1999). Synergism between *Pax-8* and *lim-1* in embryonic kidney development. *Dev Biol.* **214**, 46-59.

Carroll, T., Wallingford, J., Seufert, D. and Vize, P. D. (1999). Molecular regulation of pronephric development. *Curr Top Dev Biol.* **44**, 67-100.

Chan, T. C., Takahashi, S. and Asashima, M. (2000). A role for *Xlim-1* in pronephros development in *Xenopus laevis*. *Dev Biol.* **228**, 256-69.

Chen S., Kasama Y., Lee J. S., Jim B., Marin M., Ziyadeh F. N. (2004) Podocyte-derived vascular endothelial growth factor mediates the stimulation of alpha3(IV) collagen production by transforming growth factor-beta1 in mouse podocytes. *Diabetes.* **53**, 2939-49.

Cleaver, O. and Krieg, P. A. (1998). *VEGF* mediates angioblast migration during development of the dorsal aorta in *Xenopus*. *Development.* **125**, 3905-14.

Cleaver, O., Tonissen, K. F., Saha, M. S. and Krieg, P. A. (1997). Neovascularization of the *Xenopus* embryo. *Dev Dyn.* **210**, 66-77.

Cui S., Ross A., Stallings N., Parker K. L., Capel B., Quaggin S. E. (2004) Disrupted gonadogenesis and male-to-female sex reversal in Pod1 knockout mice. *Development.* **131**, 4095-105.

Cui S., Schwartz L., Quaggin S. E. (2003) Pod1 is required in stromal cells for glomerulogenesis. *Dev Dyn.* **226**, 512-22.

Dale L. (2000) Pattern formation: A new twist to BMP signaling. *Current Biology.* **10**, R671-3.

Dale L., and Wardle F. C. (1999) A gradient of BMP activity specifies dorsal–ventral fates in early Xenopus embryos. seminars in Cell & Developmental Biology,10, 319-326

Dale L., Howes G., Price B. M. J., Smith J. C. (1992) Bone morphogenetic protein 4: A ventralizing factor in early *Xenopus* development. *Development.* **115**, 573-585.

Davidson G., Dono R., and Zeller R. (2002) FGF signalling is required for differentiation-induced cytoskeletal reorganisation and formation of actin-based processes by podocytes. *J. Cell Sci.* **114**, 3359 - 3366.

Dehbi M., Ghahremani M., Lechner M., Dressler G., Pelletier J. (1996) The paired-box transcription factor, PAX2, positively modulates expression of the Wilms' tumor suppressor gene (WT1). *Oncogene.* **13**, 447-53.

Dehbi M., Pelletier J. (1996) PAX8-mediated activation of the wt1 tumor suppressor gene. *EMBO J.* **15**, 4297-306.

Deltas C. C. (2001) Mutations of the *Human Polycystic Kidney Disease 2* (*PKD2*) Gene. *Human Mutation.* **18**,13-24.

Demartis, A., Maffei, M., Vignali, R., Barsacchi, G. and De Simone, V. (1994). Cloning and developmental expression of LFB3/HNF1 beta transcription factor in *Xenopus laevis*. *Mech Dev.* **47**, 19-28.

Denys P., Malvaux P., Van Den Berghe H., Tanghe W., Proesmans W. (1967) Association of an anatomo-pathological syndrome of male pseudohermaphroditism, Wilms' tumor, parenchymatous nephropathy and XX/XY mosaicism. *Arch Fr Pediatr.* **24**, 729-39

Discenza M. T., and Pelletier J., (2004) Insights into the physiological role of *WT1* from studies of genetically modified mice. *Physiol Genomics.* **16**, 287-300.

Doyonnas R., Kershaw D. B., Duhme C., Merkens H., Chelliah S., Graf T., McNagny K. M. (2001) Anuria, omphalocele, and perinatal lethality in mice lacking the CD34-related protein podocalyxin. *J Exp Med.* **194**, 13-27.

Drash A., Sherman F., Hartmann W. H., Blizzard R. M. (1970) A syndrome of pseudohermaphroditism, Wilms' tumor, hypertension, and degenerative renal disease. *J Pediatr.* **76**, 585-93.

Drummond I. A., Majumdar A., Hentschel H., Elger M., Solnica-Krezel L., Schier A. F., Neuhauss S. C., Stemple D. L., Zwartkruis F., Rangini Z., Driever W., Fishman M. C. (1998) Early development of the zebrafish pronephros and analysis of mutations affecting pronephric function. *Development.* **125**, 4655-67.

Drummond I. A., Majumdar A., Hentschel H., Elger M., Solnica-Krezel L., Schier A. F., Neuhauss S. C. F., Stemple D. L., Zwartkruis F., Rangini Z., Driever W., and Fishman M. C. (1998) Early development of the zebrafish pronephros and analysis of mutations affecting pronephric function. *Development.* **125**, 4655-4667.

Dziarmaga A., Clark P., Stayner C., Julien J. P., Torban E., Goodyer P., Eccles M. (2003) Ureteric bud apoptosis and renal hypoplasia in transgenic PAX2-Bax fetal mice mimics the renal-coloboma syndrome. *J Am Soc Nephrol.* **14**, 2767-74.

Eccles M. R. (1998) The role of *PAX2* in normal and abnormal development of the urinary tract. *Pediatr Nephrol.* **12**, 712-20.

Eccles MR, He S, Legge M, Kumar R, Fox J, Zhou C, French M, Tsai RW. (2002) PAX genes in development and disease: the role of PAX2 in urogenital tract development. *Int J Dev Biol.* **46**, 535-44.

Fainsod A., Steinbeisser H., and De Robertis E. M. (1994) On the function of BMP-4 in patterning the marginal zone of the Xenopus embryo. *The EMBO Journal.* **13**, 5015-5025.

Falcon-Perez J. M., Nazarian R., Sabatti C., and Dell'Angelica E. C. (2005) Distribution and dynamics of Lamp1-containing endocytic organelles in fibroblasts deficient in BLOC-3. *J Cell Sci.* **118**, 5243-55.

Favor J., Sandulache R., Neuhauser-Klaus A., Pretsch W., Chatterjee B., Senft E., Wurst W., Blanquet V., Grimes P., Sporle R., Schughart K. (1996) The mouse Pax2(1Neu) mutation is identical to a human PAX2 mutation in a family with renal-coloboma syndrome and results in developmental defects of the brain, ear, eye, and kidney. *Proc Natl Acad Sci U S A.* **93**, 13870-5.

Ferrari C. K., (2004) Functional foods, herbs and nutraceuticals: towards biochemical mechanisms of healthy aging. *Biogerontology.* **5**, 275-89.

Fransen M. E., Lemanski L. F. (1990) Epicardial development in the axolotl, Ambystoma mexicanum. *Anat Rec.* **226**, 228-36.

Funato N., Ohyama K., Kuroda T., Nakamura M. (2002) Basic helix-loop-helix transcription factor epicardin/capsulin/Pod-1 suppresses differentiation by negative regulation of transcription. *J Biol Chem.* **278**, 7486-93.

Gallagher AR, Hidaka S, Gretz N, Witzgall R. (2002) Molecular basis of autosomal-dominant polycystic kidney disease. *Cell Mol Life Sci.* **59**, 682-93.

Gerth V. E., Zhou X., Vize P. D. (2005) Nephrin expression and three-dimensional morphogenesis of the Xenopus pronephric glomus. *Dev Dyn.* **233**, 1131-9.

Gessler M., Konig A., Arden K., Grundy P., Orkin S., Sallan S., Peters C., Ruyle S., Mandell J., Li F. (1994) Infrequent mutation of the *WT1* gene in 77 Wilms' Tumors. *Hum Mutat.* **3**, 212-22.

Gessler M., Poustka A., Cavenee W., Neve R. L., Orkin S. H., Bruns G. A. (1990) Homozygous deletion in Wilms tumours of a zinc-finger gene identified by chromosome jumping. *Nature.* **343**, 774-8.

Gnarra J. R., and Dressler G. R. (1995) Expression of Pax-2 in human renal cell carcinoma and growth inhibition by antisense oligonucleotides. *Cancer Res.* **55**, 4092-8.

Gough S. M., McDonald M., Chen X. N., Korenberg J. R., Neri A., Kahn T., Eccles M. R., Morris C. M. (2003) Refined physical map of the human PAX2/HOX11/NFKB2 cancer gene region at 10q24 and relocalization of the HPV6AI1 viral integration site to 14q13.3-q21.1. *BMC Genomics.* **4**, 9.

Green J. B. A., Cook T. L., Smith J. C., and Grainger R. M. (1997). Anteroposterior neural tissue specification by activin-induced mesoderm. *Dev. Biol.*. **94**, 8596-8601.

Green J. B., and Smith J. C. (1990) Graded changes in dose of a Xenopus activin A homologue elicit stepwise transitions in embryonic cell fate. *Nature.* **347**, 391-4.

Green J. B., Howes G., Symes K., Cooke J., and Smith J. C. (1990) The biological effects of XTC-MIF: quantitative comparison with Xenopus bFGF. *Development.* **108**, 173-183.

Gurdol F., Genc S., Yalcin O., Gultepe M. (1995) The presence of prolidase activity in amniotic fluid and its evaluation as a maturity test. *Biol Neonate.* **67**, 34-8.

Haldin C. E., Nijjar S., Masse K., Barnett M. W., and Jones E.A. (2003) Isolation and growth factor inducibility of the Xenopus laevis *Lmx1b* gene. *Int J Dev Biol.* **47**, 253-262.

Hanson, H. T. & Smith, E. L. (1949) Papain resolution of D,L-tryptophan; optical specificity of carboxypeptidase. *J Biol Chem.* **179**, 815-818.

Harland, R. M. (1991). In situ hybridization: an improved whole-mount method for Xenopus embryos. *Methods Cell Biol.* **36**, 685-95.

Hawley S. H., Wunnenberg-Stapleton K., Hashimoto C., Laurent M. N., Watabe T., Blumberg B. W., Cho K. W. (1995) Disruption of BMP signals in embryonic *Xenopus* ectoderm leads to direct neural induction. *Genes Dev.* **9**, 2923-35.

Heller N., Brandli A. W. (1999) Xenopus Pax-2/5/8 orthologues: novel insights into Pax gene evolution and identification of Pax-8 as the earliest marker for otic and pronephric cell lineages. *Dev Genet.* **24**, 208-19

Heller, N. and Brandli, A. W. (1997). *Xenopus Pax-2* displays multiple splice forms during embryogenesis and pronephric kidney development. *Mech Dev.* **69**, 83-104.

Hemmati-Brivanlou, A., Frank, D., Bolce, M. E., Brown, B. D., Sive, H. L. and Harland, R. M. (1990). Localization of specific mRNAs in Xenopus embryos by whole-mount in situ hybridization. *Development.* **110**, 325-30.

Herzer U., Crocoll A., Barton D., Howells N., Englert C. (1999) The Wilms tumor suppressor gene wt1 is required for development of the spleen. *Curr Biol.* **9**, 837-40.

Hidai H., Bardales R., Goodwin R., Quertermous T., Quertermous E. E. (1998) Cloning of capsulin, a basic helix-loop-helix factor expressed in progenitor cells of the pericardium and the coronary arteries. *Mech Dev.* **73**, 33-43.

Holewa, B., Strandmann, E. P., Zapp, D., Lorenz, P. and Ryffel, G. U. (1996). Transcriptional hierarchy in *Xenopus* embryogenesis: *HNF4* a maternal factor involved in the developmental activation of the gene encoding the tissue specific transcription factor *HNF1 alpha* (*LFB1*). *Mech Dev.* **54**, 45-57.

Horb M. E., Thomsen G. H. (1999) Tbx5 is essential for heart development. *Development.* **126**, 1739-51.

Horvat R., Hovorka A., Dekan G., Poczewski H., Kerjaschki D. (1986) Endothelial cell membranes contain podocalyxin--the major sialoprotein of visceral glomerular epithelial cells. *J Cell Biol.* **102**, 484-91.

Hsu D. R., Economides A. N., Wang X., Eimon P. M., and Harland R. M. (1998) The *Xenopus* Dorsalizing Factor Gremlin Identifies a Novel Family of Secreted Proteins that Antagonize BMP Activities. *Molecular Cell.* **1**, 673–683.

Hsu H. J., Lin G., Chung B. C. (2003) Parallel early development of zebrafish interrenal glands and pronephros: differential control by wt1 and ff1b. *Development.* **130**, 2107-16.

Hubbard T., Andrews D., Caccamo M., Cameron G., Chen Y., Clamp M., Clarke L., Coates G., Cox T., Cunningham F., Curwen V., Cutts T., Down T., Durbin R., Fernandez-Suarez X. M., Gilbert J., Hammond M., Herrero J., Hotz H., Howe K., Iyer V., Jekosch K., Kahari A., Kasprzyk A., Keefe D., Keenan S., Kokocinsci F., London D., Longden I., McVicker G., Melsopp C., Meidl P., Potter S., Proctor G., Rae M., Rios D., Schuster M., Searle S., Severin J., Slater G., Smedley D., Smith J., Spooner W., Stabenau A., Stalker J., Storey R., Trevanion S., Ureta-Vidal A., Vogel J., White S., Woodwark C., Birney E. (2005) Ensembl 2005. *Nucleic Acids Res.* **33**, D447-53.

Hutson M. R., Lewis J. E., Nguyen-Luu D., Lindberg K. H., Barald K. F. (1999) Expression of Pax2 and patterning of the chick inner ear. *J Neurocytol.* **28**, 795-807.

Irie K., Komori K., Seiki M., Tsuruga E., Sakakura Y., Kaku T., Yajima T. (2005) Impaired alveolization in mice deficient in membrane-type matrix metalloproteinase 1 (MT1-MMP). *Med Mol Morphol.* **38**, 43-6.

Ito S., Hataya H., Ikeda M., Takata A, Kikuchi H., Hata J., Morikawa Y., Kawamura S., Honda M. (2003) Alport syndrome-like basement membrane changes in Frasier syndrome: an electron microscopy study. *Am J Kidney Dis.* **41**, 1110-5.

James R. G., Schultheiss T. M. (2003) Patterning of the avian intermediate mesoderm by lateral plate and axial tissues. *Dev Biol.* **253**, 109-24.

Janssen B., Hohenadel D., Brinkkoetter P., Peters V., Rind N., Fischer C., Rychlik I., Cerna M., Romzova M., de Heer E., Baelde H., Bakker S. J., Zirie M., Rondeau E., Mathieson P., Saleem M. A., Meyer J., Koppel H., Sauerhoefer S., Bartram C. R., Nawroth P., Hammes H. P., Yard B. A., Zschocke J., van der Woude F. J. (2005) Carnosine as a protective factor in diabetic nephropathy: association with a leucine repeat of the carnosinase gene CNDP1. *Diabetes.* **54**, 2320-7.

Jones E. A. (2005) *Xenopus*: A Prince Among Models for Pronephric Kidney Development. *J Am Soc Nephrol.* **16**, 313-321.

Kestila M., Lenkkeri U., Mannikko M., Lamerdin J., McCready P., Putaala H., Ruotsalainen V., Morita T., Nissinen M., Herva R., Kashtan C., Peltonen L., Holmberg C., Olsen A., Tryggvason K. (1998) Positionally Cloned Gene for a Novel Glomerular Protein - Nephrin - Is Mutated in Congenital Nephrotic Syndrome. *Molecular Cell.* **1**, 575–582.

Kim K., Drummond I., Ibraghimov-Beskrovnaya O., Klinger K., Arnaout M. A. (2000) Polycystin 1 is required for the structural integrity of blood vessels. *Proc Natl Acad Sci U S A.* **97**, 1731-6.

Kolker S. J., Tajchman U., Weeks D. L. (2000) Confocal imaging of early heart development in *Xenopus laevis*. *Dev Biol.* **218**, 64-73.

Kostrouchova M., Housa D., Kostrouch Z., Saudek V., and Rall J. E. (2002) *SKIP* is an indispensable factor for *Caenorhabditis elegans* development. *Proc Natl Acad Sci U S A.* 99, 9254-9259.

Koziell A., Grech V., Hussain S., Lee G., Lenkkeri U., Tryggvason K., Scambler P. (2002) Genotype/phenotype correlations of NPHS1 and NPHS2 mutations in nephrotic syndrome advocate a functional inter-relationship in glomerular filtration. *Hum. Molec. Genet.* **11**, 379-388.

Kramer-Zucker A. G., Wiessner S., Jensen A. M., Drummond I. A. (2005) Organization of the pronephric filtration apparatus in zebrafish requires Nephrin, Podocin and the FERM domain protein Mosaic eyes. *Dev Biol.* **285**, 316-29.

Kraus F., Haenig B., Kispert A. (2001) Cloning and expression analysis of the mouse T-box gene Tbx18. *Mech Dev.* **100**, 83-6.

Kreidberg J. A., Sariola H., Loring J. M., Maeda M., Pelletier J., Housman D., Jaenisch R. (1993) WT-1 is required for early kidney development. *Cell.* **74**, 679-91.

Ku, M. and Melton, D. A. (1993). *Xwnt-11*: a maternally expressed *Xenopus* wnt gene. *Development.* **119**, 1161-73.

Kyuno, J., Fukui, A., Michiue, T. and Asashima, M. (2003). Identification and characterization of *Xenopus NDRG1*. *Biochem Biophys Res Commun.* **309**, 52-7.

Lassar A. B., Davis R. L., Wright W. E., Kadesch T., Murre C., Voronova A., Baltimore D., Weintraub H. (1991) Functional activity of myogenic HLH proteins requires hetero-oligomerization with E12/E47-like proteins in vivo. *Cell.* **66**, 305-15.

Lenney J. F. (1990) Separation and characterization of two carnosine-splitting cytosolic dipeptidases from hog kidney (carnosinase and non-specific dipeptidase). *Biol Chem Hoppe Seyler.* **371**, 433-40.

Lenney J. F., Peppers S. C., Kucera-Orallo C. M., George R. P. (1985) Characterization of human tissue carnosinase. *Biochem J.* **228**, 653-60.

Li D. H., Chan T., Satow R., Komazaki S., Hashizume K., Asashima M. (2005) The role of XTRAP-gamma in Xenopus pronephros development. *Int J Dev Biol.* **49**, 401-8.

Li H., Liu H., Corrales C. E., Mutai H., Heller S. (2004) Correlation of Pax-2 expression with cell proliferation in the developing chicken inner ear. *J Neurobiol.* **60**, 61-70.

Little M. H., Williamson K. A., Mannens M., Kelsey A., Gosden C., Hastie N. D., van Heyningen V. (1993) Evidence that WT1 mutations in Denys-Drash syndrome patients may act in a dominant-negative fashion. *Hum Mol Genet.* **2**, 259-64.

Little M., and Wells C. (1997) A clinical overview of WT1 gene mutations. *Hum Mutat.* **9**, 209-25.

Liu L., Done S. C., Khoshnoodi J., Bertorello A., Wartiovaara J., Berggren P. O., Tryggvason K. (2001) Defective nephrin trafficking caused by missense mutations in the NPHS1 gene: insight into the mechanisms of congenital nephrotic syndrome. *Hum Mol Genet.* **10**, 2637-44.

Lochs H., Williams P. E., Morse E. L., Abumrad N. N. and Adibi S. A. (1988) Metabolism of dipeptides and their constituent amino acids by liver, gut, kidney, and muscle. *Am J Physiol Endocrinol Metab.* **254**, E588-E594.

Logan M., and Mohun T. (1993) Induction of cardiac muscle differentiation in isolated animal pole explants of *Xenopus laevis* embryos. *Development.* **118**, 865-75.

Low S. H., Vasanth S., Larson C. H., Mukherjee S., Sharma N., Kinter M. T., Kane M. E., Obara T., Weimbs T. (2006) Polycystin-1, STAT6, and P100 function in a pathway that transduces ciliary mechanosensation and is activated in polycystic kidney disease. *Dev Cell.* **10**, 57-69.

Lu J. R., Bassel-Duby R., Hawkins A., Chang P., Valdez R., Wu H., Gan L., Shelton J. M., Richardson J. A., Olson E. N. (2002) Control of facial muscle development by MyoR and capsulin. *Science*. **298**, 2378-81.

Lu J., Chang P., Richardson J. A., Gan L., Weiler H., Olson E. N. (2000) The basic helix-loop-helix transcription factor capsulin controls spleen organogenesis. *Proc Natl Acad Sci U S A*. **97**, 9525-30.

Lu J., Richardson J. A., Olson E. N. (1998) Capsulin: a novel bHLH transcription factor expressed in epicardial progenitors and mesenchyme of visceral organs. *Mech Dev*. **73**, 23-32.

Lu W., Peissel B., Babakhanlou H., Pavlova A., Geng L., Fan X., Larson C., Brent G., Zhou J. (1997) Perinatal lethality with kidney and pancreas defects in mice with a targetted Pkd1 mutation. *Nat Genet*. **17**, 179-81.

Majumdar A., Lun K., Brand M., Drummond I. A. (2000) Zebrafish no isthmus reveals a role for pax2.1 in tubule differentiation and patterning events in the pronephric primordia. *Development*. **127**, 2089-98.

Manner J. (1999) Does the subepicardial mesenchyme contribute myocardioblasts to the myocardium of the chick embryo heart? A quail-chick chimera study tracing the fate of the epicardial primordium. *Anat Rec*. **255**, 212-26.

Mansouri A., Chowdhury K., Gruss P. (1998) Follicular cells of the thyroid gland require Pax8 gene function. *Nat Genet*. **19**, 87-90.

Masse K., Bhamra S., Haldin C. E., and Jones E.A. (2004) Cloning and characterisation of the immunophilin *X-CypA* in *Xenopus laevis*. *Gene Expr Patterns*. **5**, 51-60.

McLaughlin K. A., Rones M. S., and Mercola M. (2000) Notch Regulates Cell Fate in the Developing Pronephros. *Developmental Biology*. **227**, 567–580.

Menke A. L., IJpenberg A., Fleming S., Ross A., Medine C. N., Patek C. E., Spraggon L., Hughes J., Clarke A. R., Hastie N. D. (2003) The wt1-heterozygous mouse; a model to study the development of glomerular sclerosis. *J Pathol*. **200**, 667-74.

Miyagishi M., Nakajima T., Fukamizu A. (2000a) Molecular characterization of mesoderm-restricted basic helix-loop-helix protein, POD-1/Capsulin. *Int J Mol Med*. **5**, 27-31.

Miyagishi M., Hatta M., Ohshima T., Ishida J., Fujii R., Nakajima T., Fukamizu A. (2000b) Cell type-dependent transactivation or repression of mesoderm-restricted basic helix-loop-helix protein, POD-1/Capsulin. *Mol Cell Biochem*. **205**, 141-7.

Miyanaga Y., Shiurba R., and Asashima M. (1999) Blood cell induction in Xenopus animal cap explants: effects of fibroblast growth factor, bone morphogenetic proteins, and activin. *Dev Genes Evol*. **209**, 69-76.

Møbjerg, N., Larsen, E. H. and Jespersen, A. (2000). Morphology of the kidney in larvae of *Bufo viridis* (Amphibia, Anura, Bufonidae). *J Morphol.* **245**, 177-95.

Mochizuki E., Fukuta K., Tada T., Harada T., Watanabe N., Matsuo S., Hashimoto H., Ozato K., Wakamatsu Y. (2005) Fish mesonephric model of polycystic kidney disease in medaka (Oryzias latipes) pc mutant. *Kidney Int.* **68**, 23-34.

Moore A. W., McInnes L., Kreidberg J., Hastie N. D., Schedl A. (1999) YAC complementation shows a requirement for Wt1 in the development of epicardium, adrenal gland and throughout nephrogenesis. *Development.* **126**, 1845-57.

Morabito C. J., Dettman R. W., Kattan J., Collier J. M., Bristow J. (2001) Positive and negative regulation of epicardial-mesenchymal transformation during avian heart development. *Dev Biol.* **234**, 204-15.

Moreno R.D. (2003) Differential expression of lysosomal associated membrane protein (LAMP-1) during mammalian spermiogenesis. *Mol Reprod Dev.* **66**, 202-209.

Moriya N., Komazaki S., Takahashi S., Yokota C., and Asashima M. (2000) *In vitro* pancreas formation from *Xenopus* ectoderm treated with activin and retinoic acid. *Dev Growth Differ.* **42**, 593-602.

Mundel P., and Kriz W. (1995) Structure and function of podocytes: an update. *Anat Embryol (Berl).* **192**, 385-97.

Munoz-Chapuli R., Macias D., Gonzalez-Iriarte M., Carmona R., Atencia G., Perez-Pomares J. M. (2002) The epicardium and epicardial-derived cells: multiple functions in cardiac development. *Rev Esp Cardiol.* **55**, 1070-82.

Murre C., McCaw P. S., Vaessin H., Caudy M., Jan L. Y., Jan Y. N., Cabrera C. V., Buskin J. N., Hauschka S. D., Lassar A. B., *et al.* (1989) Interactions between heterologous helix-loop-helix proteins generate complexes that bind specifically to a common DNA sequence. *Cell.* **58**, 537-44..

Nieuwkoop P. D. and Faber J. (1994). Normal Table of Xenopus laevis (Daudin). *4th ed. Garland, New York.*

Okabayashi K., and Asashima M. (2003) Tissue generation from amphibian animal caps. *Curr Opin Genet Dev.* **13**, 502-7.

Osafune K., Nishinakamura R., Komazaki S., Asashima M. (2002) In vitro induction of the pronephric duct in Xenopus explants. *Dev Growth Differ.* **44**, 161-7.

Palmer R. E., Kotsianti A., Cadman B., Boyd T., Gerald W., Haber D. A. (2001) WT1 regulates the expression of the major glomerular podocyte membrane protein Podocalyxin. *Curr Biol.* **11**, 1805-9.

Patek C. E., Little M. H., Fleming S., Miles C., Charlieu J. P., Clarke A. R., Miyagawa K., Christie S., Doig J., Harrison D. J., Porteous D. J., Brookes A. J., Hooper M. L., Hastie N. D. (1999) A zinc finger truncation of murine WT1 results in the characteristic

urogenital abnormalities of Denys-Drash syndrome. *Proc Natl Acad Sci U S A.* **96**, 2931-6.

Paterson A. D., Pei Y. (1998) Is there a third gene for autosomal dominant polycystic kidney disease? *Kidney Int.* **54**, 1759-61

Pegova A., Abe H., Boldyrev A. (2000) Hydrolysis of carnosine and related compounds by mammalian carnosinases. *Comp Biochem Physiol B Biochem Mol Biol.* **127**, 443-6.

Pelletier J., Bruening W., Kashtan C. E., Mauer S. M., Manivel J. C., Striegel J. E., Houghton D. C., Junien C., Habib R., Fouser L., *et al.* (1991) Germline mutations in the Wilms' tumor suppressor gene are associated with abnormal urogenital development in Denys-Drash syndrome. *Cell.* **67**, 437-47.

Penga Y., Kok K. H., Xuc R., Kwok K. H. H., Tay D., Fung P. C. W., Kung H., Lin M. C. M. (2000) Maternal cold inducible RNA binding protein is required for embryonic kidney formation in *Xenopus laevis. FEBS Letters.* **482**, 37-43

Pera E. M., De Robertis E. M. (2000) A direct screen for secreted proteins in Xenopus embryos identifies distinct activities for the Wnt antagonists Crescent and Frzb-1. *Mech Dev.* **96**, 183-95.

Pera E. M., Martinez S. L., Flanagan J. J., Brechner M., Wessely O., De Robertis E. M. (2003) Darmin is a novel secreted protein expressed during endoderm development in Xenopus. *Gene Expr Patterns.* **3**, 147-52.

Pollet N., Muncke N., Verbeek B., Li Y., Fenger U., Delius H., Niehrs C. (2005) An atlas of differential gene expression during early Xenopus embryogenesis. *Mech Dev.* **122**, 365-439.

Porteous S., Torban E., Cho N. P., Cunliffe H., Chua L., McNoe L., Ward T., Souza C., Gus P., Giugliani R., Sato T., Yun K., Favor J., Sicotte M., Goodyer P., Eccles M. (2000) Primary renal hypoplasia in humans and mice with *PAX2* mutations: evidence of increased apoptosis in fetal kidneys of *Pax2*^{1Neu} +/- mutant mice. *Hum Mol Genet.* **9**, 1–11.

Putaala H., Soininen R., Kilpelainen P., Wartiovaara J., Tryggvason K. (2001) The murine nephrin gene is specifically expressed in kidney, brain and pancreas: inactivation of the gene leads to massive proteinuria and neonatal death. *Hum Mol Genet.* **10**, 1-8.

Quaggin S. E. (2002) Transcriptional regulation of podocyte specification and differentiation. *Microsc Res Tech.* **57**, 208-11.

Quaggin S. E., Schwartz L., Cui S., Igarashi P., Deimling J., Post M., Rossant J. (1999) The basic-helix-loop-helix protein pod1 is critically important for kidney and lung organogenesis. *Development.* **126**, 5771-83.

Quaggin S. E., Vanden Heuvel G. B., Igarashi P. (1998) Pod-1, a mesoderm-specific basic-helix-loop-helix protein expressed in mesenchymal and glomerular epithelial cells in the developing kidney. *Mech Dev.* **71**, 37-48.

Ranjan M., Tafuri S. R., Wolffe A. P. (1993) Masking mRNA from translation in somatic cells. *Genes Dev.* **7**, 1725-36.

Rawlings N. D., Morton F. R., Barrett A. J. (2006) MEROPS: the peptidase database. *Nucleic Acids Res.* **34**, D270-2.

Riccardi V. M., Sujansky E., Smith A. C., Francke U. (1978) Chromosomal imbalance in the Aniridia-Wilms' tumor association: 11p interstitial deletion. *Pediatrics.* **61**, 604-10.

Rieder S. E., Banta L. M., Kohrer K., McCaffery J. M., and Emr S. D. (1996) Multilamellar endosome-like compartment accumulates in the yeast vps28 vacuolar protein sorting mutant. *Mol Biol Cell.* **7**, 985-99.

Robb L., Mifsud L., Hartley L., Biben C., Copeland N. G., Gilbert D. J., Jenkins N. A., Harvey R. P. (1998) epicardin: A novel basic helix-loop-helix transcription factor gene expressed in epicardium, branchial arch myoblasts, and mesenchyme of developing lung, gut, kidney, and gonads. *Dev Dyn.* **213**, 105-13.

Ruotsalainen V., Ljungberg P., Wartiovaara J., Lenkkeri U., Kestila M., Jalanko H., Holmberg C., and Tryggvason K. (1999) Nephrin is specifically located at the slit diaphragm of glomerular podocytes. *Proc. Natl. Acad. Sci. USA.* **96**, 7962–7967.

Ryan G, Steele-Perkins V, Morris JF, Rauscher FJ 3rd, Dressler GR. (1995) Repression of Pax-2 by WT1 during normal kidney development. *Development.* **121**, 867-75.

Sambrook, J., Fritsch, E. F. and Maniatis, T. (1989). Molecular cloning: a laboratory manual.

Sanyanusin P., Norrish J. H., Ward T. A., Nebel A., McNoe L. A., Eccles M. R. (1996) Genomic structure of the human PAX2 gene. *Genomics.* **35**, 258-61.

Sanyanusin P., Schimmenti L. A., McNoe L. A., Ward T. A., Pierpont M. E., Sullivan M. J., Dobyns W. B., Eccles M. R. (1995) Mutation of the *PAX2* gene in a family with optic nerve colobomas, renal anomalies and vesicoureteral reflux. *Nat Genet.* **9**, 358-64.

Sassoe-Pognetto M., Cantino D., Panzanelli P., Verdun di Cantogno L., Giustetto M., Margolis F. L., De Biasi S., Fasolo A. (1993) Presynaptic co-localization of carnosine and glutamate in olfactory neurones. *Neuroreport.* **5**, 7-10.

Sato A., Asashima M., Yokota T., and Nishinakamura R. (2000) Cloning and expression pattern of a *Xenopus* pronephros-specific gene, *XSMP-30. Mech Dev.* **92**, 273-5.

Satow, R., Chan, T. C. and Asashima, M. (2004). The role of *Xenopus frizzled-8* in pronephric development. *Biochem Biophys Res Commun.* **321**, 487-94.

Saulnier, D. M., Ghanbari, H. and Brandli, A. W. (2002). Essential function of *Wnt-4* for tubulogenesis in the *Xenopus* pronephric kidney. *Dev Biol.* **248**, 13-28.

Saxén, L. (1987). Organogesis of the kidney. *Cambridge: Cambridge University Press.* Scharnhorst V., Van Der Eb A. J., Jochemsen A. G. (2001) WT1 proteins: functions in growth and differentiation. *Gene.* **273**, 141-61.

Schnabel E., Dekan G., Miettinen A., Farquhar M. G. (1989) Biogenesis of podocalyxin--the major glomerular sialoglycoprotein--in the newborn rat kidney. *Eur J Cell Biol.* **48**, 313-26.

Semba, K., Saito-Ueno, R., Takayama, G. and Kondo, M. (1996). cDNA cloning and its pronephros-specific expression of the Wilms' tumor suppressor gene, WT1, from Xenopus laevis. *Gene.* **175**, 167-72.

Seufert D. W., Brennan H. C., DeGuire J., Jones E. A., Vize P. D. (1999) Developmental basis of pronephric defects in Xenopus body plan phenotypes. *Dev Biol.* **215**, 233-42.

Seville, R. A., Nijjar, S., Barnett, M. W., Masse, K. and Jones, E. A. (2002). *Annexin IV* (*Xanx-4*) has a functional role in the formation of pronephric tubules. *Development.* **129**, 1693-704.

Smith J. C., Yaqoob M., and Symes K. (1988) Purification, partial characterization and biological effects of the XTC mesoderm-inducing factor. *Development.* **103**, 591-600.

Smith L. T., Lin M., Brena R. M., Lang J. C., Schuller D. E., Otterson G. A., Morrison C. D., Smiraglia D. J., Plass C. (2006) Epigenetic regulation of the tumor suppressor gene TCF21 on 6q23-q24 in lung and head and neck cancer. *Proc Natl Acad Sci U S A.* **103**, 982-7.

Tafuri S. R., and Wolffe A. P. (1990) *Xenopus Y-box transcription factors*: molecular cloning, functional analysis and developmental regulation. *Proc Natl Acad Sci U S A.* **87**, 9028-32.

Tafuri S. R., and Wolffe A. P. (1993) Selective recruitment of masked maternal mRNA from messenger ribonucleoprotein particles containing *FRGY2* (mRNP4). *J Biol Chem.* **268**, 24255-61.

Taira M., Otani H., Jamrich M., and Dawid I. B. (1994) Expression of the LIM class homeobox gene *Xlim-1* in pronephros and CNS cell lineages of Xenopus embryos is affected by retinoic acid and exogastrulation. *Development.* **120**, 1525-36.

Tamai K., Yokota C., Ariizumi T., and Asashima M. (1999) *Cytochalasin B* inhibits morphogenetic movement and muscle differentiation of activin-treated ectoderm in *Xenopus*. *Dev Growth Differ.* **41**, 41-9.

Tamura M., Kanno Y., Chuma S., Saito T., Nakatsuji N. (2001) Pod-1/Capsulin shows a sex- and stage-dependent expression pattern in the mouse gonad development and represses expression of Ad4BP/SF-1. *Mech Dev.* **102**, 135-44.

Teufel M., Saudek V., Ledig J. P., Bernhardt A., Boularand S., Carreau A., Cairns N. J., Carter C., Cowley D. J., Duverger D., Ganzhorn A. J., Guenet C., Heintzelmann B., Laucher V., Sauvage C., Smirnova T. (2003) Sequence identification and characterization of human carnosinase and a closely related non-specific dipeptidase. *J Biol Chem.* **278**, 6521-31.

Thijssen H. H., Janssen C. A., and Drittij-Reijnders M. J.(1986) The effect of S-warfarin administration on vitamin K 2,3-epoxide reductase activity in liver, kidney and testis of the rat. *Biochem Pharmacol.* **35**, 3277-82.

Tryggvason K. (1999) Unraveling the mechanisms of glomerular ultrafiltration: nephrin, a key component of the slit diaphragm. *J Am Soc Nephrol.* **10**, 2440-5

Uochi, T. and Asashima, M. (1998). XCIRP (Xenopus homolog of cold-inducible RNA-binding protein) is expressed transiently in developing pronephros and neural tissue. *Gene.* **211**, 245-50.

Varanasi R., Bardeesy N., Ghahremani M., Petruzzi M., Nowak N., Adam M., Grundy P., Shows T., Pelletier J. (1994) Fine structure analysis of the *WT1* gene in sporadic Wilms tumors. *Proc. Nati. Acad. Sci. USA.* **91**, 3554-3558.

Vize, P. D., Seufert, D. W., Carroll, T. J. and Wallingford, J. B. (1997). Model systems for the study of kidney development: use of the pronephros in the analysis of organ induction and patterning. *Dev Biol.* **188**, 189-204.

Vize, P. D., Woolf, A. S. and Bard, J. B. L. (2003). The Kidney. From normal development to congenital disease. 1st ed.: Elsevier Science, Academic Press, London.

Wallingford, J. B., Carroll, T. J. and Vize, P. D. (1998). Precocious expression of the Wilms' tumor gene xWT1 inhibits embryonic kidney development in Xenopus laevis. *Dev Biol* **202**, 103-12.

Weber, H., Holewa, B., Jones, E. A. and Ryffel, G. U. (1996a). Mesoderm and endoderm differentiation in animal cap explants: identification of the HNF4-binding site as an activin A responsive element in the Xenopus HNF1alpha promoter. *Development.* **122**, 1975-84.

Weber, H., Strandmann, E. P., Holewa, B., Bartkowski, S., Zapp, D., Zoidl, C. and Ryffel, G. U. (1996b). Regulation and function of the tissue-specific transcription factor HNF1 alpha (LFB1) during Xenopus development. *Int J Dev Biol.* **40**, 297-304.

Wheeler D. L., Barrett T., Benson D. A., Bryant S. H., Canese K., Church D. M., DiCuccio M., Edgar R., Federhen S., Helmberg W., Kenton D. L., Khovayko O., Lipman D. J., Madden T. L., Maglott D. R., Ostell J., Pontius J. U., Pruitt K. D., Schuler G. D., Schriml L. M., Sequeira E., Sherry S. T., Sirotkin K., Starchenko G., Suzek T. O., Tatusov R., Tatusova T. A., Wagner L., Yaschenko E. (2005) Database resources of the National Center for Biotechnology Information. *Nucleic Acids Res.* **33**, D39-45.

Wild, W., Pogge von Strandmann, E., Nastos, A., Senkel, S., Lingott-Frieg, A., Bulman, M., Bingham, C., Ellard, S., Hattersley, A. T. and Ryffel, G. U. (2000). The mutated human gene encoding hepatocyte nuclear factor 1beta inhibits kidney formation in developing Xenopus embryos. *Proc Natl Acad Sci U S A.* **97**, 4695-700.

Wilhelm D., Englert C. (2002) The Wilms tumor suppressor WT1 regulates early gonad development by activation of Sf1. *Genes Dev.* **16**, 1839-51.

Yamada T., and Takata K. (1961) A technique for testing macromolecular samples in solution for morphogenetic effects on the isolated ectoderm of the amphibian gastrula. *Dev Biol.* **3**, 411-23.

Yang Y., Jeanpierre C., Dressler G. R., Lacoste M., Niaudet P., Gubler M. C. (1999) *WT1* and *PAX-2* podocyte expression in Denys-Drash syndrome and isolated diffuse mesangial sclerosis. *Am J Pathol.* **154**, 181-92.

Yu S., Wang H., Davis A., and Ahmed K. (2001) Consequences of CK2 signaling to the nuclear matrix. *Mol Cell Biochem.* **227**, 67-71.

Appendix

Xenopus and mouse _Pod 1_ show the same over-expression phenotype demonstrated by _WT1 in situ_ indicating the size of the glomus.

Data from Figure 6.5A+B

	Injection					
	Experimental			Control		
	Glomus measurements		Length of	Glomus measurements		Length of
	Injected	Not injected	embryo	Injected	Not injected	embryo
1	0.020	0.020	5.490	0.030	0.030	5.550
2	0.020	0.020	5.255	0.020	0.030	5.600
3	0.020	0.030	5.100	0.030	0.040	5.205
4	0.020	0.030	5.325	0.030	0.020	5.880
5	0.020	0.020	5.200	0.020	0.030	5.120
6	0.010	0.010	5.070	0.030	0.020	5.570
7	0.020	0.030	5.305	0.040	0.020	5.425
8	0.020	0.040	5.245	0.030	0.030	5.275
9	0.020	0.020	5.235	0.030	0.030	5.490
10	0.020	0.030	5.340	0.030	0.030	5.630
11	0.020	0.030	5.150	0.030	0.040	5.065
12	0.010	0.030	4.925	0.030	0.040	5.810
13	0.030	0.030	5.335	0.030	0.030	5.850
14	0.030	0.030	5.180	0.030	0.020	6.095
15	0.020	0.040	4.880	0.020	0.030	5.570
16	0.020	0.020	4.520	0.040	0.040	5.040
17	0.020	0.040	4.635	0.040	0.030	5.335
18	0.000	0.000	4.385	0.040	0.020	5.520
19	0.020	0.020	5.150	0.030	0.050	5.570
20	0.020	0.030	5.155	0.030	0.010	4.700
21	0.040	0.040	5.245	0.030	0.030	5.755
22	0.020	0.030	5.505	0.050	0.040	5.505
23	0.020	0.030	5.135	0.020	0.030	5.805
24	0.010	0.020	5.315	0.020	0.030	5.555
25	0.020	0.020	5.010	0.040	0.020	5.665
26	0.020	0.030	4.340	0.020	0.030	5.420
27	0.020	0.040	5.230	0.040	0.020	5.750
28	0.020	0.020	5.250	0.020	0.040	5.650
29	0.002	0.020	4.585	0.020	0.020	5.625
30	0.030	0.044	5.215	0.020	0.020	5.595
31	0.011	0.020	4.945	0.030	0.020	5.605
32	0.016	0.020	5.080	0.040	0.020	5.510
33	0.031	0.030	5.410	0.040	0.030	5.580
34	0.008	0.030	5.130	0.020	0.030	5.625
35	0.026	0.033	5.265	0.030	0.030	5.375
36	0.020	0.030	5.155	0.020	0.030	5.490
37	0.030	0.030	4.995			
38	0.030	0.030	4.860			
Mean	0.020	0.027	5.093	0.030	0.029	5.523

Experimental injection = 0.6ng *Xenopus Pod 1* mRNA and *GFP* mRNA
Control injection = *GFP* mRNA

Glomus measurements in (3.d.p) mm^2
Length of embryo measured on each side. Mean value of sides for each embryo shown in (3.d.p) mm.

Kolmogorov-Smirnov test for normality: All failed

Wilcoxon matched-pairs signed-ranks test: Experimental $P < 0.0001$
Control $P = 0.4348$

Measurements taken using LUCIA G version 4.81 for NIKON Ltd. Laboratory Imaging, www.lim.cz

Statistics calculated by GraphPad InStat version 3.06 for Windows, GraphPad Software, San Diego California USA, www.graphpad.com

***Xenopus* and mouse *Pod 1* show the same over-expression phenotype demonstrated by *WT1 in situ* indicating the size of the glomus.**

Data from Figure 6.5A+B

	Injection			
	Experimental ratios		Control ratios	
	Injected	Not injected	Injected	Not injected
1	0.004	0.004	0.005	0.005
2	0.004	0.004	0.004	0.005
3	0.004	0.006	0.006	0.008
4	0.004	0.006	0.005	0.003
5	0.004	0.004	0.004	0.006
6	0.002	0.002	0.005	0.004
7	0.004	0.006	0.007	0.004
8	0.004	0.008	0.006	0.006
9	0.004	0.004	0.005	0.005
10	0.004	0.006	0.005	0.005
11	0.004	0.006	0.006	0.008
12	0.002	0.006	0.005	0.007
13	0.006	0.006	0.005	0.005
14	0.006	0.006	0.005	0.003
15	0.004	0.008	0.004	0.005
16	0.004	0.004	0.008	0.008
17	0.004	0.009	0.007	0.006
18	0.000	0.000	0.007	0.004
19	0.004	0.004	0.005	0.009
20	0.004	0.006	0.006	0.002
21	0.008	0.008	0.005	0.005
22	0.004	0.005	0.009	0.007
23	0.004	0.006	0.003	0.005
24	0.002	0.004	0.004	0.005
25	0.004	0.004	0.007	0.004
26	0.005	0.007	0.004	0.006
27	0.004	0.008	0.007	0.003
28	0.004	0.004	0.004	0.007
29	0.000	0.004	0.004	0.004
30	0.006	0.008	0.004	0.004
31	0.002	0.004	0.005	0.004
32	0.003	0.004	0.007	0.004
33	0.006	0.006	0.007	0.005
34	0.002	0.006	0.004	0.005
35	0.005	0.006	0.006	0.006
36	0.004	0.006	0.004	0.005
37	0.006	0.006		
38	0.006	0.006		
Mean	0.004	0.005	0.005	0.005

Experimental injection = 0.6ng *Xenopus Pod 1* mRNA and *GFP* mRNA
Control injection = *GFP* mRNA
Ratio of **Glomus measurement** divided by **Length of Embryo** shown in (3.d.p) mm^2/mm

Kolmogorov-Smirnov test for normality: All failed

Kruskal Wallis test P = 0.0002

Dunn's post test:
(P values)

		Experimental	
		Injected	Not injected
Control	Injected	< 0.01	> 0.05
	Not Injected	< 0.05	> 0.05

Statistics calculated by GraphPad InStat version 3.06 for Windows, GraphPad Software, San Diego California USA, www.graphpad.com

***Xenopus* and mouse *Pod 1* show the same over-expression phenotype demonstrated by *WT1 in situ* indicating the size of the glomus.**

Data from Figure 6.5C+D

	Injection					
	Experimental			Control		
	Glomus measurements		Length of embryo	Glomus measurements		Length of embryo
	Injected	Not injected		Injected	Not injected	
1	0.010	0.020	4.775	0.030	0.030	4.515
2	0.010	0.020	4.565	0.020	0.020	5.035
3	0.008	0.014	4.235	0.020	0.020	4.320
4	0.032	0.027	4.750	0.040	0.030	4.700
5	0.021	0.028	4.980	0.030	0.030	4.785
6	0.024	0.037	5.055	0.020	0.020	4.535
7	0.015	0.018	4.960	0.020	0.020	3.755
8	0.015	0.028	4.145	0.030	0.030	3.810
9	0.016	0.027	4.195	0.020	0.020	3.540
10	0.025	0.032	4.205	0.030	0.040	4.465
11	0.000	0.010	4.440	0.020	0.020	4.450
12	0.020	0.020	4.700	0.020	0.030	4.495
13	0.020	0.040	4.235	0.020	0.030	4.315
14	0.020	0.030	4.780	0.020	0.030	4.415
15	0.020	0.020	4.600	0.020	0.030	4.455
16	0.020	0.020	4.600	0.020	0.030	4.510
17	0.020	0.020	4.750	0.020	0.030	4.540
18	0.020	0.010	4.410	0.020	0.030	4.120
19	0.020	0.020	4.645	0.040	0.030	4.425
20	0.020	0.020	4.545	0.030	0.030	4.485
21	0.010	0.030	4.390	0.020	0.030	4.580
22	0.017	0.020	4.635	0.030	0.020	3.360
23	0.022	0.020	4.665			
24	0.043	0.023	4.500			
25	0.020	0.022	4.750			
26	0.013	0.029	4.530			
27	0.023	0.017	4.045			
28	0.029	0.028	4.405			
29	0.020	0.020	4.385			
30	0.020	0.020	4.685			
31	0.010	0.020	4.285			
Mean	0.019	0.023	4.543	0.025	0.027	4.346

Experimental injection = 0.6ng mouse *Pod 1* mRNA and *GFP* mRNA
Control injection = *GFP* mRNA

Glomus measurements in (3.d.p) mm^2
Length of embryo measured on each side. Mean value of sides for each embryo shown in (3.d.p) mm.

Kolmogorov-Smirnov test for normality: All failed

Wilcoxon matched-pairs signed-ranks test: Experimental P = 0.0083
Control P = 0.1294

Measurements taken using LUCIA G version 4.81 for NIKON Ltd. Laboratory Imaging, www.lim.cz

Statistics calculated by GraphPad InStat version 3.06 for Windows, GraphPad Software, San Diego California USA, www.graphpad.com

***Xenopus* and mouse *Pod 1* show the same over-expression phenotype demonstrated by *WT1 in situ* indicating the size of the glomus.**

Data from Figure 6.5C+D

	Injection			
	Experimental ratios		Control ratios	
	Injected	Not injected	Injected	Not injected
1	0.002	0.004	0.007	0.007
2	0.002	0.004	0.004	0.004
3	0.002	0.003	0.005	0.005
4	0.007	0.006	0.009	0.006
5	0.004	0.006	0.006	0.006
6	0.005	0.007	0.004	0.004
7	0.003	0.004	0.005	0.005
8	0.004	0.007	0.008	0.008
9	0.004	0.006	0.006	0.006
10	0.006	0.008	0.007	0.009
11	0.000	0.002	0.004	0.004
12	0.004	0.004	0.004	0.007
13	0.005	0.009	0.005	0.007
14	0.004	0.006	0.005	0.007
15	0.004	0.004	0.004	0.007
16	0.004	0.004	0.004	0.007
17	0.004	0.004	0.004	0.007
18	0.005	0.002	0.005	0.007
19	0.004	0.004	0.009	0.007
20	0.004	0.004	0.007	0.007
21	0.002	0.007	0.004	0.007
22	0.004	0.004	0.009	0.006
23	0.005	0.004		
24	0.010	0.005		
25	0.004	0.005		
26	0.003	0.006		
27	0.006	0.004		
28	0.007	0.006		
29	0.005	0.005		
30	0.004	0.004		
31	0.002	0.005		
Mean	0.004	0.005	0.006	0.006

Experimental injection = 0.6ng mouse *Pod 1* mRNA and *GFP* mRNA
Control injection = *GFP* mRNA

Ratio of **Glomus measurement** divided by **Length of Embryo** shown in (3.d.p) mm^2/mm

Kolmogorov-Smirnov test for normality: All failed

Kruskal Wallis test $P < 0.0001$

Dunn's post test:
(P values)

		Experimental	
		Injected	Not injected
Control	Injected	< 0.05	> 0.05
	Not Injected	< 0.001	< 0.05*

* Probably due to differences in embryo length

Statistics calculated by GraphPad InStat version 3.06 for Windows, GraphPad Software, San Diego California USA, www.graphpad.com

***Xenopus Pod 1* over-expression glomus phenotype confirmed by *xlmx1b* expression analysis.**

Data from Figure 6.7

	Injection					
	Experimental			Control		
	Glomus measurements		Length of	Glomus measurements		Length of
	Injected	Not injected	embryo	Injected	Not injected	embryo
1	0.010	0.010	3.365	0.020	0.020	4.085
2	0.008	0.010	4.255	0.020	0.030	3.775
3	0.011	0.012	4.750	0.020	0.010	3.820
4	0.010	0.012	4.325	0.020	0.010	4.455
5	0.015	0.010	4.040	0.040	0.020	4.055
6	0.018	0.013	2.605	0.020	0.020	4.400
7	0.015	0.016	3.855	0.010	0.010	2.485
8	0.009	0.010	4.565	0.020	0.020	4.115
9	0.010	0.010	4.490	0.020	0.020	3.650
10	0.008	0.010	4.225	0.010	0.010	4.090
11	0.010	0.012	4.145	0.010	0.020	3.855
12	0.005	0.009	3.840	0.020	0.020	4.365
13	0.016	0.016	4.175	0.020	0.010	3.825
14	0.010	0.012	3.945	0.010	0.020	4.855
15	0.010	0.018	4.345			
16	0.015	0.018	3.950			
17	0.015	0.010	4.270			
18	0.013	0.014	4.415			
19	0.004	0.010	3.005			
20	0.015	0.014	3.155			
21	0.012	0.003	2.925			
22	0.000	0.013	3.525			
23	0.007	0.014	3.280			
24	0.000	0.009	2.785			
25	0.000	0.014	3.535			
26	0.000	0.012	3.030			
27	0.012	0.013	3.480			
28	0.018	0.013	3.930			
Mean	0.010	0.012	3.793	0.019	0.017	3.988

Experimental injection = 0.6ng *Xenopus Pod 1* mRNA and *GFP* mRNA
Control injection = *GFP* mRNA

Glomus measurements in (3.d.p) mm^2
Length of embryo measured on each side. Mean value of sides for each embryo shown in (3.d.p) mm.

Kolmogorov-Smirnov test for normality: All failed

Wilcoxon matched-pairs signed-ranks test: Experimental P = 0.0393
Control P = 0.5781

Measurements taken using LUCIA G version 4.81 for NIKON Ltd. Laboratory Imaging, www.lim.cz

Statistics calculated by GraphPad InStat version 3.06 for Windows, GraphPad Software, San Diego California USA, www.graphpad.com

***Xenopus Pod 1* over-expression glomus phenotype confirmed by *xlmx1b* expression analysis.**

Data from Figure 6.7

	Injection			
	Experimental ratios		Control ratios	
	Injected	Not injected	Injected	Not injected
1	0.003	0.003	0.005	0.005
2	0.002	0.002	0.005	0.008
3	0.002	0.003	0.005	0.003
4	0.002	0.003	0.004	0.002
5	0.004	0.002	0.010	0.005
6	0.007	0.005	0.005	0.005
7	0.004	0.004	0.004	0.004
8	0.002	0.002	0.005	0.005
9	0.002	0.002	0.005	0.005
10	0.002	0.002	0.002	0.002
11	0.002	0.003	0.003	0.005
12	0.001	0.002	0.005	0.005
13	0.004	0.004	0.005	0.003
14	0.003	0.003	0.002	0.004
15	0.002	0.004		
16	0.004	0.005		
17	0.004	0.002		
18	0.003	0.003		
19	0.001	0.003		
20	0.005	0.004		
21	0.004	0.001		
22	0.000	0.004		
23	0.002	0.004		
24	0.000	0.003		
25	0.000	0.004		
26	0.000	0.004		
27	0.003	0.004		
28	0.005	0.003		
Mean	0.003	0.003	0.005	0.004

Experimental injection = 0.6ng *Xenopus Pod 1* mRNA and *GFP* mRNA
Control injection = *GFP* mRNA

Ratio of **Glomus measurement** divided by **Length of Embryo** shown in (3.d.p) mm^2/mm

Kolmogorov-Smirnov test for normality: All failed

Kruskal Wallis test P = 0.0002

Dunn's post test:
(P values)

		Experimental	
		Injected	Not injected
Control	Injected	< 0.01	< 0.05*
	Not Injected	< 0.01	> 0.05

* Probably due to differences in embryo length

Statistics calculated by GraphPad InStat version 3.06 for Windows, GraphPad Software, San Diego California USA, www.graphpad.com

Histochemical analysis of the *Xenopus Pod 1* over expression phenotype showed no observable effect on either pronephric tubule or duct.

PNI data from Figure 6.8

	Injection			
	Experimental		Control	
	Injected	Not injected	Injected	Not injected
1	2	3	4	4
2	5	4	5	4
3	4	4	5	5
4	4	4	4	5
5	4	5	4	4
6	3	4	3	4
7	3	4	4	4
8	4	5	5	4
9	4	5	3	5
10	4	4	5	5
11	5	4	4	5
12	5	4	5	4
13	2	4	3	4
14	4	4	5	5
15	4	4	5	4
16	3	4	5	4
17	4	5	5	5
18	3	3	4	5
19	4	4	3	3
20	2	3	4	5
21	5	4	5	5
22	5	5		
23	1	2		
Median	4	4	4	4

Experimental injection = 0.6ng *Xenopus Pod 1* mRNA and *GFP* mRNA
Control injection = *GFP* mRNA

Kolmogorov-Smirnov test for normality: Experimental Failed
Control Failed

Wilcoxon paired test: Experimental P = 0.0946
Control P = 0.5186

Statistics calculated by GraphPad InStat version 3.06 for Windows, GraphPad Software, San Diego California USA, www.graphpad.com

Histochemical analysis of the *Xenopus Pod 1* over expression phenotype showed no observable effect on either pronephric tubule or duct.

Duct morphology observations from Figure 6.8

	Injection			
	Experimental		Control	
	Injected	Not injected	Injected	Not injected
Altered	6	2	3	4
Normal	17	21	18	17

Experimental injection = 0.6ng *Xenopus Pod 1* mRNA and *GFP* mRNA
Control injection = *GFP* mRNA

Fisher's exact test:

Experimental	P = 0.2427
Control	P = 1

***Xenopus Pod 1* over-expression analysis with *lim 1* does not indicate a pronephric anlagen phenotype.**

Data from Figure 6.9

	Injection					
	Experimental			Control		
	Glomus measurements		Length of	Glomus measurements		Length of
	Injected	Not injected	embryo	Injected	Not injected	embryo
1	0.060	0.050	4.045	0.030	0.050	3.635
2	0.010	0.040	3.775	0.050	0.080	4.300
3	0.020	0.040	3.135	0.050	0.130	4.160
4	0.030	0.010	3.450	0.070	0.080	3.340
5	0.060	0.040	3.180	0.060	0.030	3.170
6	0.060	0.050	3.745	0.060	0.090	3.895
7	0.040	0.050	3.265	0.080	0.110	3.870
8	0.040	0.060	3.595	0.070	0.050	4.015
9	0.040	0.050	3.720	0.060	0.070	2.545
10	0.040	0.030	3.020	0.070	0.070	3.425
11	0.040	0.020	3.930	0.050	0.060	3.565
12	0.070	0.030	3.330	0.060	0.040	3.705
13	0.030	0.030	4.140	0.100	0.060	2.650
14	0.040	0.040	3.500	0.050	0.070	3.875
15	0.030	0.030	3.760	0.090	0.090	4.190
16	0.040	0.060	3.700	0.050	0.050	2.870
17	0.050	0.070	4.095	0.080	0.040	3.395
18	0.030	0.050	2.765	0.050	0.070	3.500
19	0.070	0.080	3.560			
20	0.040	0.050	3.905			
21	0.030	0.030	3.495			
22	0.050	0.060	3.095			
23	0.040	0.070	2.905			
24	0.070	0.040	3.680			
25	0.040	0.030	3.245			
26	0.030	0.020	3.340			
27	0.060	0.030	3.695			
28	0.060	0.060	3.780			
Mean	0.044	0.044	3.530	0.063	0.069	3.561

Experimental injection = 0.6ng *Xenopus Pod 1* mRNA and *GFP* mRNA
Control injection = *GFP* mRNA

Pronephric anlagen measurements in (3.d.p) mm ^{2}
Length of embryo measured on each side. Mean value of sides for each embryo shown in (3.d.p) mm.

Kolmogorov-Smirnov test for normality:	Experimental injected	Failed
	Experimental not injected	Passed
	Control injected	Passed
	Control not injected	Passed

Wilcoxon matched-pairs signed-ranks test:	Experimental	P = 0.7998
Two tailed paired t-test:	Control	P = 0.3922

Measurements taken using LUCIA G version 4.81 for NIKON Ltd. Laboratory Imaging, www.lim.cz

Statistics calculated by GraphPad InStat version 3.06 for Windows, GraphPad Software, San Diego California USA, www.graphpad.com

***Xenopus Pod 1* over expression does not have an effect on the heart, as indicated with *Cardiac troponin I* expression.**

Data from Figure 6.11

	Injection					
	Experimental			Control		
	Heart measurements		Length of embryo	Heart measurements		Length of embryo
	Left	Right		Left	Right	
1	0.030	0.020	4.170	0.030	0.030	4.190
2	0.030	0.040	3.790	0.040	0.020	4.060
3	0.030	0.040	3.825	0.020	0.020	4.005
4	0.030	0.050	3.785	0.020	0.010	4.130
5	0.040	0.010	4.125	0.040	0.020	3.920
6	0.010	0.020	4.340	0.030	0.030	4.090
7	0.020	0.010	3.965	0.030	0.020	3.890
8	0.020	0.020	4.470	0.050	0.040	3.875
9	0.020	0.030	4.205	0.030	0.020	4.200
10	0.020	0.030	3.845	0.030	0.030	4.310
11	0.020	0.020	4.330	0.040	0.020	3.970
12	0.020	0.030	4.240	0.030	0.030	4.245
13	0.020	0.020	4.200	0.100	0.007	3.480
14	0.020	0.020	4.430	0.020	0.015	3.965
15	0.020	0.030	4.275	0.050	0.027	3.580
16	0.030	0.030	3.995	0.040	0.033	4.010
17	0.030	0.020	4.310	0.030	0.035	4.140
18	0.020	0.030	4.025	0.020	0.037	3.435
19	0.020	0.020	4.115	0.030	0.000	2.835
20	0.010	0.020	3.605	0.020	0.030	4.275
21	0.030	0.030	3.830	0.000	0.000	3.610
22	0.030	0.020	3.780	0.060	0.030	3.070
23	0.030	0.020	3.445	0.050	0.050	3.645
24	0.030	0.010	4.070	0.030	0.030	3.260
25	0.000	0.000	3.435	0.040	0.000	2.910
26	0.030	0.020	4.230	0.000	0.000	3.385
27	0.020	0.020	2.200	0.060	0.038	3.105
28	0.010	0.040	2.320	0.050	0.017	3.730
29	0.030	0.030	3.385	0.030	0.037	4.235
30	0.030	0.030	3.760	0.009	0.034	3.330
31	0.030	0.060	2.450			
32	0.030	0.008	3.135			
33	0.000	0.000	2.705			
34	0.010	0.024	2.520			
35	0.080	0.068	1.470			
Mean	0.024	0.025	3.679	0.034	0.024	3.763

Experimental injection = 0.6ng *Xenopus Pod 1* mRNA and *GFP* mRNA
Control injection = *GFP* mRNA

Heart measurements in (3.d.p) mm^2
Length of embryo measured on each side. Mean value of sides for each embryo shown in (3.d.p) mm.

Measurements taken using LUCIA G version 4.81 for NIKON Ltd. Laboratory Imaging, www.lim.cz

***Xenopus Pod 1* over expression does not have an effect on the heart, as indicated with *Cardiac troponin I* expression.**

Data from Figure 6.11

	Injection			
	Experimental		Control	
	Ratio		Ratio	
	Left	Right	Left	Right
1	0.007	0.005	0.007	0.007
2	0.008	0.011	0.010	0.005
3	0.008	0.010	0.005	0.005
4	0.008	0.013	0.005	0.002
5	0.010	0.002	0.010	0.005
6	0.002	0.005	0.007	0.007
7	0.005	0.003	0.008	0.005
8	0.004	0.004	0.013	0.010
9	0.005	0.007	0.007	0.005
10	0.005	0.008	0.007	0.007
11	0.005	0.005	0.010	0.005
12	0.005	0.007	0.007	0.007
13	0.005	0.005	0.029	0.002
14	0.005	0.005	0.005	0.004
15	0.005	0.007	0.014	0.008
16	0.008	0.008	0.010	0.008
17	0.007	0.005	0.007	0.008
18	0.005	0.007	0.006	0.011
19	0.005	0.005	0.011	0.000
20	0.003	0.006	0.005	0.007
21	0.008	0.008	0.000	0.000
22	0.008	0.005	0.020	0.010
23	0.009	0.006	0.014	0.014
24	0.007	0.002	0.009	0.009
25	0.000	0.000	0.014	0.000
26	0.007	0.005	0.000	0.000
27	0.009	0.009	0.019	0.012
28	0.004	0.017	0.013	0.005
29	0.009	0.009	0.007	0.009
30	0.008	0.008	0.003	0.010
31	0.012	0.024		
32	0.010	0.003		
33	0.000	0.000		
34	0.004	0.010		
35	0.054	0.046		
Mean	0.007	0.008	0.009	0.006

Experimental injection = 0.6ng *Xenopus Pod 1* mRNA and *GFP* mRNA
Control injection = *GFP* mRNA
Ratio of **Heart measurement** divided by **Length of Embryo** shown in (3.d.p) mm^2/mm

Kolmogorov-Smirnov test for normality: Experimental Left = Fail Right = Fail
Control Left = Fail Right = Pass

Kruskal Wallis test P = 0.0965
Dunn's post test not performed

Statistics calculated by GraphPad InStat version 3.06 for Windows, GraphPad Software, San Diego California USA, www.graphpad.com

***Xenopus Pod 1* expression is required for glomus development as indicated by *WT1* expression**

Data from Figure 7.3

	Injection					
	40ng PMO		40ng PMO + RESCUE		40ng CMO	
	Injected	Not injected	Injected	Not injected	Injected	Not injected
No glomus present	13	0	7	1	1	0
Glomus present	9	22	30	36	31	32

Columns
40ng PMO:
40ng *Pod 1* morpholino + *GFP* mRNA

40ng PMO + RESCUE:
40ng *Pod 1* morpholino + 0.6ng *mPod 1* mRNA + *GFP* mRNA

40ng CMO:
40ng Control morpholino + *GFP* mRNA

Fisher's exact test

40ng PMO: P < 0.0001

40ng PMO + RESCUE: P = 0.0557

40ng CMO: P = 1

40ng PMO injected vs. 40ng PMO + RESCUE injected: P = 0.0037

40ng PMO injected vs. 40ng CMO injected: P < 0.0001

40ng PMO + RESCUE injected vs. 40ng CMO injected: P = 0.0602

Statistics calculated by GraphPad InStat version 3.06 for Windows, GraphPad Software, San Diego California USA, www.graphpad.com

Confirmation that *Xenopus Pod 1* expression is required for glomus development, indicated by *xlmx1b* expression

Data from Figure 7.4

	Injection					
	40ng PMO		40ng PMO + RESCUE		40ng CMO	
	Injected	Not injected	Injected	Not injected	Injected	Not injected
No glomus present	11	0	5	1	1	0
Glomus present	11	22	15	19	22	23

Columns
40ng PMO:
40ng *Pod 1* morpholino + *GFP* mRNA

40ng PMO + RESCUE:
40ng *Pod 1* morpholino + 0.6ng *mPod 1* mRNA + *GFP* mRNA

40ng CMO:
40ng Control morpholino + *GFP* mRNA

Fisher's exact test

40ng PMO: P = 0.0002

40ng PMO + RESCUE: P = 0.1818

40ng CMO: P = 1

40ng PMO injected vs. 40ng PMO + RESCUE injected: P = 0.0372

40ng PMO injected vs. 40ng CMO injected: P = 0.0006

40ng PMO + RESCUE injected vs. 40ng CMO injected: P = 0.0814

Statistics calculated by GraphPad InStat version 3.06 for Windows, GraphPad Software, San Diego California USA, www.graphpad.com

Pod 1 knock-down disrupts tubule morphology

PNI data from Figure 7.6

	Injection					
	40ng PMO		40ng PMO + RESCUE		40ng CMO	
	Injected	Not injected	Injected	Not injected	Injected	Not injected
1	2	4	4	5	5	5
2	1	5	4	4	5	5
3	1	4	5	5	3	5
4	1	4	2	3	4	4
5	4	5	4	4	5	5
6	5	5	3	5	4	5
7	3	4	5	4	3	5
8	4	2	1	4	3	4
9	2	5	5	5	4	4
10	1	3	4	4	3	3
11	1	3	4	4	5	5
12	2	4	5	4	3	5
13	4	5	3	4	5	5
14	1	4	2	3	4	4
15	2	5	4	5	5	5
16	2	5	4	5	5	5
17	1	4	5	4	5	5
18			4	4	5	5
19			4	3	4	4
20			4	4	4	3
21			3	4	5	5
22			2	3	3	4
23			3	4	3	2
24					3	3
Median	2	4	4	4	4	5

Columns

40ng PMO: 40ng *Pod 1* morpholino + *GFP* mRNA

40ng PMO + RESCUE: 40ng *Pod 1*

40ng CMO: 40ng Control morpholino + *GFP* mRNA

Kolmogorov-Smirnov test for normality:

	Injected	Not injected
40ng PMO	Passed	Failed
40ng PMO + RESCUE	Failed	Failed
40ng CMO	Failed	Failed

Wilcoxon paired test:

40ng PMO	P = 0.0004
40ng PMO + RESCUE	P = 0.0730
40ng CMO	P = 0.0897

Statistics calculated by GraphPad InStat version 3.06 for Windows, GraphPad Software, San Diego California USA, www.graphpad.com

***Pod 1* knock-down does not have an effect on early *Xlim 1* expression**

Data from Figure 7.7

	Injection								
	40ng PMO			40ng PMO + RESCUE			40ng CMO		
	Glomus measurements		Length of	Glomus measurements		Length of	Glomus measurements		Length of
	Injected	Not injected	embryo	Injected	Not injected	embryo	Injected	Not injected	embryo
1	0.030	0.040	2.360	0.030	0.010	2.440	0.070	0.040	2.290
2	0.030	0.020	2.020	0.040	0.032	2.480	0.010	0.040	2.075
3	0.040	0.020	2.315	0.020	0.019	2.060	0.020	0.020	2.530
4	0.030	0.040	2.225	0.050	0.050	2.535	0.050	0.070	2.670
5	0.040	0.050	2.265	0.020	0.040	2.540	0.040	0.030	2.650
6	0.030	0.030	2.210	0.040	0.010	2.570	0.040	0.070	2.420
7	0.030	0.030	2.385	0.030	0.040	2.425	0.040	0.050	2.500
8	0.040	0.020	2.190	0.030	0.020	2.525	0.030	0.030	1.985
9	0.030	0.040	2.245	0.010	0.020	2.510	0.040	0.040	2.530
10	0.030	0.050	2.130	0.010	0.040	2.330	0.060	0.060	2.510
11	0.050	0.040	2.075	0.030	0.040	2.755	0.070	0.060	2.565
12	0.050	0.040	2.325	0.020	0.020	2.330	0.060	0.050	2.555
13	0.060	0.030	1.860	0.020	0.006	2.370	0.020	0.040	2.060
14	0.060	0.040	2.090	0.040	0.020	2.505	0.050	0.010	1.975
15	0.020	0.020	2.255	0.020	0.030	2.605	0.050	0.040	2.570
16	0.060	0.040	1.990	0.040	0.030	2.485	0.030	0.040	2.725
17	0.050	0.040	2.285	0.040	0.060	2.585	0.050	0.040	2.035
18	0.040	0.060	2.265	0.040	0.020	2.290	0.050	0.070	2.615
19	0.040	0.020	2.415	0.030	0.020	2.425	0.040	0.040	2.685
20	0.040	0.020	2.300	0.020	0.040	2.580	0.050	0.040	2.610
21	0.020	0.030	2.175	0.030	0.030	2.425	0.040	0.030	2.745
22	0.040	0.050	2.615	0.030	0.020	2.525	0.040	0.050	2.645
23	0.030	0.020	2.145	0.040	0.040	2.530	0.050	0.040	2.460
24	0.040	0.020	2.285	0.050	0.030	2.285	0.030	0.030	2.700
25	0.030	0.030	2.065	0.030	0.050	2.380	0.050	0.040	2.555
26	0.040	0.030	2.270	0.030	0.030	2.815	0.050	0.070	2.820
27	0.020	0.040	2.680				0.050	0.040	2.220
28	0.030	0.040	2.620				0.030	0.060	2.630
29	0.040	0.030	2.410						
30	0.050	0.030	2.570						
31	0.038	0.034	2.220						
Mean	0.038	0.034	2.266	0.030	0.030	2.473	0.043	0.044	2.476

Columns

40ng PMO: 40ng *Pod 1* morpholino + *GFP* mRNA

40ng PMO + RESCUE: 40ng *Pod 1*

40ng CMO: 40ng Control morpholino + *GFP* mRNA

Glomus measurements in (3.d.p) mm²

Length of embryo measured on each side. Mean value of sides for each embryo shown in (3.d.p) mm.

Kolmogorov-Smirnov test for normality: All failed

Wilcoxon matched-pairs signed-ranks test:

40ng PMO	P = 0.1042
40ng PMO + RESCUE	P = 0.8117
40ng CMO	P = 0.6556

Measurements taken using LUCIA G version 4.81 for NIKON Ltd. Laboratory Imaging, www.lim.cz
Statistics calculated by GraphPad InStat version 3.06 for Windows, GraphPad Software, San Diego California USA, www.graphpad.com

***Pod 1* expression is required for *Pax 8* expression.**

Data from Figure 7.8

	Injection					
	40ng PMO		40ng PMO + RESCUE		40ng CMO	
	Injected	Not injected	Injected	Not injected	Injected	Not injected
Pax 8 expression absent	12	0	5	1	1	0
Pax 8 expression present	13	25	16	20	19	20

Columns
40ng PMO:
40ng *Pod 1* morpholino + *GFP* mRNA

40ng PMO + RESCUE:
40ng *Pod 1* morpholino + 0.6ng *mPod 1* mRNA + *GFP* mRNA

40ng CMO:
40ng Control morpholino + *GFP* mRNA

Fisher's exact test

40ng PMO: P < 0.0001

40ng PMO + RESCUE: P = 0.1836

40ng CMO: P = 1

40ng PMO injected vs. 40ng PMO + RESCUE injected P = 0.1283

40ng PMO injected vs. 40ng CMO injected P = 0.0022

40ng PMO + RESCUE injected vs. 40ng CMO injected P = 0.1836

Statistics calculated by GraphPad InStat version 3.06 for Windows, GraphPad Software, San Diego California USA, www.graphpad.com

***Darmin r* over-expression disrupts tubule formation.**

PNI data from Figure 8.6

	Injection			
	Experimental		Control	
	Injected	Not injected	Injected	Not injected
1	4	5	5	5
2	5	4	5	4
3	3	4	5	4
4	2	3	5	5
5	1	5	5	5
6	2	4	4	5
7	1	4	4	5
8	3	4	4	5
9	3	5	5	4
10	4	5	5	4
11	1	3	5	5
12	5	5	5	5
13	1	3	5	5
14	2	4	4	4
15	3	5	5	5
16	2	3	5	5
17	2	4	4	5
18	4	4	5	5
19	2	3	4	5
20	1	3	5	4
21			4	4
22			5	5
23			5	4
24			5	5
25			5	4
26			4	5
27			5	5
28			5	4
29			4	4
30			4	5
31			4	5
32			5	4
33			4	5
34			3	5
35			3	5
36			4	5
37			4	4
38			4	5
39			4	4
40			5	4
41			5	4
42			5	5
43			4	5
Median	2	4	5	5

Experimental injection = 0.5ng *Darmin r* mRNA and *GFP* mRNA
Control injection = *GFP* mRNA

Kolmogorov-Smirnov test for normality: All failed

Wilcoxon paired test: Experimental $P < 0.0001$
Control $P = 0.4261$

Statistics calculated by GraphPad InStat version 3.06 for Windows, GraphPad Software, San Diego California USA, www.graphpad.com

***Darmin r* over-expression does not have an effect on the glomus.**

Data from Figure 8.7

	Injection					
	Experimental			Control		
	Glomus measurements		Length of	Glomus measurements		Length of
	Injected	Not injected	embryo	Injected	Not injected	embryo
1	0.040	0.020	4.300	0.030	0.040	4.440
2	0.020	0.030	4.345	0.030	0.050	4.525
3	0.020	0.020	4.180	0.020	0.020	4.455
4	0.020	0.030	4.225	0.020	0.020	4.545
5	0.030	0.010	3.430	0.020	0.030	4.545
6	0.020	0.030	4.325	0.020	0.030	4.485
7	0.030	0.020	3.860	0.020	0.020	4.335
8	0.020	0.020	4.425	0.030	0.020	4.615
9	0.020	0.020	4.105	0.030	0.020	4.490
10	0.020	0.030	4.235	0.030	0.030	4.495
11	0.020	0.020	4.695	0.010	0.030	4.405
12	0.020	0.020	4.475	0.030	0.030	4.250
13	0.020	0.020	4.380	0.020	0.030	4.400
14	0.020	0.020	4.215	0.030	0.030	4.400
15	0.020	0.020	4.300	0.030	0.030	4.535
16	0.010	0.030	4.365	0.030	0.020	4.640
17	0.030	0.020	4.300	0.020	0.020	4.375
18	0.020	0.020	4.270	0.040	0.020	4.330
19	0.020	0.020	4.205	0.020	0.020	4.240
20	0.020	0.020	4.285	0.020	0.010	4.330
21	0.020	0.020	4.250	0.020	0.020	4.560
22	0.030	0.020	4.195	0.020	0.020	4.545
23	0.020	0.020	4.090	0.030	0.030	4.495
24	0.020	0.020	4.100	0.030	0.020	4.155
25	0.003	0.010	4.405	0.010	0.020	4.365
26	0.025	0.010	4.320	0.020	0.030	4.360
27	0.008	0.030	4.300	0.010	0.020	4.290
28	0.008	0.020	4.000	0.010	0.020	4.505
29	0.009	0.030	4.750	0.030	0.020	4.505
30	0.030	0.030	4.180	0.030	0.020	4.355
31	0.018	0.020	4.240	0.030	0.040	4.420
32	0.020	0.020	4.160	0.040	0.030	4.395
33	0.024	0.020	4.215	0.020	0.020	4.555
34				0.030	0.030	4.395
Mean	0.020	0.022	4.246	0.024	0.025	4.433

Experimental injection = 0.5ng *Darmin r* mRNA and *GFP* mRNA
Control injection = *GFP* mRNA

Glomus measurements in (3.d.p) mm^2
Length of embryo measured on each side. Mean value of sides for each embryo shown in (3.d.p) mm.

Kolmogorov-Smirnov test for normality: All Failed

Wilcoxon matched-pairs signed-ranks test: Experimental P = 0.5477
Control P = 0.5958

Measurements taken using LUCIA G version 4.81 for NIKON Ltd. Laboratory Imaging, www.lim.cz

Statistics calculated by GraphPad InStat version 3.06 for Windows, GraphPad Software, San Diego California USA, www.graphpad.com

***Darmin r* over-expression reduces the size of the pronephric anlagen.**

Data from Figure 8.8

	Injection					
	Experimental			Control		
	Glomus measurements		Length of	Glomus measurements		Length of
	Injected	Not injected	embryo	Injected	Not injected	embryo
1	0.030	0.030	2.290	0.040	0.040	2.505
2	0.040	0.030	2.075	0.049	0.040	2.125
3	0.020	0.030	2.530	0.010	0.030	2.440
4	0.020	0.040	2.670	0.032	0.040	2.480
5	0.040	0.030	2.650	0.039	0.020	2.060
6	0.050	0.040	2.420	0.050	0.050	2.535
7	0.030	0.030	2.500	0.040	0.050	2.540
8	0.030	0.030	1.985	0.030	0.040	2.570
9	0.020	0.040	2.530	0.040	0.030	2.425
10	0.040	0.030	2.510	0.020	0.030	2.525
11	0.050	0.030	2.565	0.020	0.050	2.510
12	0.040	0.050	2.555	0.040	0.040	2.330
13	0.040	0.050	2.060	0.040	0.030	2.755
14	0.030	0.060	1.975	0.020	0.020	2.330
15	0.040	0.060	2.570	0.026	0.020	2.370
16	0.020	0.020	2.725	0.020	0.040	2.505
17	0.040	0.060	2.035	0.030	0.020	2.605
18	0.040	0.050	2.615	0.030	0.040	2.485
19	0.020	0.040	2.685	0.060	0.040	2.585
20	0.020	0.040	2.610	0.020	0.040	2.290
21	0.020	0.040	2.745	0.020	0.030	2.425
22	0.030	0.020	2.645	0.040	0.020	2.580
23	0.050	0.040	2.460	0.030	0.030	2.425
24	0.020	0.030	2.700	0.020	0.030	2.525
25	0.020	0.040	2.555	0.040	0.040	2.530
26	0.030	0.030	2.820	0.030	0.050	2.285
27	0.030	0.040	2.220	0.050	0.030	2.380
28	0.040	0.020	2.630	0.030	0.030	2.815
29	0.040	0.030	2.365	0.045	0.040	2.265
30	0.030	0.040	2.720	0.025	0.050	2.275
31	0.030	0.050	2.525	0.030	0.040	2.350
32	0.020	0.050	2.390	0.045	0.050	2.295
33				0.040	0.040	2.495
34				0.020	0.020	2.290
35				0.030	0.020	2.470
36				0.040	0.040	2.450
Mean	0.032	0.038	2.479	0.033	0.035	2.440

Experimental injection = 0.5ng *Darmin r* mRNA and *GFP* mRNA
Control injection = *GFP* mRNA

Pronephric anlagen measurements in (3.d.p) mm²
Length of embryo measured on each side. Mean value of sides for each embryo shown in (3.d.p) mm.

Kolmogorov-Smirnov test for normality: All failed

Wilcoxon matched-pairs signed-ranks test: Experimental P = 0.0199
Control P = 0.3319

Measurements taken using LUCIA G version 4.81 for NIKON Ltd. Laboratory Imaging, www.lim.cz

Statistics calculated by GraphPad InStat version 3.06 for Windows, GraphPad Software, San Diego California USA, www.graphpad.com

***Darmin r* over-expression reduces the size of the pronephric anlagen.**

Data from Figure 8.8

	Injection			
	Experimental ratios		Control ratios	
	Injected	Not injected	Injected	Not injected
1	0.013	0.013	0.016	0.016
2	0.019	0.014	0.023	0.019
3	0.008	0.012	0.004	0.012
4	0.007	0.015	0.013	0.016
5	0.015	0.011	0.019	0.010
6	0.021	0.017	0.020	0.020
7	0.012	0.012	0.016	0.020
8	0.015	0.015	0.012	0.016
9	0.008	0.016	0.016	0.012
10	0.016	0.012	0.008	0.012
11	0.019	0.012	0.008	0.020
12	0.016	0.020	0.017	0.017
13	0.019	0.024	0.015	0.011
14	0.015	0.030	0.009	0.009
15	0.016	0.023	0.011	0.008
16	0.007	0.007	0.008	0.016
17	0.020	0.029	0.012	0.008
18	0.015	0.019	0.012	0.016
19	0.007	0.015	0.023	0.015
20	0.008	0.015	0.009	0.017
21	0.007	0.015	0.008	0.012
22	0.011	0.008	0.016	0.008
23	0.020	0.016	0.012	0.012
24	0.007	0.011	0.008	0.012
25	0.008	0.016	0.016	0.016
26	0.011	0.011	0.013	0.022
27	0.014	0.018	0.021	0.013
28	0.015	0.008	0.011	0.011
29	0.017	0.013	0.020	0.018
30	0.011	0.015	0.011	0.022
31	0.012	0.020	0.013	0.017
32	0.008	0.021	0.020	0.022
33			0.016	0.016
34			0.009	0.009
35			0.012	0.008
36			0.016	0.016
Mean	0.013	0.016	0.014	0.015

Experimental injection = 0.5ng *Darmin r* mRNA and *GFP* mRNA
Control injection = *GFP* mRNA

Ratio of **Pronephric anlagen measurement** divided by **Length of Embryo** shown in (3.d.p) mm²/mm

Kolmogorov-Smirnov test for normality:

Experimental injected = Failed — Control injected = Passed
Experimental not injected = Failed — Control not injected = Failed

Kruskal Wallis test P = 0.2307
Dunn's post test not performed

Statistics calculated by GraphPad InStat version 3.06 for Windows, GraphPad Software, San Diego California USA, www.graphpad.com

Duct morphology observations from *Darmin r* over-expression

	Injection			
	Experimental		Control	
	Injected	Not injected	Injected	Not injected
Altered	5	8	4	3
Normal	29	26	27	28

Experimental injection = 0.5ng *Darmin r* mRNA and *GFP* mRNA
Control injection = *GFP* mRNA

Fisher's exact test:

Experimental	P = 0.5387
Control	P = 1

Nephrostome morphology observations from *Darmin r* over-expression

	Nephrostomes Disrupted	Nephrostomes Matching	Number of embryos
Darmin r inj	14	30	44
GFP inj	5	48	53

Experimental injection = 0.5ng *Darmin r* mRNA and *GFP* mRNA
Control injection = *GFP* mRNA

Fisher's exact test: P = 0.0091

Plasmid maps

pCMV SPORT6 *Xenopus Pod 1*

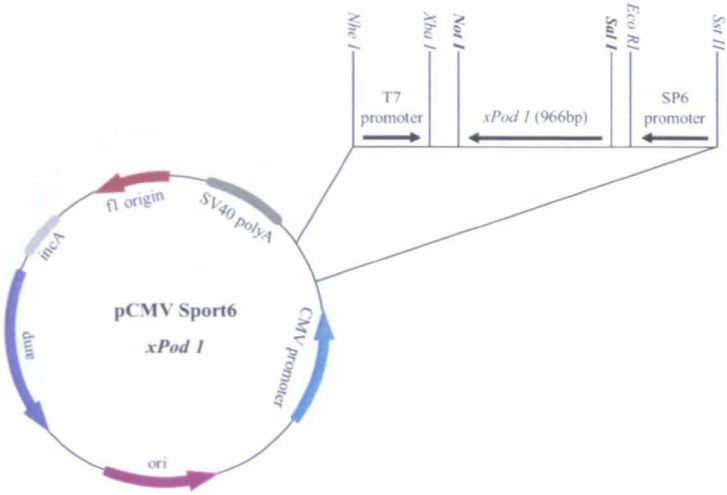

pCS2+ *Xenopus Pod 1*

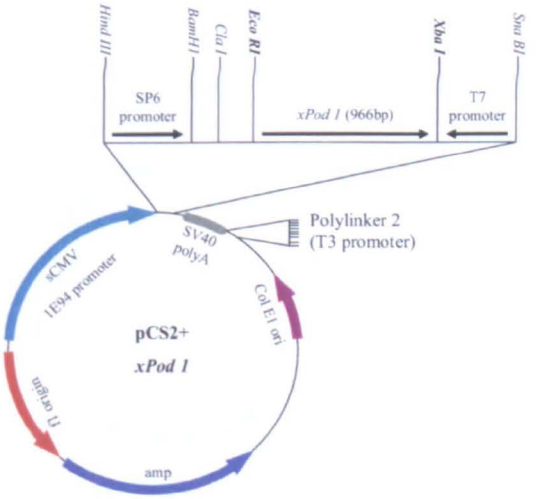

pCS3+ MT *Xenopus Pod 1*

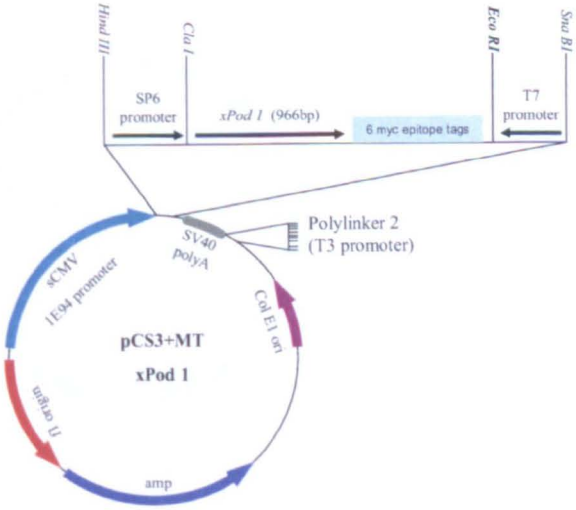

pCMV SPORT6 Mouse *Pod 1*

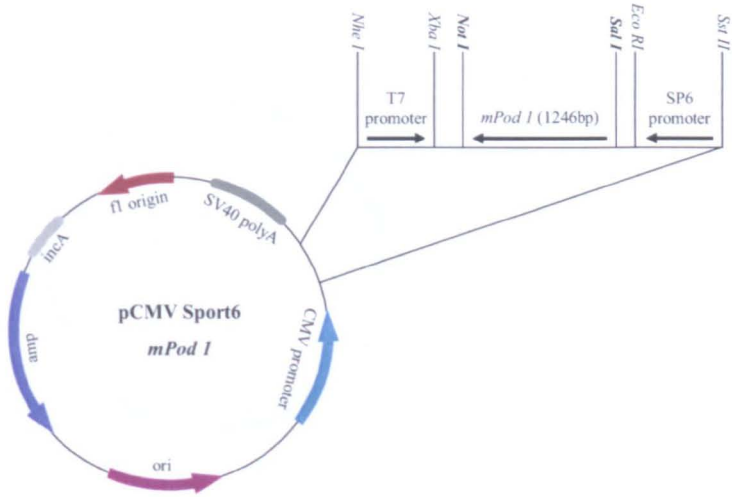

pCS2+ Mouse *Pod 1*

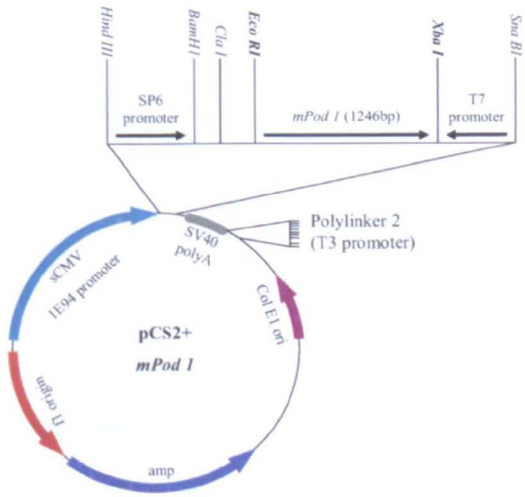

pBluescript SK (+) RA + A/RA clones except 18B1

Clones
- 3B5 (547bp)
- 6C5 (559bp)
- 10A7 (808bp)
- 15B7 (607bp)
- 18C2 (575bp)

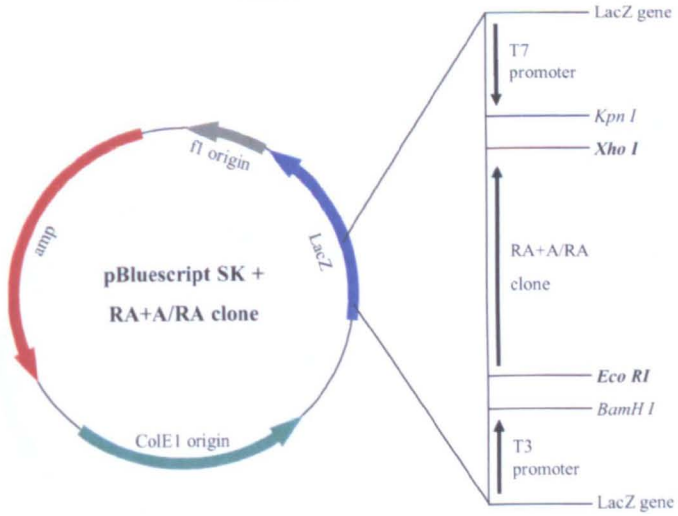

pBluescript SK (+) RA + A/RA
clone 18B1 (800bp)

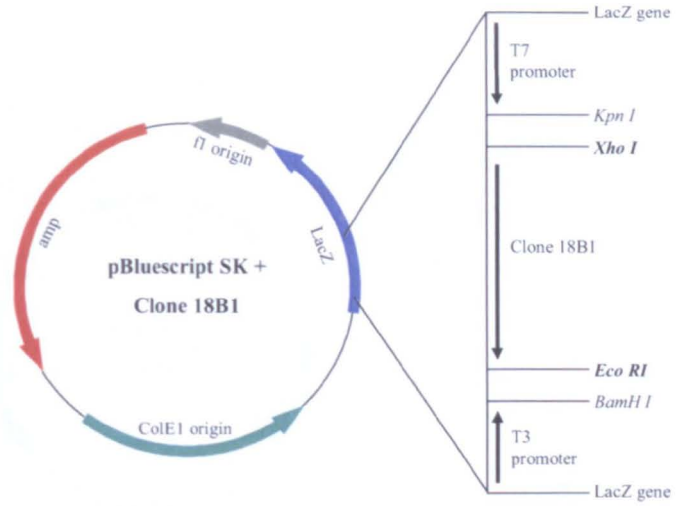

pBluescript SK (+) RA + A/A
clones
2b5 (851bp)
4c1 (1003bp)
5f6 (786bp)
6a4 (1044bp)
12a1 (828bp)
12b3 (710bp)
15b2 (864bp)
15c7 (912bp)
18c1 (771bp)
20c1 (900bp)
31b4 (635bp)
41b2 (1004bp)
46c9 (1385bp)

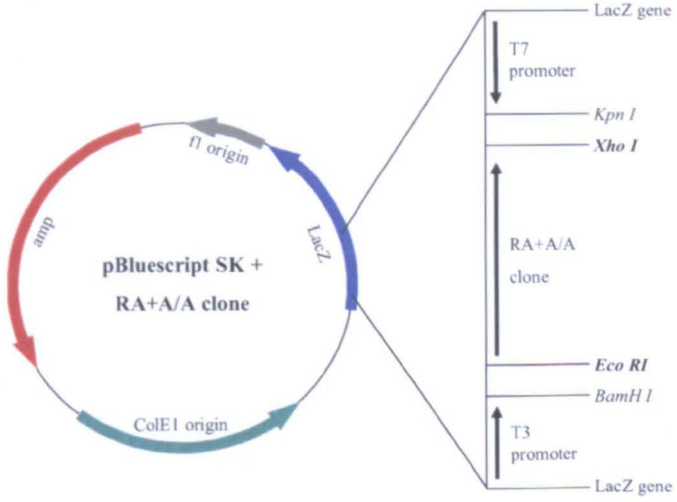

pCMV SPORT6 xl.5110

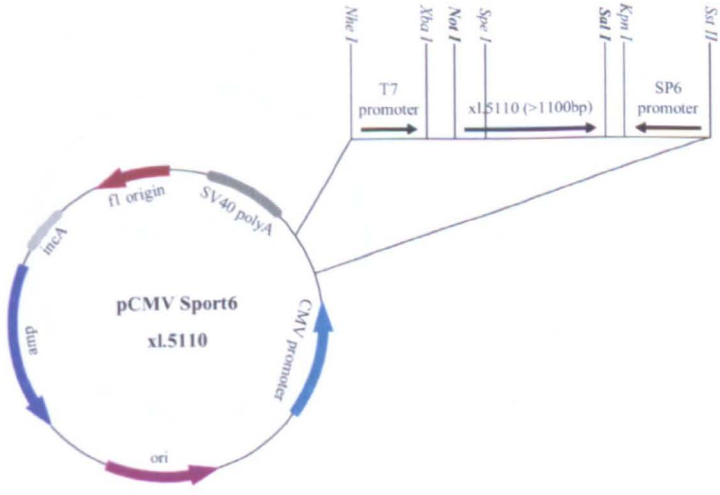

pCMV SPORT6 xl.5983

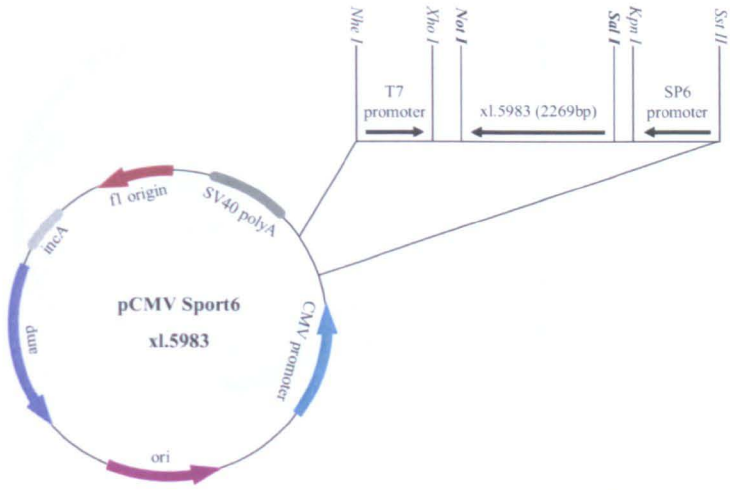

pBluescript SK (+) xl.12848

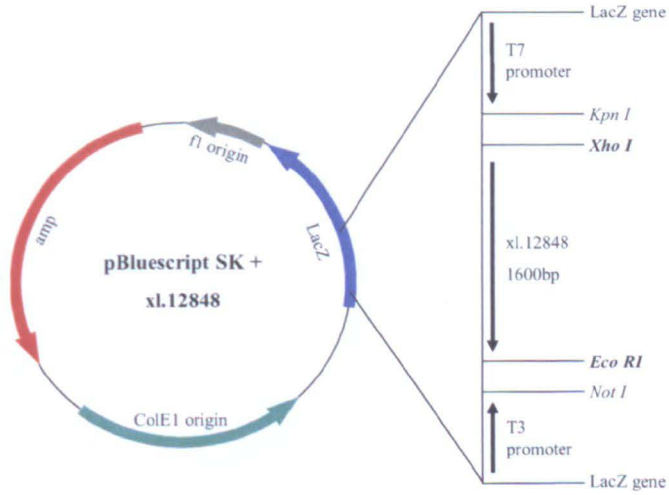

pBluescript SK (+) xl.16795

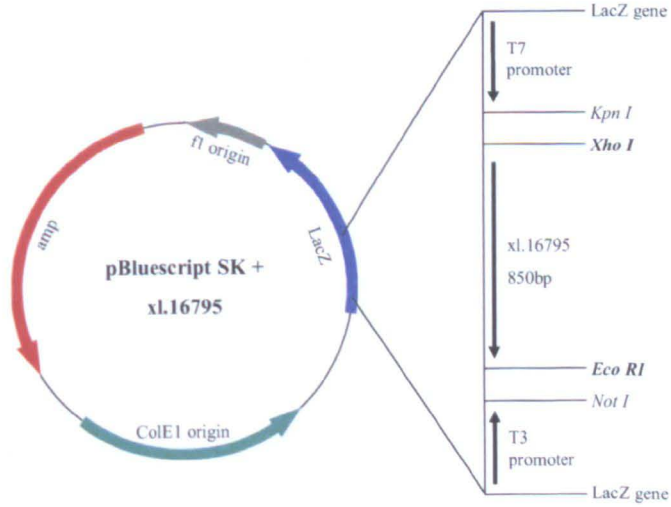

pSP64 Xβm *Xenopus E12*

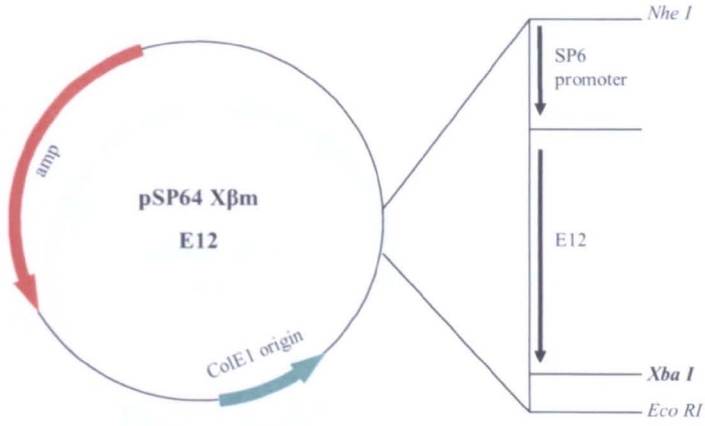

pGEM-T easy human *E47*

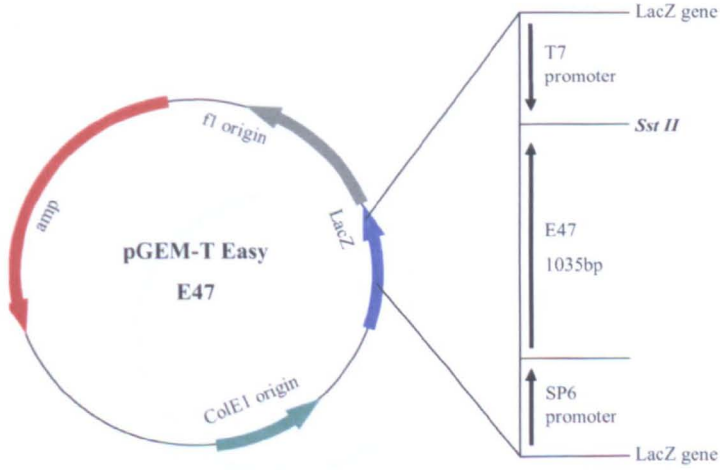

pBluescript KS (+) Mouse *HEB*

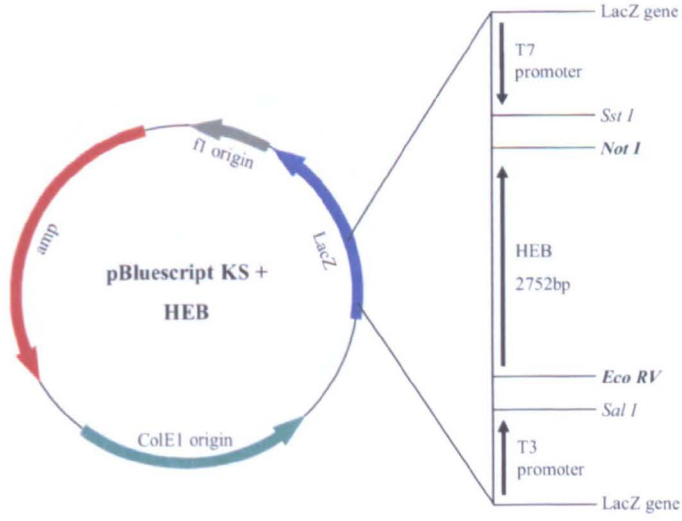

pBluescript KS (+) Mouse
ITF2b

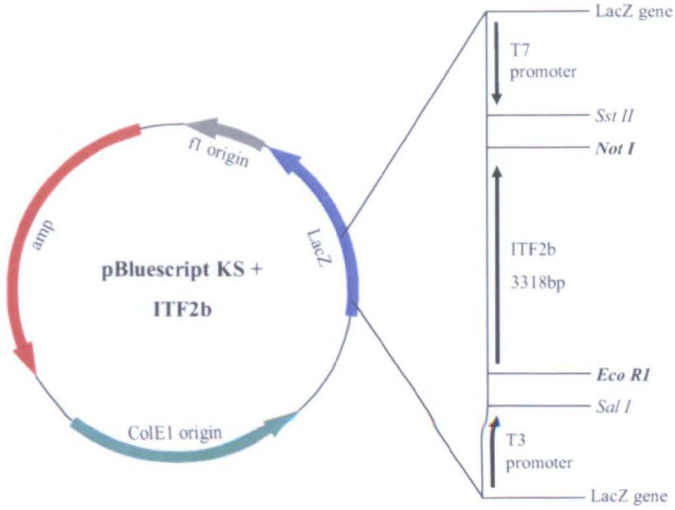

pCS2+ *Xenopus Pax 8*

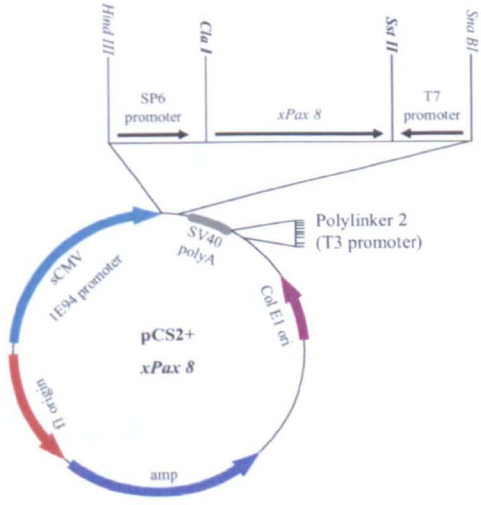

pSP64TS *Xenopus WT1*

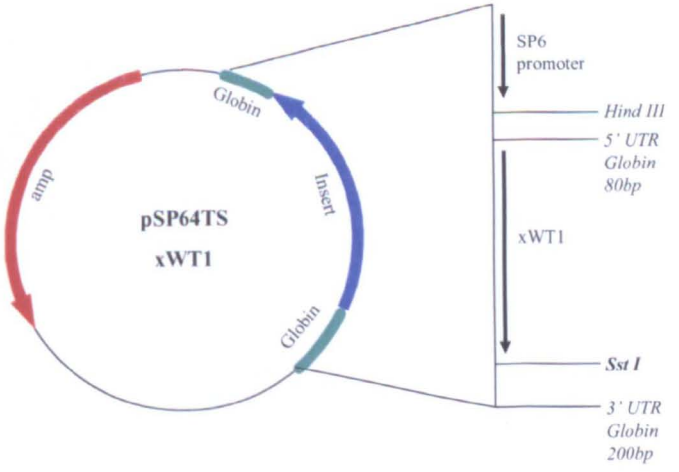

pGEM-7 Zf *Xenopus WT1*

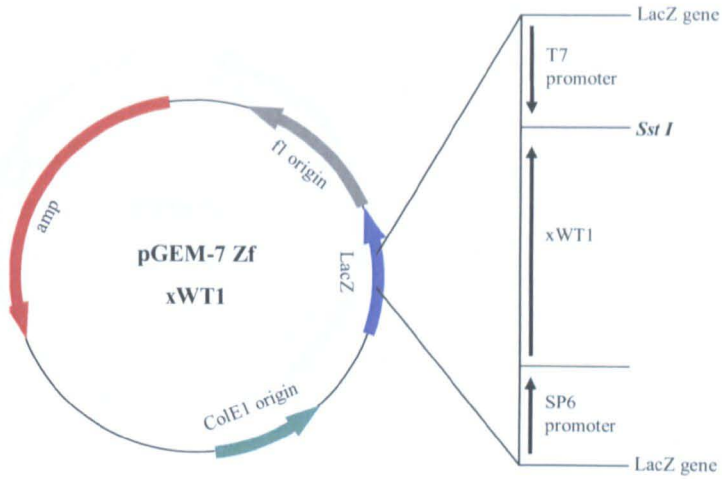

pBluescript KS + *Xlim1*

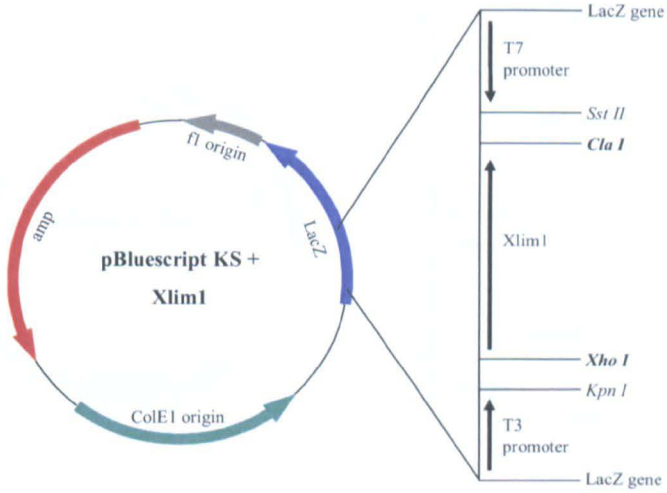

pSP64 Xβm *Xlim1*

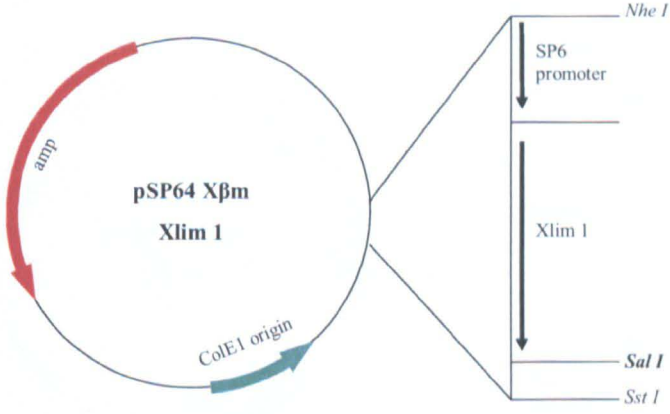

pSP64TS *Xenopus Pax 2*

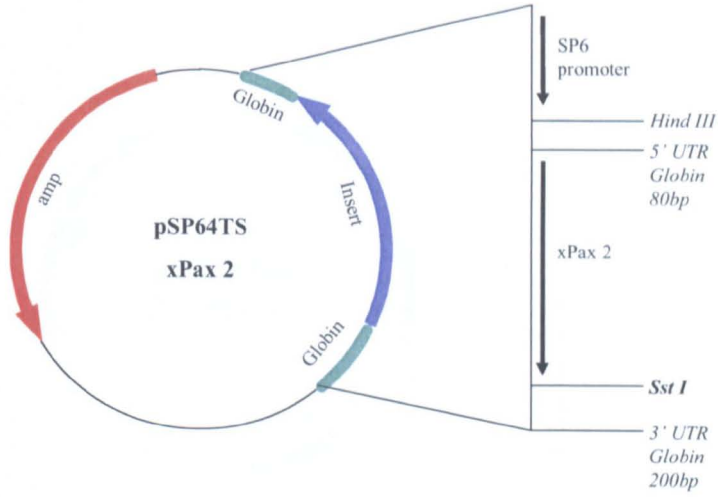

pBluescript KS + *β-tubulin*

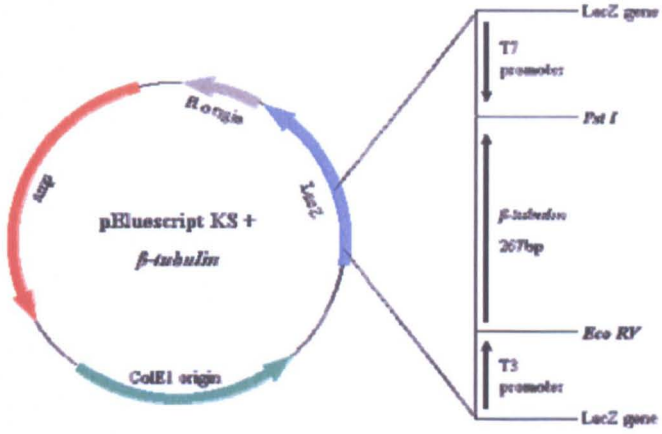

pGEM-T Easy *Xlmx1b*

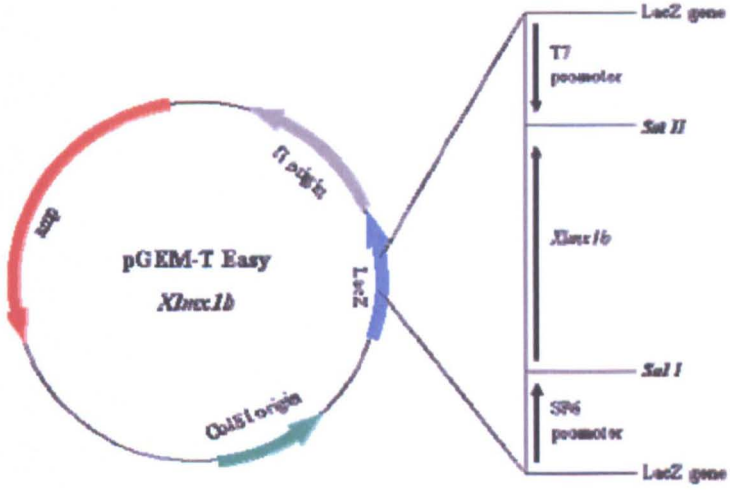

pGEM-T Easy *Xenopus*
Cardiac troponin I (Fragment)